Vulnerability of Mojo Drinking Water Supply Well Aquifer to Anthropogenic Development

By Getachew Abebe

Addis Ababa University

June, 2015

School of Graduate Studies
Addis Ababa Institute of Technology

Vulnerability of Mojo Drinking Water Supply Well Aquifer to Anthropogenic Development

By Getachew Abebe

Thesis Submitted to Addis Ababa Institute of Technology, School of Graduate Studies in partial fulfillment of the requirements for the Degree of Masters of Science in Civil Engineering under Hydraulic Engineering.

Dr. Mebruk Mohammed

Thesis Advisor

Addis Ababa, Ethiopia

June, 2015

Addis Ababa University

School of Graduate Studies

Addis Ababa Institute of Technology

Thesis Submitted to Addis Ababa Institute of Technology, School of Graduate Studies in partial fulfillment of the requirements for the Degree of Masters of Science in Civil Engineering with Hydraulic Engineering.

Date defended--------------------

Members of Examining Board

-- ------------------------------

(Chairman) (Signature)

-- -------------------------------

(Advisor) (Signature)

-- -----------------------------

(Internal examiner) (Signature)

--------------------------------------- -----------------------------

(External examiner) (Signature)

Certification

The undersigned certify that he has read the thesis entitled: **Vulnerability of Mojo Drinking Water Supply Well Aquifer to Anthropogenic Development** and hereby recommend for acceptance by the Addis Ababa University in partial fulfilment of the requirements for the degree of Master of Science.

Dr. Mebruk Mohammed

(Supervisor)

Date

Declaration

I hereby declare that all information in this document has been obtained and presented in accordance with academic rules and ethical conduct. I also declare that, as required by these rules and conduct, I have fully cited and referenced all material and results that are not original to this work.

Getachew Abebe

Signature _____________

Faculty of Technology

Addis Ababa University

Abstract

Ethiopia's Water Resources Management Policy of 1999 gives highest priority to supply drinking water as a national wide. Accordingly MoWE called attention to solve problems associate to unstable states of deficient supplies and increasing demands. Mojo Town with rapid incremental population, the former existing water supply scheme found inadequate to meet the increasing demands of water for domestic uses. Hence, new water supply project for the Mojo town has been executed and its works of construction on progress so far to alleviate such escalating demands for the potable water due to advancing developments. The Mojo water supply scheme depends on groundwater as the sole resource of drinking water from boreholes at Mojo well field. This well field system is designed containing of three deep boreholes where development for each closer to Mojo Perennial River. All over again, this river is basically apprehensive of contaminants because of existences of more than seventeen factories of tanneries, oil factories, waste disposal site and six depots in which roughly all have established at about the brink of this river and most of the factories have not been facilitated with waste treatment plants so that these can be considered as the main sources of potential threats. Therefore; this research paper was primarily initiated attributable to these conditions and was been conducted. As a return of this study, the maximum radius of influences was established fixing to be 3853m considering the entire pumps in the boreholes were assumed working at once under case scenario of the wells operation with aquifer maximum transimissivity and minimum storativity and with the designed pumping rates. The minimum length of the plume position which existing at closest distant from well head is discovered at 2034m at the downstream of the well field. So the contaminant plume is circumscribed in the influence zone of the pumping when the boreholes will start functioning. It also elaborates the particular radii of influences as results of operating boreholes and realizes that the cones of depressions are interacting with the Mojo perennial River and this river is suspicious agents of the potential threats of contaminants sites as previously described. Capture zone was also delineated at mean distance of 110m from the wells head considering case scenario when the boreholes are all simultaneously operating, visualizing that this may supportive in deciding remedying measures to protect the potential threatening of the contaminants from admittances into the boreholes at time when pumps in boreholes will be under equipped to operation. In determinations of differentiating influences of the long term operating boreholes, the superposed drawdown for groups and individual boreholes under varying aquifer parameters was approximated and noticed the intersecting of cones of depressions arrangements and thus in this coincidence it recognized the happenstances of well interference at the Mojo well field while the boreholes are operating.

Acknowledgements

My heartfelt gratitude and thanks first of all attends to my advisor Dr. Ing., Mebruk Mohammed, for his clever engineering insights that inspired me, for the intellectual and keen observations, for his invaluable assistance, support and guidance offered in dealing with the problems encountered from the beginning to the completion of this research work. His critical comments and valuable advices helped me to take this research in the right direction.

I sincerely thank the financial support provided by Ethiopian Roads Authority (E.R.A.) and for the opportunity providing and relevant data offering by Water Works Design and Supervision Enterprises (WWDSE) and.

I would like to acknowledge the Desta Horrecha Consult (DH) for the contribution of the field pumping test and data which was vital to the analysis of this research works.

I would like to give my special thanks to my wife and families for their help and encouragement during my postgraduate studies.

Table of Contents

Lists of Figures

Lists of Tables

List of Acronyms and Abbreviations

AAIT	Addis Ababa Institute of Technology
ASTER	A Surface Topography Elevations Roaster
MOWE	Ministry of Water and Energy
DEM	Digital Elevation Map
GIS	Geographical Information Systems
WWDSE	Water Work Design and Supervision Enterprise
Masl	Meter above Sea Levels
MBH1-OTD	Mojo Borehole no. 1 Observed Test Data
MBH2-OTD	Mojo Borehole no. 2 Observed Test Data
MBH3-OTD	Mojo Borehole no. 3 Observed Test Data
MBH1-APP	Mojo Borehole no. 1 Data Adjusted for Partial Penetration
MBH2-APP	Mojo Borehole no. 2 Data Adjusted for Partial Penetration
MBH3-APP	Mojo Borehole no. 3 Data Adjusted for Partial Penetration
MBH1-AP&UP	Mojo Borehole no.1 Data Adjusted for Partial Penetration and Unconfined aquifer
MBH2-AP&UP	Mojo Borehole no.2 Data Adjusted for Partial Penetration and Unconfined aquifer
MBH3-AP&UP	Mojo Borehole no.3 Data Adjusted for Partial Penetration and Unconfined aquifer
CSA	Central Statistical Agency
PW1-ORC	Pumping Well no.1 Observed Recovery Data ry
PW2-ORC	Pumping Well no.2 Observed Recovery Data

PW3-ORC	Pumping Well no.3 Observed Recovery Data
PW1-APPRC	Pumping Well no.1 Adjusted Recovery for Partial Penetration
PW2-APPRC	Pumping Well no.2 Adjusted Recovery for Partial Penetration
PW3-APPRC	Pumping Well no.3 Adjusted Recovery for Partial Penetration
PW1-APP&UCRC	Pumping Well no.1 Adjusted Recovery for Partial Penetration and Unconfined
PW2-APP&UCRC	Pumping Well no.2 Adjusted Recovery for Partial Penetration and Unconfined
PW3-APP&UCRC	Pumping Well no.3 Adjusted Recovery for Partial Penetration and Unconfined
T_{max}	Maximum Transmissivity
T_{Avg}	Average Transmissivity
T_{min}	Minimum Transmissivity
S_{max}	Maximum Storativity
S_{Avg}	Average Storativity
S_{min}	Minimum Storativity
K_{Avg}	Average Hydraulic conductivity
MJBH-1	Mojo Borehole no. 1
MJBH-2	Mojo Borehole no. 2
MJBH-3	Mojo Borehole no. 3
T_{T1}	Transmissivity Approximated by Theis Curve-Matching Method*
S_T	Storativity Approximated by Theis Curve-Matching Method
K_T	Hydraulic Conductivity Approximated by Theis Curve-Matching Method

T_{CJ}	Transmissivity Approximated by Cooper- Jacob Method
S_{CJ}	Storativity Approximated by by Cooper- Jacob Method
K_{CJ}	Hydraulic Conductivity Approximated by by Cooper- Jacob Method
T_R	Transmissivity Approximated by Theis Recovery Method
K_R	Hydraulic Conductivity Approximated by Theis Recovery Method
	*the number indexed represents the no.1-well number
UTM	Universal Transverse Mercator
WRT	With Respect To
Δ	Symbol delta (Change of drawdown per log cycle/ slope of the drawdown)

1. Introduction

1.1. Background Information

Globally, demands for water supplies are significantly increasing along with drastic population growth, conflicts over agricultural land and pastures, change of climate, environmental protection and governing laws and regulations for water use and allocations. On the other hand existing fresh water to alleviate such increasing demands in the world amounts only 3% and the remaining 97% is salt water in the oceans. Out of the available 3% of the fresh water two-third is stored in form ice in the Arctic and about 2% of the liquid fresh water is surface water, of which is considerably refilled by groundwater. This represents wells and pumps 98% of the world's liquid fresh water (Bouwer, 2002). Hence, groundwater is generally potable at source. It's in situ accessibility and low temporal variability is making it the most important source of water supply for rural communities. However, such available groundwater sources may find deep and tapping may lodge deep drilling in some areas and its development complicated by highly variable hydrogeological conditions rendering the task of management fraught with uncertainty (Taylor & Barrett, 1999). In order to secure the foodstuffs the agriculture sector has a special prominence concerning this problem, since of the competition over water particularly from the municipal and industrial sectors, which affect the efficient use of the available water resources. All of these issues raise the need for adequate, inexpensive, unsophisticated and socially accepted measures awareness of the management to meet the growing demand and to make the growth sustainable involving treating water and wastewater, and groundwater/surface water conjunctive use.

Ethiopia's Water Resources Management Policy of 1999 gives highest priority to drinking water supply over other uses. Accordingly, MoWE has currently launched 15 towns Water Supply Project to promote sustainable water supply development and management as National wide. As a case Mojo Town with high increasing rate of population due migrations from different direction of nearby rural regions, is one of the towns which has been encompassed in this package. For the reason that, an on-going rapid incremental population of Mojo Town's the former water supply scheme found insufficient to meet the domestic water supply to the town dwellers. With objective to alleviate sufficient water supply to Mojo town population, the MoWE called attention to the severing problem of water shortages, the Mojo Water Supply Project launched, implemented and its construction is presently on progress. The source for the new water supply project is Mojo well field located at North West of the Mojo town. Three deep boreholes developed and ready to supply water to the town as soon as the main and service pipe line construction works will be completed.

The report of this research works is compiled by five main chapters. The first chapter is introduction part as tried to overview the source of the water supply in brief at the preceding paragraph of this section. The second section of this report contained the literature reviews and it dealt with the entire relevant citation of literatures as understandings frame of references those which applicable to the study area and it involved in details how the investigation had been through with respect to the scientific findings of the relevant previous studies and the text books of the groundwater. The third portion of the report incorporated the methods used to carry on the investigations. In this section the methods and the procedures thoroughly followed has been integrated in details. To briefly summon up, the primary and secondary pumping test data were collected and thoroughly adjusted for necessary adjustment prior to engage in the analysis. There exist various versions of Aquifer Test Software in analysis of well pumping test. Under this study, an EXCEL tool is used to solve Theis, Cooper-Jacob equations and the curve fitting concluded on windows of Excel Spread Sheet (2007). As an additional the estimations of the parameters is also carried out by Aquifer Test Software 3.5 via automatic curve fitting method with intention to make a comparison. In practical it is a challenging task for radial flow to resolve the solution of the governing differential equation in unsteady state flow (non-equilibrium) condition. Thus, the Theis type-curve fitting method is one of the widely applied methods, to determine the aquifer parameters and simplified such bulky tasks. This type-curve-matching with pumping test data conducted by adopting the EXCEL spread sheet, as EXCEL tool permits of the data entry and handling plotting features effectively. Moreover; all operations in this method are done within EXCEL itself with no needs of macro programming and additional numerical calculation. This method prefered to for it is handy and cheap to apply in analysing the pumping test data for determination of the aquifer parameters. The model simulation through principle of superposition is carried out and composite solutions of drawdown for different scenario predicted. To conduct this simple well hydraulic model simulation analysis software such as Surfer 11 and Global Mapper 12 are utilised.

The fourth and the fifth section of this report are compiling the result and discussion and the conclusions and recommendations parts. The results of the established radii of influences and delineated capture zone of recharge boundary have been organized and detail discussions has also made under the potion of result and discussions at the fourth chapter. The interference of pumping wells also checked based on situation all boreholes are simultaneously put into operational with constant pumping rates at this chapter. The last chapter is chapter five and this section includes conclusions and substantial recommendations forwarded depending on the findings of the research study. Generally, this research report has substantially incorporates all sequences and processes which has been gone through whilst carrying on the analyses in estimating the parameters of the aquifer of the study area, in conducting simple hydraulic simulation to resolve composite drawdown for grouping boreholes in well field via principle of superposition and the final outputs of this case study is thoroughly integrated through in the body of the report.

1.2. Description of the study area

The study area is located in Oromia Reginal State, Eastern Shoa Zone, Ada'a and Lume Wereda between 40 -70km from capital city, Addis Ababa. The study area in Lume wereda will consider Mojo town drinking water supply form boreholes where as the Ada'a wereda refers to supply water for irrigation from multi-boreholes developed for this purpose. The Mojo town is situated 70 km from Addis Ababa with growing industrial and basic service and one of high potential for development. Town municipal & water utility office population estimate of the town for the current year (2011) is indicated to be in the range of 32,000- 36,000. The feasibility study, Metefrea Consulting, 2010, projection for the year 2010 estimated population of the town to be 47,473. According to the recent (2011) Central Statistical Agency (CSA) projection, town population projection indicates 34,968 of which male and female accounts 16,989 and 17979 respectively. Currently the main sources of water production for domestic use in Mojo town are eight drilled bore holes. The design period of the Mojo town Domestic Water production is completed and very old. About 4 boreholes have completed their design period. Moreover the treatment plant of the town is not functional. In addition to this although Mojo River is found at adjacent to Mojo town it is polluted by the nearby industrial discharge. So, it couldn't serve as an alternative source for domestic water production for the town. Mojo town is finding as one industrial town in the country with over 17 tanneries processing and the giant steel and metal factory also allocated 300 hectare of land at the edge of the town that expected to increase workers and population migration to the town. Growing Investment activities and the dry port terminal establishment are also expected to be the engine for development of the town that adds additional demand for basic service in the short or long time period. According to the recent study (Metaferia Consulting engineers, 2010) water born and water related diseases most affecting children under five were typhoid fever, and Amebiasis and the top ten diseases.

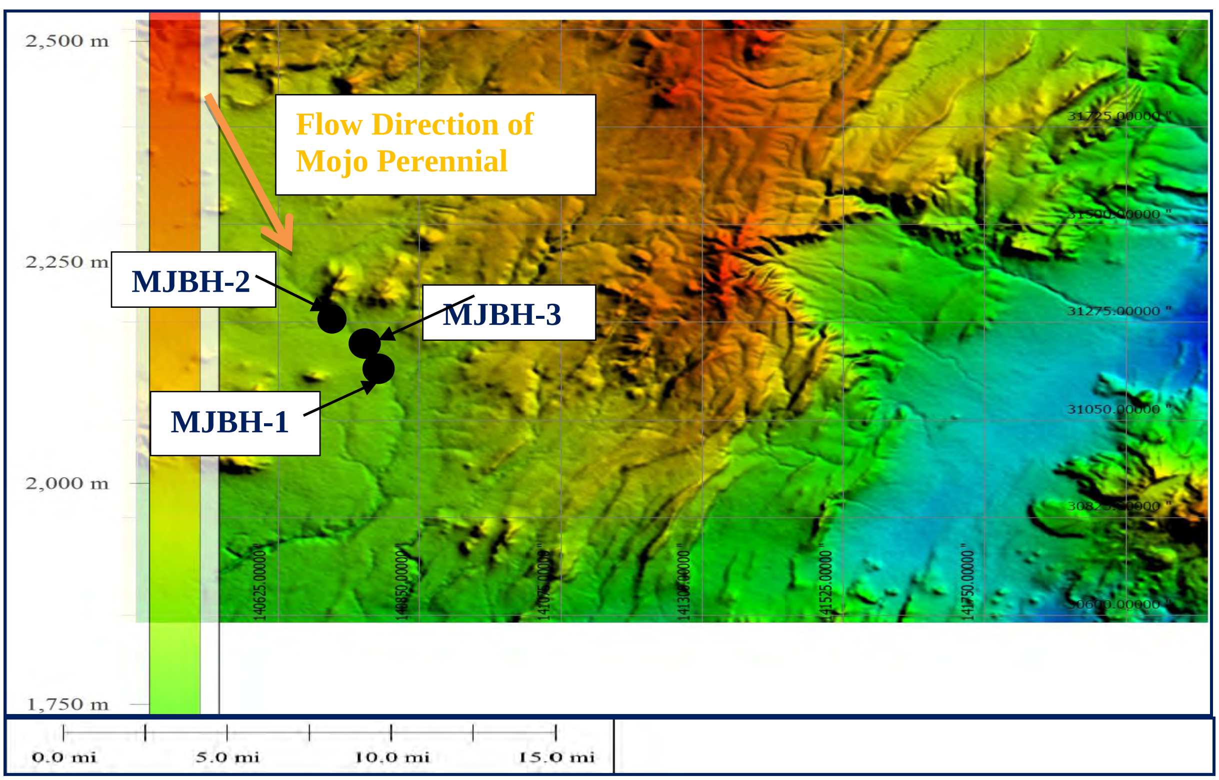

Figure 1. Map of the study area organized from DEM and Boreholes Location

1.3. Statement of the Problem

The locations of Mojo boreholes are closer to Mojo Perennial River. In our opinion based on observation and organized data there might be a gap in providing sufficient space between the existing river and locations of the wells. As discussed by Stevee and Walton stated that the location of pumping well should be far away from hydraulic boundaries in distance equal to or exceeding the thickness of the aquifer to permit cessation of drawdown trends before the influence boundary conditions affects drawdown data (Sevee, 1991(Walton, 1987).

In spite of this evidence, the radius of influences and recharge boundaries of the developed wells were not established.

The sources of potential threats those possibly subsist in the vicinity of the wells such as: - Natural, Industrial, Agricultural practices, Urban wastes materials damping sites and Human activities are what remarkably call notice in selecting the appropriate position of well field for water supply purpose. But as it understood from the executed settings of the developed boreholes, this important issue seems not considered in line to minimize the vulnerability of anthropogenic development may be resulted from the potential threats abovementioned. For instance most of Tanneries developed at Mojo Town have not facilitated by waste removal treatment plants and the harmful chemicals and solute are sending directly into the closer river.

Similarly the treatment plant of the town is not functional. As a result the Mojo River exists at adjacent to Mojo town is polluted by the nearby industrial discharge. For that reason, it cannot serve as an alternative source for domestic water production for the town.

The main source of water production for domestic use in Mojo town is groundwater which are eight drilled boreholes serving at this time. But the design period of those boreholes to supply domestic water production is completed and very old. Thus, the alternative for the new water supply project to alleviate the increasing demands for water is also groundwater.

However; the water produced from the existing boreholes there confirmed to consist of pollutants which cause water born and water related diseases according to the recent study of (Metaferia Consulting engineers, 2010). The water born and water related diseases those most affecting children under five were typhoid fever, amebiasis and the top ten diseases.

Hence, this research was initiated to substantiate whether the new water supply project in which its source assumed from the groundwater via the well filed location set up closer to the Mojo River can interact with this river or not. Note that construction of this new water supply is currently underway and the boreholes had been developed and yet not starting functioning.

1.4. Objective of the study

1.4.1. General objective

The general objective of this research is to establishing radius of influences. Accordingly, the radii of influences established and the capture zones also determined for pumps operating in the boreholes under various operational conditions at Mojo well field. In view of that, understanding of this may be utilized in generating improved decisions in planning water resource managements and remedying protections against threats possibly solidify by developments conditions of human beings.

1.4.2. Specific objectives

The specific objectives of the study were:

1. Determining the aquifer parameter. The aquifer parameters were determined by conducting the analytical solution through the analyses of the Theis curve matching, Copper-Jacob and residual drawdown methods.

2. Identifying the potential threatening sources. The sources of potential threats exist within the vicinity of the well field had been identified. These included, Natural, Industrial practices, Agricultural practices, urban wastes materials damping sites and Human beings activities as effect developments. This information was consumed as input when the radius of influence of pumping wells fixed.

3. Checking for well interference. The occurrences of well interference were determined whilst in partial or entire wells supposed operating altogether in the well field.

2. Literature Review

2.1. Impact of Environment and Effect of Pumping

Wells drilled into the saturated zone are pumped and groundwater extracted for different purposes. Regularly most of the water pumped for the purposes of irrigation, water supply and industrial uses. When the pumping rate of discharge increases, wells in a groundwater basin always have some long-term effects on other wells or the volume stored in the basin. In many cases, often pumping wells located near to streams because a noticeable reduction in groundwater level and water discharge from the stream to aquifer. That is why Harr, advocates “The interaction between well discharge and groundwater discharge to a nearby stream was a key technical issue in A Civil Action, a popular nonfiction book and movie about a trial involving contaminated water supply wells”, (Harr, 1995). The owners of industries and tanneries those defendants in the regulation getup were major organizations that owned polluted sites and discharge to the streams near the water supply wells. If the supply wells pulled most of their water from the nearby stream, then a significant fraction of the pollutants in the well water could have come from such sites upstream into the stream, and the poisoned water might be extracted. That is why the investigation of environmental impact on water supply and other many different kinds of issues fascinate the attention of the scientists nowadays.

2.1.1. Sources of Potential Threats

The potential threat is referred non-point and point sources that possibly imminent to the groundwater contamination. Groundwater contamination is addition of any solute into the hydrological system as a result of man’s activity (Freeze and Cherry 1979). It can take place from non-point-source like percolation from agricultural fields on account of application of fertilizers and pesticides and from point source like waste disposal sites. This problem has become more severe in the last few decades to our country Ethiopia as a result of increased industrialization, urbanization and agricultural activities which have seriously deteriorated the quality of both surfaces and sub surfaces water resources. The major sources of potential threats those possibly will subsist in the vicinity of radius of influence are the cited underneath:-

2.1.1.1. Natural

This phenomenon is one of the threat sources for occurrence of groundwater contamination due to natural causes clearly in dissolution of aquifer materials. Fluoride-rich water in East African Rift Valley, e.g. Ethiopia is associated with calcium deficient volcanic rocks and calcium poor granitic rocks (Smedley 1992). Arsenic (As) in drinking water has received much attention in recent years as evidence of its detrimental health effects has grown (Welch and Stollenwerk 2003).

2.1.1.2. Industrial Activities

The waste water discharged from industries conveys with it a variety of dissolved and suspended impurities, the composition of which depends on the type of industries and the processes used. At several places, the effluents have been discharged to the streams and rivers with no provision of proper treatment schemes and consequently create the problems of surface water and groundwater contaminations. In the developing countries like Ethiopia, for instance Eastern Zone massive Industries located at midway of Mojo and Dukam towns such problems might be happened. Some researchers have discovered that high concentrations of Cr, Pb and Zn in surface water and groundwater are reported from several places due to industries (Kakar 1988, 1990; Handa 1994).

2.1.1.3. Agricultural Activities

These are also most potential threatening sources which cause contamination of groundwater due to greater use of inorganic fertilizers and pesticides for obtaining higher crop yields. This event might be the case in the developing countries as massive Industries are in expanding. The use of such pesticides is more rapid in many developing countries than in the developed world. The inorganic fertilizers are the source of nitrogen, phosphorous and potassium. If the NO_3^- concentration exceeds 50 mg/l, it becomes undesirable for drinking purposes. The NO_3^- concentration is usually higher in shallow aquifers but with time and greater input, deeper aquifers are also likely to be contaminated. The various pesticides with higher solubility in water have significant mobility in some type of aquifer materials, such as clean sands and gravels (Freeze and Cherry 1979).

2.1.1.4. Urban Waste Disposal

The majority of the urban solid waste is likely to dispose in sanitary landfills. At some places, hazardous waste viz. organic chemicals and pesticides also disposed in these landfills. The sanitary landfills are made in natural depressions or in man-made excavations like abandoned quarries etc. The leachate from landfills may contain large number of potential contaminants threats. Therefore, it can cause severe damage to groundwater quality. The problem is more acute in humid climate, especially in permeable and fractured formations where water-table is at shallow depths. The leachate plume may extend to distances of several hundred metres in permeable formations which may last for many decades. Therefore, landfill sites should be selected by necessary hydrogeological investigations to minimize the groundwater threaten by the leachate. Currently, with increasing population, the leachates from landfills pose a major environmental problem. According to lately published paper the predominantly NO_3 content in groundwater from a landfill located in fractured zones will be increased which necessitates to drop solutions to protect groundwater quality (Dey et al. 2003). The effect of consuming drinking water that being poisoned by these potential contaminants could cause brain disorder and liver damage etc.

2.1.1.5. Human Activities

In addition to the sources of potential threats for groundwater contamination mentioned above, there are several other causes of deterioration of water quality due to human activities viz. deforestation, over-irrigation, road salts, sewage sludge, urban runoff, deep well disposal of liquid waste, flower farming etc. Deforestation may cause rise in water-table and subsequent increase in the salinity of groundwater (Ruprecht and Schofield 1991).

2.1.1.6. Remediation

The impact of environmental investigations and remediating contaminated sites has been occupied by more groundwater scientists in the past several decades than any other type of investigation. The result of the investigation directs that certain contaminants require more active remediation efforts. Consequently, new technologies and methods are constantly innovated to take active remediation. This remediation might involve construction of trenches where contaminants are captured or destroyed, pumping and treating water, injecting air, or other schemes. Kresic Neven (2009).

2.1.2. Collection of Pumping Test Data

The test data groups are very important to make a meaningful discussion on the processing variables. There are two main groups: and these include both primary and secondary essential data collection at field investigation and office work stage. The primary data gathering includes the works accomplished at the field investigation level. This task was carried out by collecting data on the sites using different instruments to discover existing physical features and barriers. The secondary data collections again categorized into two types i.e. point data and spatial information. The point data are the data that are generated at a specific geographical point. This data type may assume many forms. For examples: - geological data, such as borehole logs; hydrogeological data, such as depths to water level and yields; construction data, such as casing, piezometer, borehole development and costs; type of equipment, such as pumping equipment and recorders; geophysical data, including surface and borehole measurements; hydraulic properties of the aquifer(s), such as transmissivity and storage; water abstraction and groundwater level records; hydrochemistry; other information, such as topography and surface drainage. The term spatial in secondary data gathering recommends that point data are displayed in the geographical context, such as on a map. Whereas the term information proposes that the point data have been processed, usually to the extent that the original values for variables can no longer be recognised. Examples of variables with spatial associations contain the geological log, which has a vertical dimension, and surface geophysics, which has both horizontal and vertical dimensions. The management of data and information can be gathered under main headings of graphs and statistical tables and displays. In addition to the data above-mentioned, the following data are also requiring: - local well name and owner, date drilled, well use, location by legal description, such as latitude and longitude coordinates (UTM), and approximate location relative to local landmarks, elevation of land surface and measuring point, well depth, size and type of casing, location and arrangement of screen openings (Ground Water Studies).

2.1.3. Topography and Digital Elevation Model (DEM)

Topography is defined by a DEM that describe the elevation of any point in a given area at a specific spatial determination. The digital elevation model (DEM) is any digital representation of a topographic surface and it is specifically made available in the form of raster or regular grid of spot heights. A surface topography has pronounced influence on groundwater occurrence. Digital Elevation Model (DEM) forms a very basic and important input in any study of the earth's surface features. It is significant to delineate the topographic map and to analyse the river patterns of the land surface terrain. It can be obtained in many ways. Digitization of topographic maps followed by interpolation has been a widely used practice for generating DEM. However, the major shortcomings of this are lower accuracy due to deformation of topographic map paper and many generalizations during topographic map preparation. There are various available software packages for generating DEM. One of that DEM software is ASTER. A 90 m by 90 m resolution DEM was obtained from Water Works Design and Supervision Enterprise (WWDSE). The supposed area under influence of pumping is delineated and Mojo River is generated from DEM. Elevation of the study area ranges from

1757 amsl to 1838 amsl surrounding the well field in study region. (B.B.S Singhal and R.P. Gupta, 2010).

2.1.4. Pumping Well Location

The location of the pumping well should be far enough away from hydraulic boundaries to permit recognition of drawdown trends before boundary conditions influence the drawdown data (Sevee, 1991). So as to minimize the effect of stream, river or lake bed infiltration, it should be located at a distance equal to or exceeding the aquifer thickness from the possible boundary (Walton, 1987). Nevertheless, if the intent is to induce recharge, then the pumping well should be located as close to the boundary as possible (Sevee, 1991). The appropriate depth should be determined from exploratory boreholes or logs from nearby wells. (U.S. EPA Guidance, 1995).

2.2. Pumping Tests Data and Adjustment of Data for Analyses

The water supply wells for drinking water, irrigation, and industrial purposes are drilled after assembling data on the hydrogeology of the region (previous drilling data, well data, and geologic maps). Test wells are drilled and hydraulic testing is done to estimate the long-term discharge capacity. The water chemistry is checked to make sure that the water is suited for its intended purpose. If the test results are favorable, production wells are then designed and installed. One of the measurements to be taken during a pumping test is the measurement of the water levels in the test wells and the piezometers. However; for this study, there were no test wells and piezometers. Instead observations for water level measurements and pumping tests conducted in single pumping well (Charles R. Fitts, 2002).

2.2.1. Single Well Test

A single-well test is a test when there are no piezometers existing. In situations when data from observation wells are not available, it is possible to obtain useful data from production wells. The test in a single well involves pumping, displacing, or adding water and measuring changes in water levels in the well. Such type of test allows a rapid and economical calculation of K and T of the zone of interest at a single location. It can also determine response criteria for observation wells in multiple well pumping tests. So using the data that measured from changes in water-level during pumping or recovery which is conducted in the well itself, the hydraulic parameters of the aquifer can be determined in many conditions (U.S. EPA Guidance, 1995).

2.2.2. Observation Wells and Piezometers

The data on groundwater heads and the chemical composition are obtained at observation wells or piezometers. An observation well is a non-pumping well used to observe the height of the water table. Whereas a piezometer is a non-pumping well, generally small in diameter, that is used to measure the groundwater head. The observation well generally of larger diameter than a piezometer and may be screened throughout the thickness of the aquifer. The piezometer is an open-ended pipe, placed in a borehole that has been drilled to the desired depth in the ground. The number depends on test objectives and available resources for test program. The field test data from single pumping well can give aquifer characteristics (T and S). But reliability of estimates increases with additional observation points. Normally three wells at different distances are needed for time-distance analysis (Kruseman and de Ridder). There is no maximum number; because anisotropy, homogeneity, and boundaries can be deduced from response.

2.2.3. Categories of the Aquifers

Aquifers are classified into two broad categories. They are either unconsolidated aquifers or consolidated fractured aquifers. The unconsolidated aquifer again subdivided into three types naming: confined, unconfined and leaky aquifers. The unconfined aquifer is one where the water table occurs within the aquifer layer. The unconfined aquifers are also called water table or phreatic aquifers. In a confined aquifer, the whole thickness of the aquifer layer is saturated and there is a confining layer above. The water level in a non-pumping well in a confined aquifer rises above the top of the aquifer.

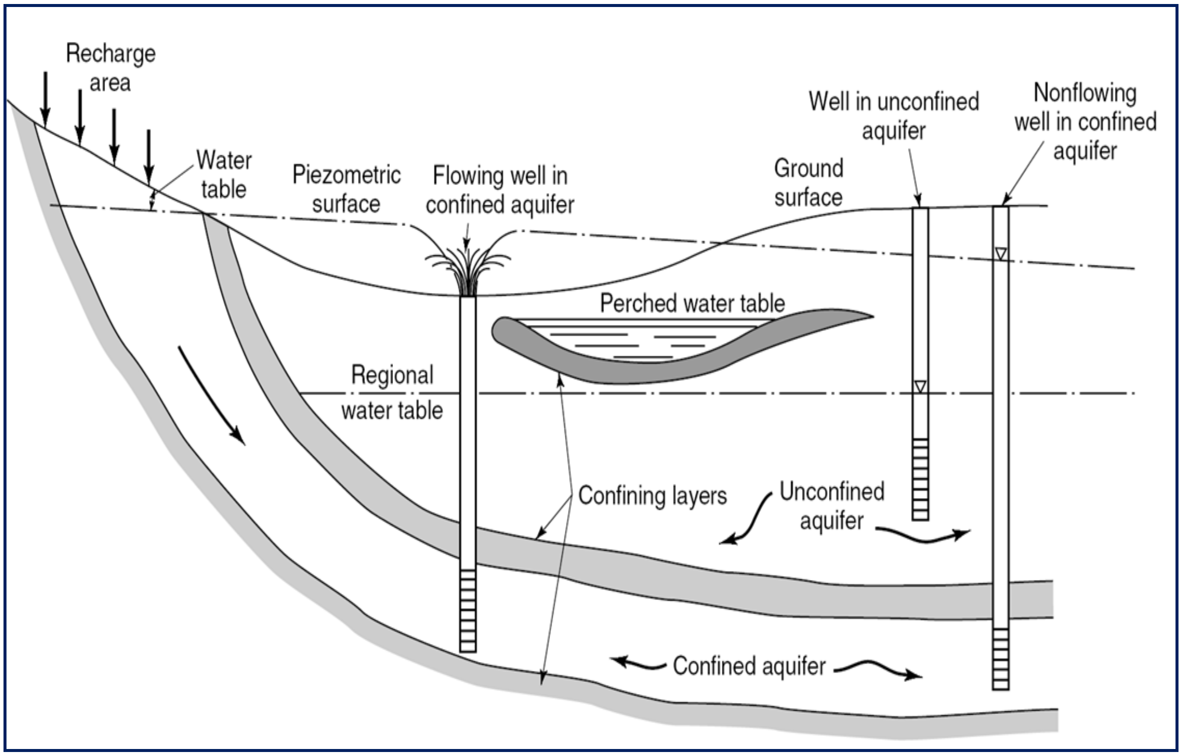

Figure 2. Vertical cross-sections through an unconfined aquifer and a confined aquifer. Source: Types of aquifers (from U.S. Bureau of Reclamation (1981), P-144).

The aquifer system has to be precisely known to assist an easy calculation of its hydraulic characteristics. So interpreting a pumping test is primarily a matter of identifying an unknown system. This system identification comprises the construction of diagnostic plots and specialized plots. The diagnostic plots are log-log plots of the drawdown versus time since pumping started. The specialized plots are referring to semi-log plots of drawdown versus time. In order to select appropriate theoretical model both plots must be constructed for it is a crucial step in the interpretation of pumping tests.

2.2.4. Characteristics of Unconfined Aquifer

The characteristics of the aquifer can be decided based on the response that the pumping causes a cone of depression trend that creates in the water table while dewatering water from the aquifer. As pumping continues, the cone expands and deepens the level of water in the well, and the flow towards the well has clear vertical component. Therefore; some basic characteristics of unconfined aquifers whilst subject to pumping operation, unconfined aquifers, and the water levels in piezometers near the well often tend to decline at a slower rate than that described by the Theis equation. The time-drawdown curve on log-log paper commonly shows a typical S-shape. At the present time, the widely used explanation of this S-shaped time-drawdown curve is based on the concept of delayed water table response. The researcher who first discovered and announced this concept is Boulton (1954, 1963). He called the concept ‘delayed yield’. Although the concept he developed useful in practice, an empirical constant known as Boulton’s delay index is not defined and not clearly related to any physical phenomenon. The concept of delayed water table response was further developed by Neuman (1972, 1973, 1979); Streltsova (1972a and b, 1973, 1976); Gambolati (1976) and Philippe Renard (2005).

2.2.5. Adjustment of Pumping Test Data

The test data obtained from the observed water levels might have to be corrected for external influences prior of being used in the analysis. The local movement in the hydraulic head or water table has to be analyzed so as to discover out whether the correction is indispensable or not. The test data that ultimately suitable for these purposes are the water-level measurements those had taken in a pumping test itself or in a piezometer. But measurements taken at the test site for some days before and after the test can also be used. If, after the recovery period, the same constant water level is observed as during the pre-testing period, it can safely be assumed that no external events influenced the hydraulic head during the test. If, however, the water level is subject to unidirectional or rhythmic changes, it will have to be adjusted. Amongst of the applicable test data adjustments the following mutual corrections are presented.

2.2.5.1. Adjustments of Pumping Test Data for Unconfined Aquifers

The observed drawdowns from unconfined aquifers are required correction for unconfined before using for analysis to estimate aquifer parameters, when the drawdowns in this aquifer are large compared with the aquifer's original saturated thickness. This correction is only needed when the maximum drawdown at the end of the test is larger than 5% of the original saturated aquifer thickness. According to the recommendation forwarded by Jacob (1944), the adjusted drawdown for an unconfined aquifer is given by: -

$$\mathbf{s_c = s * \left(1 - \frac{s}{2b}\right)} \qquad (\mathbf{2.1})$$

Where:-

b = is the initial saturated thickness;

s = is the measured drawdown and

s_c = is the corrected drawdown.

If the drawdown is not corrected, the Jacob and Theis analysis underestimates the true transmissivity under saturated conditions by a factor of s_c/s. Accordingly the gathered test data is adjusted for unconfined aquifer by using the above equation as supposed by Cooper-Jacob. (U.S. EPA Guidance, 1995)

2.2.5.2. Correction for Partial Penetration

The Theis method assumes that pumping wells fully penetrate the aquifer and all releases from storage are derived directly and solely from the aquifer being pumped. Partial penetration of the well into the aquifer causes vertical component flow to happen in the vicinity of the well and as effect additional head loss is occurred. When the well only partially penetrates the aquifer, the average flow path length is increased so that a greater resistance to flow is encountered. The analysis of the partially penetrating case is difficult but (Kozeny;

1933) provides a practical method to estimate the change in specific capacity (Q/s). (Kozeny; 1933) contributes the following approximate reduction factor to correct specific capacity (Q/s) for the effects of partial penetrations.

$$\mathbf{F} = \frac{\mathbf{L}}{\mathbf{b}}\left[\mathbf{1} + \mathbf{7}\cos\left({}^{\pi\mathbf{L}}/_{\mathbf{2b}}\right)\sqrt{{}^{\mathbf{r}}/_{\mathbf{2L}}}\right] \qquad (\mathbf{2.2})$$

Where

b = is the total aquifer thickness (m)

r = is the well radius (m); and

L = is screen length (m).

The equation is valid for L/b < 0.5 and L/r > 30. Accordingly the required correction for the possible effect of partial penetration is conduct supposing the average values of the casing arrangements of the wells and the proposed reduction factor valued as the above equation so as to use the adjusted data for the analysis of such conditions.

2.2.5.3. Adjustment for Well Loss and Well-Bore Storage

The drawdown data obtained from single pumping well tests can be used to define the characteristics of aquifers parameters in many occasions. However; the drawdown and recovery data from such single pumped well tests are influenced by well losses and well bore storage. In theory of hydraulics of well flow, the well is assumed to have an infinitesimal radius so that the well bore storage can be ignored. Consequently, almost all theoretical models assume a line source or sink, which means that well-bore storage effects can be neglected. As a matter of fact, well bore storage is large by comparison with the storage in an equal volume of aquifer material. As effect these wells acquire certain dimensions and some water might be stored. Therefore, in a single-well test, well bore storage must be considered while analyzing the drawdown data. This occasion is particularly true when pumping tests are carried out in large-diameter dug wells and the early time drawdown test data is considered for the analyses. Reasoning that the larger the diameter of the well, the more waters it will store, and the less the condition of line source or sink will be satisfied.

Obviously, the effects of well-bore storage will appear at early pumping times, and may last from a few minutes to many minutes, depending on the storage capacity of the well. So as to recognize whether the early time drawdown data are dominated by well bore storage, a log-log plot of drawdown s versus pumping time t should be completed. If the early time drawdown plots as a straight-line segment with a slope of unity, we can conclude that the effect of well bore storage exists. If a pumping test is conducted in a large-diameter well and drawdown data from those sources will also be affected by the well-bore storage in the pumped well. This is because a significant amount of fluid may be contained in the pumping well when its radius is large enough. But when the radius of the pumping well is small and the early-time straight-line segment slope in a log-log plot is less than unity at the early pumping time, the well bore storage can be disregarded. Moreover, "Kruseman and N.A. de Ridder suggested that the Curve-fitting methods and straight line methods have been developed and are applicable to analyze single-well tests, even when the early time data are affected by well bore storage (G.P. Kruseman and N.A. de Ridder, 1994)". Hence, correction for the well loss and bore storage loss are not considered in this investigation considering that the radii of the pumping wells are small and curve fitting is applicable to analyze single-well tests.

2.3. Pumping Test Analyses and Methods to Estimate Aquifers' Parameters

The reliable value for the parameters of the geological formations of the aquifers through which the groundwater is moving has to be determined by the geologist or engineer. One of the most effective methods of achieving such values which have been proved in many practical ways is the Pumping Test Analyzing Method. The deed of analyzing and evaluating the pumping test data, however, is as much an art as a science. It is said an art because different types of aquifers can exhibit similar drawdown behaviors, which demand interpretational skills on the portion of the geologist or engineer (G.P. Kruseman and N.A. de Ridder, 1994). It is also a science because it is established on theoretical models that the geologist or engineer must recognize on thorough investigations that he must conduct into the geological formations in the test area. One of the comprehensive methods of analyzing aquifers test data is applicable for many investigations to fit the measured drawdown with standard simulated type - curve using Analytic Solution or Curve Fitting Technique. The analytical solution methods use classical mathematical approaches to resolve differential equations into exact solutions. These solution techniques require assumptions of homogeneity and are limited to one dimensional and two dimensional problems. Owing to a number of simplifying assumptions regarding the ground water system, such models enable investigators to conduct a quick preliminary analysis of ground-water contamination and to perform sensitivity analysis which are necessary to obtain the solution. Even though these assumptions do not necessarily dictate that analytical models cannot be used in realistic situations, they do require sound professional experience and judgment in practical application to field situations. It is also true that in many field situations few data are available; complex numerical models are often of limited consumption. So that other different techniques such as: -log-log plots or semi-log plots and further techniques for the recovery stages can be implemented for estimating aquifers parameters from the pumping tests data. In the case of the curve-fitting techniques the field results are plotted and matched against the results of the analytical solutions.

In order to conduct curve fitting for gathered pumping test data, the type of aquifer and test data change have to be resolute in the first step. As these topics is already cited thoroughly in subsections from 2.2.5.1 to 2.2.5.3 of the literature review parts, the duty of fitting between the type – curve and the corrected drawdown versus time plot is accepted there by overlapping two plots, adjusting that both plots ensured to have the same scale. Then the guess of the parameters for each well or multiple wells are concluded manually. In addition to the mentioned techniques, Aquifer Test Model is also applied to analyze the gathered data from pumping tests. In such model the solution methods offered to incorporate the broad ranges of physical conditions of confined and unconfined aquifers. The pumping tests data usually involves pumping from a single well or several testing data from different observation wells and piezometers fixed from hours to weeks. Noticing from varies tests data exhibitions, that the heads measured at the pumping well and/or nearby observation wells decline over time as a result of operating pumps. These tests are used to measure the average horizontal hydraulic conductivity, transmissivity, and storativity of the layer being pumped. For the sake such aquifers parameters cannot be measured directly in a test, a variety of techniques are demanded to determine these aquifers characteristics. Among those methods the Aquifer Testing Model using the solutions advisor, is one of the common techniques for carrying on analyzing of pumping tests (Thomas Röhrich, 2002).

The intention why the supposed analyzing of pumping tests by means of the Aquifer Testing Model technique is conducted and presented here in the scope of this research work, simply for mere compression between the manual curve fitting method which is produced by excel spread sheet and automatic curve fitting technique that completed by Aquifer Test Model. Then the estimation of the aquifers parameters for each well is concluded via curve–fitting and Aquifer Test Model methods both in manual and automatic curve fitting techniques respectively. So as to carry on the analysis the following three common approaches are comprised in sequences: - ***Theis's Curve-Fitting Method, Cooper and Jacob Drawdown versus Time Graph and Residual Drawdown versus Time Graph*****.**

2.3.1. Theis's Curve-Fitting Method

Theis (1935) distinguished that when a well penetrating an extensive confined aquifer is pumped at a constant rate, the influence of the discharge extends outward with time. The rate of reduction in head multiplied by the storativity and summed over the area under the influence of pumping, equals to the volume of water to be extracted. Theis's equation is written as:

$$\mathbf{h_0 - h = s = \frac{Q}{4\pi T}\int_u^\infty \frac{e^{-u}}{u}\,du = \frac{Q}{4\pi T}W(u)} \qquad \textbf{(2.3)}$$

Where:

$s = h_0 - h$ = the drawdown in m measured in a piezometer at a distance r in m from the well;

Q = the constant well discharge in m^3/s;

T = the transmissivity of the aquifer in m^2/s;

W(u)= is a particular exponential integral, with u as the argument, which in this usage is read as the well function of u.

S = the storage coefficient;

t = the time since pumping started.

$$\mathbf{u} = \frac{\mathbf{r^2S}}{\mathbf{4Tt}} \text{ and } \mathbf{S} = \frac{\mathbf{4Ttu}}{\mathbf{r^2}} \qquad (2.4)$$

W(u) is the exponential integral and symbolically written as W(u), which is commonly read as 'well function of u' or 'Theis well function'. This well function W(u) and its argument u are also specified as 'dimensionless drawdown' and 'dimensionless time', respectively. It can be written as a series:

$$\mathbf{W(u) = -0.5772 - \ln u + u - \frac{u^2}{2.2!} + \frac{u^3}{3.3!} - \frac{u^4}{4.4!}} \qquad (2.5)$$

The utmost familiar type of aquifer test is the constant-discharge pumping test. The discharge Q is pumped at constant rate for the test duration at a given well, while drawdown against time since pumping started is measured at the pumping wells and/or nearby observation wells. The parameters Q, r, and s versus t are measured and whereas unknowns T and S are to be calculated. The Theis equation/analytic solutions for the radial/well flow do not allow direct calculation of the parameters (i.e. T and S) for the constraints measured in the test due to the appearance of the two unknowns and the nature of the exponential integral in the equation. On the other hand; a solution can be found by a curve fitting technique for this technique is quite versatile, and may be applied to a variety of solutions. Equation (2.3) can be written as:

$$\mathbf{\log s = \log\left(\frac{Q}{4\pi T}\right) + \log\ (W(u))} \qquad (2.6)$$

$$\mathbf{\log (t) = \log\left({}^{r^2S}/_{4T}\right) + \log({}^{1}/_{u})} \qquad (2.7)$$

The right-hand terms in each of these two equations is a constant on a fixed radial distance r. This implies that the curve fitting method is based on the fact that when s is plotted versus t and W(u) versus 1/u on the same log-log paper the resulting curves (the data curve and the type curve, respectively) ought to have the same shape, but either has to be offset horizontally and vertically by the constants Q/(4πT) and $4T/(r^2S)$. The vertical offset is Q/(4πT) which can be used to calculate T, whereas the horizontal offset is $4T/(r^2S)$ which may be used to calculate S/T. The calculated values for W(u) corresponding to 1/u had been tabulated and widely published in groundwater text books (G.P. Kruseman and N.A. de Ridder, 1994). The two curves have made to match, the coordinates of an arbitrary matching point are the related to values of s, t, 1/u, and W(u) and the unknowns T and S are computed with equations (2.8) and (2.9)respectively.

The following procedures are gone through while conducting the curve-fitting task

1. The plots of drawdown (s) versus pumping time (t) at three boreholes on log−log paper are prepared in Excel Spread Sheet, using the same scale paper as a log−log plot of W (u) versus 1/u which is previously produced in similar manner.
2. The two plots on excel window is overlaying and until the best fitting point of the two curves as much as possible. The axes of both plots are kept parallel while doing the curve fitting.
3. Recording the s, t, W (u), and (1/u) at the best fitting point by selecting any point that is on both sheets of the log−log graph paper. This point, called the match point, is arbitrarily chosen because only the ratios s/W(u) and t/(1/u) are important, and these ratios are independent of the location of the match point. It is convenient for the following calculations to choose the match point either where W(u) =1, (1/u) = 10
4. Then T is Calculated for each wells using

$$\mathbf{T} = \frac{\mathbf{Q}}{\mathbf{4\pi\Delta s}}\mathbf{W(u)} \qquad (\mathbf{2.8})$$

5. S is Calculated for each wells using

$$\mathbf{S = \frac{4Ttu}{r^2}} \qquad (2.9)$$

2.3.2. Cooper and Jacob Drawdown versus Time Graph

The analysis of Theis method was modified by Cooper and Jacob (1946) who well known that when the pumping well has been running for some time, u becomes small and the higher power terms of the infinite series becomes insignificant. Kevin M. Hiscock recommended that for small values of u (u < 0.01) at large values of time, t, the sum of the series beyond the term $\mathbf{\ln u}$ in the expansion of the well function, W(u) in equation $(\mathbf{2.5})$ can be ignored (Kevin M. Hiscock, 2002). So that drawdown, s, can be approximated as:

$$\mathbf{s = \frac{Q}{4\pi T}(-0.5772 - \ln u)} \qquad (2.10)$$

In confined aquifers the condition that u be small is usually satisfied at moderate distances from the well within an hour or less. When u <0.05, we can ignore all higher powers of u, hence:

$$\mathbf{T = \frac{Q}{4\pi(h_0 - h)}\{-0.5772 - \ln\left(\frac{r^2\,S}{4Tt_0}\right)\}} \qquad (2.11)$$

By substituting equation $(\mathbf{2.10})$, $\mathbf{u = {r^2S}/{4Tt_0}}$ for u in equation $(\mathbf{2.11})$ and observing that $\mathbf{\ln u} = \mathbf{2.3 \ln u}$, gives

$$\mathbf{s = \frac{2.3Q}{4\pi T}\log_{10}\frac{2.25Tt_0}{r^2S} = \frac{Q}{4\pi T}\ln\frac{2.25Tt_0}{r^2S}} \qquad (2.12)$$

Since Q, r, T and S have constant values, a plot of drawdown, s, against the logarithm of time, t, should give a straight line. Then at the final outcome we can get

$$\mathbf{S = \frac{2.25Tt_0}{r^2}} \qquad (2.13)$$

$$\mathbf{T = \frac{2.3Q}{4\pi\Delta(h_0 - h)} = \frac{2.3Q}{4\pi\Delta s}} \qquad (2.14)$$

Where: -

Δs or $\Delta(h_0\text{-}h)$ = the drawdown per log cycle of time;

S = storativity;

r = the radial distance to the well and

t_0 = the time, where the straight line intersects the zero-drawdown

The following procedures are gone through while conducting the curve-fitting task

1. Drawdown, s versus the corresponding time, t plot is produced on semi-log paper (t on log scale) and a straight line is drawn through the plotted points.
2. The straight line is extended until it is intercepting the time axis at the point where drawdown, s = 0 and the initial time, t0 is read from the prepared graph.
3. From the prepared plot the slope of the straight line (i.e. the drawdown difference per log cycle) of time is determined. Letting s=ax + y such that when s=0, the slope is computed as 0=ax + y implies a=-y/x
4. Finally, the obtained values of the measured parameters are substituted in the equations (2.13) and (2.14) the required parameters (S and T) are computed respectively.

The following Theis-Cooper-Jacob Assumptions are considered when estimating the aquifer parameters by using Cooper and Jacob Drawdown versus Time Graph. Due to the fact that the real aquifers rarely conform to the assumptions made for Theis-Cooper-Jacob non-equilibrium analysis, the collected pumping test data is adjusted against external and internal influence conditions in order to take into consideration the underlying basic assumptions suggested hereunder (Cooper-Jacob, 1946).

1. Isotropic, homogeneous, uniform thickness
2. Fully penetrating well
3. Laminar flow
4. Flat potentiometric surface
5. Infinite areal extent
6. No recharge

"If some or all of these assumptions is the failed to meet the conditions, there will be indications to "non-ideal" behavior and deviations from the Theis and Cooper-Jacob analytical solutions for radial unsteady flow (Lecture Materials, AAiT, 2012. Dr. Mebruk M.)".

2.3.3. Recovery/Residual Drawdown versus Time Graph

The analysis of recovery test is also used to quantify aquifers hydraulic parameters. The data that was collected during the pumping period of single well tests and the recovery test data which was collected after the pumping had stopped are consumed to carrying on the analyzing of pumping tests. Kruseman and N.A. de Ridder stated that soon as the pump is shut down after completion of a pumping test, the water levels in the well and the piezometers will begin to rise. They defined this rise in water levels to be called as residual drawdown (s'). According to their articulation the residual drawdown (s') is the difference between the original water level before the start of pumping and the water level measured at time (t') after the cessation of pumping (G.P. Kruseman and N.A. de Ridder, 1994).

"Kevin M. Hiscock points out that the rate of recharge to the well during the recovery period on average is assumed to be equal to the mean pumping rate as an effect it is in contrasting to the drawdown phase when the pumping rate is likely to vary. The monitoring of the recovery phase is beneficial as the rate of recharge can be assumed to be constant and it satisfies one of the Theis solution basic assumptions. It is well known that the Theis method requires that pumping is continuous. Hence, in order this method to be applied to the recovery phase of a pumping test; a hypothetical situation must be conceptualized. If a well is pumped for a known period of time and then switched off, the next drawdown will be the same as if pumping had continued and a hypothetical recharge well with the same discharge was superimposed on the pumping well at the time the pump is switched off (Kevin M. Hiscock, 2002)". Thus, the hydraulic theory of well and aquifer performance assumes that water level changes during the recovery period are the result of input from an imaginary recharge well. It has been said that the time drawdown curve for the pumping period becomes a straight line on a semi-log paper. The same simplification can be used for the time-recovery plot, where the horizontal scale represents the log of time during the recovery period and the vertical scale represents the water level recovery (s-s'). The recharge and the discharge thus cancel each other out, resulting in an idle well, as is required for the recovery period. Therefore; from the principle of superimposition of drawdown, the residual drawdown s’ after a pumping test with a constant discharge is given by:

$$\mathbf{s' = \frac{Q}{4\pi T}\{W(u) - W(u')\}} \qquad (2.15)$$

Where: -

t = is time measured since the start of pumping and

t’ = is time since the start of the recovery phase

$$\mathbf{u' = \frac{r^2S'}{4Tt'}} \qquad (2.16)$$

$$\mathbf{u = \frac{r^2S}{4Tt}} \qquad (2.17)$$

When u and u’ are sufficiently small values and large values of t’, the well functions can be approximated by the above equation is written as:

$$\mathbf{s' = \frac{Q}{4\pi T}\left(\ln\frac{4Tt}{r^2S} - \ln\frac{4Tt'}{r^2S'}\right)} \qquad (2.18)$$

Where: -

s’ = residual drawdown

S = storativity during recovery

S’ = storativity during pumping

t = time in days since the start of pumping

t’= time in days since the cessation of pumping

r= distance from well to piezometer

When s and s’ are constant and equal and T constant the above equation can be rewritten as:

$$\mathbf{s' = \frac{2.3Q}{4\pi T}\log\frac{t}{t'}} \qquad (2.19)$$

Hence, a plot of residual drawdown, s’, versus the logarithm of t/t’ (t/t’ on logarithmic scale) should provide a straight line. The gradient of the line equals 2.3Q/4πT so that Δs’, the change in residual drawdown over one log cycle of t/t', enables a value of transmissivity to be found from:

$$\mathbf{T} = \frac{\mathbf{2.3Q}}{\mathbf{4\pi\Delta s'}} \qquad (\mathbf{2.20})$$

Where: -

Δs' = is the residual drawdown difference per log cycle of t/t'

It is not possible for a value of storage coefficient S, to be determined by this recovery test method although, unlike the Theis and Cooper–Jacob methods, a reliable estimate of transmissivity can be obtained from measurements in either the pumping well or observation well.

The procedures engaged while determining the aquifer parameter via the analyzing of the recovery testing phase are: -

1. For each observed value of s', the corresponding value of t/t' is calculated;
2. The plots for s' versus t/t' on semi-log paper for each pumping well is prepared;
3. Then fitting a straight line through the plotted points is carried out;
4. The slope of the straight line is determined;
5. Lastly, the known values of Q and Δs' are substituted in equation (2.20) the value of transmissivity T is calculated.

2.4. Establishing Radius of Influences

Water supply for varies consumptions in numerous communities is available from groundwater wells. The water level within the well drops, whilst water is extracting from a well. The well causing a lowering of the water level which extending outward from the well as water in the adjoining aquifer flows towards the well. Such declines in water level is greatest immediately adjacent to the well and decreases radially outward by creating a feature called the cone of depression. As pumping continues, the cone of depression stretches out farther gathering water from a larger cylindrical volume surrounding the well. The spreading out of the cone of depression will continue until the volume of water captured by the well equivalents the pumping rate. Similarly aquifer water, the water drawn by a well can also be recharge from the ground surface, adjacent aquifers, rivers, lakes or oceans. Water resistant boundaries formed by low hydraulic conductivity materials such as bedrock, faults, etc. will cease the progress of the cone of depression at their localities. Awareness of the drawdown in water level and pattern of groundwater flow resulting from pumping well is essential for evaluating environmental impacts in masses of situations. An extreme descent in the levels of groundwater over regional scales can effect in adverse impacts to river flows, vegetation and the use of shallow wells. By the side of sites of groundwater pollution, the cone of depression can expand outward from the pumping well and capture the contaminated water. Despite of the fact that the well capture zone of the potential treat or contaminated water is desired with a remediation action, the situation could be destructive with a well supplying drinking water. When the worst-case scenario occurred, contamination of drinking water wells may get aggravation in resulting of serious illnesses and the communities might loss of their drinking water source. (Harr, 1995). Therefore; establishing the extents radius of influence/recharge boundaries of the wells for drinking water supply and effect of their interference at specific locality in determined zone of captures is the main objective of the study in order to proceeds with the appropriate remedial way out to minimize the risk of drinking water contaminations. In line of managing such burning problem, the Principle of the Superposition and its practical application in area of the groundwater well hydraulics is well pragmatic under this study.

2.4.1. Principle of Superposition and Image Wells Analyses

Principle of superposition is a powerful defined technique for analyzing certain types of complex groundwater flow problems. The principle of superposition is a simple concept that has significant applications in well hydraulics of groundwater and modeling of groundwater systems in many areas of science and technology. Many text books on groundwater provide some explanations about this subject matter. Among the other authors, “Bear and Walter” are those who to be mentioned. “Walter J. Karplus, briefly explains the superposition theorem as: In linear systems the response due to a number of excitation may be found by adding algebraically the response due to each excitation taken separately, while the other excitations are reduced to zero (Walter J. Karplus, 1958)”. In terms of groundwater models, this statement means that calculated changes in head can then be added to other head distributions to construct solutions corresponding to combined boundary conditions. “Bear, also contributes the most comprehensive cites readily about the principle of superposition (Bear, 1979)”. He states that the solutions to individual parts of a problem can be added together so as to achieve the required composite solutions. This principle applies to linear systems or processes those generally governed by the linear differential equations. Such linearity behavior of the governing equations in the systems of groundwater flow principally allows for its implementation.

In this we can build up the solution to a more complicated problem by simply summing up solutions to simpler problems. Thus, the resulting composite solution might be an actual solution of the complex problems. For instance, from the settings of pumping wells, we have solutions for a single well in an infinite aquifer; these solutions would possibly extend to more realistic problems. The conditions where this idea is valuable in pumping problems are including: - An infinite aquifer with multiple wells; Non-infinite aquifers with a no-flux boundary condition; Non infinite aquifers with a fixed head boundary condition and combinations of the above cases. Hence, the principle of the superposition is applicable to the linear conditions to establish recharge boundaries by the image well analysis and impact of pumping on a well flow fields for the case of unconfined aquifers providing that the drawdown is much smaller relative to the full saturated thickness of the aquifer (as a rule of thumb, 10 percent or less than the aquifer thickness). (Gordon D. Bennett, 1976); as cited in the report of U.S. Geological Survey Open File Report 84-459; March, 1849).

2.4.2. Image Wells Analyses and Boundary Conditions

Pumping tests sometimes have to be performed near the boundary of an aquifer. A boundary may be either a recharging boundary (e.g. a river or a canal) or a barrier boundary (e.g. an impermeable valley wall). When an aquifer boundary is located within the area influenced by a pumping test, the general assumption that the aquifer is of infinite areal extent is no longer valid. By means of various boundaries and boundary configurations, there are different methods of analysis that can be developed for confined or unconfined aquifers. So, by introducing imaginary wells, or image wells, we can transform an aquifer of finite extent into one of seemingly infinite extent, which allows us to use the non-equilibrium Theis or the (Cooper and Jacob 1946) techniques to conduct the analysis.

2.4.2.1. Method of Image Wells Analyses by Recharge/ Fixed Head Boundaries

In several circumstances, a field site may have more than one pumping well. In such occasions a multiple cones of depression can likely intersect and result in greater drawdown than foreseeable from a single pumping well. For example, the equation governing groundwater flow (Laplace equation) is linear, the drawdown at any point is found by summing the drawdowns produced by all the wells. Theoretically all the solutions are assumed to have infinite horizontal extent aquifers. In reality, most aquifers will be bounded by recharge sources or boundaries such as ocean, lakes and perennial rivers or impermeable boundaries including alluvial sandy clay and bedrock contact.

The mutual non-infinite aquifer condition we often must deal with is that of a perennial river boundary. For easiness, the perennial river is often modeled as a fixed-head boundary condition. So that the principle of superposition by practice of the Theis equation in unconfined aquifer, may be used in the calculation of the drawdown at a certain point in space and time due to the effect of a well field, while a set of pumping wells are operating simultaneously; recharge/fixed-head boundaries and no-flow boundaries that cause to become the aquifer semi-infinite. The advantage of utilizing the technique of superposition is that equations will result in cones of depression which extend an unrealistic distance beyond these boundaries.

The imaginary wells called image wells as per Figure 3 and 4 demonstrates underneath, can again be applied in order to simulate the effects of the realistic problem of the fixed head boundary. In the occurrence of the recharge boundary, when the cone of depression reaches a recharge source, the rate of drawdown declines as the well immediately receives water from the source. The cone of depression will not extend preceding the recharge boundary and will have less drawdown than simulated by the Theis equation. Under these conditions we are interested in resolving for the drawdown profile.

The effect of a recharge boundary is simulated by applying an image well analysis method that injects water into the aquifer by engaging the following paces: -

1. The image well is placed across the boundary at the same distance that the pumping well is far apart from the boundary (mirror image);
2. At a given point of known radial distance from the pumping well, drawdown for the pumping well is calculated by using the Theis equation;
3. Similarly, at that same point of known radial distance from the image well, the potentiometric buildup (or negative drawdown) from the image well injecting water is calculated by means of the Theis equation (in this case Q will be negative);
4. Then the drawdown and the head buildup are summed to give the drawdown expected in the presence of a recharge boundary.

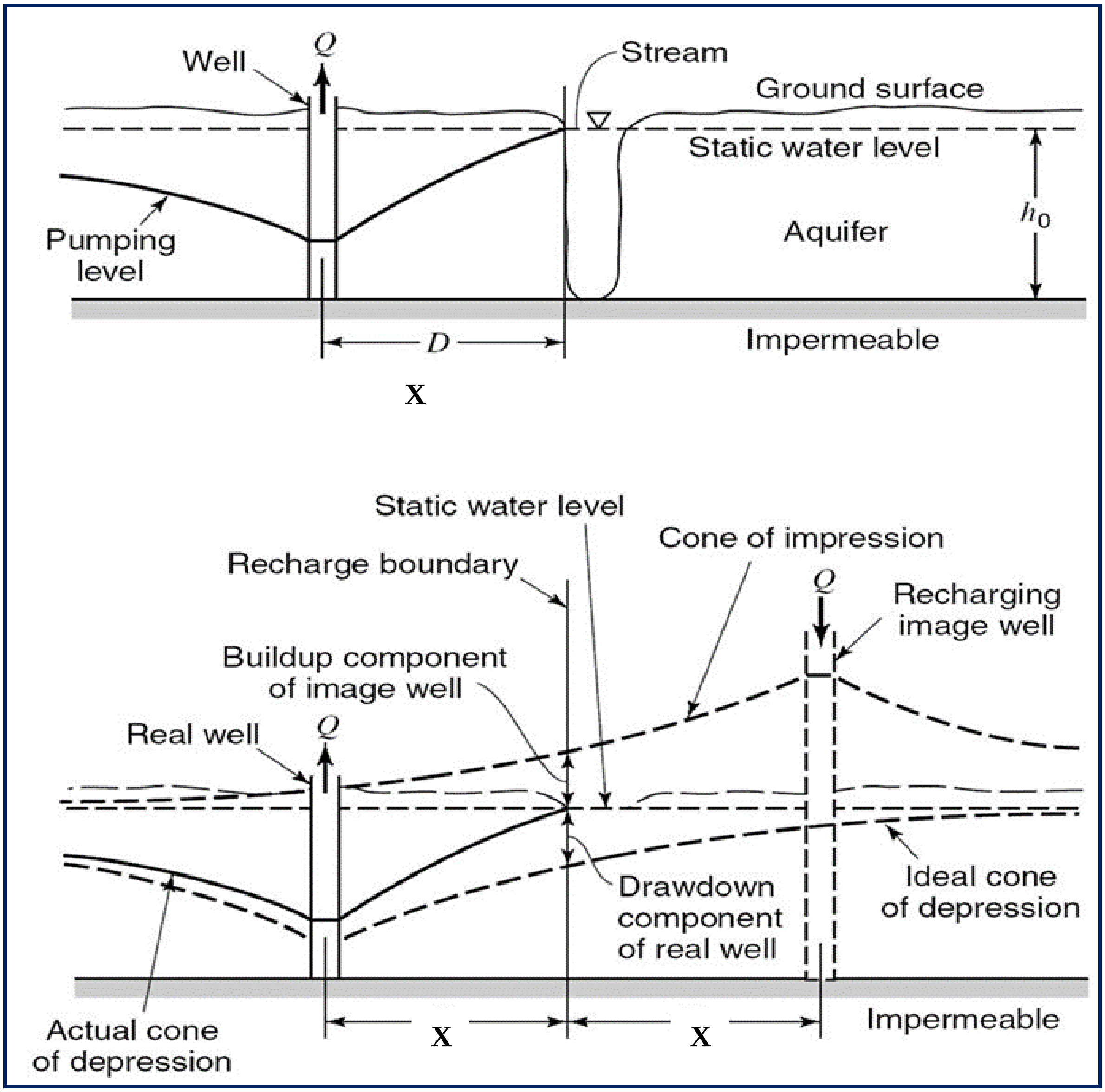

Figure 3. Method of image analysis by fixed head boundary (source: Bear, 1979)

Explicitly, if an image well recharging (negative pumping rate) at the same rate as the real well is placed at a symmetric distance on the other side of the boundary and add up the drawdowns (which can organize due to superposition) the solution will ensure that:

1. The head is equal to the fixed value at the boundary, and
2. All flow that would have been unavailable to the real well if it were in an infinite aquifer (due to drawdown) will instead be supplied by the image well, thereby decreasing the drawdown everywhere in the real domain.

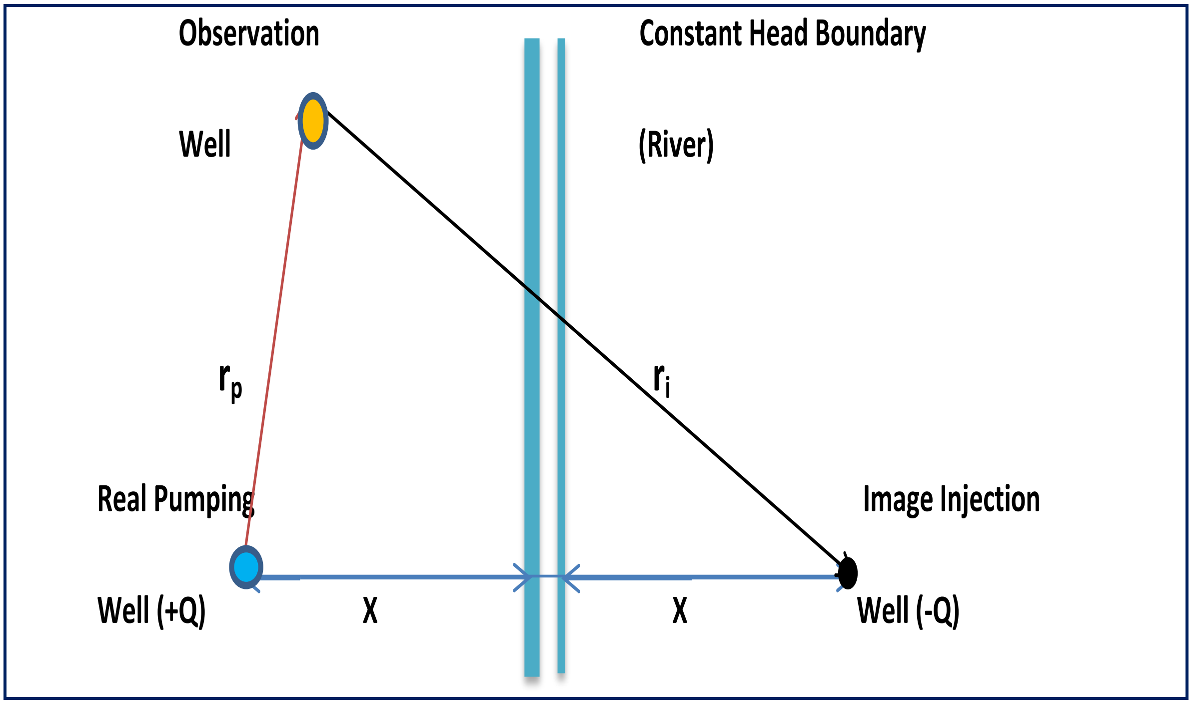

Figure 4. Diagram illustrates arrangements of real pumping and image injection wells

Hence the drawdown anywhere in the domain for the real problem can be computed by the Theis Equation, Equation (2.3) that represents the drawdown distribution in time and space due to a single well operating at a constant rate Q in a homogenous, isotropic, horizontal, constant thickness confined aquifer.

If the well is pumping at rate Q for any time (t), and the real/pumping well/ is pumping at rate $Q = Q_p$, then it will cause drawdown $s = s_p$,

Then placing a mirror image injection well, injecting at the same rate but on the other side of the constant head boundary $Q_p = -Q_i$ at a distance X, causing drawdown $s_p = -s_i$,

Then, $s = s_p + s_i$

Hence the solution for adding image wells to a real pumping well can be written: -

$$s = s_p + s_i = \frac{Q_p}{4\pi T} W(u_p) + \left(\frac{-Q_i}{4\pi T}\right) W(u_i) \qquad (2.20)$$

$$u_p = \frac{r_p^2 S}{4Tt} \quad \text{and} \quad u_i = \frac{r_i^2 S}{4Tt} \qquad (2.21)$$

Where: -

s = the actual resulting drawdown from summing up the drawdowns of real and image wells;

s_p = the drawdown from real pumping well;

s_i = the drawdown from image pumping well;

Q = the constant well discharge in m^3/s;

Q_p = the constant pumping rate of real well in m^3/s;

Q_i = the constant pumping rate of imagel well in m^3/s;

T = the transmissivity of the aquifer in m^2/s;

W(u) = is a particular exponential integral, with u as the argument, which in this usage is read as the well function of u;

S = the storage coefficient;

t = the time since pumping started;

r_p , r_i = are the distances from the pumping and image wells respectively in radial coordinates;

(x_{pw}, y_{pw}) = is a point of the pumping well in the plane of Cartesian coordinates and

(x_{iw}, y_{iw}) = is a point of the image well in the plane of Cartesian coordinates.

(x, y) = is representing any arbitrary points in vicinity of the wells field such that (x_1, y_1; x_2, y_2..........x_n, y_n)

In the equations above r_p and r_i are putting in radial coordinates. However; the values for r_p and r_i were calculated in excel spread sheet by writing in the form of Cartesian coordinates systems of any arbitrary points of (x, y) plane and their respective resulting values then inserted into the required equations. Thus, r_p and r_i were arranged and computed as:

$$\mathbf{r_p = \sqrt{(x_{pw} - x)^2 + (y_{pw} - y)^2}}$$

$$\mathbf{r_{pi} = \sqrt{(x_{pi} - x)^2 + (y_{pi} - y)^2}}$$

Along the boundary, where $r_p = r_i$, the drawdown from real pumping well is balanced by the image injection well, such that s = 0, preserving the constant head boundary condition. Hence,

$$s = \frac{2.3Q_p}{4\pi T}\log_{10}\frac{2.25Tt}{r_p^2S} + \frac{2.3(-Q_i)}{4\pi T}\log_{10}\frac{2.25Tt}{r_i^2S} \qquad (2.23)$$

$$s = \frac{Q_p}{4\pi T}\ln\frac{2.25Tt}{r_p^2S} - \frac{(Q_i)}{4\pi T}\ln\frac{2.25Tt}{r_i^2S} \qquad (2.24)$$

Letting $Q_p = -Q_i = Q$ and simplifying equation (2.24) gives

$$s = \frac{Q}{4\pi T}\ln\left(\frac{r_i^2}{r_p^2}\right) \qquad (2.25)$$

Note: For a constant head/recharge boundary, for all points on the boundary $r_p = r_i$ the drawdown is zero.

2.4.2.2. Method of Image Wells Analyses by Barrier / No-Flux Boundaries

The image well analysis in the event of the barrier/impermeable boundaries, enhanced drawdown will effect as the spread of the cone of depression is concluded and all water pumped is removed from storage in the aquifer. In the direction to simulate the impermeable boundary using a pumping and image well analysis, the procedures will be as follows: -

1. The image well is placed across the boundary at the same distance as the pumping well is away from the boundary (mirror image);
2. At a given arbitrary point of known radial distance from the pumping well, drawdown for the pumping well is calculated by using the Theis equation;
3. In similar manner using the same arbitrary point at equal radial distance from the image well, the drawdown for the image pumping well is calculated by means of the Theis equation (at this time Q will be positive);
4. Then two drawdown values are summed to give the drawdown that projected in the presence of an impermeable boundary.

The actual solution to such more complicated problem can be obtained by applying again the principle of superposition for its simplicity. So as to model the realistic problem, the concept of an image well analysis should be carried out to simulate the effects of the impermeable boundary. Obviously, the image well which assumed pumping at the same rate as the real well can be placed at a symmetric distance on the opposite side of the boundary (i.e. as a mirror image) as Figure 6 shows. In favor of the principle of superposition, we can sum up the drawdowns which will ensure that: -

1. The gradient in head is zero at the boundary, and
2. All flow that would have been captured by the real well if it were in an infinite aquifer will instead be captured by the image well, thereby increasing the drawdown everywhere in the real domain.

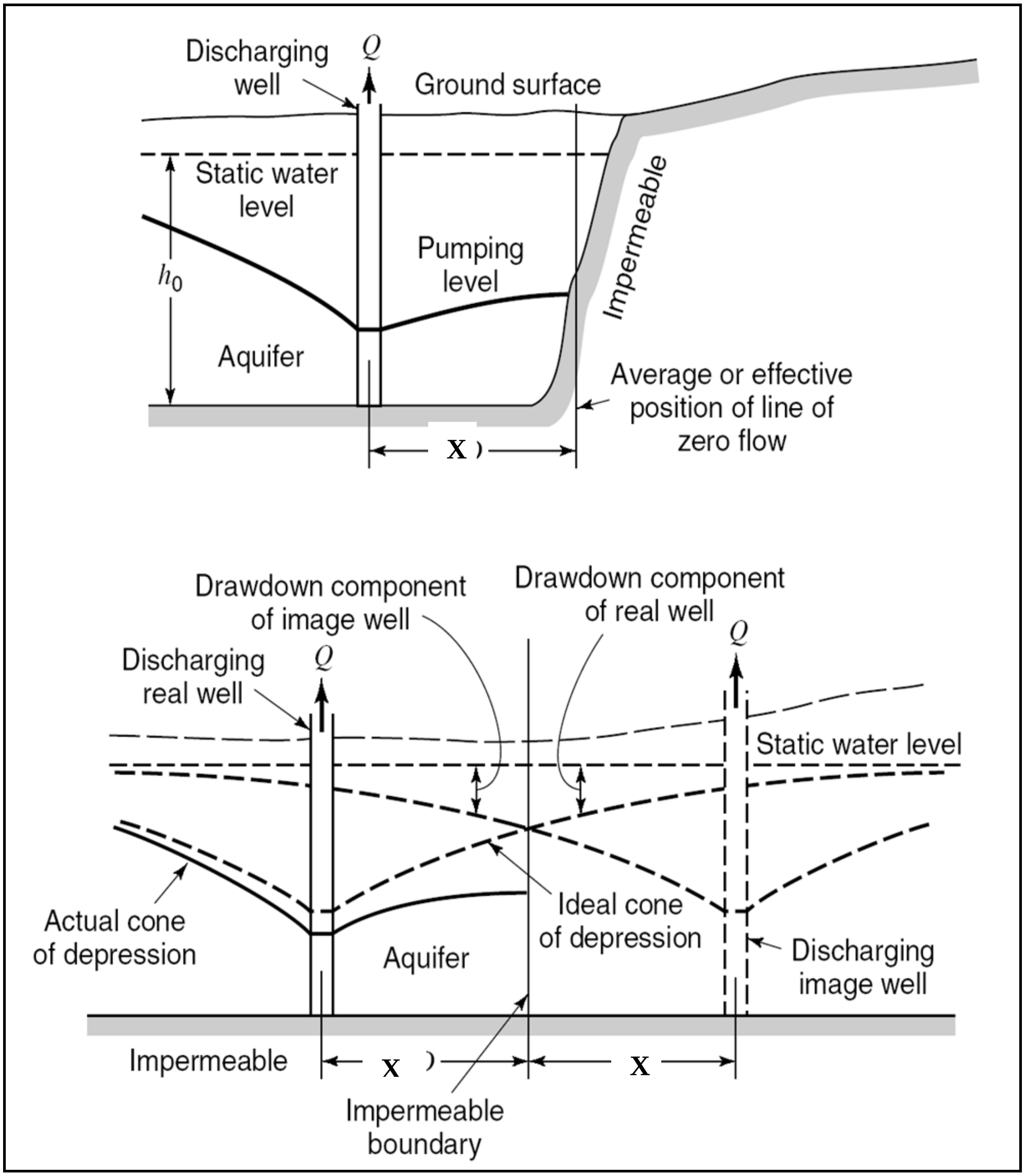

Figure 5. Method of image analysis by fixed head boundary (source: Bear, 1979)

In realistic problems we are often dealing with a non-infinite aquifer (i.e. there is some sort of boundary within the radius of influence of the pumping well). In the case above there is an impermeable boundary meaning that there is no flux at that boundary. The differences between the actual head (drawdown) and that predicted by a single pumping well (in an infinite aquifer) solution are:

1. The gradient in head must be zero at the boundary, and
2. The presence of the boundary will reduce the flow to the well from that portion of the domain, thereby reducing the head (increasing the drawdown) everywhere as the flow must be replaced from other portions of the domain.

So as to determine the actual solution to such more complicated problem we can use the principle of superposition to our advantage. To model the realistic problem, we can use the concept of an "image well" to model the effects of the impermeable boundary. Obviously, if we place an image well pumping at the same rate as the real well at a symmetric distance on the other side of the boundary (i.e. as a mirror image) and add up the drawdowns (which we can do due to the principle of superposition) we will ensure that:

1. The gradient in head is zero at the boundary, and
2. All flow that would have been captured by the real well if it were in an infinite aquifer will instead be captured by the image well, thereby increasing the drawdown everywhere in the real domain.

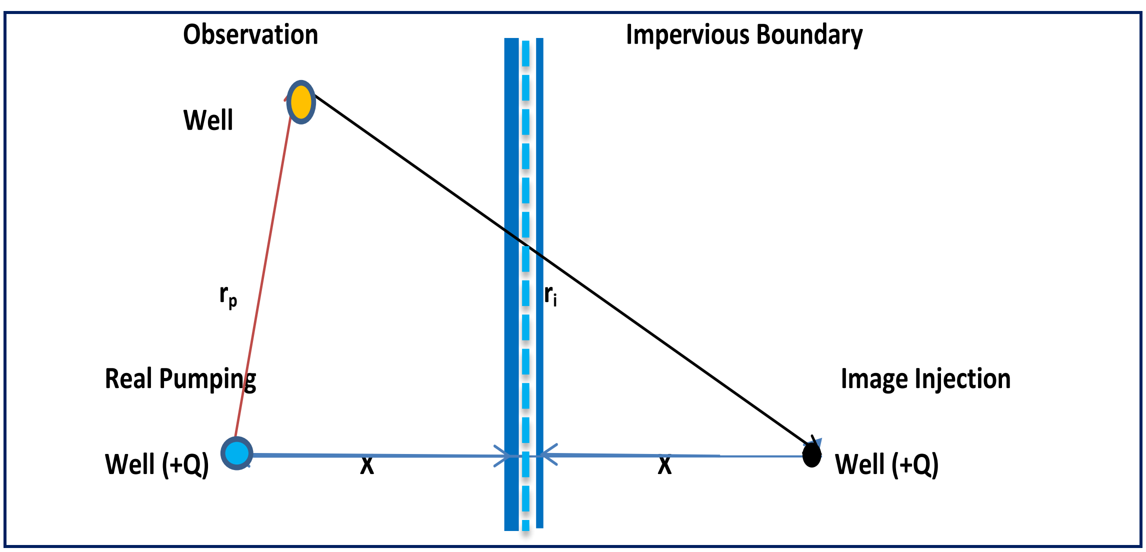

Figure 6. Diagram illustrates arrangements of real pumping and image injection wells

Hence the drawdown anywhere in the domain for the real problem can be computed by the Theis Equation, Equation (2.3) that represents the drawdown distribution in time and space due to a single well operating at a constant rate Q in a homogenous, isotropic, horizontal, constant thickness confined aquifer.

If the well is pumping at rate Q for any time (t), and the real/pumping well/ is pumping at rate $Q = Q_p$, then it will cause drawdown $s = s_p$,

Then placing a mirror image injection well, injecting at the same rate but on the other side of the impervious boundary $Q_p = + Q_i$ at a distance X, causing drawdown $s_p = s_i$, Then, $s = s_p + s_i$

Hence the solution for adding image wells to a real pumping well for the impervious boundary can be written: -

$$s = s_p + s_i = \frac{Q_p}{4\pi T} W(u_p) + \left(\frac{+Q_i}{4\pi T}\right) W(u_i) \quad (2.26)$$

$$u_p = \frac{r_p^2 S}{4Tt} \quad \text{and} \quad u_i = \frac{r_i^2 S}{4Tt} \quad (2.27)$$

Where: -

s = the actual resulting drawdown from summing up the drawdowns of real and image wells;

s_p = the drawdown from real pumping well;

s_i = the drawdown from image pumping well;

Q = the constant well discharge in m^3/s;

Q_p = the constant pumping rate of real well in m^3/s;

Q_i = the constant pumping rate of imagel well in m^3/s;

T = the transmissivity of the aquifer in m^2/s;

W(u) = is a particular exponential integral, with u as the argument, which in this usage is read as the well function of u.

S = the storage coefficient;

t = the time since pumping started.

r_p , r_i = are the distances from the pumping and image wells respectively.

Along the boundary, where $r_p = r_i$ the gradient from real well is balanced by the gradient from image well, such that ∂s⁄∂x=0, preserving the no flux Boundary Condition. So that

$$s = \frac{2.3Q_p}{4\pi T}\log_{10}\frac{2.25Tt}{r_p^2 S} + \frac{2.3Q_i}{4\pi T}\log_{10}\frac{2.25Tt}{r_i^2 S} \qquad (2.28)$$

$$s = \frac{Q_p}{4\pi T}\ln\frac{2.25Tt}{r_p^2 S} + \frac{Q_i}{4\pi T}\ln\frac{2.25Tt}{r_i^2 S} \qquad (2.29)$$

Since $Q_p = -Q_i = Q$ and by simplifying equation (2.24) it gives

$$s = \frac{Q}{4\pi T}\ln\left(r_p^2\, r_i^2\right) \qquad (2.30)$$

Note: For a no flux/barrier boundary, for all points on the boundary $r_p = r_i$ the drawdown is doubled.

2.4.2.3. Establishing Radius of Influences

The principle of radius of influence of a well has of limited rehearsal nowadays. Nevertheless, from a practical point of view it is quiet of interest such as the established radius of influence assistances to have a readily available idea about the size of the capture zone of ground water models which is perturbed by a pumping well. The radius of influence is established according to the Cooper-Jacob equation. This is preferable equation to for the Theis equation denotes to the radius of influence that extends to the infinite in a well pumped at a constant radius. This condition has slight significance in the practical world where a very small drawdown can be neglected. Hence then it is usually accepted that a realistic estimation of the radius of influence can be obtained from the Cooper – Jacob equation (Cooper and Jacob, 1946). This study take into consideration wells those pumping in an unconfined aquifer without recharge, in unsteady state.

$$s = \frac{Q}{4\pi T}\ln\frac{2.25Tt}{r^2 S} \qquad (2.31)$$

According to equation (2.31) at any time t, the radius of influence R_{cj} is given by

$$R_{cj} = \sqrt{\frac{2.25Tt}{r^2}} \qquad (2.32)$$

At an occasions when the pumping tests carried out close to a boundary, equation (2.32) is used to evaluate the distance between the imaginary well and the required point where the drawdown is measured (de Marsily, 1986).

The following state must be true when and where s =0 in equation (2.31)

$$\frac{2.25Tt}{r^2S} = 1 \qquad (2.33)$$

Where: R_{cj} = is radius of influence computed by the Cooper – Jacob equation and the other variable as described earlier.

2.5. Demarcation of Capture Zone for Mojo Pumping Boreholes

A capture zone is including up gradient and down gradient potentiometric and encompasses the volume of water that operating wells extract from the porous media of the aquifer. So that it is very important to establish the area of the capture zone to decide the remediation action to be implemented during design and operation of pumping wells for the designed purposes particularly water supply systems. To carry out the delineation of the capture zone the following assumption are considered. The aquifer is homogeneous, isotropic and has infinite horizontal areal extent; uniform condition flow be comes up; an unconfined aquifer is assumed to have horizontal impervious at the base with no infiltration no vertical recharge and no leakage; the specific yield of unconfined aquifer is neglected, the Duppuit assumption of the vertical gradients are neglected; the constant pumping rate is assumed and the well is fully penetrated and open throughout the thickness of the unconfined aquifer (Stack; 1989) and Marsily ; 1986). The equation used for the computation of the capture zone edge when the conditions of the steady state have reached in unconfined aquifer is as of that discussed by (Todd; 1980 and Grubb; 1993).

In the case of the single well with uniform at infinite time (steady state) a quick and simple analysis is an important for determining capture zone of many hydrogeological projects. This is due to potentials and boundary conditions considered are linear and homogeneous; and the linearity of such difficult potentials can be solved according to the principle of the superposition. Through the technique of the superposition the complex potential are superimposing (summing up) for the supposed uniform flow and this gives the composed solution to the given problems. This becomes more simply when using the appropriate aquifer parameters by applying the concept of the discharge potential theory.

Fienen et al. (2005) presented an algorithm for quick delineation of capture zones using complex discharge potentials for steady-state and two dimensional flows in a homogeneous domain with anisotropic transmissivities. Yeo and Lee (2003) suggested an alternative analytical steady-state solution to deal with arbitrarily located multi-injection pumping wells. An analytical solution to calculate flow around two arbitrarily located wells derived by Shan in a confined aquifer based on potential theorem and the principle of superposition (Shan; 1999). As numerous studies show the hydraulic boundaries have important effects on the configurations of the capture zone. There are two different kinds of hydraulic boundaries such as constant heads along the streams or impermeable boundaries where abstraction of flows may exist near pumping wells. In his studies Stack had used image well theory assuming linearity in the governing equations of flow in porous media (Strack; 1989).

In order to model the boundary, one may apply the theory of real and imaginary wells through the principle of superposition. In this methodology, an imaginary injecting well is placed across the boundary to offset the drawdown at the boundary due to the pumping well. In concept of the image well, an imaginary pumping or injecting well is added to satisfy the constant or no-flow boundary conditions, respectively. The Hydraulic connection between a stream and an aquifer is serious point in capture zone delineation for a pumping well. The stream is considered a fully penetrating boundary and is hydraulically connected with the aquifer through the entire aquifer thickness as some studies discussed (Intaraprasong and Zhan 2007; Newsom and Wilson 1998). These studies have considered the stream a constant head boundary and functional image well theory to obtain secured solutions for the flow configuration. The presented solutions for the capture zone near a stream, it is usually assumed that the regional flow is perpendicular to the stream axis (Intaraprasong and Zhan 2007; Strack 1989). The capture zone delineation in such configurations is crucial for both water-resources management and environmental engineering applications where the stream water should be for the water supply consumptions. Supposing there is pollution in the stream, one practical concern is to delineate the location and pumping rate of the well so that the pollution does not enter the aquifer or the well. These precautions may be effectively addressed through the delineation of the capture zone.

In his study Grubb provided the solution of the capture zone in unconfined aquifer (Grubb; 1996). The requirement for this condition is to have the head in two pumping wells along the axis the groundwater flow direction. Then as per the equation of Grubb the shape of the capture zone is given by

$$\mathbf{x} = \frac{-\mathbf{y}}{\tan\left[\pi \mathbf{K}\left(\mathbf{h}_1^2 - \mathbf{h}_2^2\right)\mathbf{y}/\mathbf{QL}\right.} \qquad (6.1)$$

The maximum width of the capture zone is computed by the Grubb equation as

$$\mathbf{y}_{\mathbf{max}} = \pm \frac{\mathbf{QL}}{\mathbf{K}\left(\mathbf{h}_1^2 - \mathbf{h}_2^2\right)} \qquad (6.2)$$

The position of the stagnation point where the down-grading edge of the capture zone ends, at point y=0 is also given by

$$\mathbf{x}_0 = \frac{-\mathbf{QL}}{\mathbf{K}\pi\left(\mathbf{h}_1^2 - \mathbf{h}_2^2\right)} \qquad (6.3)$$

Where:-

h_1 and h_2 = are the up-gradient and down- gradient head in the monitoring wells;

x and y = are the direction of the points defined;

L = is the distance between the monitoring wells

Q = is the pumping rate (m^3/s or m^3/day); and

K = is the hydraulic conductivity (m/s or m/day)

2.6. Determination of Wells interference for Mojo Pumping Boreholes

Theoretically, wells should be positioned adequately far from each other, at a distance more than two times the radius of influence which would only work in case there is no interference among the wells. This is because the radius of influence will usually large enough in the case of the confined aquifer. However; this would probably exception in a phreatic aquifer that positioned closer to a river.

When operation of pumping begins in the pumped well, a region of reduced water pressure is formed around the pumped well. In general the movement of water is towards the potentiometric low heads and largely gradient inclines to the center of pumped well. This arrangement is known as the cone of depression. The cone of depression continues to develop as long as the well is pumping exclusive of somewhere the recharge region may encompass into the process.

The rate of drawdown is initially rapid, as the well extracts water from storage in a small region. Progress of operation through extra time, the heads lowers in an ever larger zone about the well, so the rate of drawdown tapers off over time. The amount of drawdown grows indefinitely if the aquifer is homogeneous and isotropic, the base of the cone of depression is circular and the growth of the radius of that circle has a definite relationship with the elapsed pumping time.

As the radius inedible, as a result of pumping, water level is lowered and a cone of water-table depression in an unconfined aquifer may take place. Solutions to find the total drawdown can be found using the equilibrium (Thiem) or non-equilibrium (Theis) equations through the principle of superposition of well drawdown analysis and are of practical use in designing layout systems of a multiple well field to minimize interference between well drawdowns or in designing an array of wells for the purpose of dewatering a ground excavation site.

In well fields where more than one pump or several pumping wells may exist in a given well field such that those wells are extracting the ground water from aquifer the same field, interference of the pumping wells is a crucial unease to take into account in designing and treating the locations of the pumping wells. This is to resolve the spacing there to be provide between the pumping wells so as to minimize the occurrence of transecting cones of depression as effect of operating wells which subsequently generates interferences in layout system of the well field.

The total drawdown of the individual pumping wells is the linear addition of every well operating in multiple well systems as the superposition permits addition to determinate the effect of drawdowns. It is well known that, in phreatic aquifer in which the value of the transsimissivity varies with the saturated thickness and where the drawdown is relatively insignificant with extensive saturated thickness of aquifer, the linear superposition technique predicts a composite solution of drawdowns and this composed drawdown miscalculates the real drawdowns may result.

As a consequence of saturated thickness reduces the transmissivity also decreases, the multiple well systems operating in the aquifer develops a greater value of composite hydraulic gradient than that of equivalent confined aquifer as response of reimbursing the diminished value of the aquifer transinmissivity. So that determining existence of wells interference is necessary to design the layout system of multiple pumping wells to minimize chance of well interference in the well field.

3. Methodology

The Mojo Wells Field was constructed at nearby to Mojo Town for drinking water supply purpose. The study site is located in Oromia Regional State, Eastern Shoa Zone, Ada'a and Lume Wereda between 70km from capital city. The geographical location of the study area of the wells field are between $8^0$37'N:$39^0$03'E and $8^0$41'N:$39^0$07'E. At about 4km apart in the North outskirt of the Mojo Town and all the three wells have no observation wells so far the water level measurement has been done in the pumping well. Thus the observed pumping test data is a data obtained from single well pumping testing data. The Elevation of the study area ranges from 1838 amsl to 1757amsl.

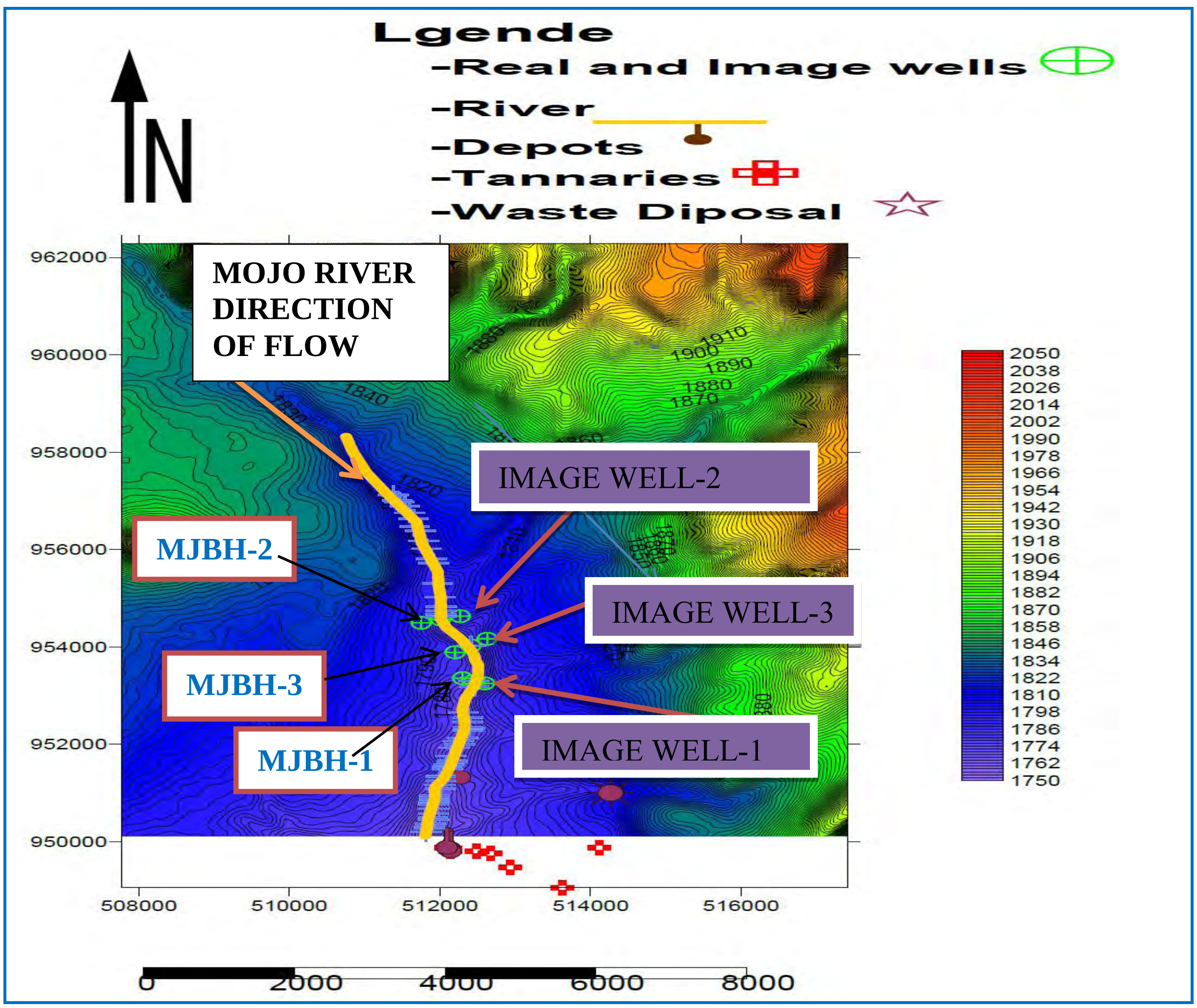

Figure 7. Map of the study area and locations of wells studied for this investigation

3.1. Data Collection and Analysis

In this portion of the work effort applied to incorporate both primary and secondary essential data collection at field investigation and office work stage so as to achieve the objective of the study. The primary data gathering includes the works accomplished at the field investigation level. This task was carried out by collecting sites using GPS instrument to discover existing physical barriers and possible threaten potential sources surrounding Mojo Water Supply Wells field and Mojo Town itself as towns may be harbor for contamination of groundwater resources. The secondary data colleting refers the activities accomplished at the office work stage. This comprises the gathering of validated and organized data (secondary data) of Borehole information such as:- constant rate test, step drawdown test, recover test, final drawdown, pumping duration, static water level, dynamic water level, well depth, design discharge, water quality such as: detailed hydro chemical, and pH, borehole diameter, casing arrangement properties and Digital elevation model (DEM) that are essential input data for computations of parameters in order to identify the physical characteristics of the aquifers.

This duty covers the methods employed to achieve the subject matter as the citation of literature review on modeling books is substantially completed at the office work level. The data collected from field investigation and office work are adjusted and made ready for computer code that aids for producing modeling such as Aquifer Test, Global Mapper 12 and Surfer 11, and so on. The source from which the single wells pumping test data gathered is DH-consultant who has undertaken the contract of Mojo Water Supply wells field construction. The source of digital map (DEM) is Water works Study Design and Supervision Enterprise (WWSDE). In line of recognizing the physical characteristics of the aquifers, the necessary parameters such as the aquifer's design discharge, transmissivity and storage coefficient are computed. Such duty of approximating the aquifers parameters for each well is concluded via curve–fitting by basic EXCEL tool and Aquifer Test Model methods in manual and automatic fitting means respectively based on the data collected from the specified firms. With the intention of carrying analysis on the pumping test data, three common methods are included: - Theis's Curve-Fitting Method, Cooper and Jacob Drawdown versus Time Graph

Cooper and Jacob Drawdown versus Time Graph and Residual Drawdown versus Time Graph are sequentially applied as described in depth at the chapter of literature review. Finally, the best fitting values that obtained from manual curve fitting method by means of basic excel tool (2007) is utilized in the analysis of the aquifer parameters estimations.

3.2. Estimation of Aquifers Parameters Using Pumping Test Data

The general method of analyzing aquifers test data for this study is to match the measured drawdown with standard simulated type - curve using Analytic Solution Model. In order to conduct curve fitting for gathered pumping test data, the type of aquifer has to be determined first and the pumping test data has to be adjusted against possibility of external influences may take place. Thus, a log-log graph of the measured drawdown as a function of time since pumping started was plotted for each well. Then curve fitting for each three well with different standard type curves is manually organized. Based on judgments of the visual observations undertaken from the curve fitting and duration of pumping period that lasting during pumping test recorded, the category of the aquifer is recognized. Afterwards to the aquifer categorization, modification for the measured drawdowns against to the influential conditions those might have been encountered during the operation of pumping test is completed earlier than that the measured data being consumed for investigation to evaluation the parameters of the aquifer. Hence, the measured drawdown data, observed in individual single well pumping test data, are corrected for necessary adjustments. This corrected drawdown (observed) data as a function of time since pumping started is plotted on log-log scale for each well on Spread sheet (Excel 2007). Correspondingly the Theis Type – Curve of well function W(u) versus 1/u within the same scale is plotted on Excel Spread Sheet using values of W(u) on Y-axis and 1/u on X-axis from table of ground water books (Kruseman and De-Ridder- 1994).

Fitting between the Theis type - Curve and the corrected drawdown versus time plot carried by overlapping adjusting both plots to have the same scale on excel window. Then the corrected drawdown versus time plot is fitted with the type - curve by moving, keeping the horizontal axis parallel and overlapping until the best matching point reached. Then the estimation of the aquifer parameters for particular well i.e. MJBH-1, MJBH-2 and MJBH-3 are concluded manually. The same have been adopted by making use of Cooper - Jacob approach, but in semi-log (Log time versus drawdown) for equitable aquifer parameter estimation.

Since the data collected in these boreholes include the recovery data, residual drawdown versus time from the time when pumping has stopped is also used in estimation of the aquifer parameters.

These three methods abovementioned are working for an ideal unbounded aquifer. Hence; assessment should be made around the boreholes site for availability of natural and manmade groundwater flow boundaries. As per the assessment there lays Mojo Perennial River that bounds the boreholes at site of the well field in the East direction. The existence of this river may develop boundary effect in deciding the radius of influence for group of pumping boreholes especially in case aquifer is unconfined. As the results of various study distinguished that when one or more boundary conditions exists, the above listed three approaches may result in different aquifer parameters with a varying magnitude. Since our study is to indicate the radius of influence of the well field site and to identify the possible environmental concerns around the well site, three ranges of values of aquifer properties determined for well field site are used. These are the maximum, average and minimum transmissivity and storativity values respectively which obtained through valuation characteristics of the aquifer.

Supposing that the manual curve fitting method for this analysis may be exposed to personal judgment and miscalculation, simple well hydraulics model functions of Theis solution and Copper - Jacob approximation methods by using Aquifer Test software is also implemented as supplementary for approximation of aquifer parameters. The objective of conducting analyzing the pumping tests by Aquifer Testing Model technique and presented here in the scope of this research ***is simply to generate a mere comparison*** between the manual curve fitting method which produced by excel spread sheet and automatic curve fitting technique that completed by Aquifer Test Model.

The Aquifer Test is used to analyze data gathered from pumping tests. Solution methods available in Aquifer Test cover the full range of physical settings of unconfined and confined aquifers.

In Aquifer Tests software, the following analysis methods are used for pumping tests:-

- **Theis (1935)**
- **Cooper-Jacob Time-Drawdown (1946)**
- **Theis Recovery (1935)**

In Aquifer Test, Theis (1935) used in the software provides a flexible, user-friendly environment that allows to be more efficient in aquifer testing projects. The corrected pumping test data was directly entered in Aquifer Test via the keyboard, imported from a Microsoft Excel (version 5/95) workbook file. The well data such as well screen length, static water levels, well dimension including radius of well and radius of casing, well coordinate, saturated thickness, design discharge and well elevations were produced in spread sheet and saved as tab limited text format. These wells data imported to Aquifer Test. Time since pumping started and the measured water levels for both observed and corrected pumping test data is prepared in data logger format and imported to Aquifer Test. Test data for recovery test data was inserted from a spreadsheet by "cutting and pasting" through the clipboard. The correction done for unconfined aquifer permits the Theis, Cooper-Jacob and Theis Recovery solutions for the analysis of pumping test data recorded for an unconfined aquifer. Then the drawdown versus time, Theis (1935), Cooper – Jacob and Theis Recovery (1935) plotted successively. The Automatic Curve Fitting option then used to fit the data with a type curve. Since the auto fit is not always provide with right fitting value, manual fitting the test data with a type curve was also carried out using options provided in Aquifer Test.

We completed this analysis as an auxiliary only anticipating comparing and contrasting the approximated results of aquifers parameters obtained from estimations carried out in both ways, there to redo the analysis in case that the result will deviate from the normal ranges.

However, deciding that the estimated values from two methods are nearly equivalent, ***measured parameters values obtained from the manual curve fitting method by basic excel tool is considered/consumed*** for calculating unknowns parameters to determine the properties of aquifer at the well filed site. This technique preferred to software since it permits easy data entry and to effectively handling plotting features by toggling on at no fill option of the plotting area to have transparent on excel sheet window in overlapping operation the test data to match with the Theis type curve. Furthermore, all operations in this method could be done within EXCEL itself and then no require of macro programming and additional numerical calculation. It is also cheap and one could easily adopt in analyzing the pumping test data for determination of the aquifer parameters.

As it can be observed from the computed values of transmissivity, that the basic assumption considered the aquifer is an isotropic is not more valid for achieved values of transmissivities are different for the three wells and in the meantime transmissivity in unconfined aquifers is not constant. This situation agrees with what Papadopolus stated "The Theis Model is similar to an anisotropic model except that the transmissivity for the latter model characterized with directional transmissivity and prevails an ellipse form (Papadopolus, 1965)". This means that the maximum transmissivity (Tmax) in the direction of high permeability or porous media and the minimum transmissivity (Tmin) in low permeability direction of the aquifer media.

Therefore, the geometric mean value of the coefficient storage and transmissivity is considered in conducting the analysis of model simulation to resolve composed drawdown by superposition technique. The maximum value may aid the water management body in making conservative decisions whereas the minimum one may shows to take optimistic precautions with respect to coverage of the radius of influence being established adopting speculated value ranges of the aquifer parameters.

3.3. Principle of Superposition

Implementing the principle of the superposition technique, the final solution achieved by using linear combination of solutions resulting drawdowns those predicted from superimposing individual operating wells in he given well field. In virtue of its predictions, the superposition can provide composite solutions to the three boreholes at Mojo well filed site. Since the results of the estimated aquifers' parameters computed manually by the curve fitting technique in excel spread sheet already produced , proceeding the detailed steps cited in the section of the literature review and methodology parts, the geometric mean values of transmissivities and storage coefficients are arranged to simulate drawdowns solution through the principle of superposition. The geometric mean values generated from maximum, minimum and average values of transmissivities and storativities being computed for individual Mojo Water Supply Boreholes namely MJBH-1, MJBH-2 and MJBH-3.

To do so map for the study area is taken from the available digital elevation model (DEM) using Global Mapper software edited version 12. The DEM aids to delineate the area that might be under the influences of pumping and to analyze the recharge boundary patterns of the surface environment. The digital representation of a topographic surface of the well field site generated and transmitted to an appropriate UTM map to enable digitalizing the girds in forms of Cartesian coordinates. In order to facilitate this action a 90 m by 90 m resolution DEM was obtained from the Water Works Design and Supervision Enterprise (WWDSE). Global mapper 12 software and Surfer 11 software adopted to export DEM into UTM working area map.

Then the UTM configured to the form of raster or regular grid of interested area representative spot heights and available contours generated through consuming the configured coordinates and GPS locations data composed during data collection. The shortest distance between the real and image wells from the existing straight constant head boundary and the position of the imaginary wells fixed for each boreholes. Then there by using digitalized coordinates setting up around well field from surfer map which assumed as input of arbitrary synthetic observation spots in predicting of expected drawdowns along with the analysis of real and image wells using the theory of superposition.

The alignment of Mojo River also correspondingly delineated from DEM. In conducting the initial trial analysis work, five thousand arbitrary points digitalized from generated surfer map and superimposing for individual and then summing up to resolve the composite solutions of entire pumping wells as a collectives. This trial was going on for constant rates of the designed discharging capacity of the boreholes. To estimate the radius of influence for each different scenario, arbitrary points surrounding the well field are first created then the trial check analyzed, and the drawdown at the extreme boundary are seen at extreme of boundary. The edge at extreme of the boundary indicates the influence region if and only if zero draw down is obtained. If the drawdown at these extreme ends of the region is still positive, the number of arbitrary points should be increased until the limits of the boundary locations prevails no more drawdowns.

Thus the numbers settings of arbitrary observation points digitalized to increase to eleven thousand and sixteen thousand to run second and third trials and the coverage area of the pumping under the influence developed to see the effect of the predicted drawdown with respect to distance from the pumping boreholes. Observing that the more number of the arbitrary points setting up surrounding the boreholes to the furthest, the more increased is area of analysis, i.e. increasing the distance of synthetic observation arbitrary points, points at which no more drawdown will be obtained. Hence, the number settings of the arbitrary observation points enlarged to forty six thousand points. In undertaking this required point where the drawdown is maintaining constant and at the limit edges of the recharging boundary the composite drawdowns become equal to zero is satisfied.

Therefore; by means of the digitalized coordinates of surfer map as simple input of 46,000 selected arbitrary theoretical observation spots and the geometric mean of the approximated aquifers parameters the prediction of expected drawdowns along with the analysis of real and image wells are accomplished for each borehole for changeable discharging rates of assumed possible case scenarios. To make this, the principle of superposition technique is implemented. The designed pumping rates of the boreholes is manipulated to be reduced by half amount of the designed rate capacity and supposing in the occurrence that may demand for water supply rises so the rates will also increases, then increasing designed rate by double amount to create scenario to note the effect of simulated drawdowns configurations. Then resulted composite solutions gained from the superimposing, contour line distribution of the simulated drawdown is plotted to note the configuration of cones of depression displays as an influence of operating boreholes exerted on the nearby river at vicinity of the well field location. The cooper-Jacob, Theis equation and superposition methods are also implemented to establish the radius of influence and capture zone of the recharge boundary.

3.4. Demarcation of Capture Zone for Mojo Pumping Boreholes

A capture zone is including up gradient and down gradient potentiometric and encompasses the volume of water that operating wells may extract from the porous media of given aquifer. With the purpose of establishing the demarcation of the recharge boundary initiating, from its significant the area of the capture zone is delineated to convey improved understanding to decide the remediation action to be implemented during design and operation of pumping wells particularly when the systems designed for water supply purposes. To carry out the delineation of the capture zone the following assumption are considered. The aquifer is homogeneous, isotropic and has infinite horizontal areal extent; uniform condition flow be comes up; an unconfined aquifer is assumed to have horizontal impervious at the base with no infiltration no vertical recharge and no leakage; the specific yield of unconfined aquifer is neglected, the Duppuit assumption of the vertical gradients are neglected; the constant pumping rate is assumed and the well is fully penetrated and open throughout the thickness of the unconfined aquifer (Stack; 1989) and Marsily ; 1986). The equation used for the computation of the capture zone edge when the conditions of the steady state have reached in unconfined aquifer is as of that discussed by (Todd; 1980 and Grubb; 1993). In the case where water supply boreholes situated closer to the stream such that potential treats to contaminate the existing nearby river is anticipated, one practical concern is to delineate the locations and pumping rate of the well securing that the pollution does not enter the aquifer or not cross the threshold to the pumping well. These precautions may be effectively addressed through the delineation of the capture zone. According to his study Grubb provided the solution of the capture zone in case of unconfined aquifer (Grubb; 1996). The requirement for this condition is to have the head in two pumping wells along the axis the groundwater flow direction. Then, even though test data from pumping well test/piezometeic not available here in this study we utilized heads data collected from single well pumping test data, to furnish demarcations of the capture zone for Mojo boreholes well field. This is carried out considering two proximate pumping wells are operating simultaneously by keeping their designed capacity rate in the first scenario. Then the by manipulating designed rate into half and also there by doubling the designed rates, demarcation of recharge zone is computed to convey the optimal position of the capture zone so as to enable in making suitable decision of the well protection.

3.5. Determination of Boreholes Interference at Mojo Well Field

The Theis Prediction (pumping test planning) method is used in this study to determine whether there are interferences among the bore wells exist or not. By this method interference checked between two wells while operating separately by entering the value of transmissivity and storativity value obtained individual well pumping test data, whereas the geometric mean value when the wells are operating simultaneously. The discharge rate is varied to ensure that a measurable water level drawdown is kept constant over certain time with no radius of influence interfere with the adjacent pumping well.

In target to minimize wells interference and to design non interfering systems layout of multiple well fields where more than one pump or several pumping wells may exist in a given well field such that those wells are capturing groundwater from aquifer of the same field, considerations of the subject matter is fundamental task in designing and fixing appropriate locations of the pumping wells. Out of which the one is to resolve the spacing there to be provide between the pumping wells so as to minimize the occurrence of transecting cones of depression as effect of operating wells which subsequently generates interferences in the layout system of the well field. The total drawdown of the individual pumping wells is the linear addition of every well operating in multiple well systems as the superposition permits addition to determinate the effect of drawdowns. Despite of truth that transmissivity in unconfined aquifer is varying due to fluctuating nature of saturated thickness of the unconfined aquifer, the linear superposition technique predicts a composite drawdown from summing up individual drawdowns in multiple pumping well field miscalculate the resulting drawdowns with comparative to real drawdown may resulted therein. For instance as the saturated thickness reduces the transmissivity also decreases, the multiple well systems operating in the aquifer develops a greater value of composite hydraulic gradient than that of equivalent confined aquifer as response of compensating the diminished value of the aquifer transinmissivity. So that we have implemented geometric mean values of transimissivities which were approximated through various determination methods descried in the preceding sections whilst conducting the simulation of composed drawdown solutions by the principle of superposition. Therefore; realization of wells interference is necessary scheduling the operation and maintaining the continual function of pumping wells in multiple well field system (C.W. Fetter, 2002).

For the occasions of multiple well system forming a well field, the cones of depression of the operating wells intersect and each well interfere with one another due to the increase of the drawdown as the pumping lift created. Well interference between the boreholes develop due to the intersection of cones of depression inventing from these pumping wells in the well field while all are operating simultaneously. Such overlapping of cones of depression in multiple well systems is recognized as interference of one pumping well with others.

Therefore; to facilitate interpretation of complicated water level changes caused by well interference effects from multiple pumping wells, the simulated drawdown have been plotted with respect to areal coverage when pumping wells are running at the same times. In the case of Mojo well field there are three pumping wells which thought to extract water from the aquifer at this well field. At the first phase of the project one well is proposed as a standby and the remaining two wells to be exact MJBH-1 and MJBH-2 are operational. But MJBH-3 will also be operational in the second phase facing to alleviate the increasing demand for water supply. With the purpose of doing we have simulated composed drawdown considering all the three pumps are simultaneously operating in full capacity of designed rates since applying to operative the third borehole will not be avoidable after a session, owing to fact that demands for water supply rises with growth of population and economy. Seeing from this point of view the third pump which is not working at the moment is included assuming it will be put in operational later on may be in the second stage of project.

Regarding rates of pumping at the boreholes, constant pumping rates are assumed there but at different time the designed pumping capacities of the boreholes manipulated to new rates such that the pumping rates are setting up to run within double and half rates of their designed capacity. This is conducted to create alternative case scenarios by the higher and lower rating of pumping operations which provides a chance to detect the features of the overlapping situation when well interference may be resulted as of pumping boreholes operating progressive in the described well field.

4. Results and Discussion

4.1. Comparison between Manual Curve-Matching and Automatic Curve-fitting by Computer

From the comparisons completed among particular wells there by using the values of various transmissivities and storativities calculated and tabulated in Table 1 and 2 via both the manual and the automatic curve fitting methods, we can recognize that values of the transmissivities approximated for the three wells are not the same and this prevails that the transmissivity in unconfined aquifers is not constant. Thus the basic assumption that Theis (1935) model anticipated that all wells in confined aquifer is an isotropic where the transmissivity (T) is independent of direction is not more valid.

Attributable to this context, “Papadopolus, 1965 stated that Theis Model is similar to an anisotropic model except that the transmissivity for the second model characterized with directional transmissivity and displays a profile of an ellipse (Papadopolus, 1965)”. This means that the maximum transmissivity (T_{max}) in the direction of high permeability or porous media, the minimum transmissivity (T_{min}) in low permeability and the average transmissivity (T_{avg}) in the mean permeability direction through media of the aquifers. Therefore, the geometric mean values of the model parameters transmissivity (T) and storage coefficient (S) is considered in evaluating the superposition modeling.

Accordingly, the geometric mean values from the analysis accomplished by manual curve-fitting and that of Aquifer Test 3.5 Software methods are tabulated and presented beneath for comparing and contrasting purpose in the line of the aquifers parameters valuations. From comparisons it is noticed that the achieved geometric mean values of the aquifer parameters analyzed by means of both methods are approximately correspondent. Even so, the approximated parameters values as possessions of the aquifer at well field those achieved from the analysis accomplished using tools of Excel Spread Sheet (Excel-2007) by the manual curve-fitting technique is applied for the evaluating real pumping and imaginary wells through the principles of superposition.

Table 1: *Summary of Geometric Mean Results for the Analysis Completed by Excel Spread Sheet /Manual Curve-Fitting/ Method*

Name of Boreholes	Aquifer Paramaters						
	Transmissivity (m^2/s)			Storativity			Horizontal hydraulic conductivity (m/s)
	T_{max}	T_{avg}	T_{min}	S_{max}	S_{avg}	S_{min}	K_{Avg}
MJBH-1 MJBH-2 MJBH-3	3.63E-03	3.40E-03	3.15E-03	2.93E-02	2.03E-02	1.12E-02	9.02E-06

Table 2: *Summary of Geometric Mean Results for the Analysis Completed by Aquifer Test 3.5 Software Method for Comparison*

Name of Boreholes	Aquifer Paramaters						
	Transmissivity (m^2/s)			Storativity			Horizontal hydraulic conductivity (m/s)
	T_{max}	T_{avg}	T_{min}	S_{max}	S_{avg}	S_{min}	K_{Avg}
MJBH-1 MJBH-2 MJBH-3	3.79E-03	3.00E-03	2.30E-03	4.11E-03	4.11E-03	4.11E-03	7.62E-06

4.2. Results of Recharge Boundary Response to Three Pumping Wells Operating Simultaneously via Superposition Technique

In case of boundary conditions where the area of interest under the influence of pumping is concerned, the basic assumption that the aquifer is of infinite areal extent is no longer functional. From the determination result of the aquifer category, it is observed that both plots of the log-log and semi-log of the observed drawdowns as a function of time and from judgments that drive through comparing the resulted plots with the simulated standard Theis type curves, the characteristics of Mojo well field aquifer prevails ***the effect of recharging boundary condition and partiality of the wells penetrations in unconfined aquifer***. The recharge boundary is reflected as a boundary that concerns to a constant head state, where the drawdown is maintained constant and equal to zero on progress of time. So as to handle such groundwater problem (i.e. recharge boundary condition), the principle of superposition is engaged in the calculation of the drawdown at a certain point in space due to the effect of a set of pumping wells operating simultaneously and the recharge boundary renders the aquifer to seemingly finite state. In the case of the Theis Equation, the principle of superposition gives final solutions to the problems by using linear combination of elementary solutions.

So as to conduct the analysis of superposition principles, which permits the applications of the non-equilibrium Theis or the (Cooper and Jacob 1946) techniques, we must first transform an aquifer of finite extent into one of apparently infinite extent there by introducing imaginary wells, or image wells analyses. To compute solution of the superposed drawdowns using Theis Equation (2.20) firstly, the geometric mean values generated from maximum, minimum and average values of transmissivities and storativities are computed for individual Mojo water supply boreholes namely MJBH-1, MJBH-2 and MJBH-3. The results of the geometric mean values of the estimated aquifers' parameters (transmissivities and storage coefficients) which were computed and tabulated in summary of geometric mean results for the analysis completed by the method of Excel tools as Table 1 shows used to carry on simple model simulation to have composite drawdowns solution by superposing technique. In order to generate the available contours for the synthetics drawdowns at any arbitrary points those likely be occurred in ranges of interested areal converges under the influences as effect of the pumping boreholes, by using the tabularized geometric mean of the estimated aquifers parameters and the digitalized coordinates of 46,000 selected arbitrary theoretical representative observations spots from surfer map as detailed in the methods portion as input and the established shortest distance of the real and image wells from the existing straight constant head boundary, simulation of model via the principle of superposition along with the analyses of real and image wells for individual three wells and two wells in case the pumps are operating simultaneously and then by adding the linear individual solutions to predict the composite solutions of drawdowns expected to result as influences of mutual pumping operating under differing situation of the boreholes at the Mojo well field is carried out as per represents procedurally.

The drawdown at any point in the area of influence caused by the discharge of three boreholes is equal to the sum of the drawdowns caused by each well discretely.

$$s_t = s_{pw1} + s_{pw2} + s_{pw3} \tag{4.1}$$

Let the three wells in Mojo well field are pumping at rates of Q_{pw1}, Q_{pw2} and Q_{pw3} causing drawdowns s_{pw1}, s_{pw2} and s_{pw3} respectively.

For the stated three pumping boreholes, total drawdown is the sum of the contribution from each well such that:

$$s_t = s_{pw1} + s_{pw2} + s_{pw3}) = \frac{Q_1}{4\pi T} W(u_{pw1}) + \frac{Q_2}{4\pi T} W(u_{pw2}) + \frac{Q_3}{4\pi T} W(u_{pw3}) \tag{4.2}$$

Then placing a mirror image injection well, injecting at the same rate but on the other side of the constant head boundary gives, $Q_{pw1} = -Q_{iw1}$, $Q_{pw2} = -Q_{iw2}$, and $Q_{pw3} = -Q_{iw3}$ at a distance X, causing drawdown $s_{pw1} = -s_{iw1}$, $s_{pw2} = -s_{iw2}$, and $s_{pw3} = -s_{iw3}$ respectively.

Hence the solution for adding image wells to a real pumping well can be written as

$$s_t = (s_{pw1} - s_{iw1}) + (s_{pw2} - s_{iw2}) + (s_{pw3} - s_{iw3}) = \frac{Q_1}{4\pi T}W(u_{pw1}) + \left(\frac{-Q_1}{4\pi T}\right)W(u_{iw1}) + \frac{Q_2}{4\pi T}W(u_{pw2}) + \left(\frac{-Q_2}{4\pi T}\right)W(u_{iw2}) + \frac{Q_3}{4\pi T}W(u_{pw3}) + \left(\frac{-Q_3}{4\pi T}\right)W(u_{iw3}) \qquad (4.3)$$

$$u_{pw} = \frac{r_{pw}^2 S}{4Tt} \qquad (4.4)$$

$$u_{iw} = \frac{r_{iw}^2 S}{4Tt} \qquad (4.5)$$

The values for r_p and r_i were calculated in EXCEL spread sheet marks in the form of Cartesian coordinates systems of any arbitrary points of (x, y) plane and their respective resulting values then inserted into the required equations and computed as:

$$r_{pw} = \sqrt{(x_{pw} - x)^2 + (y_{pw} - y)^2}$$

$$r_{iw} = \sqrt{(x_{pi} - x)^2 + (y_{pi} - y)^2}$$

Where: -

s_t = is the total drawdown at any given arbitrary point;

s_{pw1}, s_{pw2} and s_{pw3} = are the drawdowns at any arbitrary point caused by the operating wells no. 1, 2, and 3 in well field;

s_{iw1}, s_{iw2} and s_{iw3} = are the drawdowns at any arbitrary point caused by the image wells no. 1, 2, and 3 in well field;

Q_{pw1}, Q_{pw2} and Q_{pw3} = are the pumping rates of discharging well no. 1, 2, and 3 respectively.

$-Q_{iw1}$, $-Q_{iw2}$ and $-Q_{iw3}$ = are the injecting rates of image well no. 1, 2, and 3 respectively.

r_{pw1}, r_{pw2} and r_{pw3} = are the distances from the pumping wells to any arbitrary point of well no. 1, 2 and 3 respectively;

r_{iw1}, r_{iw2} and r_{iw3} = are the distances from the image wells to any arbitrary point of injection well no. 1, 2 and 3 respectively;

Alongside the recharge boundary, where $r_{pw} = r_{iw}$, the drawdown from real pumping well is balanced by the injecting image well, such that s = 0, maintaining the constant head boundary condition. Hence, substituting the above itemized wells parameters in to equation no. (4.3) and simplified equation no.(4.4) gives more simpler equation which is expended in excel spread sheet to compute the composite drawdown of the operating three wells through the principle of superposition.

$$s_t = \frac{Q_1}{4\pi T} \ln\left(\frac{r_{iW1}^2}{r_{pW1}^2}\right) + \frac{Q_2}{4\pi T} \ln\left(\frac{r_{iW2}^2}{r_{pW2}^2}\right) + \frac{Q_3}{4\pi T} \ln\left(\frac{r_{iW3}^2}{r_{pW3}^2}\right) \qquad (4.6)$$

Subsequently, the configured digitalized coordinates of theoretical observation arbitrary spots and the computed values of merged superposition solutions of the synthetic drawdowns predicted for three boreholes operating simultaneously with capacity of designed pumping rates are organized hereunder, and for other scenarios of the altered discharging rates are taken over at the APPENDIX-A sections of this report.

Table 3: *Estimated Aquifer Hydrogeological Parameters*

Aquifer Parameters	Aquifer Parameters						Horizontal hydraulic conductivity (m/s)	Water Level in operating well during pumping test (m)	Water Level in operating well after correction (m)
	Transmissivity (m2/s)			Storativity					
	T_{max}	T_{Avg}	T_{min}	S_{max}	S_{Avg}	S_{min}	K_{Avg}	h_w	h_w
MJBH-1	0.0036	0.0034	0.00315	0.0293	0.0203	0.0112	9.02E-06	320.43	328.074
MJBH-2								374.13	379.53
MJBH-3								373.13	381.85

Table 4: Operating wells data

Name of Pumping wells	Location in Cartesians coordinate		Transmissivity used	Operating rate (m^3/s)	Remark
	X-coordinate	Y-coordinate			
MJBH-1	512300.00	953358.00	0.003625974	0.0450	Designed (Q), T_{max}
			0.003396217	0.0450	Designed (Q), T_{avg}
			0.003146958	0.0450	Designed (Q), T_{min}
MJBH-2	511750.00	954495.00	0.003625974	0.0450	Designed (Q), T_{max}
			0.003396217	0.0450	Designed (Q), T_{avg}
			0.003146958	0.0450	Designed (Q), T_{min}
MJBH-3	512200.00	953889.00	0.003625974	0.0483	Designed (Q), T_{max}
			0.003396217	0.0483	Designed (Q), T_{avg}
			0.003146958	0.0438	Designed (Q), T_{min}

4.2.1. Effect of Recharge Boundary on Mojo Well Field in Event Pumping Wells Effective Simultaneously

The effect of recharge boundary is dispensed here in by implementing the Theis equation and the principle of superposition. The contour lines plots of the composite drawdowns produced based on Theis solution that assumes radial flow to a well of constant discharge in an infinite aquifer. As a matter of fact there presents Mojo Perennial River closer to the well field, the effect of the recharge boundary condition is sensible to deal with for the theoretically predicted drawdown normally imagines of radially symmetric features of contour line trend may deviate from the actual configurations. Hence, mentioning the Mojo Perennial River as a case of recharging source since it exists nearby to Mojo boreholes which developed for drinking water supply project, discharging real pumping boreholes and their corresponding injecting imaginary wells were properly setting up and image well analyses had been carried on in order to compute the required solutions for composite drawdowns. These composite solutions are calculated through the principle of superposition adopting general equation of the Theis Equation. In the direction of resolving for required composite solutions of the drawdowns in this technique, initially the drawdowns that may originate from each borehole had been predicted particularly by superimposing. Then by accumulating up the resulting superposed predicting drawdowns that originates from each borehole, the composed drawdown that can be occurred everywhere in the well field is accomplished. The resulting composite drawdown solution represents accumulative effect that the existence of such recharge boundary may prevails in response to withdrawal actions the operating pumps apply in the boreholes around the vicinities of field at phase they eventual pumping out the water normally available there in aquifer at the Mojo well field site. Accordingly, the graphical demonstrations as the outcome is given in Figures 8, 10 and 12 that shows the contour line plot distributions of the composite drawdowns solution for selected designed operating rates when the pumps in three boreholes at Mojo water supply well field are all operating simultaneously. These contour lines plots for simulated solutions of the composite drawdowns are completed in the well field by using the hydrogeological parameters listed in Table 3 and specified locations of the boreholes, several synthesized arbitrary observations points digitalized from the digital map of the well field site, pumps operating rates and duration of operating period for pumps assumed any time (t) allowing for a case that the boreholes in service are simultaneously functioning.

The contour lines plots for the simulated drawdowns solution are accomplished for three scenarios through computing the simulation attributing variable values of the approximated parameters in valuation the properties of the aquifer in study area adopts to possess at different times for example transmissivity (i.e. T_{max}, T_{avg} and T_{min}). So that the configurations of the contour lines plots of the composed drawdowns as Figure 8, 10 and 12 illustrates, simulated imputing approximated values of transimissivities; T_{max}, T_{avg} and T_{min} respectively and with those parameters given in the mentioned tables at any time (t).

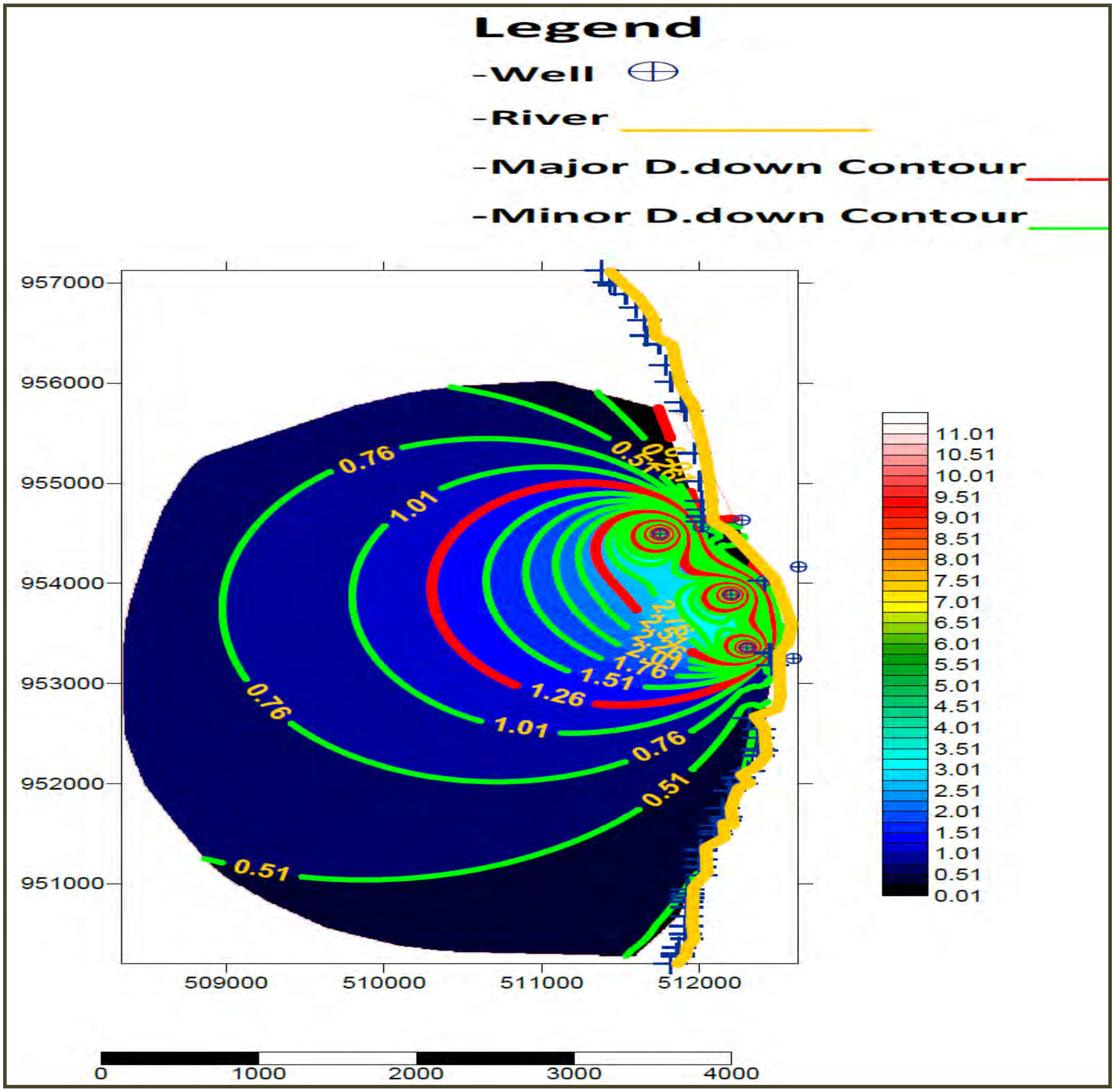

Figure 8. Plot of simulated composite drawdown contour lines distributions produced in unconfined aquifer as a result of a recharge boundary and three wells operating simultaneously located at (xw, yw) as indicated in Table 4 and numerous digitalized arbitrary coordinates, by the operating rates of 0.045 m3/s, 0.045 m3/s and 0.04383 m3/s for MJBH-1, MJBH-2 and MJBH-3 respectively, the drawdown contour lines prepared at any time (t) letting the aquifer at well field adopts maximum approximated transmissivity (Tmax).

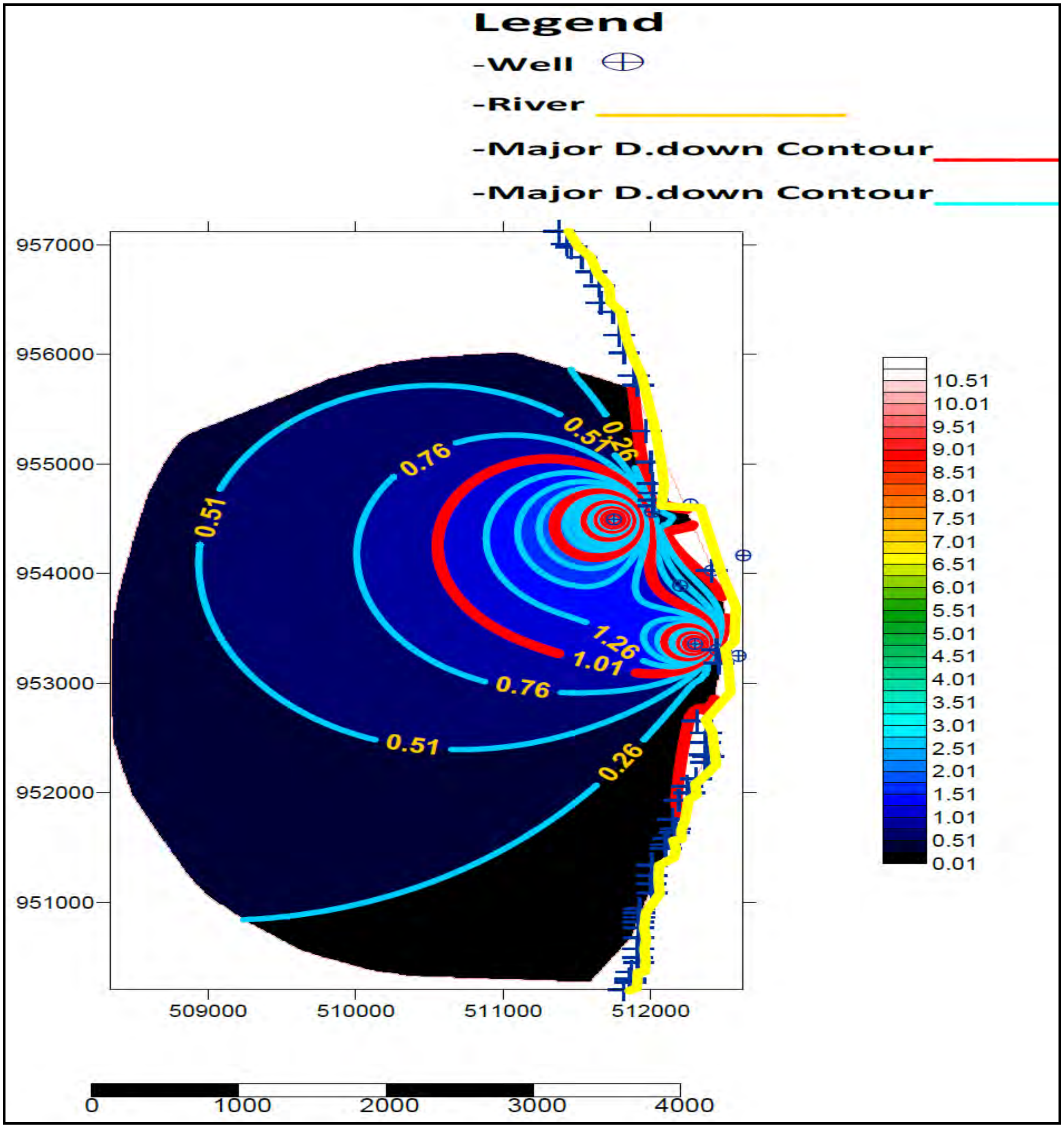

Figure 9. Plot of simulated composite drawdown contour lines distributions produced in unconfined aquifer as a result of a recharge boundary and two wells operating simultaneously located at (x_w, y_w) coordinates: - (512300.00, 953358.00) and (511750.00, 954495.00), by designed rates of 0.045 m^3/s for MJBH-1 and 0.045 m^3/s for MJBH-2, the contour lines prepared for simulated drawdown at any time (t) supposing the aquifer takes maximum estimated transmissivity (T_{max}).

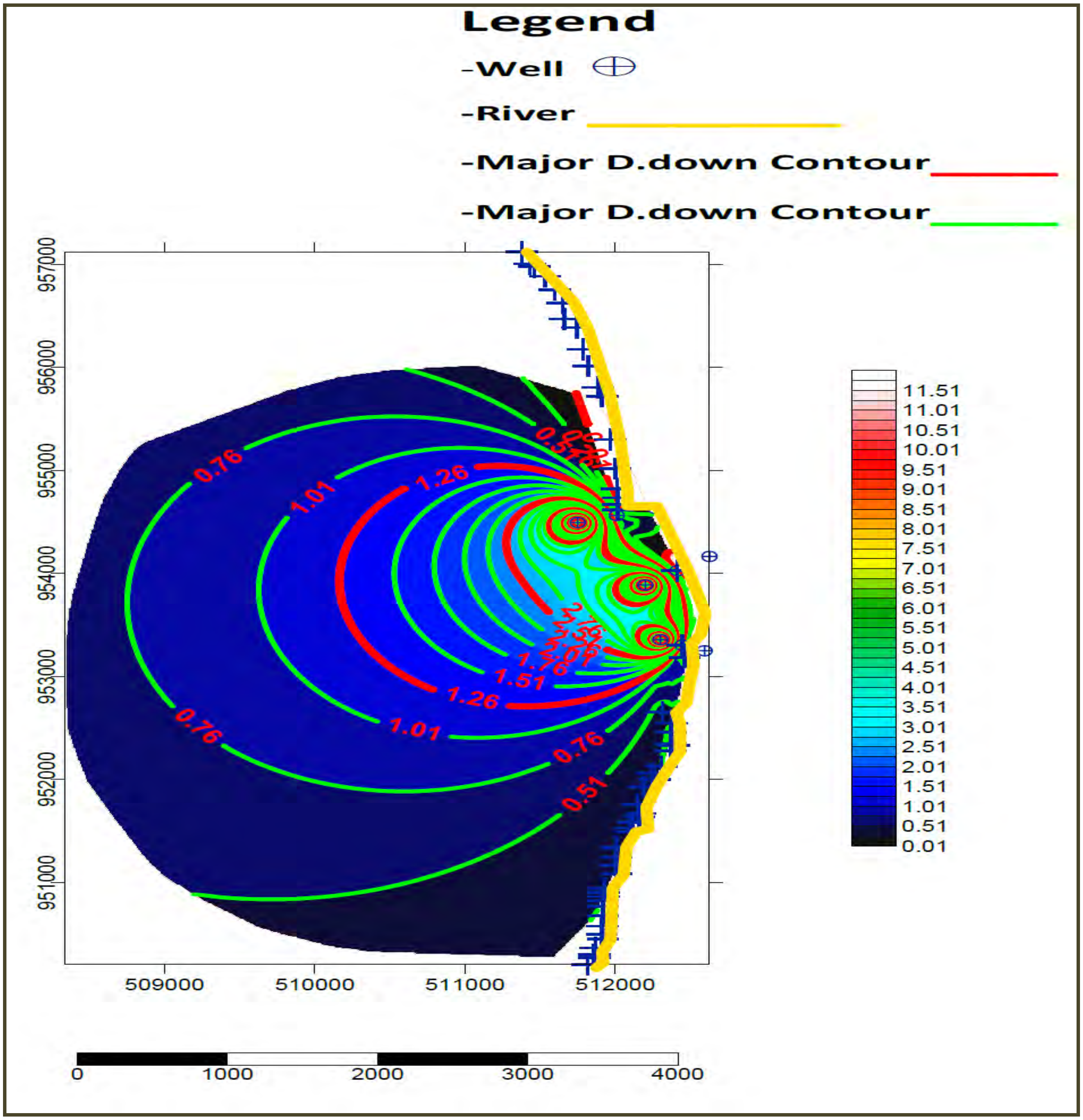

Figure 10. Plot of simulated composite drawdown contour lines distributions produced in unconfined aquifer as a result of a recharge boundary and three wells operating simultaneously located at (xw, yw) as indicated in Table 4 and numerous digitalized arbitrary coordinates, by the operating rates of 0.045 m3/s, 0.045 m3/s and 0.04383 m3/s for MJBH-1, MJBH-2 and MJBH-3 respectively, the drawdown contour lines prepared at any time (t) letting the aquifer at well field adopts approximated average transmissivity (Tavg).

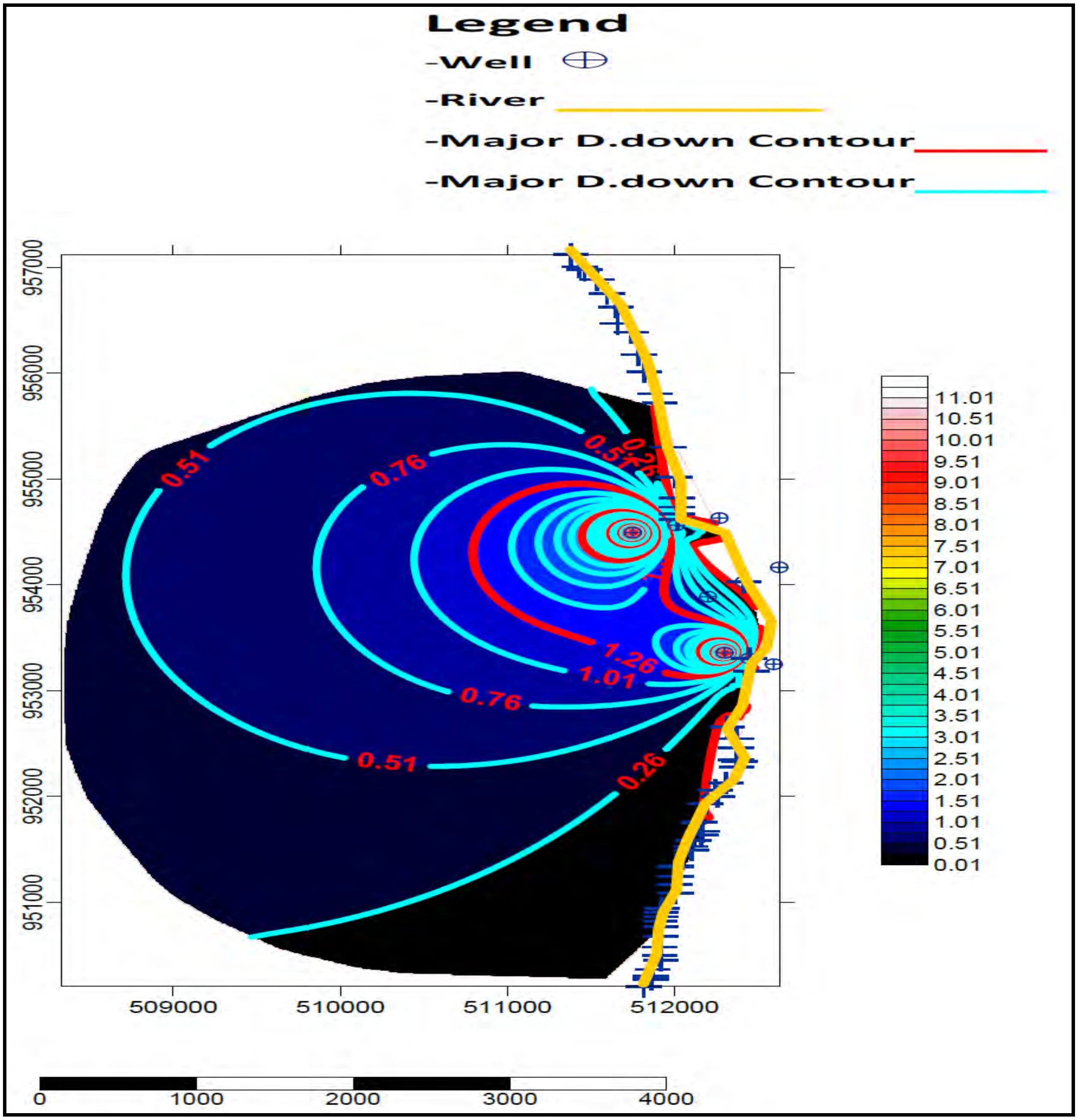

Figure 11. Plot of simulated composite drawdown contour lines distributions produced in unconfined aquifer as a result of a recharge boundary and two wells operating simultaneously located at (x_w, y_w) coordinates: - (512300.00, 953358.00) and (511750.00, 954495.00), by designed rates of 0.045 m^3/s for MJBH-1 and 0.045 m^3/s for MJBH-2, the contour lines prepared for simulated drawdown at any time (t) supposing the aquifer at well field takes theapproximated average transmissivity (T_{avg})).

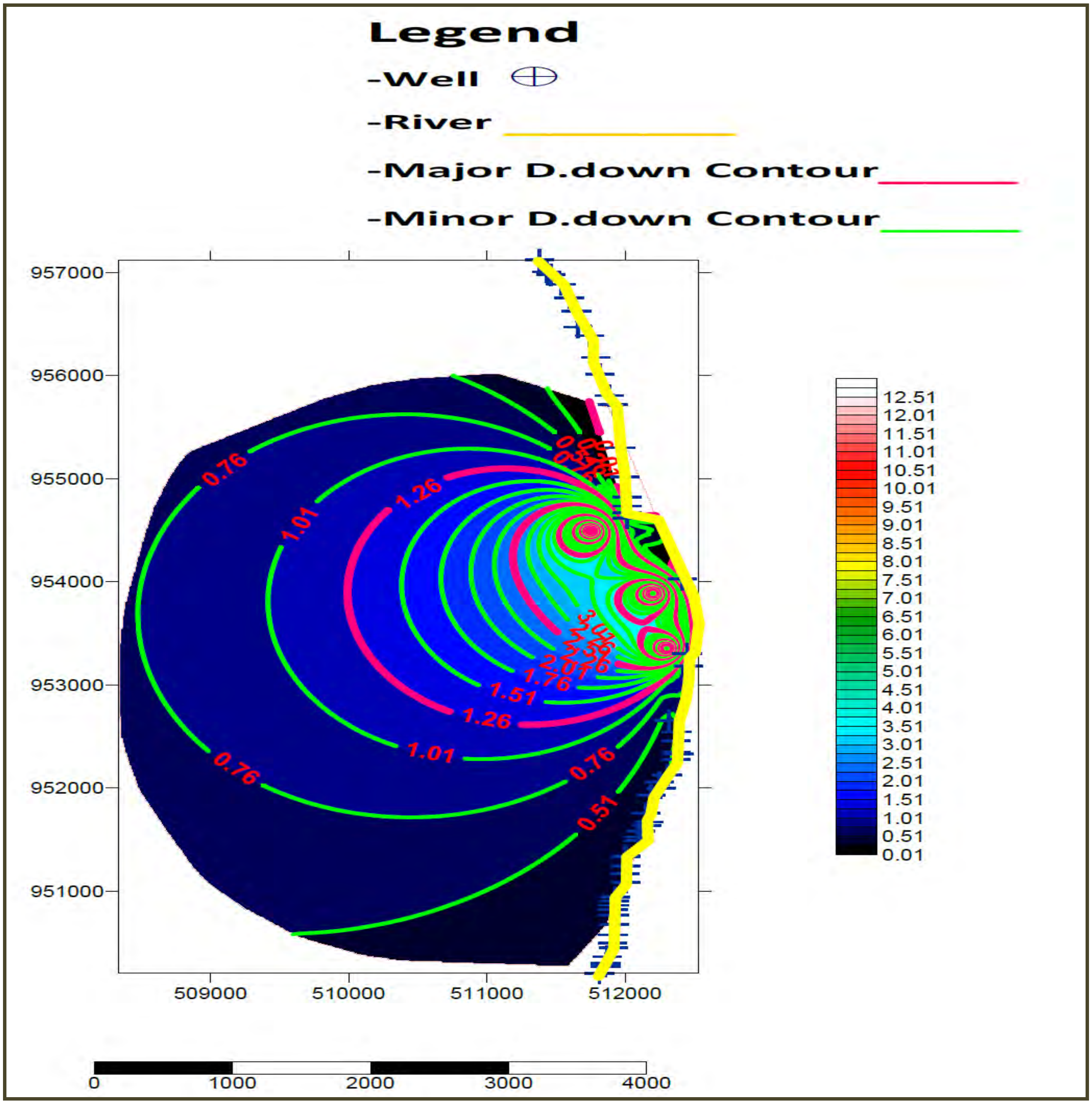

Figure 12. Plot of simulated composite drawdown contour lines distributions produced in unconfined aquifer as a result of a recharge boundary and three wells operating simultaneously located at (x_w, y_w) as indicated in Table 4 and numerous digitalized arbitrary coordinates, by the operating rates of 0.045 m^3/s, 0.045 m^3/s and 0.04383 m^3/s for MJBH-1, MJBH-2 and MJBH-3 respectively, the drawdown contour lines prepared at any time (t) letting that the aquifer at well field adopts the estimated minimum transmissivity (T_{min}).

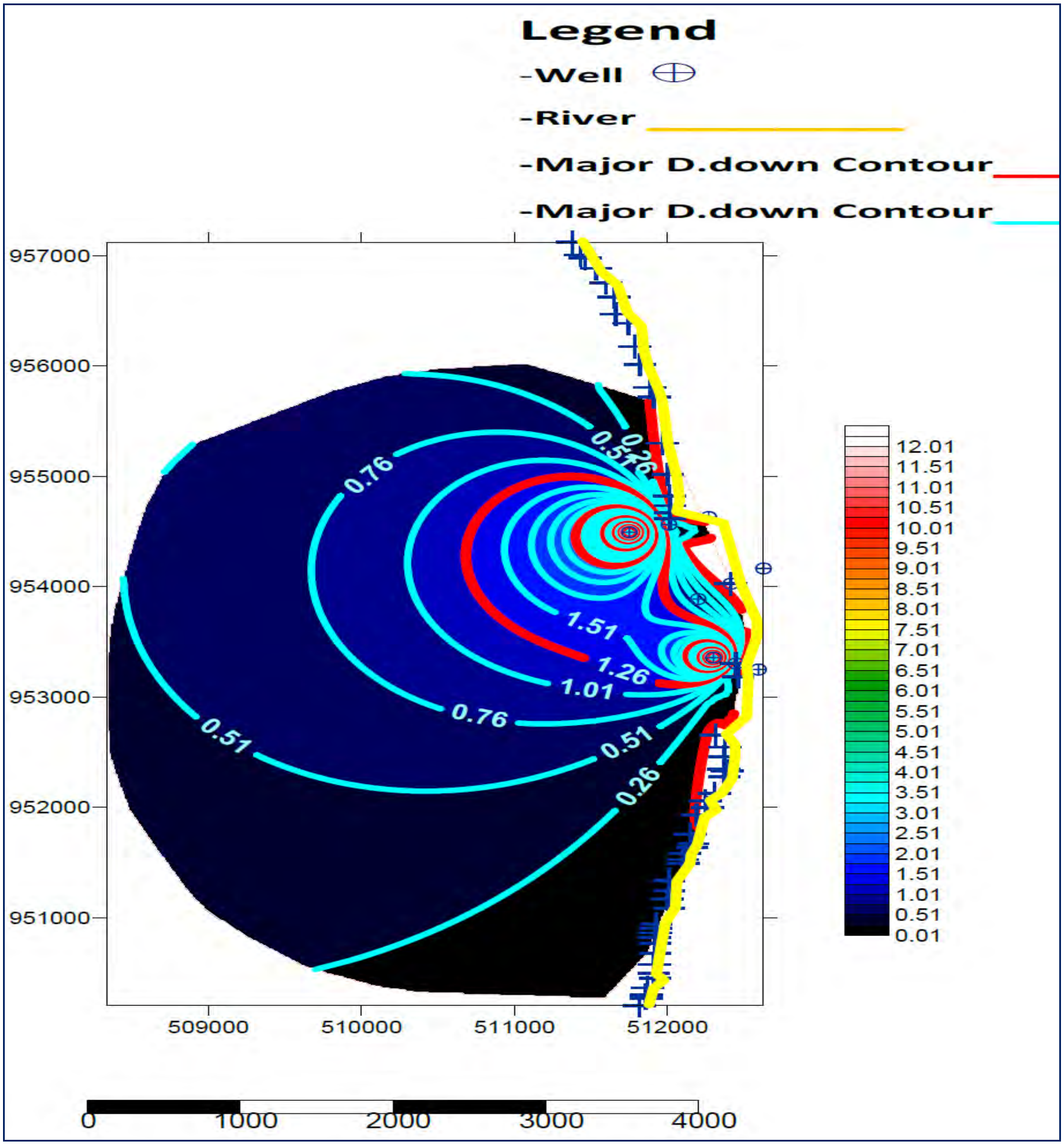

Figure 13. Plot of simulated composite drawdown contour lines distributions produced in unconfined aquifer as a result of a recharge boundary and two wells operating simultaneously located at (x_w, y_w) coordinates: - (512300.00, 953358.00) and (511750.00, 954495.00), by designed rates of 0.045 m^3/s for MJBH-1 and 0.045 m^3/s for MJBH-2, the contour lines prepared for simulated drawdown at any time (t) supposing the aquifer at well field takes the approximated minimum transmissivity (T_{min}).

It is interesting to note that from trends of contour lines plots produced for the composed drawdown displays a densely configured contours in the direction of the exiting Mojo Perennial River since the pumping boreholes are developed closer to the this river so it evidently influences the drawdown configuration in performance role of recharging source of boundary condition.

Regarding the subject matter "Sevee and Walton, recommend that a pumping well should be placed at a distance equal to or exceeding the thickness of the aquifer from the potential hydraulic boundaries in order to minimize the influence of river bed infiltration except that when the intention is to induces recharging from such sources (Sevee, 1991 and Walton, 1987)". The distance between the river and MJBH-1, MJBH-2 and MJBH-3 is 156.52m, 268.16m and 254.54m respectively. Whereas; the depth of excavation for MJBH-1, MJBH-2 and MJBH-3 is 358m, 416m and 410 respectively so that the distance between spots where the setting up of the boreholes concluded and stretches of the Mojo river escarpment nearby the well field is small comparative to ***thickness of the aquifer***. Moreover, this Perennial River situates at relatively higher elevations than that of the static water tables average altitudes as per discovered during the pump test as Table 18 shows. Then recharge area is characterized by higher elevations than the aquifer and contour lines plots display that the flow to the wells diverge forming ***radial asymmetry*** arrangement towards a source of the recharging boundary, the Mojo river, as the demonstrated Figure from 8 up to 13 shows so that the formulated assumption by Theis that flow to a well of constant discharge in an infinite aquifer is radial symmetric is not more functional for this case.

As far as the distance kept between the river and the operating boreholes so nearer and enhancing rate of depletion from river to aquifer largely depends on such factor, also there by noting that the river exists at higher average elevation than that of the static water levels and combining these facts by venue up on the orientations that the drawdown contour graphs demonstrations, the river is understood that it delivers a stream flow into the aquifer at well field site. Therefore; this Perennial River is the potential recharge source for the three boreholes those have been developed intending to supply drinking water to Mojo town.

As consequences of existing Mojo Perennial River as a recharging source of boundary condition in proximity to the boreholes, the distribution of contours lines plots resulting from simulated composite drawdowns display configurations of flow lines to grow dense surrounding an escarpment of the recharging boundary region and becomes more and more dense while progressing beginning from extreme verge of the recharge region in direction towards the center point of pumping wells. Whereas the structures of these contour lines distributions plots show the simulated drawdowns reduce as going on in other side of recharging boundary starting from origin of the operating boreholes and the shrinkage of the cones of depression increases and the space between successive lines far reaching and indicates that this diminishing act of the drawdowns comes to a cessation unify with zero zone as going further and further and the influence of operating pumps will no influence the drawdowns in the defined well field.

At this point there are no more extensions for cone of depressions and no more drawdowns to be measured so that a state of steady state condition has been taken place in partial to the direction from the boreholes to the edge of the stream. As Figures schematized from 8 up to 15 shows the plot display also the distributions of drawdown lines at about the center portion of the well field spacing among the successive lines are realized denser and the stress of superposed drawdowns mass bulge to about the middle borehole direction and progressively shifting of the mass expands from North East skirt towards the center there by encompassing more area and to the North West border within the region of the well field the system.

According to information furnished from the resident water supply authority of Mojo town we understood that the authority wishes to use boreholes MJBH-1 and MJBH-2 for meeting public demands by supplying drinking water from abstraction of the two boreholes at a rate of designed capacity of each 3,888.00 m^3/day. That is why the study incorporates as another scenario as Figure 9, 11 and 13 shows aspiring to diagnose features probably take places in the well field as a result that in the event only two pumping boreholes setting up both wells implementing by the same period during first phase of the project. Whilst there two boreholes are scheduled to be operational at the same time the consolidation of the cones of depressions reliefs comparing with the cases scenarios in which the entire boreholes are set up operative simultaneously. The distributions of cones for resulted drawdowns as contour plots display more gatherings of the cones of the depressions draw together towards North East around the borehole no. 2 when compared with the cases of three wells as the schematic on the Figures 8, 10 and 12 clearly illustrates. Moreover, as the Figures 9, 11 and 13 depicts the spaces among the successive contour lines wider than these cases in which all three pumping well are operating collectively. The spacing gets wider and wider to the furthest edge of the boundary at opposite side of well with respect to the recharging river boundary.

As alternate case when the pumps in all the boreholes are manipulated to work with constant rates but with altering discharging rate at different time, we noticed that density of the contours lines distributions of the simulated drawdown gets denser and the cones of depressions show spreading to have covered large areal extent as influences of the pumping boreholes operating at the same time. This event noticed to existence as effect of the contour lines plots organized increasing the rate of pumping in doubling the rates of designed capacity and the entire boreholes set up to operate simultaneously as one scenario.

The resulted composite drawdown is intensifying by double amount than the case that the boreholes arranged to be operated with their designed pumping rates. Correspondingly, the distribution of the contours lines of the resulting drawdown is shrinking within the well field system. As the configurations of the contour lines shortens, quiet the radius of influence displays insignificant extensions in system range of the well field but the overlying effect of the simulated drawdowns prevails increasing and the gap between successive contour lines become more compressed. The consolidations of contour lines trends illustrate as very massive surroundings vicinity of the boreholes there to coining from the origin. The intensity of overlapping of the composed drawdowns lines configurations as Figure 14 and 15 demonstrates for the higher discharging rates of pumping boreholes is higher as approaching the origin and eventually the denser inclination progresses to drop nearer towards boundary of the recharging river. On the other hand, the simulated composite drawdowns in the case scenario that the discharging rates set to reduce by half amount of the deigned capacity of the boreholes, the density of the contour lines distributions shows patterns of diminishing by relative to the first case in which the pumping boreholes are fixed to operating simultaneously by their full capacity pumping rates. For the case when the entire pumping boreholes operating by designed capacity rates simultaneously and when the discharging rates increased assuming pumps may operate by double amount rates of that of the designed capacity of the pumps in the boreholes and when two of them fixed to functioning by the same specified pumping rates, using maximum, average and minimum transmissivities, approximated as properties of the aquifer at the well field are thoroughly presented as the Figures 8, 9, 10, 11, 12, 13 and 14 clearly illustrate, for the purpose of comparison the effect of manipulating the rates of discharge scenarios, supposing that the aquifer in which the pumping boreholes operating, adopts the approximated specified transimissivities values for both conditions.

Moreover, and for the others cases of the described scenarios when the rates of pumping made increased and reduced, similar plots of the contour lines distributions for the simulated composite drawdowns are also produced for different conditions of the pumping rates but affixed at APPENDIX B which is presented at annex section of this report.

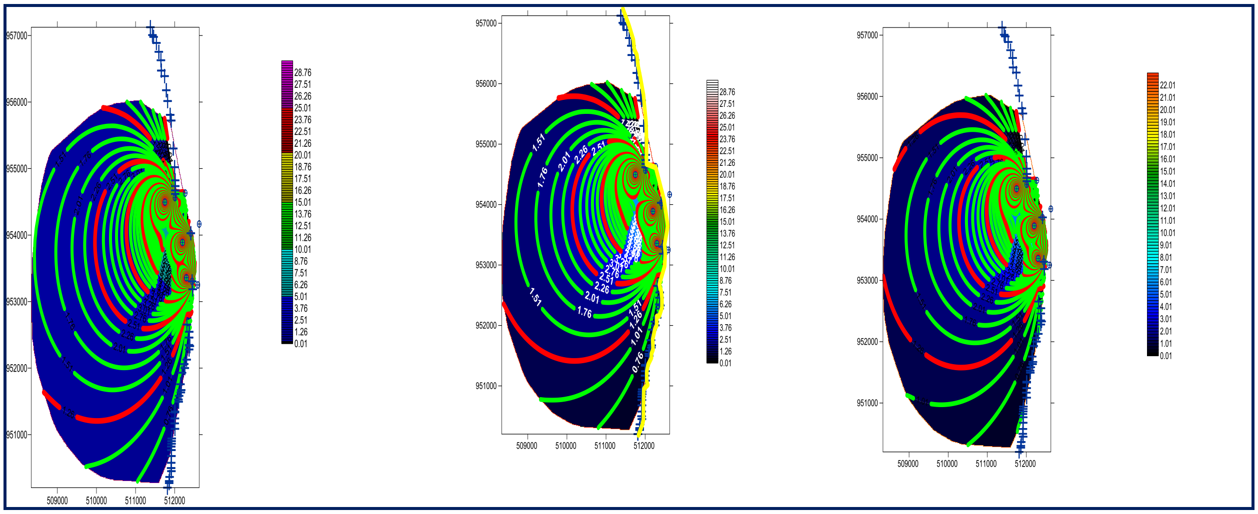

Figure 14. Plot of simulated composite drawdown contour lines distributions produced in unconfined aquifer as a result of a recharge boundary and three wells operating simultaneously located at (x_w, y_w) as indicated in Table 4 and numerous digitalized arbitrary coordinates, by doubling the rates of pumping of that of the designed rates capacity of the wells i.e. 0.09 m^3/s, 0.09 m^3/s and 0.08776 m^3/s for MJBH-1, MJBH-2 and MJBH-3 respectively, the drawdown contour lines prepared at any time (t) supposing the aquifer at well field takes the approximated transmissivities (T_{min}), (T_{avg}), (T_{max}) in sequence from left to right as shown

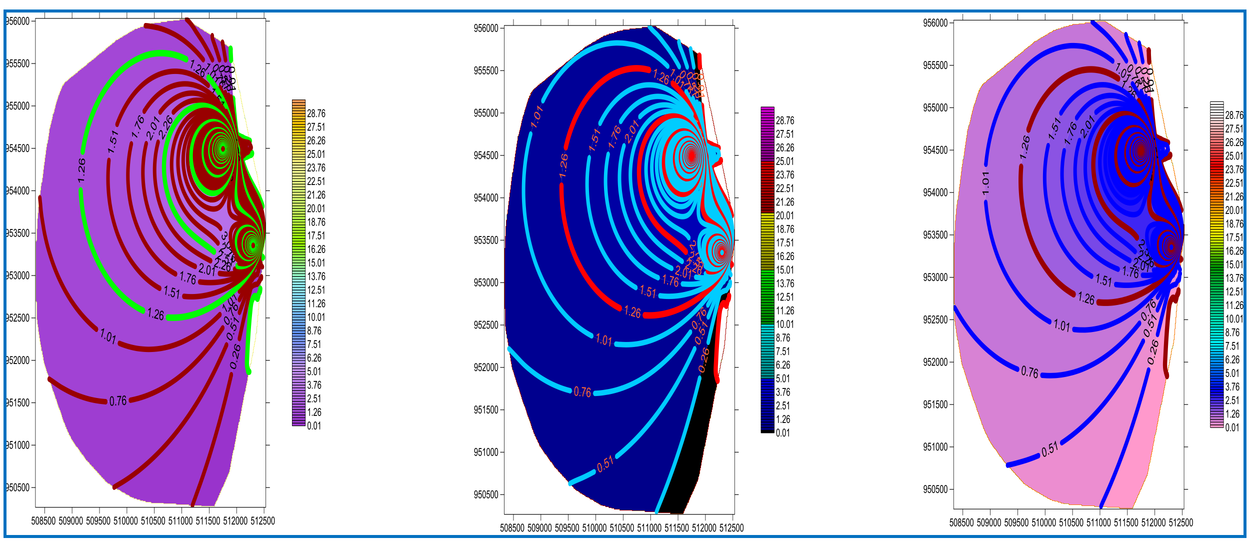

Figure 15. Plot of simulated composite drawdown contour lines distributions produced in unconfined aquifer as a result of a recharge boundary and two wells operating simultaneously located at (x_w, y_w) coordinates: - (512300.00, 953358.00) and (511750.00, 954495.00), by doubling the rates of pumping of that of the designed rates capacity of the wells i.e. 0.090 m^3/s for MJBH-1 and 0.09 m^3/s for MJBH-2, the contour lines prepared for simulated drawdown at any time (t) supposing the aquifer at well field takes the approximated transmissivities (T_{min}), (T_{avg}), (T_{max}) in sequence from left to right as shown in the figure above.

4.3. Established Radius of Influence

The radius of influence is the region of group well fields where the potentiometric head is lowered for the reason of the boreholes are operating to capture groundwater in the field of that aquifer. As most of the time the flow proceeds from the high point of the well field site of aquifer into the low spot in the boreholes, results in forming a cone of depression which also known as zone of (well) influence. On such occasion flow must converges towards the boreholes and since the extent through which the flow occurs decreases to the direction of the boreholes, the hydraulic gradient must be steeper to toward the boreholes and flatter in outward direction except that boundary may hinder its extension. As the operation of the boreholes going on the outwards extensions of the wells influences decreases and eventually maintained to point where no more drawdowns to be measured.

In view of that, the radius of influence for operation conditions of the boreholes at Mojo well field is established based on the stretches of the boreholes influences from the origins of the boreholes to settings of digitalized arbitrary observation points all over the vicinity of the well field where extensions for cones of depressions of the composed drawdown achieves a cessations at extreme bounds. From the produced distributions of flow lines plots, rapid drawdown prevails at the initial stage of the pumping boreholes and as the operations of pumping in the boreholes getting progresses, the composite drawdown diminishingly returns to maintain constant and ultimately approaches equal to zero as influences of entire functioning of the boreholes in the well field. Hence, at occasions such situation comes true the radius of influence can be established from the Cooper – Jacob equation.

$$\mathbf{s = \frac{Q}{4\pi T} \ln \frac{2.25Tt}{r^2 S}} \qquad (4.7)$$

In his study Marsily discovered that at on occasions when the pumping tests carried out nearby to a boundary, equation (4.9) is used to evaluate the distance between the recharging image well and the required point where the drawdown is measured (de Marsily, 1986). As Table 5 shows values that computed radius of influences for individual well appreciable equivalent with the straight stretches of length from the river those had been used to locate the imaginary injecting wells with equal distance but on the other side of the river. As the distances for the three boreholes from the pumping wells and the distance from the assumed imaginary wells to the desired point at which the drawdown evaluated (i.e. verge of the recharging perennial river in this case) are equals and as a result the simulated drawdown at these points are satisfying the reality in maintaining equality with zero as expected. Provided that when and where s=0, the later equality in equation (4.7) must become into existence.

So that:

$$\frac{2.25Tt}{r^2S} = 1 \qquad (4.8)$$

The radius of influence R_{cj} at any time t, through conferring to equation (4.9) is given by:

$$R_{cj} = \sqrt{\frac{2.25Tt}{S}} \qquad (4.9)$$

In favor for coincidence of the necessitating event that permits the application Copper – Jacob equation to establish the radii of influences of the pumping boreholes in the well field, since the shortest distances those utilized in setting the real pumping wells and the injecting imaginary wells are substantiating the reality in maintaining the composite drawdown at verge of the river equality with zero, the of influences for the mojo boreholes are established those dimensions consumed in the simulation of the required composite drawdowns.

Therefore; the radius of influences for the particular borehole i.e. MJBH-1=156.52m, MJBH-2=268.16m and MJBH-3=254.54m from the center of the boreholes towards the embankment edge of the closer recharging Mojo River. Thus, for the boreholes in Mojo well field, for the determined of influences, corresponding time may last for water to rejoins is accordingly calculated as:

$$R_{cjpw1} = \sqrt{\frac{2.25Tt_{p1}}{S}} \quad (4.8a)$$

$$R_{cjpw2} = \sqrt{\frac{2.25Tt_{p2}}{S}} \quad (4.8b)$$

$$R_{cjpw3} = \sqrt{\frac{2.25Tt_{p3}}{S}} \quad (4.8c)$$

Where:-

Q = is pumped flow (m^3/s)

r = is any distance from the well (m)

$R_{(cj)}$ = is radius of influence according to the Cooper - Jacob equation (m)

s = is drawdown in general (m)

S = is storage coefficient (dimensionless)

T = is transmissivity (m^2/s)

Using the Cooper- Jacob equation as described above, the aquifer hydrological parameters as tabulated in Table 3, the next times (i.e. t_1, t_2 and t_3) those may possible that the nearby river needs to respond against continual influences of the pumping boreholes signifying to the established radius of influences (viz. R_{cipw1}, R_{cipw2} and R_{cipw3}) for individual borehole is calculated and presented as tabulated in Table 5. The pumping times durations (t_{p1}, t_{p2} and t_{p3}) those recorded until three consecutive similar drawdowns had been observed there in MJBH-1, MJBH-2 and MJBH-3 boreholes respectively during the pumping test are presented as Table 5 shows for proportionality.

***Table 5:** Established radius of influence and its associated time*

Descriptions	Names of the Boreholes			Remarks
	MJBH-1	MJBH-2	MJBH-3	
Shortest distance at right angle to the recharging river used in the simulation where distance from real and image well equals and considered as radius of influences (m)	R_{cipw1}	R_{cipw2}	R_{cipw3}	
	156.52	268.16	254.54	
Calculated time for corresponding radius of Influence for each wells that takes to arrive at point where simulated drawdown (s=0), (sec)	t_1	t_2	t_3	
	33,583.44	98,573.80	88,815.47	(T_{max}, S_{min})
	101,227.60	297,122.30	267,708.65	(T_{min}, S_{max})
	65,137.46	191,190.85	172,263.89	(T_{avg}, S_{avg})
Duration of time that had been taken during pumping test when there three constant reading of the drawdowns observed, for comparisons (sec)	86,400	244,800	172,800	

***Table 6:** Recalculated distance from the center of the boreholes to the recharging river using time equivalent to testing time resulted in achieving three consecutive drawdowns in well during pumping test*

Descriptions	Names of the Boreholes			Remarks
	MJBH-1	MJBH-2	MJBH-3	
Established radius of influences for the boreholes	156.52	268.16	254.54	
Distance recalculated for time travel equivalent to testing time that were resulted in reading three conductive drawdowns in the well (m)	150.67	258.13	245.02	T_{min},S_{avg}
	161.73	277.08	263.01	T_{max},S_{avg}
	156.52	268.16	254.54	T_{avg},S_{avg}
Calculated time for corresponding radius of Influence which is closer to the time at which three consecutive reading were obtained (s=0), (sec)	65,137.46	191,190.85	172,263.89	T_{avg},S_{avg}

As per the results of the estimated times shown in Table 5 and the distances resulted from recalculating using the corresponding times of of influences of the boreholes as tabulated in Table 6 shows, the resulting times are comparative to the duration of pumping test times which expected in accomplishing a state of equilibrium and the distances recalculated are also equivalent to the determined radius of influence which resulting zero drawdowns, from these conditions a conclusion drives that there is a reality of perfect hydraulic connection between the pumping boreholes and the conveying media of the aquifer ranges the adjacent river that may also extends to the spots of the imaginary wells locations.

As the Figure from 17 up to 29 clearly illustrate, the results from superposing of the simulated drawdowns contour lines plots the influence of entire pumping boreholes drives the cones of depression to develop an unconventional formations as it ranges further up gradient and lesser down gradient. Such occurrences of events may suggests to come about due to the fact of the existing recharging boundary condition at the closeness of the pumping boreholes and this condition is already substantiated as there lays the Mojo Perennial River. From the mean time the effect of recharge boundary is to retard the rate of drawdown, change in drawdown can become zero if the well comes to be supplied entirely with recharges water. Since the initial basic assumptions to conduct analyses, the formations of the aquifer are homogeneous and isotropic, the cone of depression for the image well touches the boundary at the same time that the actual cone touches it. From this point on, as pumping continues, the effect on the shape of the cone of depression of the pumped well is exactly the same as that of a real well located where the image well is postulated reasoning that the river is exactly undertaking the action of the injecting those imaginary wells supposed to perform. Then through the analytical solution and the principle of the superposition, the accumulating up of a series of drawdowns resulting from pumping and injection wells located according to the geometry of the boundary which specified, solutions of composite drawdown obtained in which that distributions of the contours lines plots of resulting composite drawdown represents the drawdowns of radial symmetric in which the arrangements of their cones of expansions in the well field area are showing uniform.

However; from the simulated drawdown contour plots trends indicated we have noticed that the calculation of the cone of influence and hypothetical cones of depression is not analogous such that the resulted configurations of the cones of depression trends are radial asymmetric. Hence then it is usually accepted that a realistic estimation of the radius of influence can be obtained from the Cooper – Jacob equation (Cooper and Jacob, 1946). We prefer to this equation because the Theis equation denotes to the radius of influence that extends to the infinite in a well pumped at a constant radius. As a result the study takes into attentions by supposing the aquifer where the pumping boreholes locate is the unconfined aquifer in which these wells may operate under unsteady state condition and devoid of local recharge to the aquifer. Hence, the radius of influence and estimations of its respective time is established by using the Cooper–Jacob equation listed at (4.7) herein as this equation is commonly accredited in obtaining a realistic approximation (Cooper and Jacob, 1946) through setting boundary condition and the principle of superposition.

To carry out the fixing task of the radius for the three boreholes completed through conducting various trials to fix the contour line plot for composite drawdown until defined shape for the configurations of the radius of influence that obtained from the last minimum drawdown contour line, by selecting from the contour lines graphs which already organized in surfer. Then for the minimum composite drawdown being selected, the of influences those are directly involved during superposition in simulating the resulted composite solution that represents the effects of operating entire pumps at three boreholes , have been filtered from the numerous portion of data, to have the particular radius of extent for each wells out of sets of extents which were supposed, summed up jointly and resulted the representative composite drawdown at that point and time, that is identical to the selected drawdown presents defined shape for extending cone of depression of contour line at end region inside the well field system. Henceforth, the related radius of influence /well of influence also represent the distances of the resulted composite drawdowns that obtained from accumulations of the distances of the three boreholes and such that the composite drawdown for defined extent is the same everywhere in the well field, so it lays on the same contour lines plots at any space and time away from the origins of the boreholes. This is because the distribution of contour line for a particular resultant drawdown is the same anywhere in the field and shows an overall effect/stress that the entire pumping wells may put on to the aquifer when all/partial operating simultaneously Figures from 8 up to 17 illustrates.

As the main objective of this study is to identify the potential threats of the water contaminants and establish defined radius of influence in target of that the pollutants threats will not acquire interactions with the water supply boreholes. In order to secure this target we have fixed the extent of the radius of influence by approximating the extent of radial extensions of the cones of depressions for different scenario of the constant pumping rates to systematically evaluate the extensions of the radius of influences with respect to the identified localities of the potential threatening of the pollutants.

Table 7: *Expected potential threatening sites existing around Mojo well field as observed during field assessment works.*

Descriptions of the detected sites of potential threats	**Coordinates locations**		**Distance from the boreholes to the supposed threats sites (m)**		
	Easting	**Northing**	**MJBH-1**	**MJBH-2**	**MJBH-3**
Mojo waste damping site	514266	951002	3068.53	4304.80	3550.09
Mojo tannery	512265	951324	2034.30	3212.55	2565.82
East African tannery	512134	949857	3504.93	4653.87	4032.54
Friendship tannery	512142	949811	3550.52	4700.37	4078.41
Three Privates Limited Tanneries at left edge of Mojo River just beside the friendship	512091	949881	3483.28	4626.58	4009.48
WAS Wadial sundus petroleum co. LTD	512489	949806	3557.02	4746.88	4093.22
Yetebaberut petroleum co. LTD	514117	949874	3929.34	5191.95	4449.17
OILIBYA petroleum co. LTD	512668	949762	3614.78	4821.20	4153.45
Total no-1 petroleum co. LTD	512933	949475	3934.26	5157.51	4474.45
Total no-2 petroleum co. LTD	513627	949053	4504.88	5756.60	5042.14

Accordingly, by making a reduction to the simulated composite drawdowns, fixed radius of influences conducted. For high transmissivity value is lowered to have relatively seemingly defined shape for the configured plots of contours lines for the simulated drawdowns. Whereas the simulated drawdown value is increased for the low transmissivity and average transmissivity in slightly small figure in order to have comparatively equivalent radius of influences within similar cones of depression patterns and area in the well field. The designed capacity of pumping rates in the boreholes are also manipulated by increasing their designed rate with double amount and in alternative scenario by diminishing the same rates in half rate and using different values of the simulated composite drawdowns which completed via superimposing of multiple operating boreholes in the well field

Therefore; These are done for various cases of scenarios adopting different values of the approximated transimmissivity and storativity values letting such that the aquifer at the well field possesses those parameters as its property and for pumping rates of different values that the boreholes operating under various conditions, in order to reach an out most approximation, thus implications may useful in scheduling improved water resources management and planning conditions of pumping operation and making suitable protections of the environmental impacts while in line to secure sustainable withdrawing water from the aquifer at needed well field. So that the extent that it covers for different pumping rates while the pumps are operating simultaneously and estimated time travels are tabulated as Tables from 8 up to 12 shows in this sub section. Similarly the times and extensions for the remaining others scenarios for comparing are clearly deferred in the Tables affixed at the portion of B1 up to B4 shows.

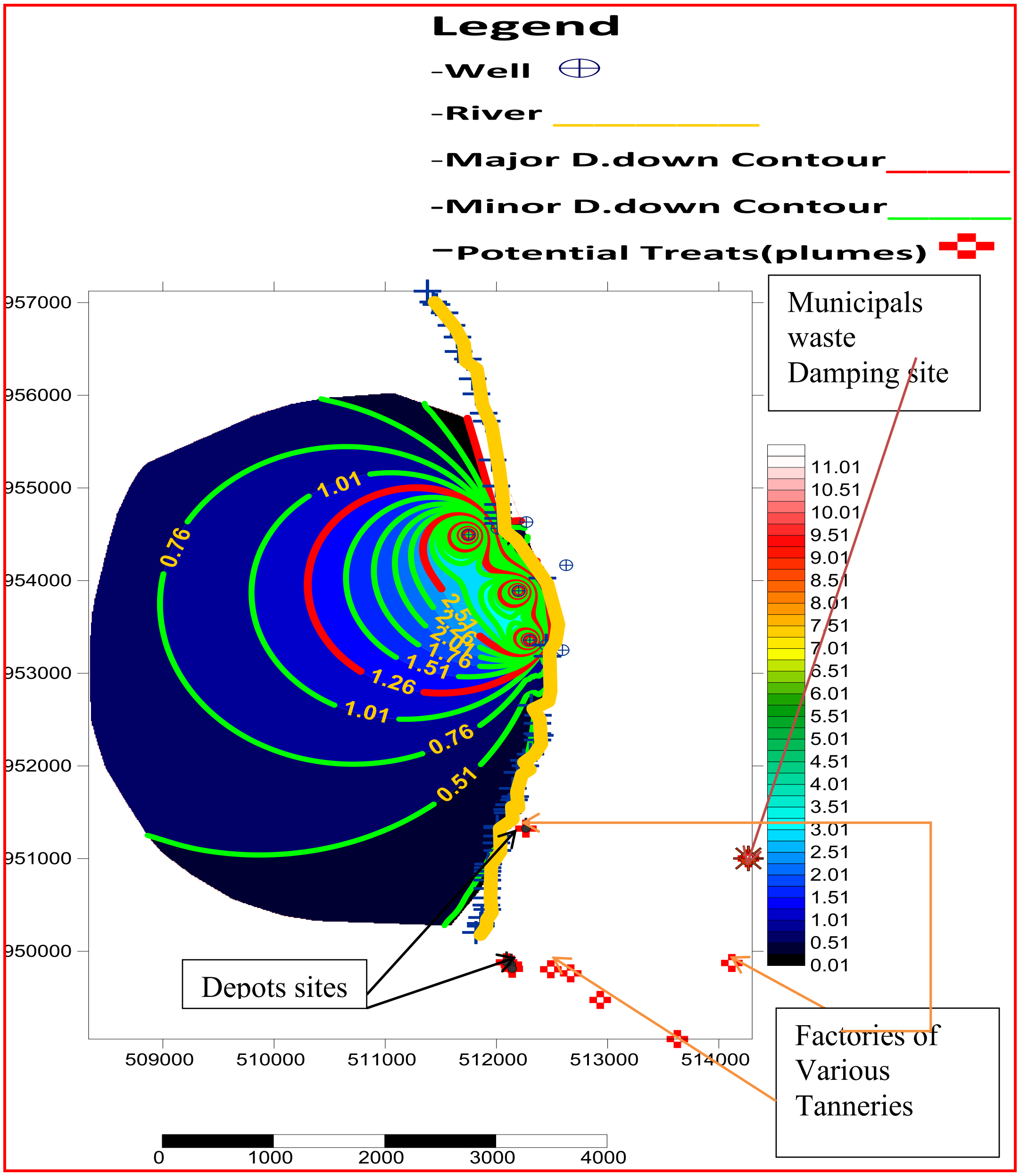

Figure 16. Schematic view of the distributions of the cones of wells influences as superposed for three wells are operating simultaneously with designed capacity of pumping rates with respect to the vicinity of the potential threats those detected during field assessment tasks.

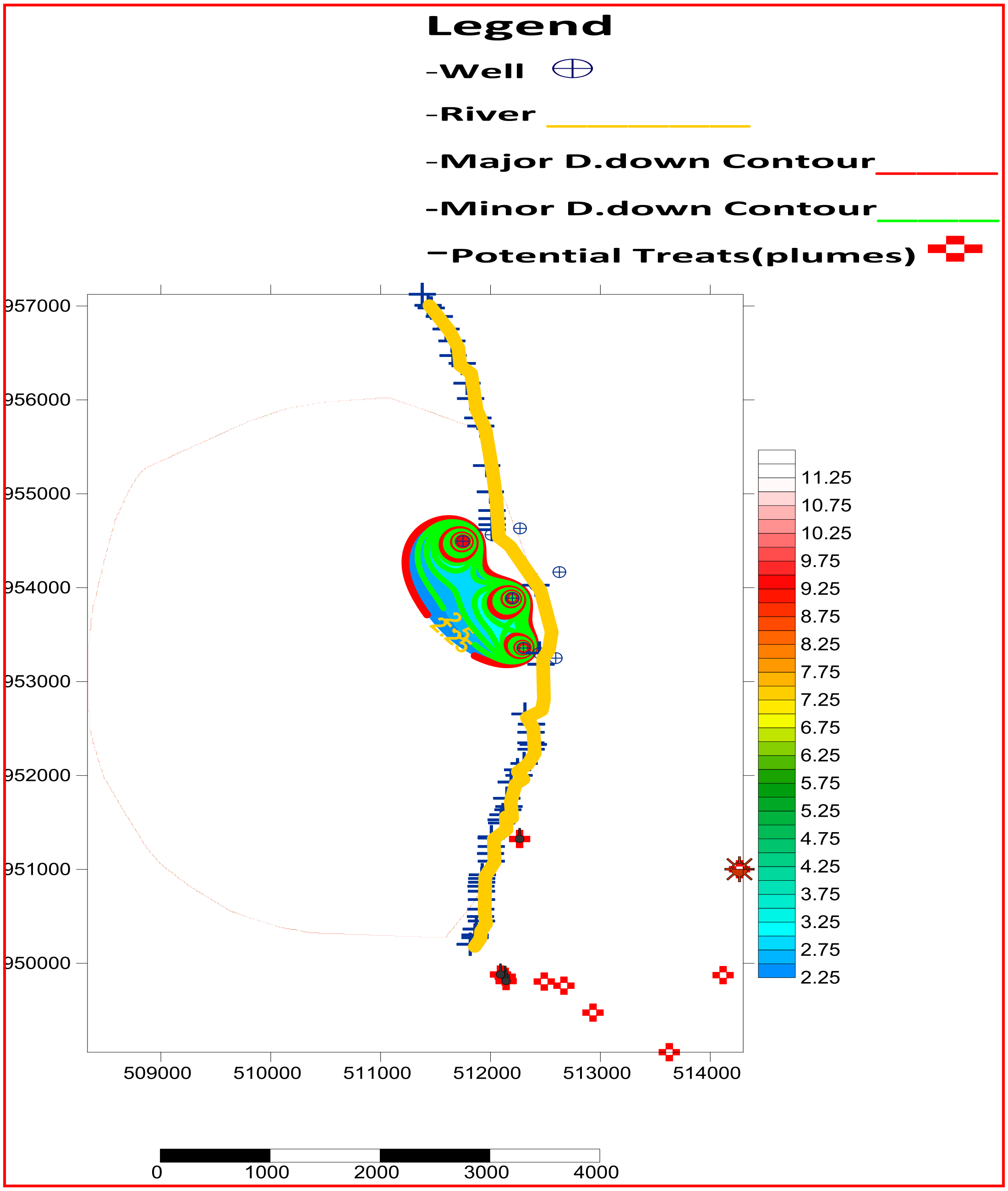

Figure 17. Schematic view of the contraction radius of influence in occasion say that the water level at the well field required to depressed by 2.25m for protecting entrance of the potential threaten pollutants when the pumps at the boreholes in operation by the designed capacity rates with respect to the vicinity of the potential threats those detected during field assessment tasks.

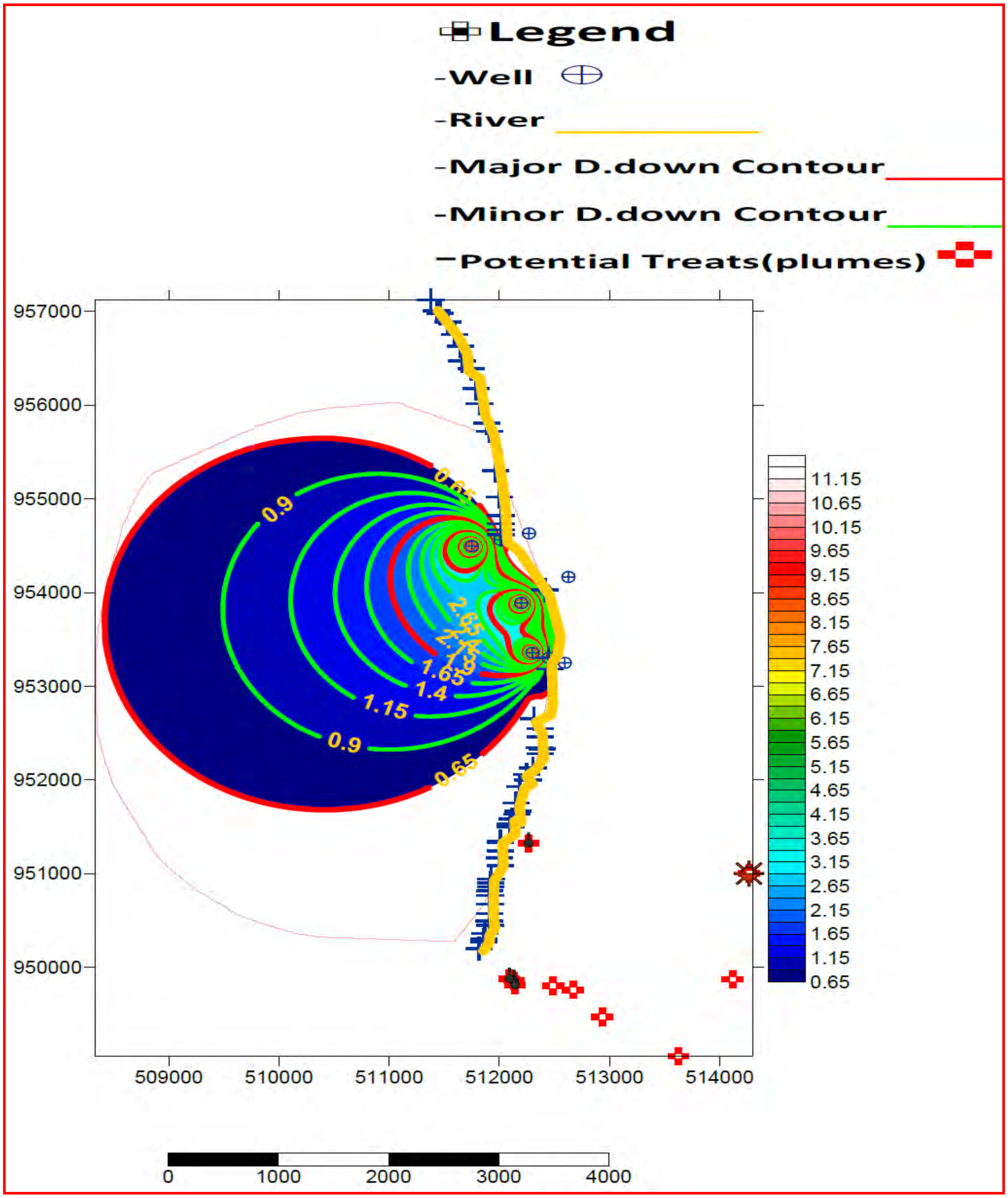

Figure 18. Schematic view of the time honored radius of influence in attempt to have defined shape for cone of depression magnitude in the well field setting the superposed drawdowns diminishing by 0.65m from the constant head in which the boreholes are assumed to operate with their designed capacity of pumping rates and letting the aquifer to adopt the maximum estimated transmissivity value at case the pumps at the boreholes are all functioning, then the extents of the cone of influence configures a shape as illuminates with respect to the existing potential threaten locations those surrounding the well field

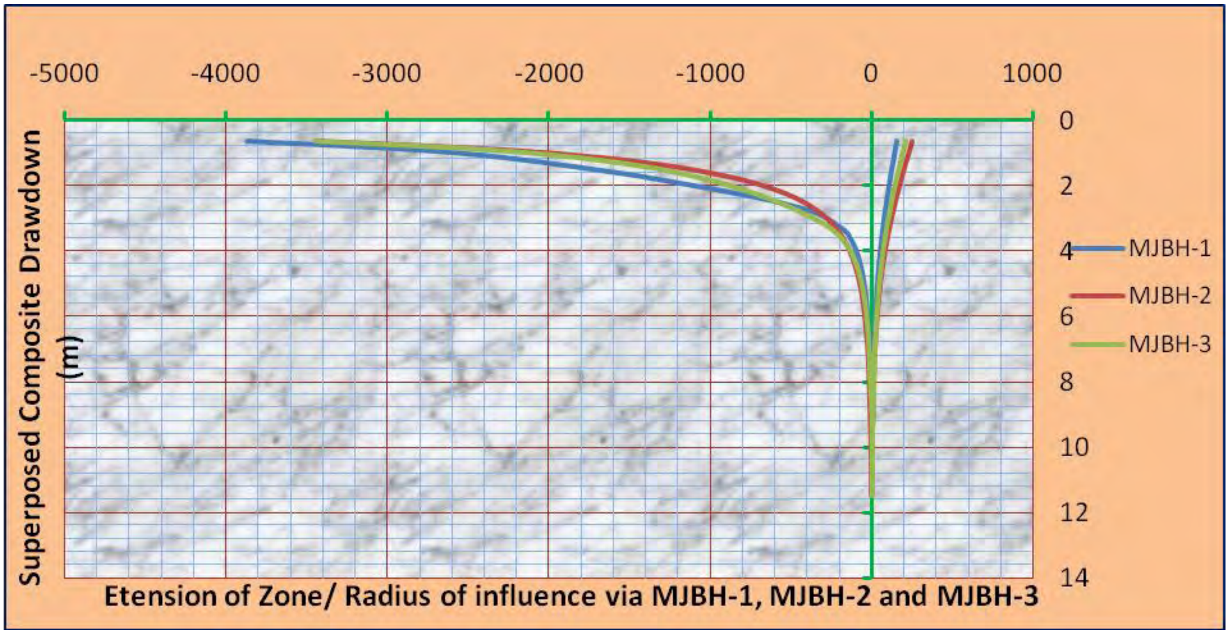

Figure 19. Depiction of the crosectional views of the extensions profiles of the radius of influence of Figure 18 crossways along the MJBH-1,MJBH-2 and MJBH-3

Table 8. *Fixed radius of influences and its corresponding time for designed discharge of the wells*

<table>
<tr><th colspan="2" rowspan="2">Descriptions</th><th colspan="3">Name of Boreholes</th><th rowspan="2">Remark</th></tr>
<tr><th>MJBH-1</th><th>MJBH-2</th><th>MJBH-3</th></tr>
<tr><td rowspan="2">Parameters Adopt to the Aquifer at Mojo Well Field</td><td>Approximated Transmissivity (m^2/s)</td><td>0.003626</td><td>0.003626</td><td>0.003626</td><td>Maximum Transmissivity, T_{max}</td></tr>
<tr><td>Storativity</td><td>0.01116</td><td>0.01116</td><td>0.01116</td><td>Minimum Storativity, S_{min}</td></tr>
<tr><td colspan="2">Constant Pumping Rate(m^3/s)</td><td>0.045</td><td>0.045</td><td>0.04383</td><td>Pumps operating by rates of designed capacity</td></tr>
<tr><td rowspan="2">Fixed Radius of Influence (m)</td><td>Extents(m)</td><td>153.82</td><td>316.11</td><td>218.82</td><td rowspan="2">Contour line/Cone of depression from well origin to the recharge river region where the composite drawdown depressed to depth of 0.65m below the constant head</td></tr>
<tr><td>Travel Time (Days)</td><td>0.73</td><td>3.06</td><td>1.5</td></tr>
<tr><td rowspan="2">Fixed Radius of Influence (m)</td><td>Extents(m)</td><td>3854.65</td><td>3551.44</td><td>3782.57</td><td rowspan="2">Contour line/Cone of depression from well origin to the right edge where the composite drawdown depressed to a depth 0.65m below the constant head</td></tr>
<tr><td>Travel Time (Days)</td><td>456.35</td><td>386.36</td><td>446.42</td></tr>
</table>

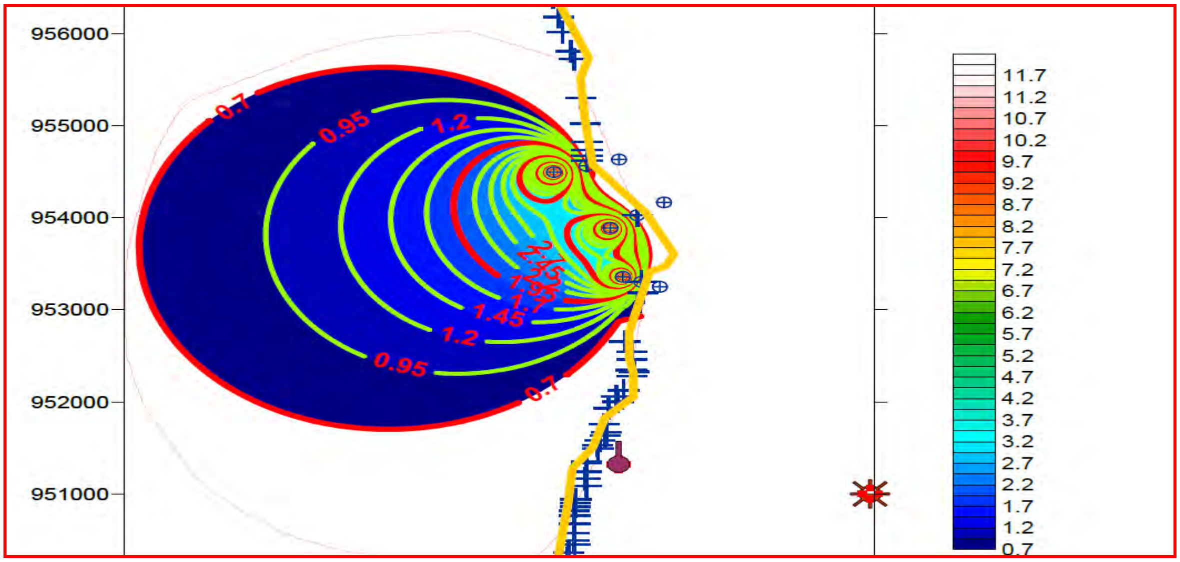

Figure 20. Schematic view of the established radius of influence in attempt to have defined shape for cone of depression magnitude in the well field setting the superposed drawdowns falling by 0.70m from the constant head in which the boreholes are assumed to operate with their designed capacity of pumping rates and letting the aquifer to adopt average estimated transmissivity value at case the pumps at the boreholes are all functioning, the extents of the cones of influence configures a shape such illuminates with respect to the existing potential threatening locations those surrounding the well field

***Table 9:** Fixed radius of influences and its corresponding time for designed discharge of the wells*

Descriptions		**Name of Boreholes**			**Remark**
		MJBH-1	**MJBH-2**	**MJBH-3**	
Parameters Adopt to the Aquifer at Mojo Well Field	***Approximated Transmissivity (m^2/s)***	0.003396	0.003396	0.003396	Average Transmissivity, T_{avg}
	Storativity	0.02032	0.02032	0.02032	Average Storativity, S_{avg}
Constant Pumping Rate(m^3/s)		0.045	0.045	0.04383	Pumps operating by rates of designed capacity
Fixed Radius of Influence (m)	**Extents(m)**	153.8238	250.7459	207.1445	Contour line/Cone of depression from well origin to the recharge river region where the composite drawdown depressed to depth of 0.70m below the constant head
	Travel Time (Days)	1.415	3.787	2.639	
Fixed Radius of Influence (m)	**Extents(m)**	3852.741	3505.962	3728.353	Contour line/Cone of depression from well origin to the right edge where the composite drawdown depressed to a depth 0.70m below the constant head
	Travel Time (Days)	890.2739	737.472	848.7003	

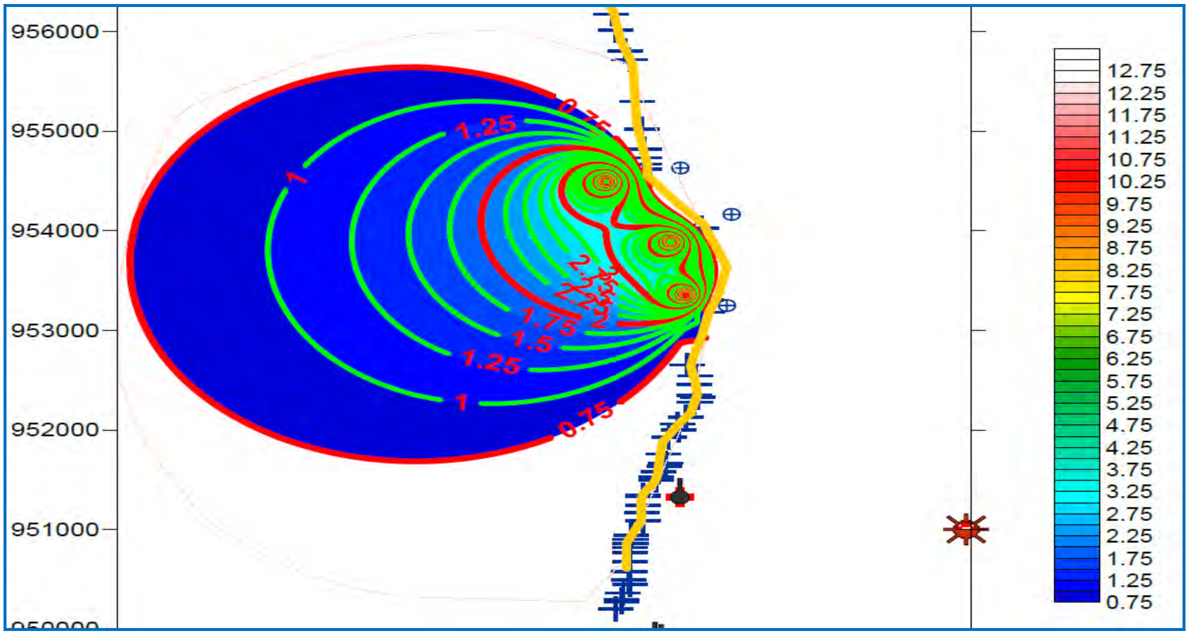

Figure 21. Schematic view of the fixed radius of influence in attempt to have defined shape for cone of depression in the well field setting the superposed drawdowns dropping by 0.75m from the constant head at case in which the boreholes are assumed to operate with their designed capacity of pumping rates and letting the aquifer adopts minimum estimated transmissivity value at case the pumps at the boreholes are all functioning, the extents of the cones of influence configures a shape as such illuminated with respect to the existing potential threatening locations those surrounding the well field

Table 10: *Fixed radius of influences and its corresponding time for designed discharge of the wells*

Descriptions		**Name of Boreholes**			**Remark**
		MJBH-1	**MJBH-2**	**MJBH-3**	
Parameters Adopt to the Aquifer at Mojo Well Field	***Approximated Transmissivity (m^2/s)***	0.003147	0.003147	0.003147	Minimum Transmissivity, T_{min}
	Storativity	0.02926	0.02926	0.02926	Maximum Storativity, S_{max}
Constant Pumping Rate(m^3/s)		0.045	0.045	0.04383	Pumps operating by rates of designed capacity
Fixed Radius of Influence (m)	**Extents(m)**	184.57	382.5	218.82	Contour line/Cone of depression from well origin to the recharge river region where the composite drawdown depressed to depth of 0.75m below the constant head
	Travel Time (Days)	3.160	13.570	4.520	
Fixed Radius of Influence (m)	**Extents(m)**	3852.741	3505.962	3728.353	Contour line/Cone of depression from well origin to the right edge where the composite drawdown depressed to a depth 0.75m below the constant head
	Travel Time (Days)	890.2739	737.472	848.7003	

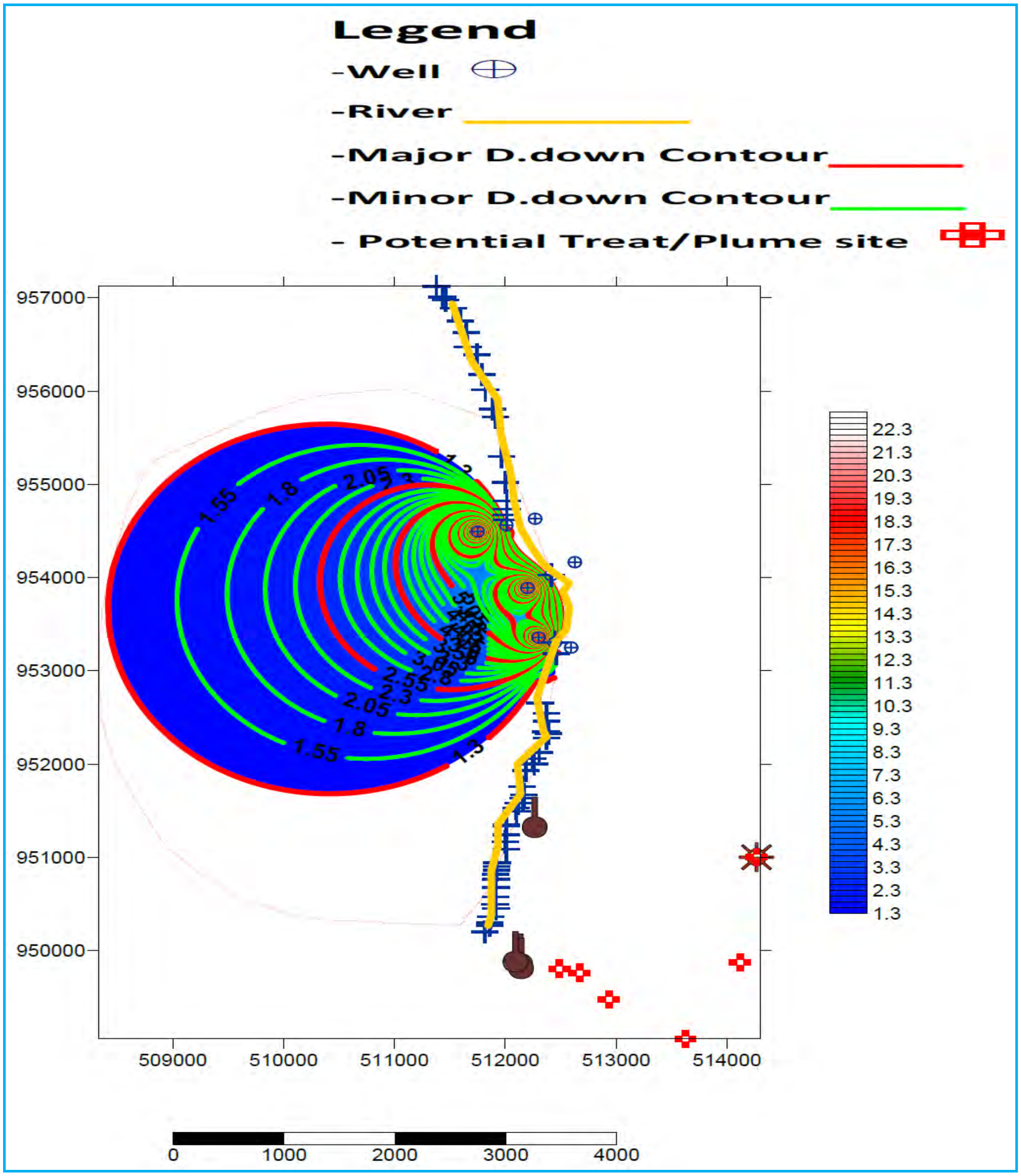

Figure 22. Schematic view of the tapered radius of influence in attempt to have defined shape of cones of depressions in the well field setting the superposed drawdowns to sink by 1.3m from the constant head in this case the boreholes are assumed to application with increased rates such as doubling that of designed capacity of pumps in the boreholes and the aquifer adopts maximum estimated transmissivity value whereas the pumps at the boreholes are all functioning, the extents of the cones of influence formation appears as per illuminated with respect to the existing potential threaten locations those surrounding the well field

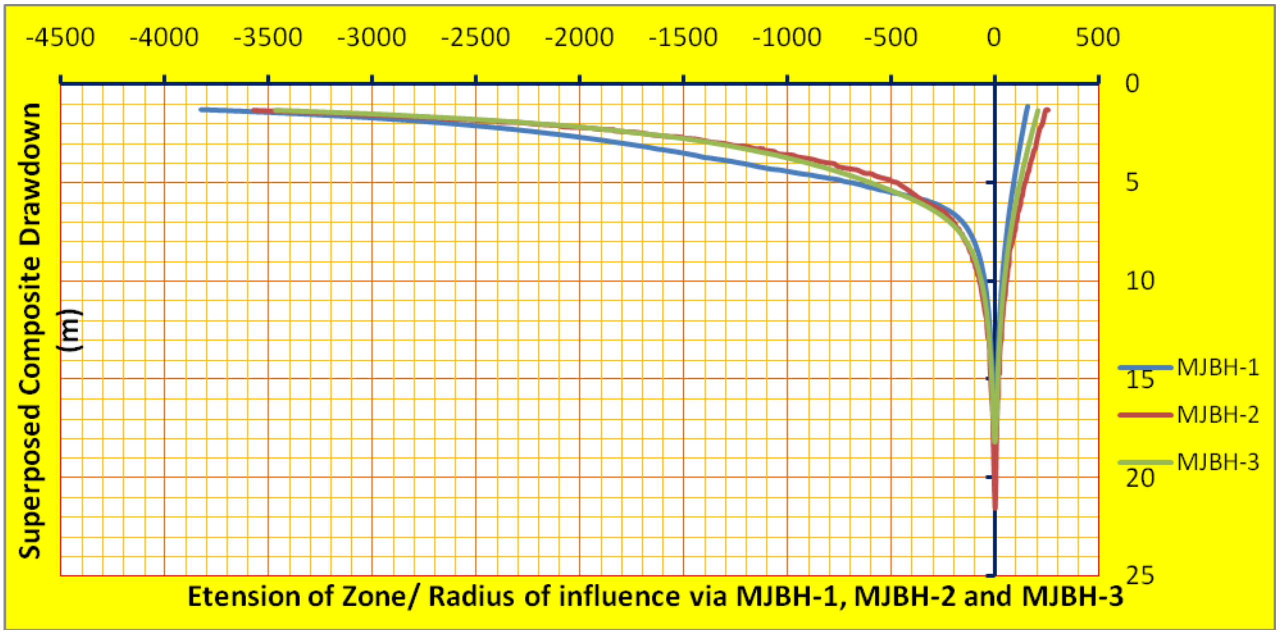

Figure 23. Depiction of the crosectional views of the extensions profiles of the radius of influence of Figure 22 transversely along the MJBH-1,MJBH-2 and MJBH-3

Table 11: *Fixed radius of influences and its corresponding time for designed discharge of the wells*

Descriptions		**Name of Boreholes**			**Remark**
		MJBH-1	**MJBH-2**	**MJBH-3**	
Parameters Adopt to the Aquifer at Mojo Well Field	***Approximated Transmissivity (m^2/s)***	0.003626	0.003626	0.003626	Maximumu Transmissivity, T_{max}
	Storativity	0.01116	0.01116	0.01116	Minimum Storativity, S_{min}
Constant Pumping Rate(m^3/s)		0.09	0.09	0.08776	Pumps operating by double rates of designed capacity
Fixed Radius of Influence (m)	**Extents(m)**	184.57	316.11	218.82	Contour line/Cone of depression from well origin to the recharge river region where the composite drawdown depressed to depth of 1.3m below the constant head
	Travel Time (Days)	1.05	3.06	1.5	
Fixed Radius of Influence (m)	**Extents(m)**	3854.65	3551.44	3782.57	Contour line/Cone of depression from well origin to the right edge where the composite drawdown depressed to a depth 1.3m below the constant head
	Travel Time (Days)	456.35	386.36	446.42	

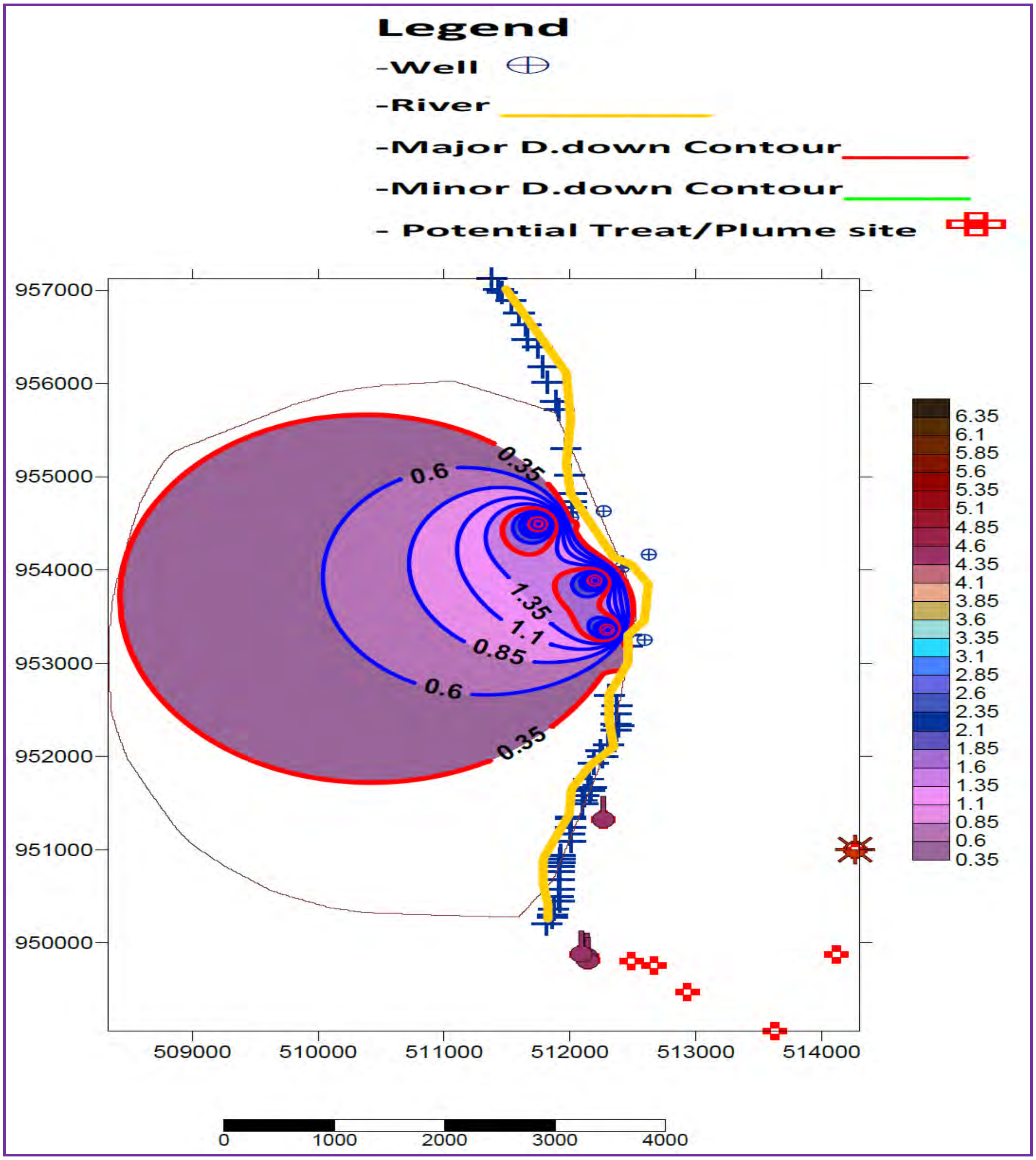

Figure 24. Schematic view of fixed radius of influence in attempt to have defined shape of cones of depressions in the well field setting the superposed drawdowns sinking by 0.35m from the constant head in this case when the boreholes are operating decreasing by the half rates from that of the designed capacity of pumps in the boreholes and the assumed aquifer adopts maximum estimated transmissivity value while the pumps at the boreholes are functioning, the determined extent of the cone of influence arrangement appears as such illuminated with respect to the existing potential threaten locations those surrounding the well field

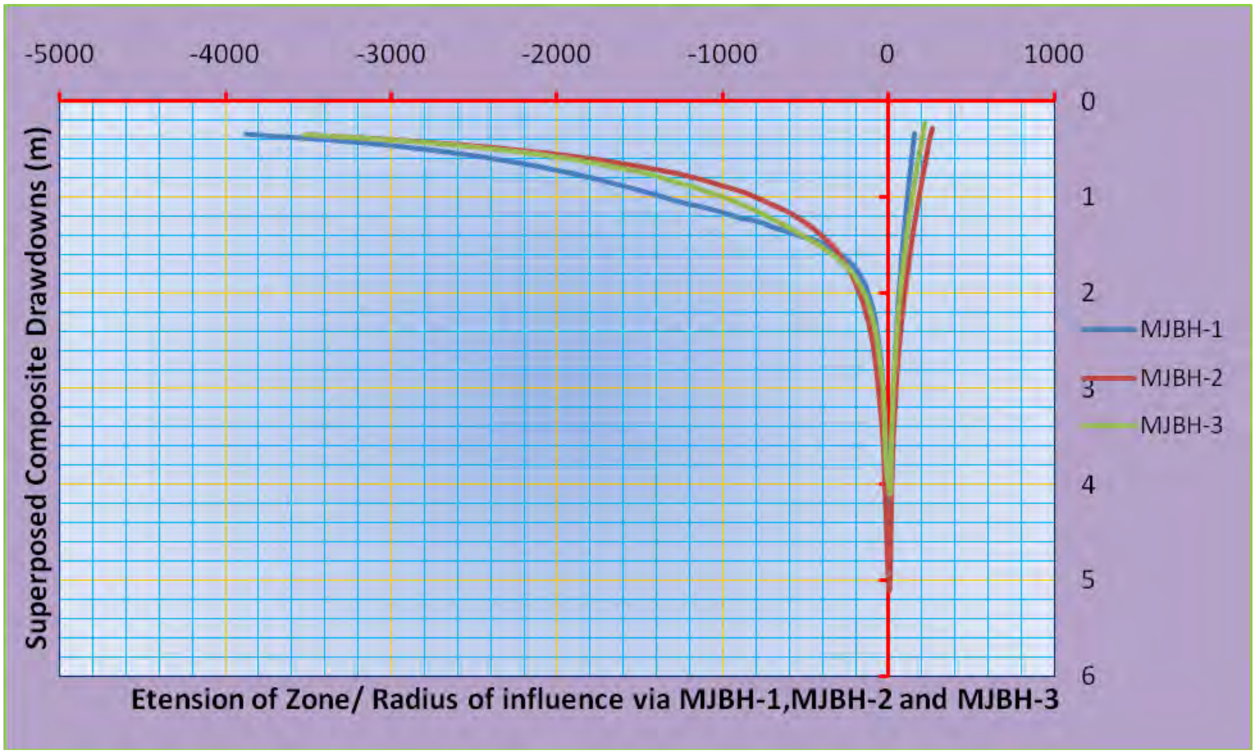

Figure 25. Depiction of the correctional views of the extensions profiles of the radius of influence of Figure 24 crosswise along the MJBH-1, MJBH-2 and MJBH-3

Table 12: *Fixed radius of influences and its corresponding time for designed discharge of the wells*

Descriptions		Name of Boreholes			Remark
		MJBH-1	MJBH-2	MJBH-3	
Parameters Adopt to the Aquifer at Mojo Well Field	***Approximated Transmissivity (m^2/s)***	0.003626	0.003626	0.003626	Maximum Transmissivity, T_{max}
	Storativity	0.01116	0.01116	0.01116	Minimum Storativity, S_{min}
Constant Pumping Rate(m^3/s)		0.09	0.09	0.08776	Pumps operating by half rates of designed capacity
Fixed Radius of Influence (m)	**Extents(m)**	151.68	249.52	208.97	Contour line/Cone of depression from well origin to the recharge river region where the composite drawdown depressed to depth of 0.35m below the constant head
	Travel Time (Days)	0.74	2	1.44	
Fixed Radius of Influence (m)	**Extents(m)**	3621.72	3279.45	3502.15	Contour line/Cone of depression from well origin to the right edge where the composite drawdown depressed to a depth 0.35m below the constant head
	Travel Time (Days)	423.7	346.76	402.83	

This circumstance may be resulted as immediate to initiate of pumping operations in the boreholes, a region of reduced water pressure is formed around the pumped wells. Because it obvious that water normally moves from high to low gradient, movement of water is pointing from recharging river to the aquifer since the surface recharge boundary (Mojo River in this case) exists at higher elevation than static water levels closer to the pumping boreholes, water pumped into the aquifer from the river/image well provided that the aquifer has a hydraulic connection with the river. Then flow of water proceeds from the well field site aquifer into the boreholes in which results in forming a cone of depression which also known as zone of influence. On this occasion as water must converges on to the boreholes from all directions and because the area through which the flow occurs decreases toward the well and, the hydraulic gradient must be steeper to toward the boreholes as the illustrations of the profiles of the extensions for cones of depressions on Figures 22, 23, 24, 32, 33, and 34 depict the steeper slopes are noted to be towards the recharging river boundary. The groundwater within the areal extent of the cone of depression is flowing towards the well. The configurations of the contour lines plots of cone of depression show that the shape of the cone is created very quickly, and then the cone goes downward. Through the advancements of pumping in the boreholes the cone of depression expands and holds more areal coverage in well field and ultimately can be captured out of the aquifer. However, capture zones must be defined by the length of time of capture water at the farthest radial distance within the cone of depression will take longer to reach the well than water within close proximity of the well. In the Theis equation, drawdown is inversely proportional to transmissivity meaning higher transmissivity values result in lower drawdown values. The slope of the cones of depression and its radius of influence depends on the type of aquifer and its hydraulic characteristics. So that in the aquifers of high transmissivity, the gradient of cone of depression is less and its radius is large, as compared with aquifers of low transmissivity. Henceforth, the shape and the size of cones of depressions are dependent primarily upon the wells pumping rate, elapsed time since start of pumping, aquifer transmissivity, aquifer type, and aquifer storativity. Such incident appears gradually in unconfined aquifer and time travel for the confined one is faster than the unconfined aquifer because the storage coefficient of an unconfined aquifer closely approximates the specific yield of the material in the aquifer so the cone of depression expands slowly. Instead, a lowering of the water table results in the aquifer with a low transmissivity which will cause increase of the drawdown in the boreholes initially and as well in the aquifer gradually. Therefore, the distributions plots of the contours lines of the simulated drawdown solution as the above figures illustrate, are asymmetric, irregular and display an elongation to North East wards reason that different types of transmissivity of the aquifer considered in conducting the simulation of the composite drawdown. As it can be noticed from the produced plots, the simulated drawdown in which the aquifer adopts approximated value of maximum transmissivity (T_{max}) diminishes earlier and but at further distance from the origin of the pumping well than those cases in which the aquifer adopts to maintain estimated an average and minimum transmissivity values T_{avg} and T_{min} respectively. In the case of aquifer assumes to adopt minimum transmissivity value the drawdown reduces as influence of operating boreholes continual and drops of composite drawdown takes place progressively with time whereas for case when using the average value the drawdowns value falls at mean of the two extreme scenarios described.

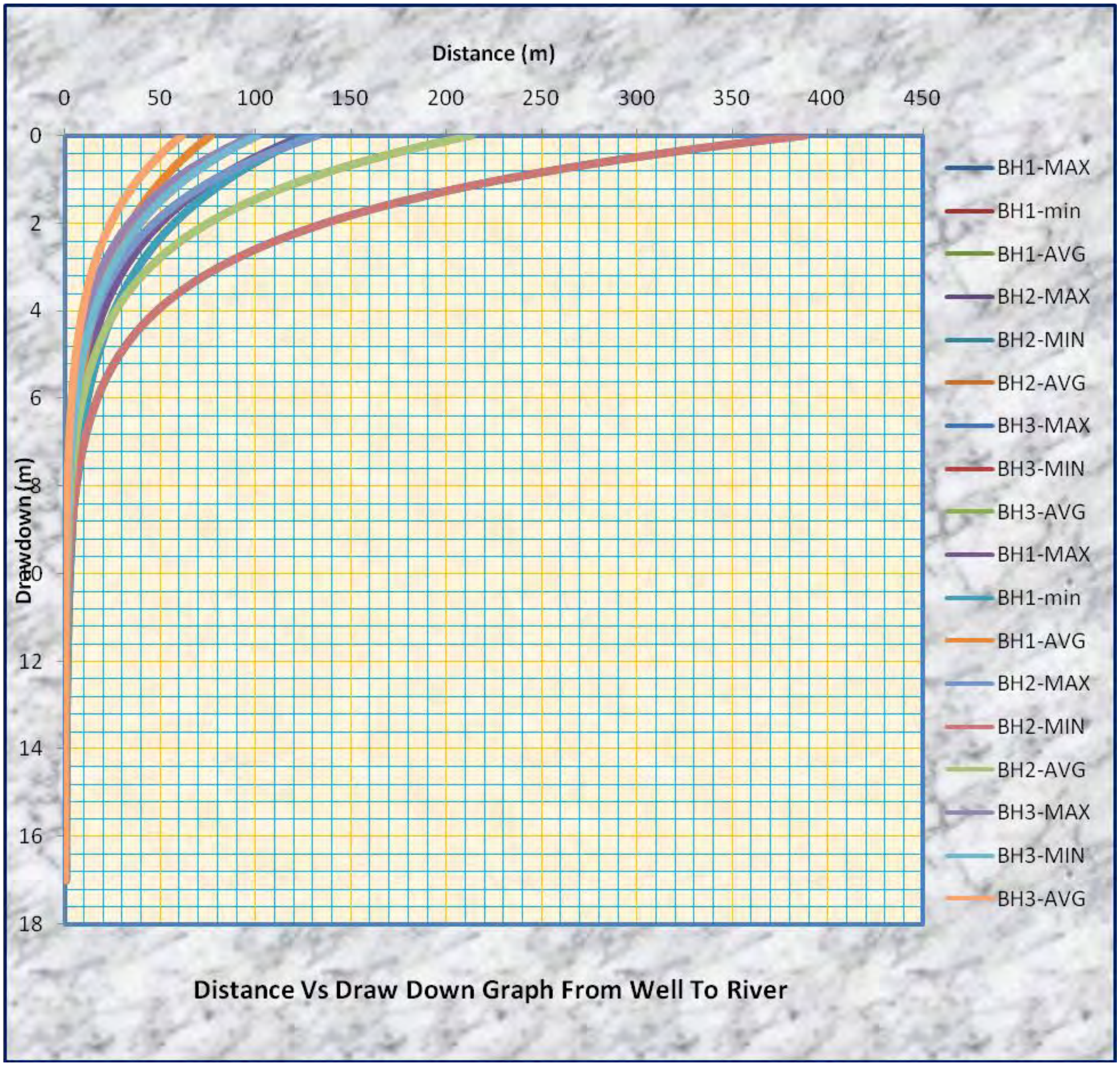

Figure 26. Distance drawdown computed by Duppuit's Equation to illustrate how sharper the slopes are to the direction of the river.

4.4. Established Capture Zones Result

A capture zone is including up gradient and down gradient potentiometric and encompasses the volume of water that operating wells extract from the porous media of the aquifer. So that it is very important to establish the area of the capture zone to decide the remediation action to be implemented during design and operation of pumping wells for the designed purposes particularly water supply systems. To carry out the delineation of the capture zone the following assumption are considered. The aquifer is homogeneous, isotropic and has infinite horizontal areal extent; uniform condition flow be comes up; an unconfined aquifer is assumed to have horizontal impervious at the base with no infiltration no vertical recharge and no leakage; the specific yield of unconfined aquifer is neglected, the Duppuit assumption of the vertical gradients are neglected; the constant pumping rate is assumed and the well is fully penetrated and open throughout the thickness of the unconfined aquifer (Stack; 1989) and Marsily ; 1986) The equation used for the computation of the capture zone edge when the conditions of the steady state have reached in unconfined aquifer is as of that discussed by (Todd; 1980 and Grubb; 1993).

In his study Grubb provided the solution of the capture zone in unconfined aquifer (Grubb; 1996). The requirement for this condition is to have the head in two pumping wells along the axis the groundwater flow direction. Then as per the equation of Grubb the shape of the capture zone is given by

$$\mathbf{x} = \frac{-\mathbf{y}}{\tan\left[\pi K\left(h_1^2 - h_2^2\right)y/QL\right.} \qquad (6.1)$$

The maximum width of the capture zone is computed by the Grubb equation as

$$\mathbf{y_{max}} = \pm\frac{QL}{K\left(h_1^2 - h_2^2\right)} \qquad (6.2)$$

The position of the stagnation point where the down-grading edge of the capture zone ends, at point y=0 is also given by

$$\mathbf{x_0} = \frac{-QL}{K\pi\left(h_1^2 - h_2^2\right)} \qquad (6.3)$$

Where:-

h_1 and h_2 = are the up-gradient and down- gradient head in the monitoring wells;

X and y=are the direction of the points defined;

L = is the distance between the monitoring wells

Q = is the pumping rate (m^3/s or m^3/day); and

K = is the hydraulic conductivity (m/s or m/day)

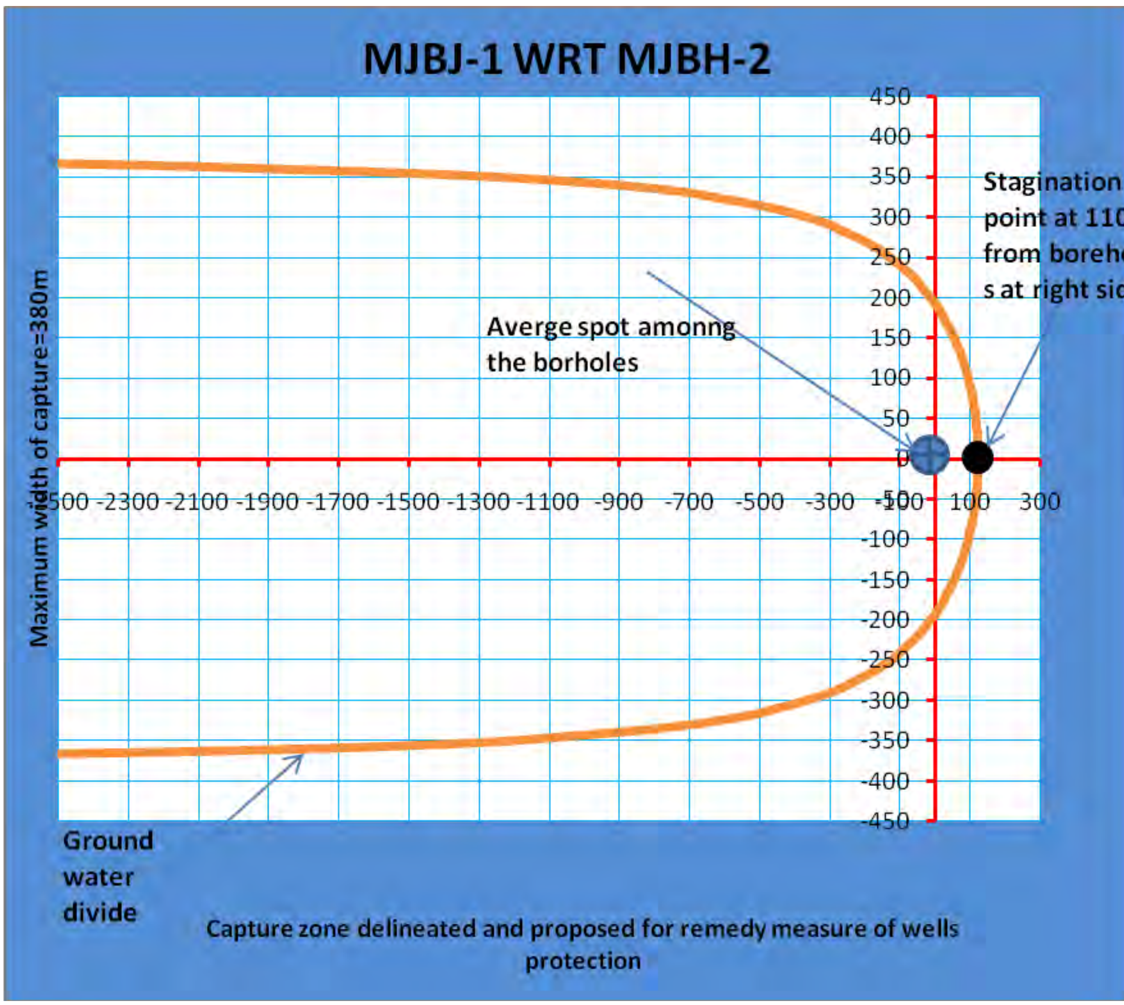

Figure 27. Diagram of the capture zone delinated for the case while the entire boreholes at the well field all are assumed operational and it is slected and recommend for the well head protectio purpose out of the other senarios as this can represent the effect of all pumping operations for the designed pumping rates of the wells

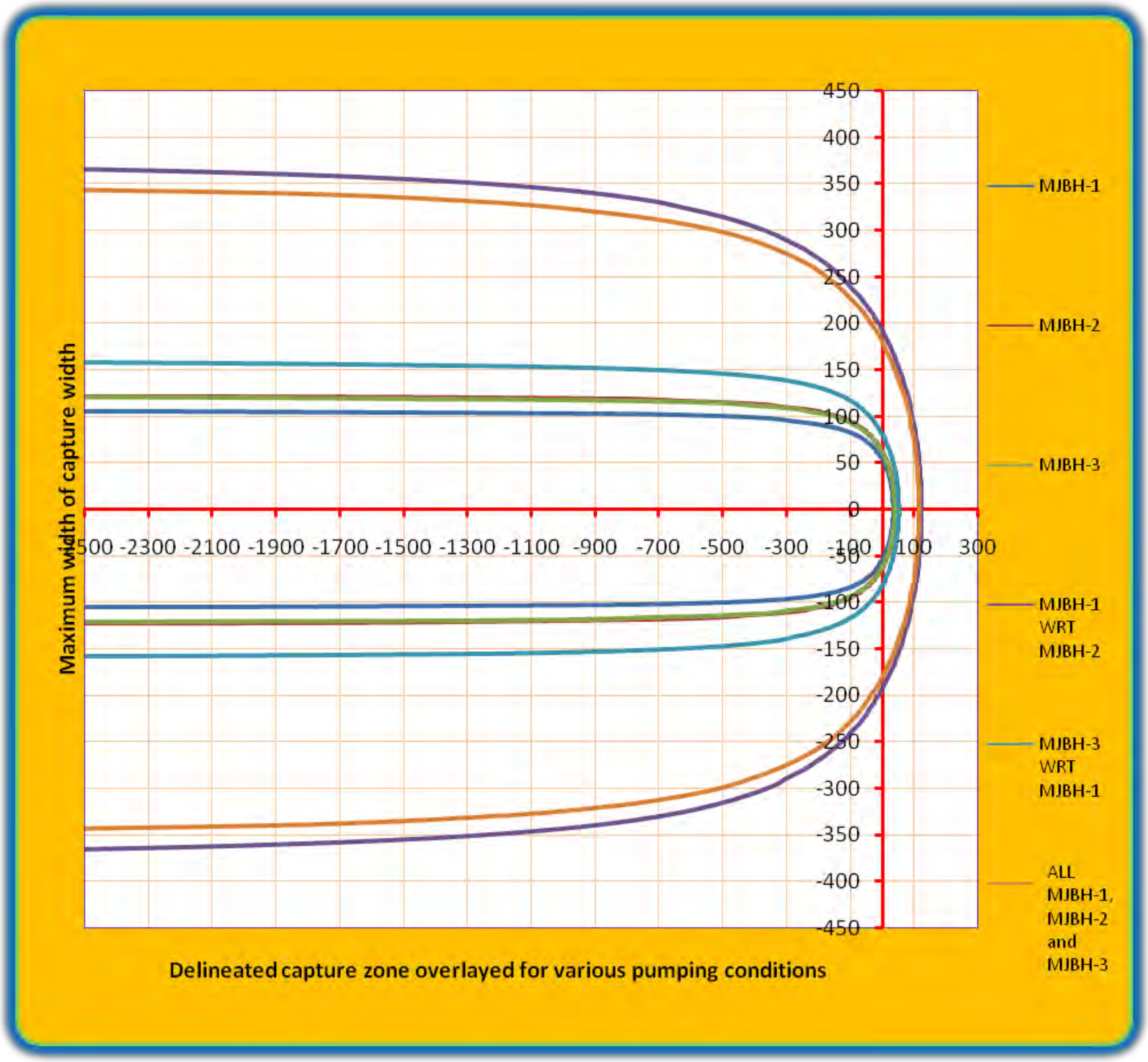

Figure 28. schematized capture zones delineated fro the various cases of senarios as the legned indicate at right edge of the diagram and overlapped to clearly illustrate the situation varying combiations of pumping operations

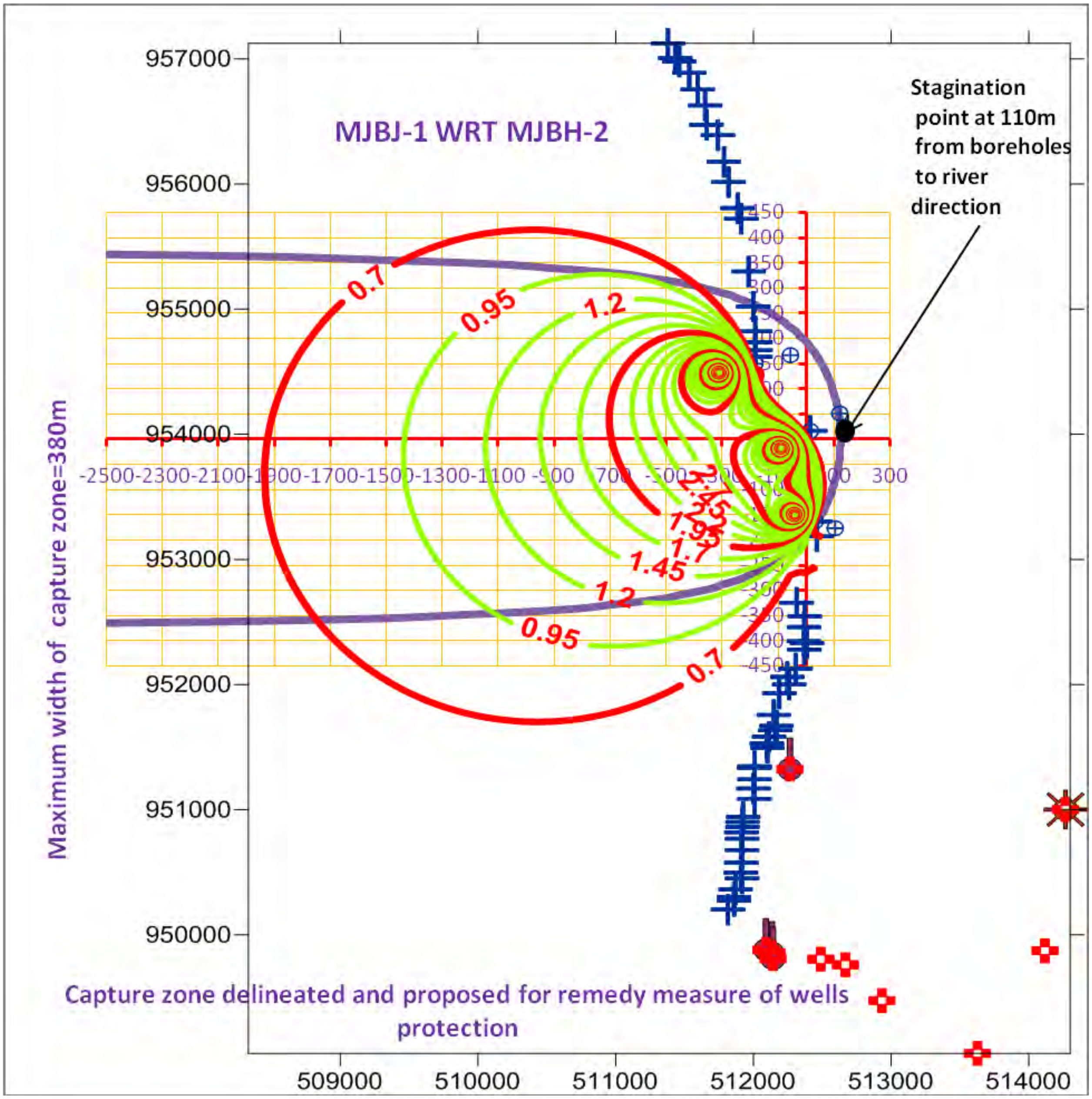

Figure 29. schematic illustration of capture zones delineated and selected for broholes head protection for the case in which all the three boreholes in the well field are supposed in opertion for the designed pimping rate capacities and the aquifer accepts the maximum transmissivity approximated and it is overlaid by the fixed radius of the simulate drawdowns cotour lines plots in attampt to display that the cones of the wells influence extending passing the delineated zone.

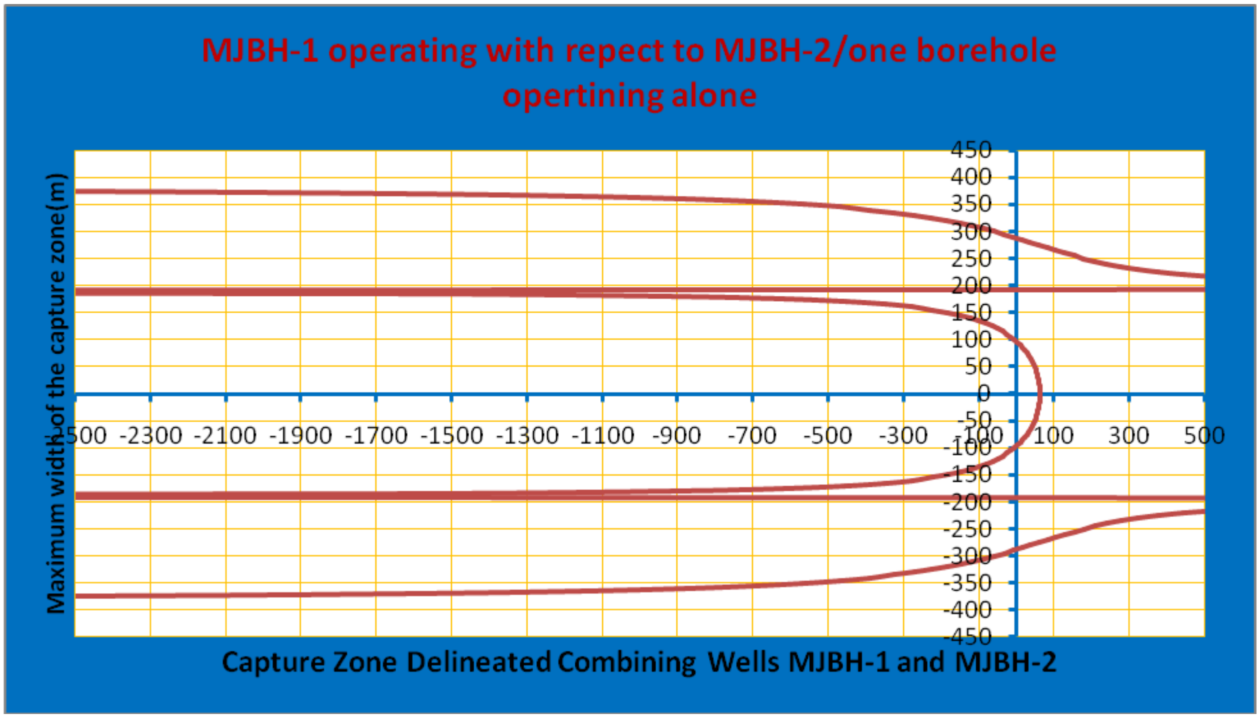

Figure 30. Capture zone delinated for senarios when MJBH-2 and MJBH-1 are assumed oeprating in incombinon or when ether of the two well is working only.

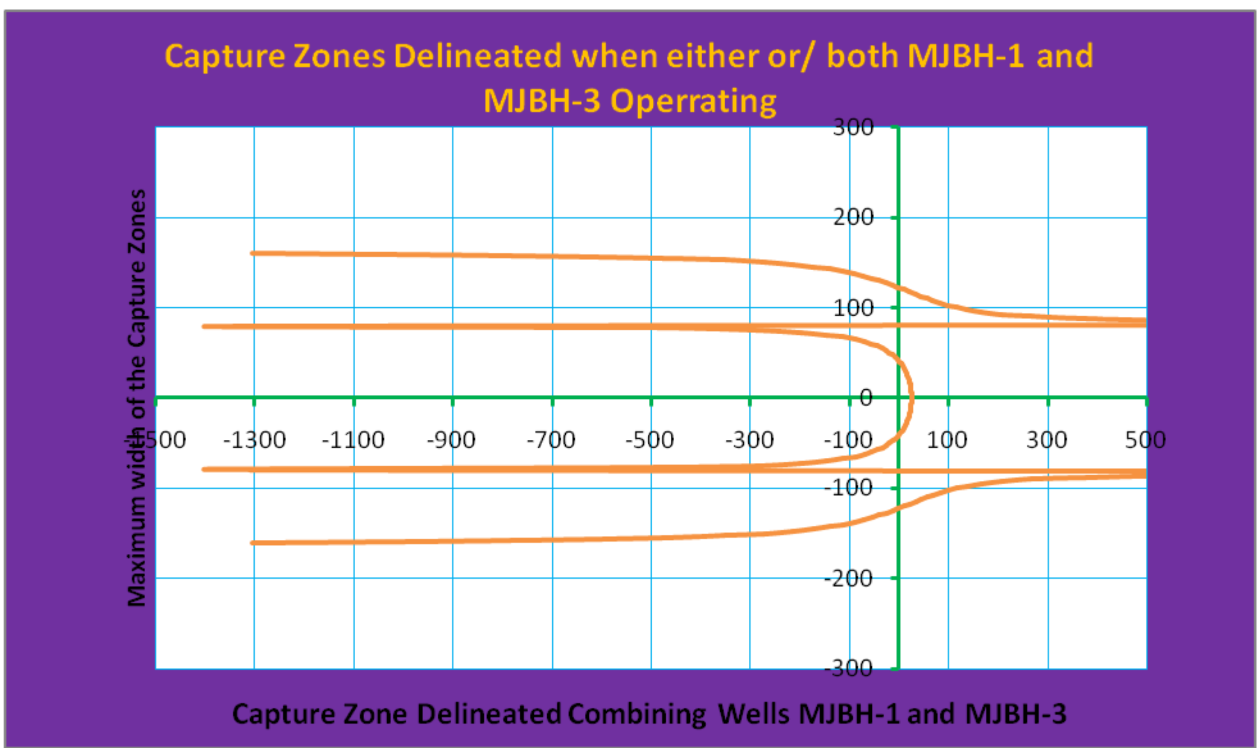

Figure 31. Capture zone delinated for senarios when MJBH-1 and MJBH-3 are assumed oeprating in incombinon or when ether of the two well is working in particular.

Table 13: *Explanation of the boreholes data*

Descriptions	Name of the boreholes		
	MJBH-1	**MJBH-2**	**MJBH-3**
X (UTM, m)	512300	511750	512200
Y (UTM, m)	953358	954495	953889
Original ground elevation of the boreholes a.s.l (m)	1785	1803	1790
Original ground elevation of the river a.s.l (m)	1772.39	1782.17	1778.05
Depth of excavations of the boreholes(m)	358	416	410
SWL(m)	12.9	24.5	14.55
DWL(m)	24.67	17.37	22.32
shortest distance from the boreholes to recharging river(m)	152.52	268.16	254.45
Spaces between the boreholes(m)	0	1263.04	540.33
	1263.04	0	754.81
	540.33	754.81	0
Designed capacity of pumping rates in boreholes(m3/s)	0.045	0.045	0.04383

Table 14: *Delineated dimensions of the capture zones/boundary for different options of the boreholes operation conditions*

Descriptions	**Names of the boreholes, Operating conditions and combination of boreholes considered**			**Remarks**
	MJBH-1	**MJBH-2**	**MJBH-3**	
Saturated aquifer thickness (m)	345.10	391.50	395.45	
Smaller hydraulic conductivity (adopts K_{min}, (m/s)	0.0000083	0.0000083	0.0000083	
Up gradient (h_1, m)	333.89	380.00	383.95	Potentiometric from recharge river to operating boreholes
Down gradient (h_2, m)	345.39	395.17	398.05	

Stagnation point stretch to the river (expected plume site), x_{stg} (m)	33.94	39.60	39.05	Boreholes operating Particularly
Maximum width of the capture zone/recharge boundaries , $\pm y_{max}$ (m)	106	124	122	
Maximum Length of $\pm x_0$ at down gradient where y=0, (m)	(5793.11, 1)	(12350, 1)	(7106, 1)	
Stagnation point stretch to the river (expected plume site), x_{stg} (m)	61.07	61.07		Boreholes operating Particularly
Maximum width of the capture zone/recharge boundaries , $\pm y_{max}$ (m)	190	190		
Maximum Length of $\pm x_0$ at down gradient where y=0, (m)	6269.08	6269.08		
Stagnation point stretch to the river (expected plume site), x_{stg} (m)	25.97		25.97	Boreholes operating Particularly
Maximum width of the capture zone/recharge boundaries , $\pm y_{max}$ (m)	81.59		81.59	
Maximum Length of $\pm x_0$ at down gradient where y=0, (m)	3593.40		3593.40	
Stagnation point stretch to (expected plume site), x_{stg} (m)	122	122		For two boreholes operating in the well field with respect to location and settings
Maximum width of the capture zone/recharge boundaries , $\pm y_{max}$ (m)	380.00	380.00		
Maximum Length of $\pm x_0$ at down gradient where y=0, (m)	12549.66	12549.66		
Stagnation point stretch to the river (expected plume site), x_{stg} (m)	51.26		51.26	For two boreholes operating in the well field with respect to location and settings
Maximum width of the capture zone/recharge boundaries , $\pm y_{max}$((m)	160		160	
Maximum Length of $\pm x_0$ at down gradient where y=0, (m)	7815.32		7815.32	
Up gradient (h_1, m)	365.85	365.85	365.85	Potentiometric from recharge river to operating boreholes (average assumed)
Down gradient (h_2, m)	379.54	379.54	379.54	
Stagnation point stretch to the river (expected plume site), x_{stg} (m)	***110***	***110***	***110***	***For entire boreholes operating in well field with respect to wells setting and site conditions***
Maximum width of the capture zone/recharge boundaries , $\pm y_{max}$(m)	***350.0***	***350.0***	***350.0***	
Maximum Length of $\pm x_0$ at down gradient where y=0, (m)	***20500.00***	***20500.00***	***20500.00***	

4.5. Determination of Boreholes Interference at Mojo Well Field

Interference of the pumping wells is a crucial unease to take into account in designing and treating the locations of the pumping wells, in the well fields where more than one pump or several pumping wells may exist and those wells are extracting water from the well field of the same aquifer. The main purpose of leading this is to resolve the spacing there to be provide between the pumping wells in target to minimize the occurrence of transecting cones of depression which subsequently generates interferences in layout system of the well field as influence of operating wells. The total drawdown of the individual pumping wells is the linear addition of every well operating in multiple well systems as the superposition permits addition to determinate the effect of drawdowns. So that awareness about the existence of wells interference is necessary to design the layout system of multiple pumping wells and substantial helpful in making decision during planning the activities of pumping operation and maintenances of pumping wells to secure sustainable abstractions of the boreholes in the well field.

For the case of multiple well system forming a well field, the cones of depression of the operating wells intersect and each well interfere with one another due to the increase of the drawdown as the pumping lift created. Such overlapping of cones of depression in multiple well systems is recognized as interference of one pumping well with others.

At the boreholes of Mojo well field site there are three pumping wells which supposed to extract and deliver groundwater to the main risings of Mojo water supply system from the aquifer at this well field. During the first phase of the project one borehole is projected as a standby and the remaining two wells namely MJBH-1 and MJBH-2 are operational. However, as per information obtained from resident water supply authority, MJBH-3 will also be operational in the second phase to alleviate the increasing demand for water supply. So that we have simulated the drawdown considering all three pumps are operating simultaneously with their full capacity as the application of operating the third boreholes will be obvious after a while due to fact that demand for water supply rises with growth of population and economy. From this point of view the third pump which is not working for this time is included assuming it will be functional in second stage of project.

The interference between the pumping boreholes can be developed due to the intersection of cones of depression originating from these operating boreholes in the well field when all of them are operating simultaneously. In order to simplify interpretation of complicated fluctuations of water level caused by well interference effects from multiple pumping wells, the simulated drawdown have been plotted with respect to areal coverage when pumping wells are running at the same times.

Hence, pointing toward realization of pumping wells interferences in the field system, the required composite solutions are simulated to predict the resulted drawdown that represents the entire influences of the working boreholes in the system at every point therein the identified well field through principle of superposition adopting let the aquifer in said field possesses the assumed properties of geometric mean values which previously approximated including transmisivity and storativity for different scenarios values and an average hydraulic conductivity values. Then using the Theis equation via the method of superposition for multiple pumping wells, and the distribution of contour line plots of the composite solution drawdown is plotted for the entire boreholes operating collectively. From the produced distributions of the contours lines section in which the cones of depressions are overlapping is detected. As per the configurations of these overlapping indicates, the boreholes are recognized to prevail interference one with each other while all/ partially operating in Mojo well field.

As a matter of existing boundary condition, when increasing the amount of pumping rates and the composite drawdown simulating by technique of superposition, expansion of cones of depression would apply a change to the configurations of the resulted drawdown contour lines plots such that increased drawdown should occur at both borders of the boundaries. Based on the radial distances from the pumping wells to the boundary, increased drawdown at the boundary could be calculated for the delineated boundary conditions. In order to have various cases of scenarios, the constant pumping rate conjugated with the existing recharging boundary condition is also evaluated. Nevertheless, the constant pumping rate assumed, the rate of pumping is manipulated to vary at different time so that options be available to note various conditions, there by letting the boreholes made to operate constantly with double pumping rates and half pumping rates that of the designed rate capacity for which the pumps in the boreholes planned to rate throughout the project life span. At low pumping rates the drawdown is smaller in which the pumps may withdraw some volume of water from the aquifer itself and the rest water that enters from the stream to the aquifer. Generally, gaining water from recharging of the adjacent stream/river for the aquifer or losing its storage to the existing closer river largely depends on the distance between the boreholes and the boundary and the location of the media with respect to potentiometric aspects. As clearly described in the earlier chapters of this study the elevation of the Mojo River lays at relatively higher spot relative to lower situation of water tables in the aquifer of the well field site definitely the river delivers water to the adjoining aquifer as fast as removal made from it by the continual pumping operations.

The total volume of water that can be extracted from this perennial river depends largely on rate of depletion from the river to the aquifer and on the distance between the operating wells and the river. However, the volume of depletion water which may be extracted directly from the river under varying scenarios of the boreholes operations conditions and the corresponding time needed for these process to end is not incorporated in this study. Whereas, as the upward swing of drawdown contours level drawn for the three boreholes laterally to the perennial river indicates effluent condition, the superposed drawdown mounds represent the recharge area.

Hence, the study determines there is interference of one well with each other as there is exhibition of overlapping cones of depression when all pumps are operating simultaneous in well field. As the Figures from 32 to 52 and sections shows the depths of overlapping increases with increasing the pumping rate as the drawdown increase. The interference becomes small when the rate of pumping decline but it is not possible to extract the designed amount of water supply.

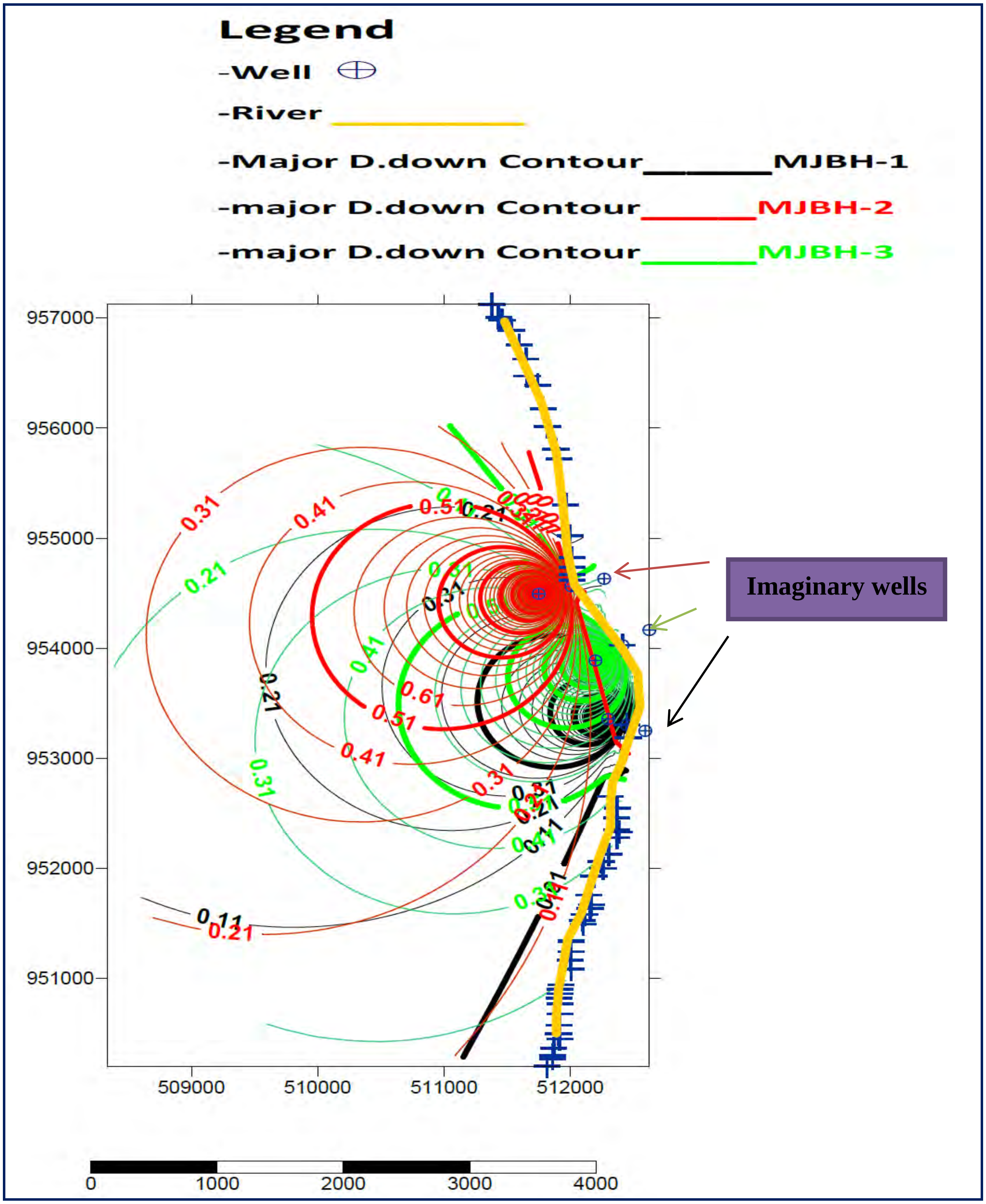

Figure 32. Schematic plan view illustrating possible well interference configuration of contour lines distributions in which the drawdowns computed by superposition for individual three pumping boreholes and the plots conducted for the particular boreholes and overlaid to note marginal overlapping states of the cones of depressions as the above plot plan view shows at case when the pumps at every boreholes are all operating by the designed discharge rates and the aquifer letting adopts maximum transmissivity T_{max}.

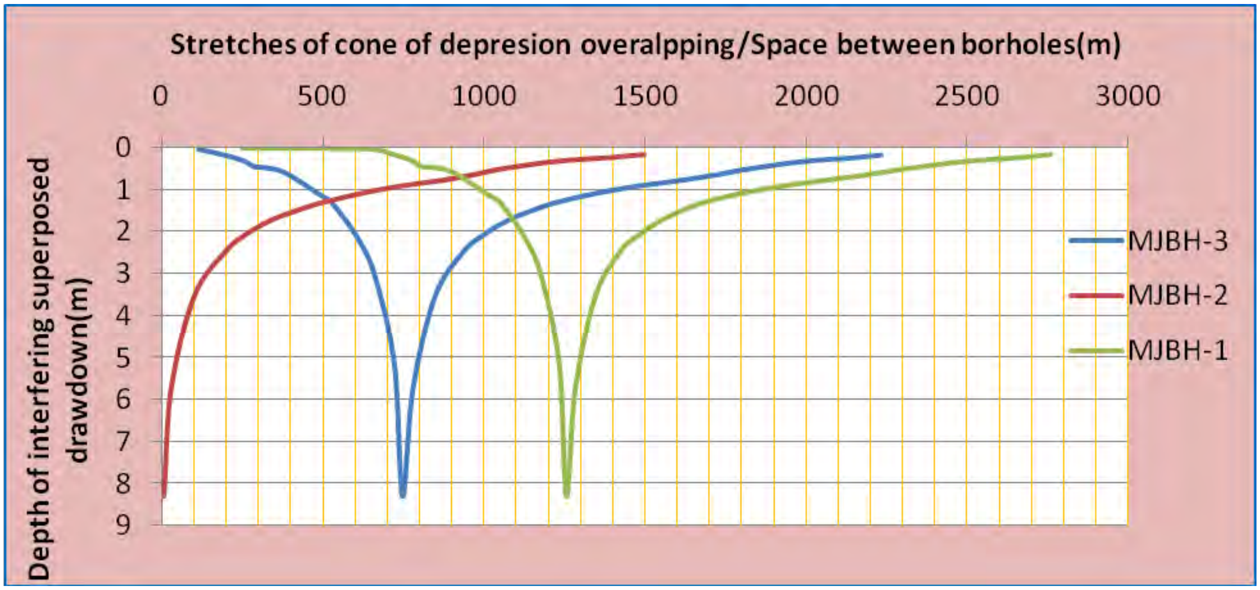

Figure 33. Schematic cross section illustrating possible well interference configuration explain potential drawdown interference between the operating boreholes when the rates of designed capacities in the wells assumed and the aquifer attains maximum transmissivity T_{max} for the plan view of the Figure 32 in which particular superposed drawdown for each boreholes overlaid.

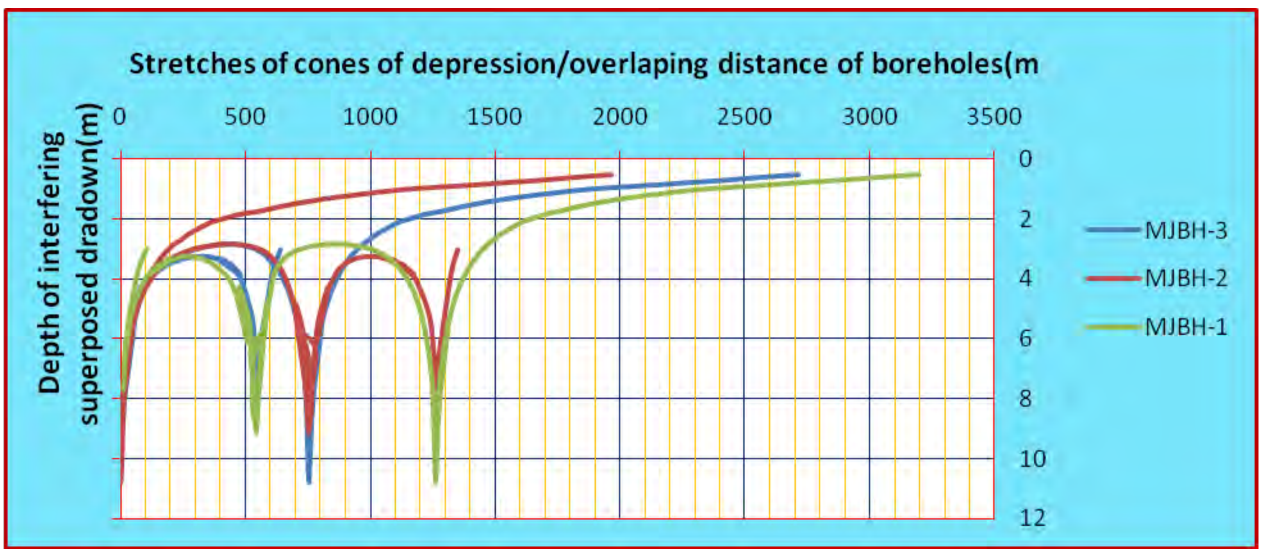

Figure 34. Schematic cross section illustrating possible well interference configuration explain potential drawdown interference between the operating boreholes when the rates of pumps in the wells assumed to operate by designed discharge rates capacity and the aquifer attains maximum transmissivity T_{max} for case the resulted drawdowns of all three pumping boreholes superposed and overlaid as plan view of the Figure 8 shows.

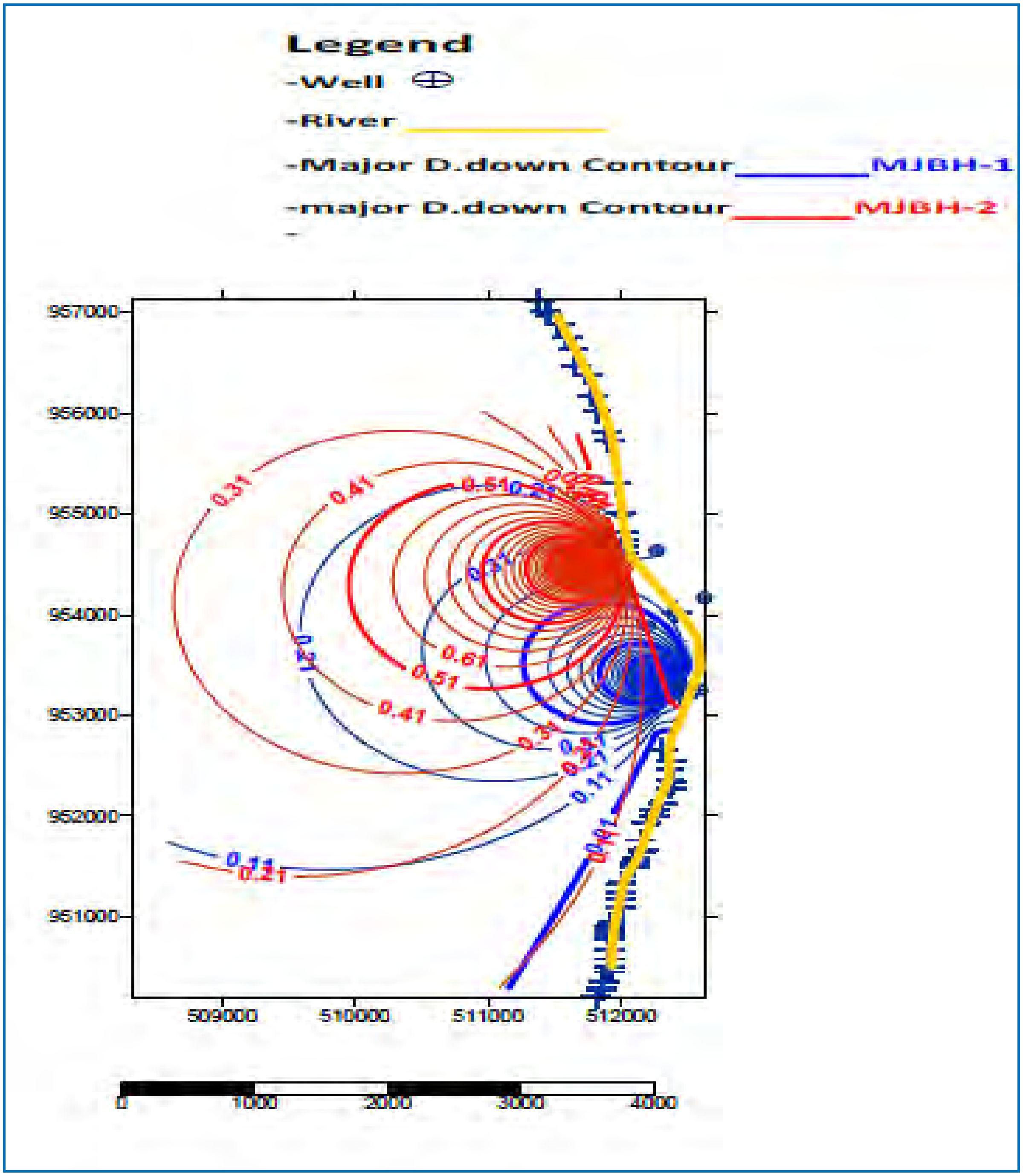

Figure 35. Schematic plan view illustrating possible well interference configuration of contour lines distributions in which the drawdowns computed by superposition for individual two pumping boreholes and the plots conducted for the particular boreholes and overlaid to note marginal overlapping states of the cones of depressions as the above plot plan view shows at case when the pumps at every boreholes are all operating by the designed discharge rates and the aquifer letting adopts maximum transmissivity T_{max}.

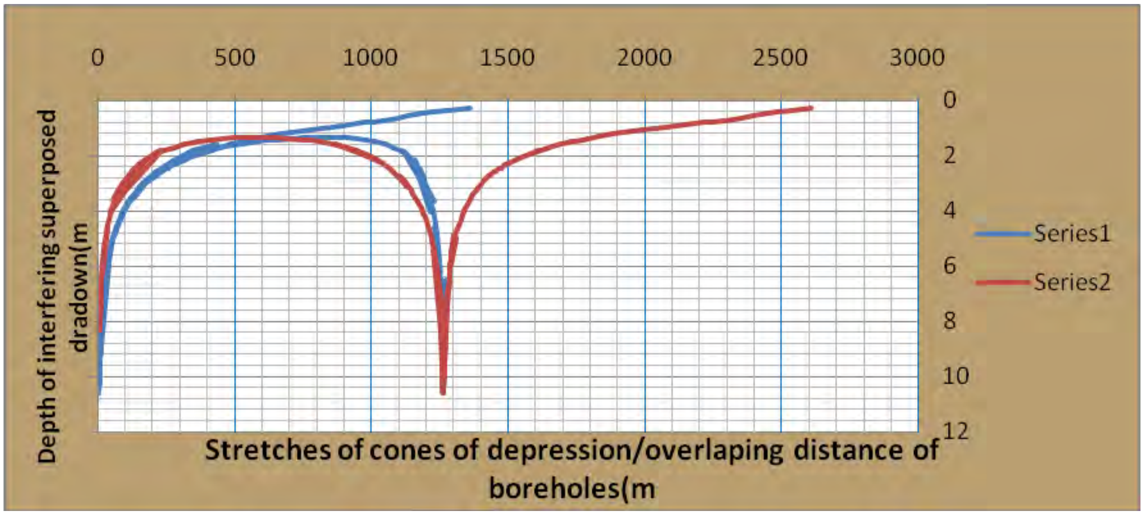

Figure 36. Schematic cross section illustrating possible well interference configuration explain potential drawdown interference between the operating boreholes when the rates of designed capacities in the wells assumed and the aquifer attains maximum transmissivity T_{max} for the case of only two wells as plan view of the Figure 9 shows in which particular superposed drawdown for each boreholes overlaid.

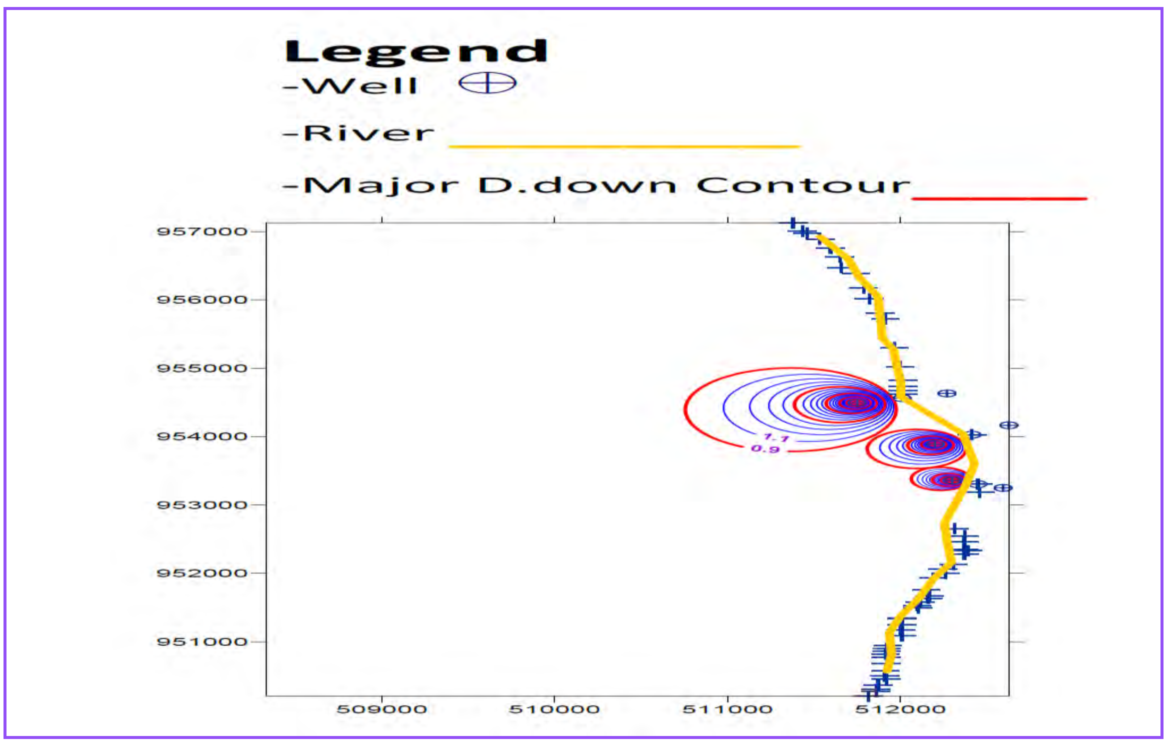

Figure 37. Schematic plan view of the cones of the depressions of the particular operating wells superposed for every operating borehole and plotted to illustrate the arrangements of the simulated drawdown with no wells interfering with drawdowns of 1.65m, 0.9m, 1.75m and in MJBH-1, MJBH-2 and MJBH-3 respectively.

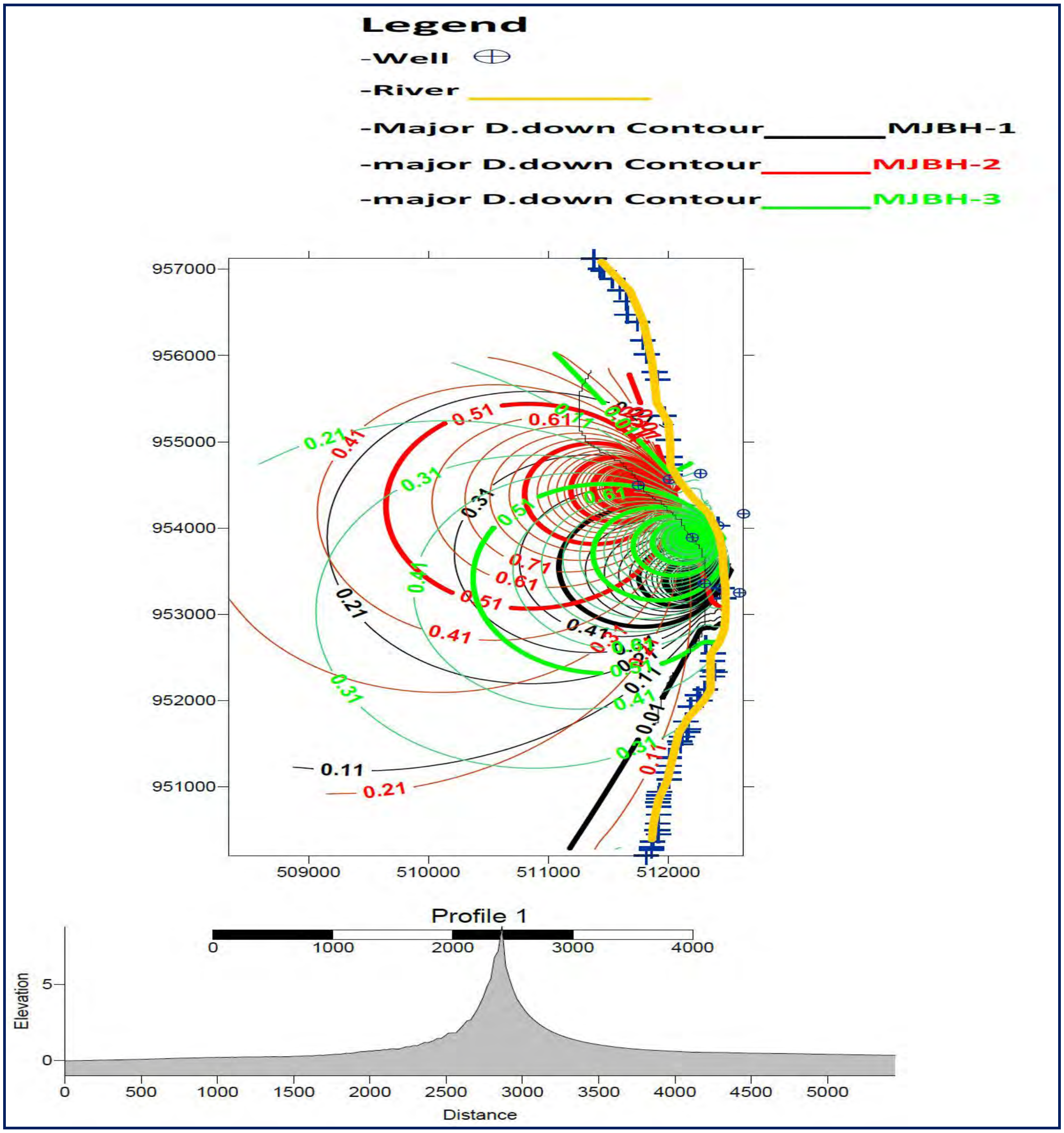

Figure 38. Schematic plan view illustrating possible well interference configuration of contour lines distributions in which the drawdowns computed by superposition for individual three pumping boreholes and the plots conducted for the particular boreholes and overlaid to note marginal overlapping states of the cones of depressions as the above plot plan view shows at case when the pumps at every boreholes are all operating by the designed discharge rates and the aquifer letting adopts minimum transmissivity T_{mjn}.

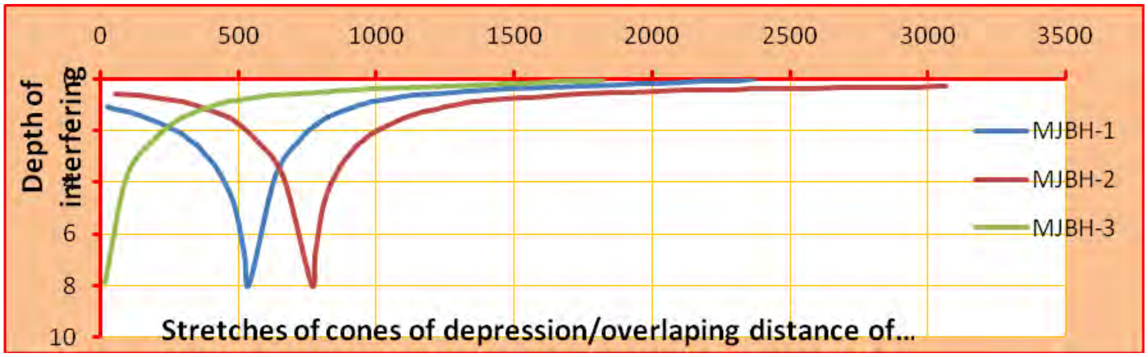

Figure 39. Schematic cross section illustrating possible well interference configuration explain potential drawdown interference between the operating boreholes when the rates of designed capacities in the wells assumed and the aquifer attains minimum transmissivity T_{min} for the plan view of the Figure 38 in which particular superposed drawdown for each boreholes overlaid.

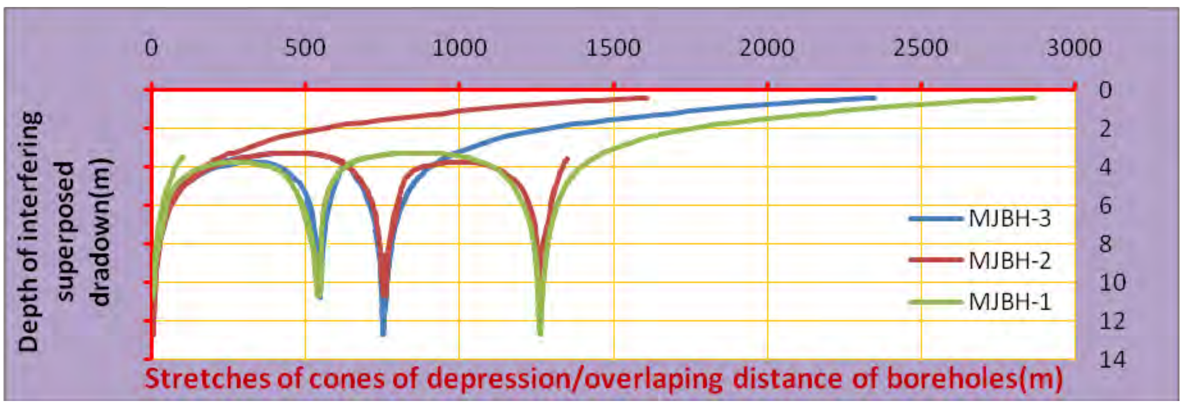

Figure 40. Schematic cross section illustrating possible well interference configuration explain potential drawdown interference between the operating boreholes when the rates of pumps in the wells assumed to operate by designed discharge rates capacity and the aquifer attains minimum transmissivity T_{min} for case the resulted drawdowns of all three pumping boreholes superposed and overlaid as Figure 12 shows.

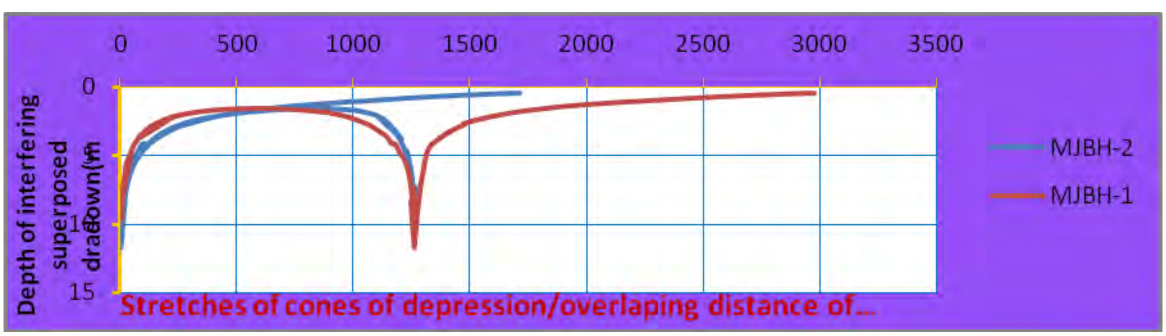

Figure 41. Schematic cross section illustrating possible well interference configuration explain potential drawdown interference between the operating boreholes when the rates of designed capacities in the wells assumed and the aquifer attains minimum transmissivity T_{min} for the case of only two wells pumping boreholes superposed and overlaid as plan view of the Figure 13 shows.

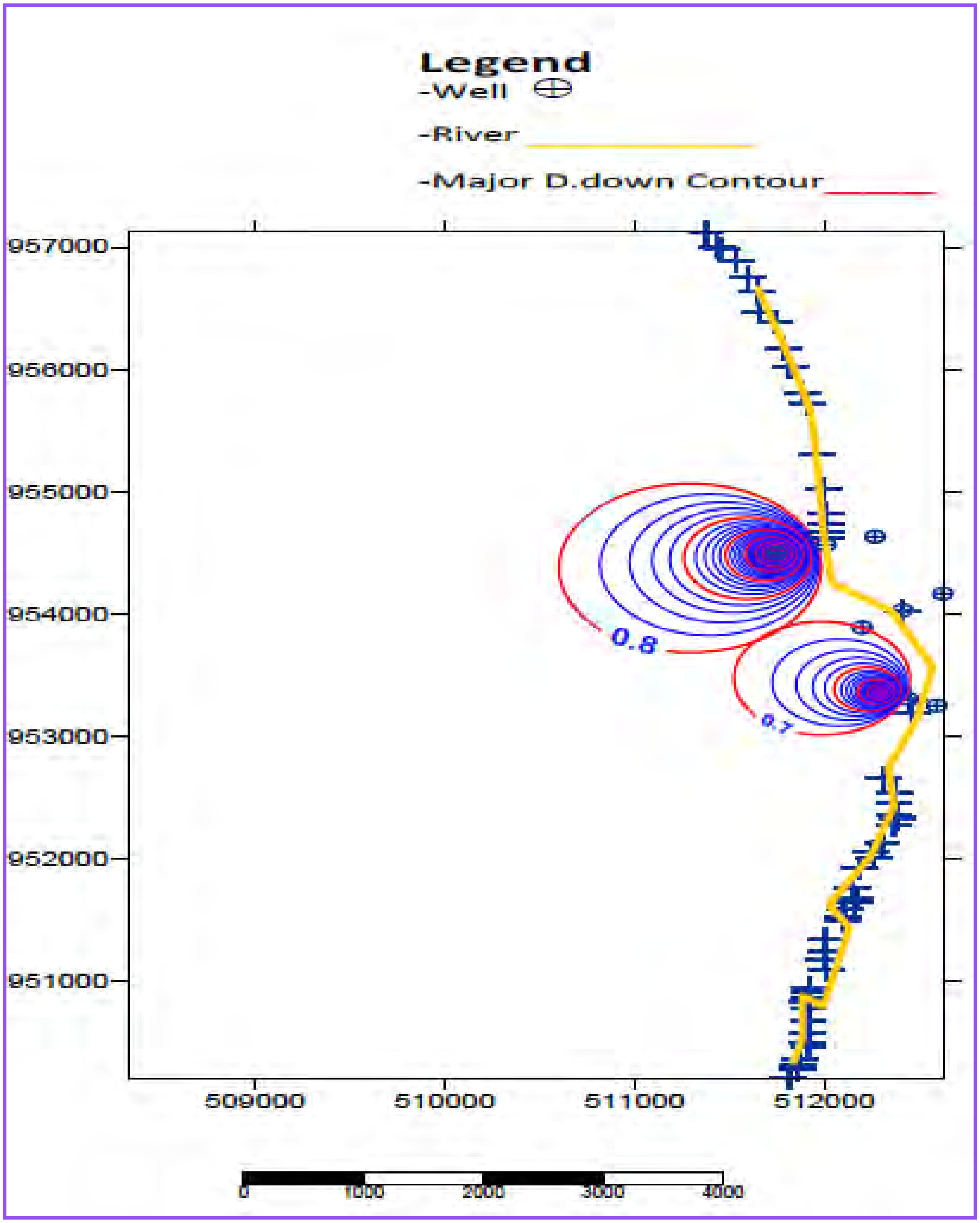

Figure 42. schamatic plan view of the cones of the dpresiions of the particular operating wells superposed for every operating boreholes and ploted to illustrate the arrangments of the simulated drawdown without well interfering for two wells operating at the well field that drawdown in MJBH-1=0.7m and MJBH-2=0.8m

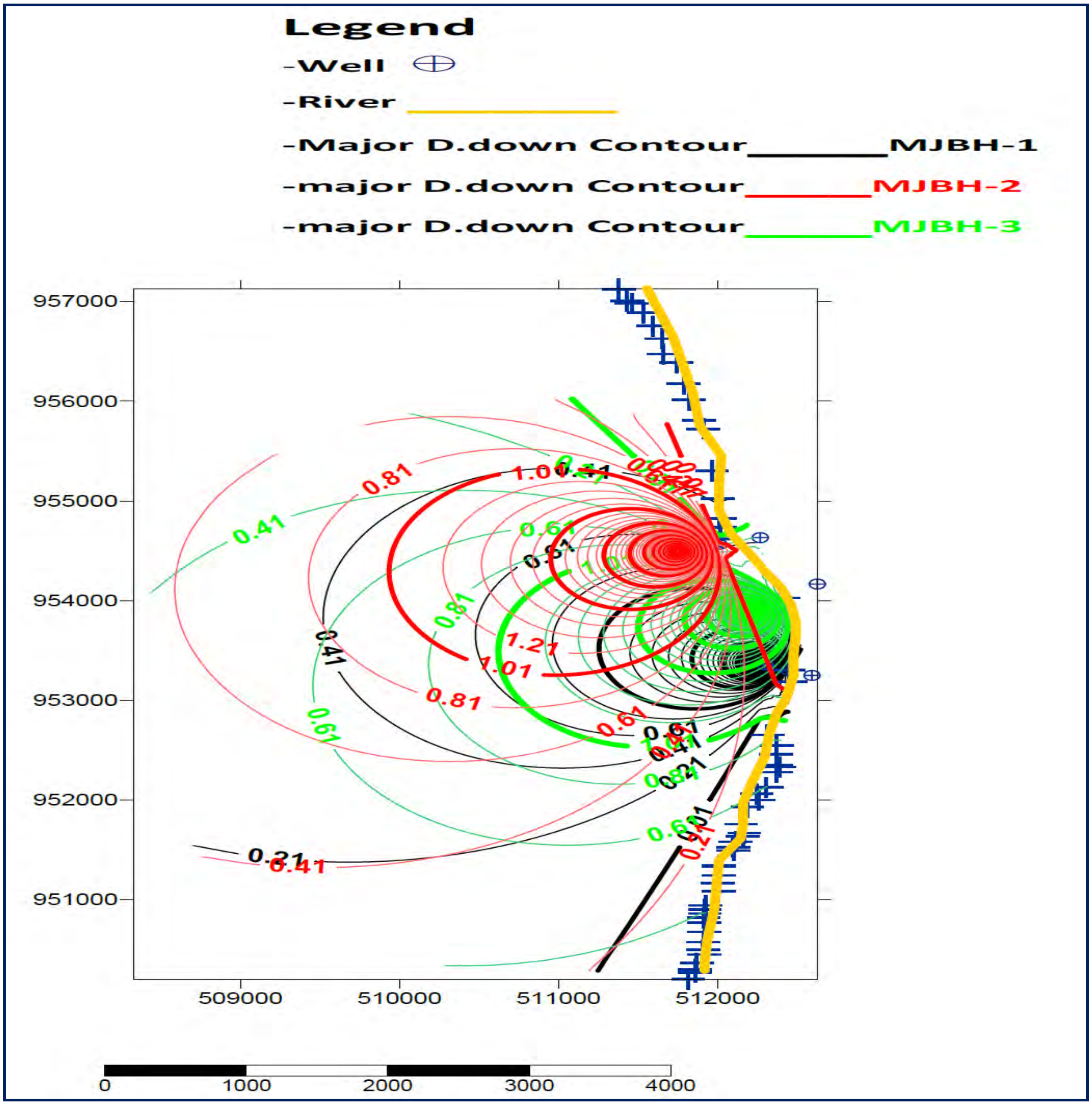

Figure 43. Schematic plan view illustrating possible well interference configuration of contour lines distributions in which the drawdowns computed by superposition for individual three pumping boreholes and the plots conducted for the particular boreholes and overlaid to note marginal overlapping states of the cones of depressions as the above plot plan view shows at case when the rate of the pumps at every boreholes are all operating there by doubling the rates of designed discharge capacities of wells and the aquifer is letting to adopt a value of maximum transmissivity T_{max} estimated.

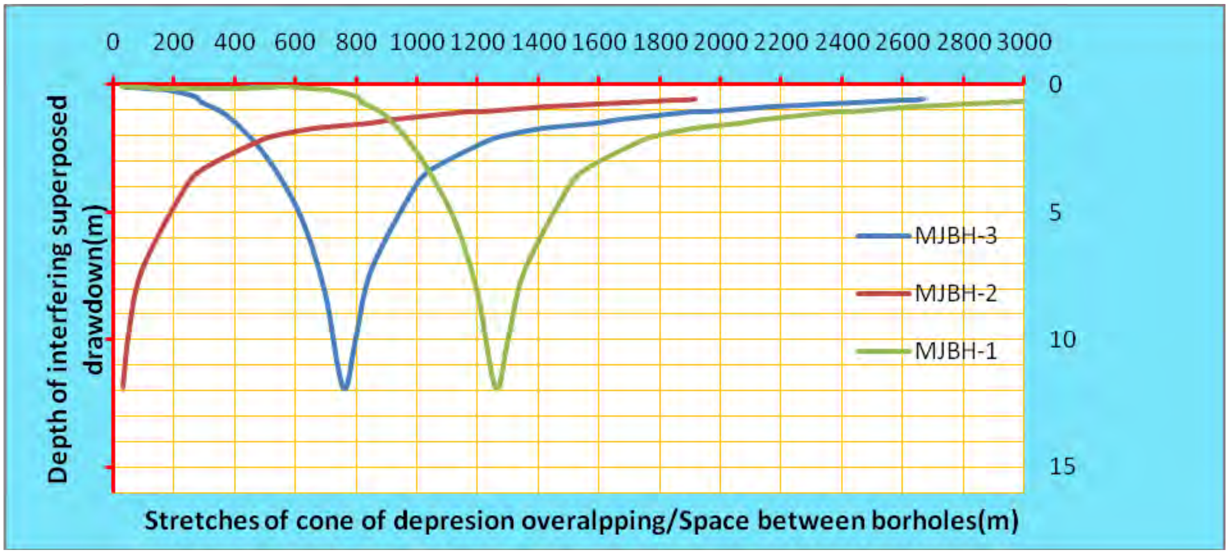

Figure 44. Schematic cross section illustrating possible well interference configuration explain potential drawdown interference between the operating boreholes when the pumps in the wells assumed to operate by double rates of the designed capacities and the aquifer attains minimum transmissivity T_{min} for case the individual drawdowns superposed for every three pumping boreholes and overlaid as the plan view of Figure 43 shows.

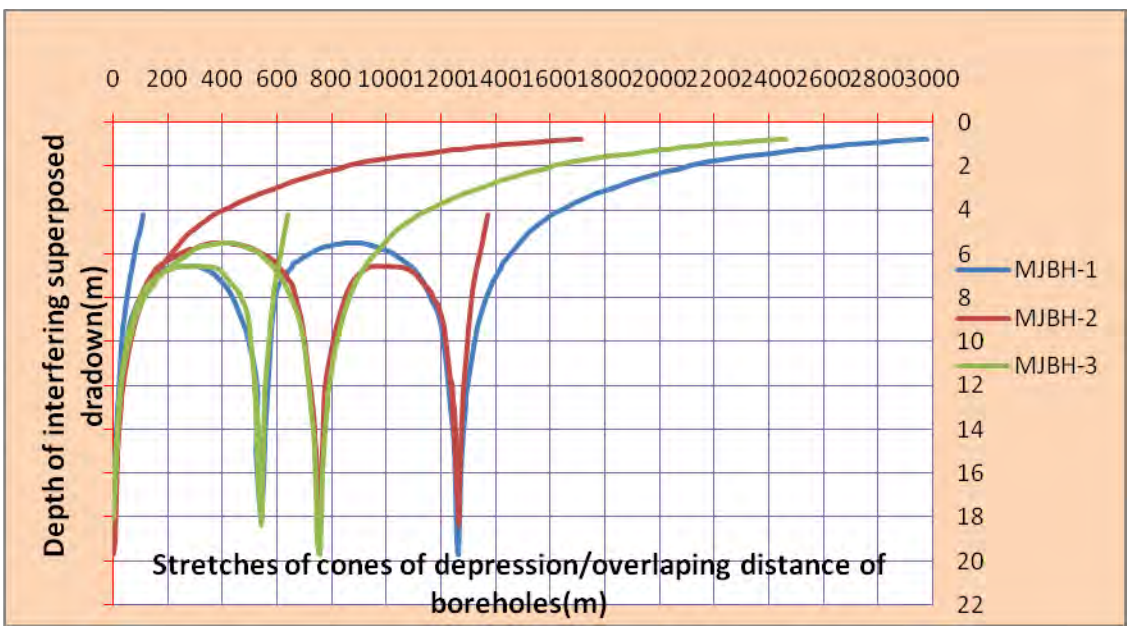

Figure 45. Schematic cross section illustrating possible well interference configuration explain potential drawdown interference between the operating boreholes when the rates of designed capacities in the wells assumed doubled and the aquifer attains maximum transmissivity T_{max} for case the resulted drawdowns of all three pumping boreholes superposed and overlaid.

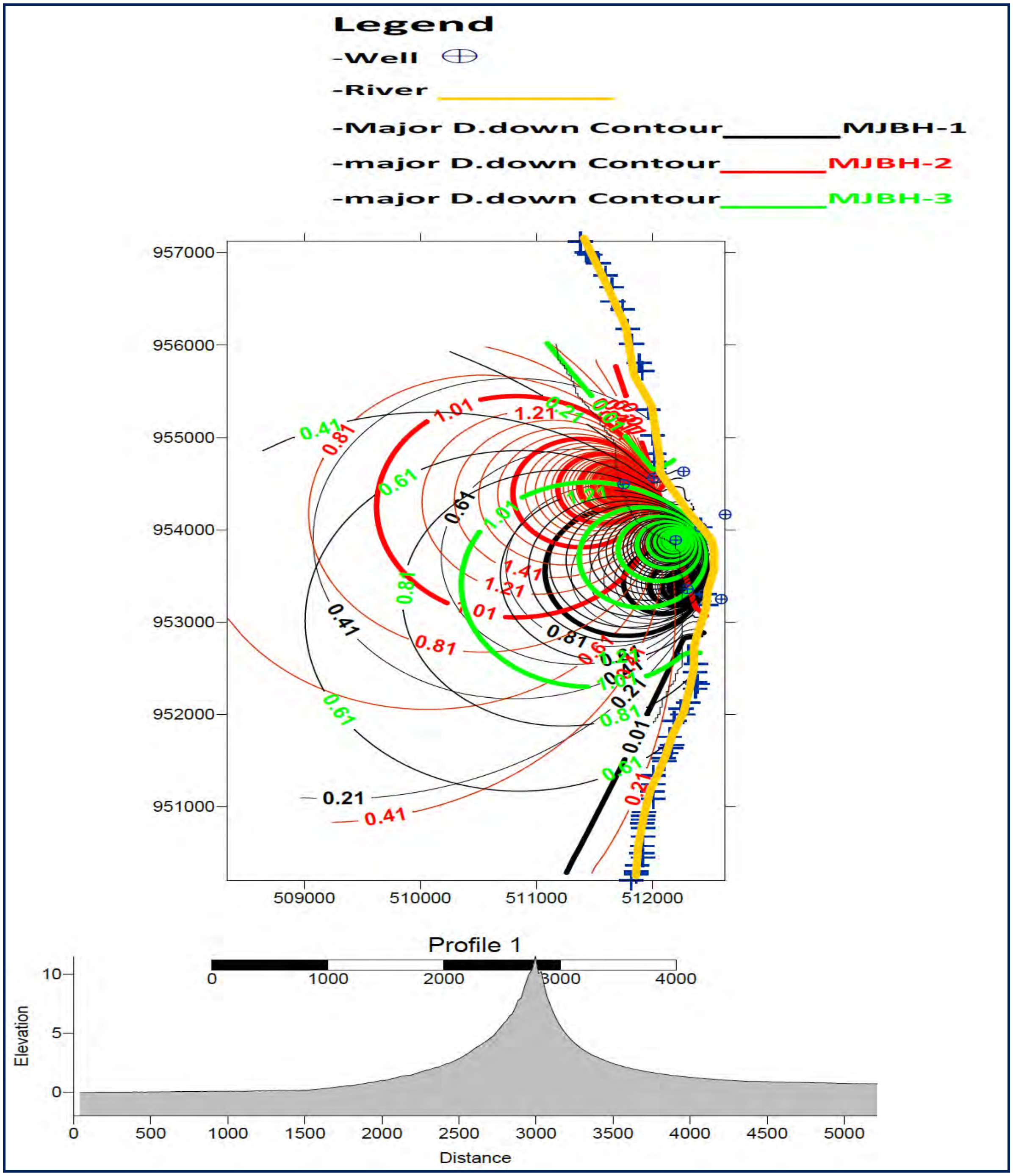

Figure 46. Schematic plan view illustrating possible well interference configuration of contour lines distributions in which the drawdowns computed by superposition for individual three pumping boreholes and the plots conducted for the particular boreholes and overlaid to note marginal overlapping states of the cones of depressions as the above plot plan view shows at case when the rate of the pumps at every boreholes are all operating there by doubling the rates of designed discharge capacities of wells and the aquifer is letting to adopt a value of minimum transmissivity T_{min} estimated.

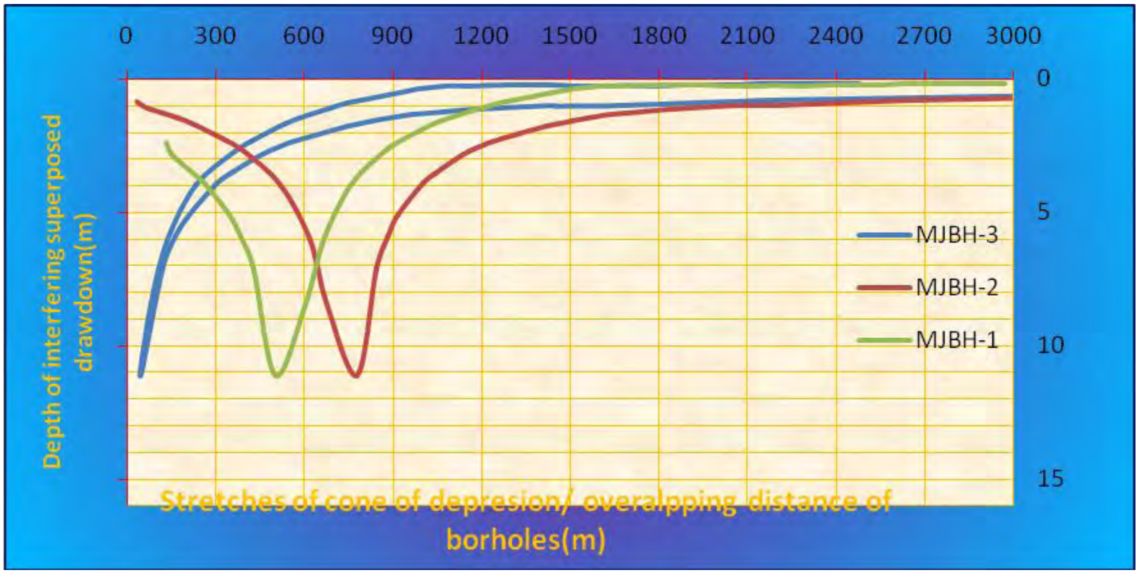

Figure 47. Schematic cross section illustrating possible well interference configuration explain potential drawdown interference between the operating boreholes when the rates of designed capacities in the wells assumed doubled and the aquifer attains minimum transmissivity T_{min} for the plan view of the Figure 46 in which particular superposed drawdown for each boreholes overlaid.

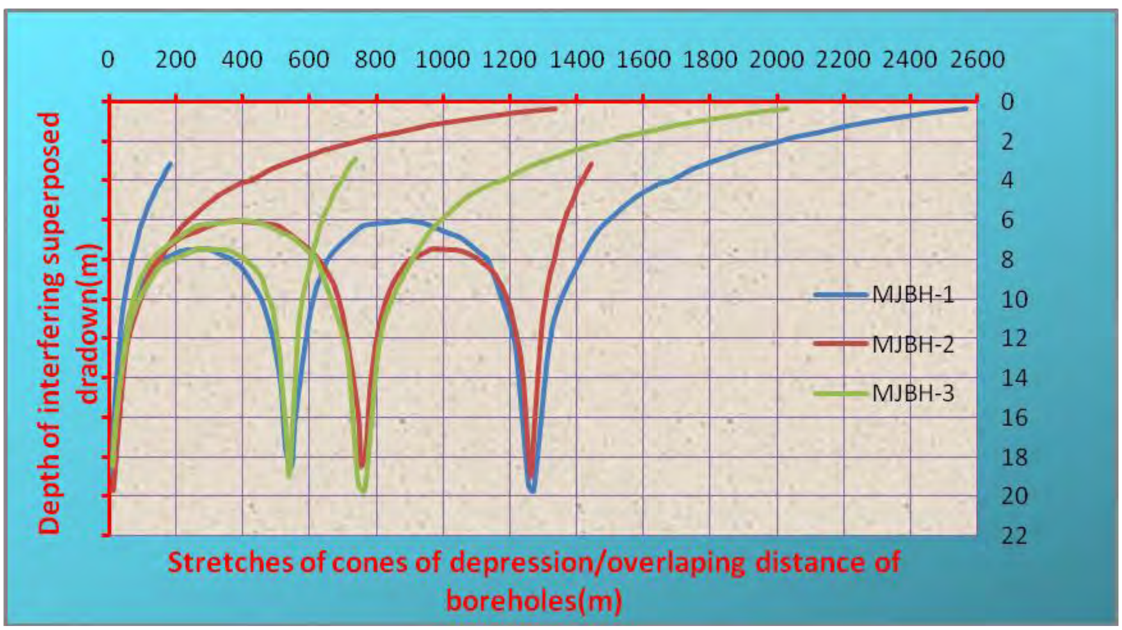

Figure 48. Schematic cross section illustrating possible well interference configuration explain potential drawdown interference between the operating boreholes when the rates of designed capacities in the wells assumed doubled and the aquifer attains minimum transmissivity T_{min} for case the resulted drawdowns of all three pumping boreholes superposed and overlaid.

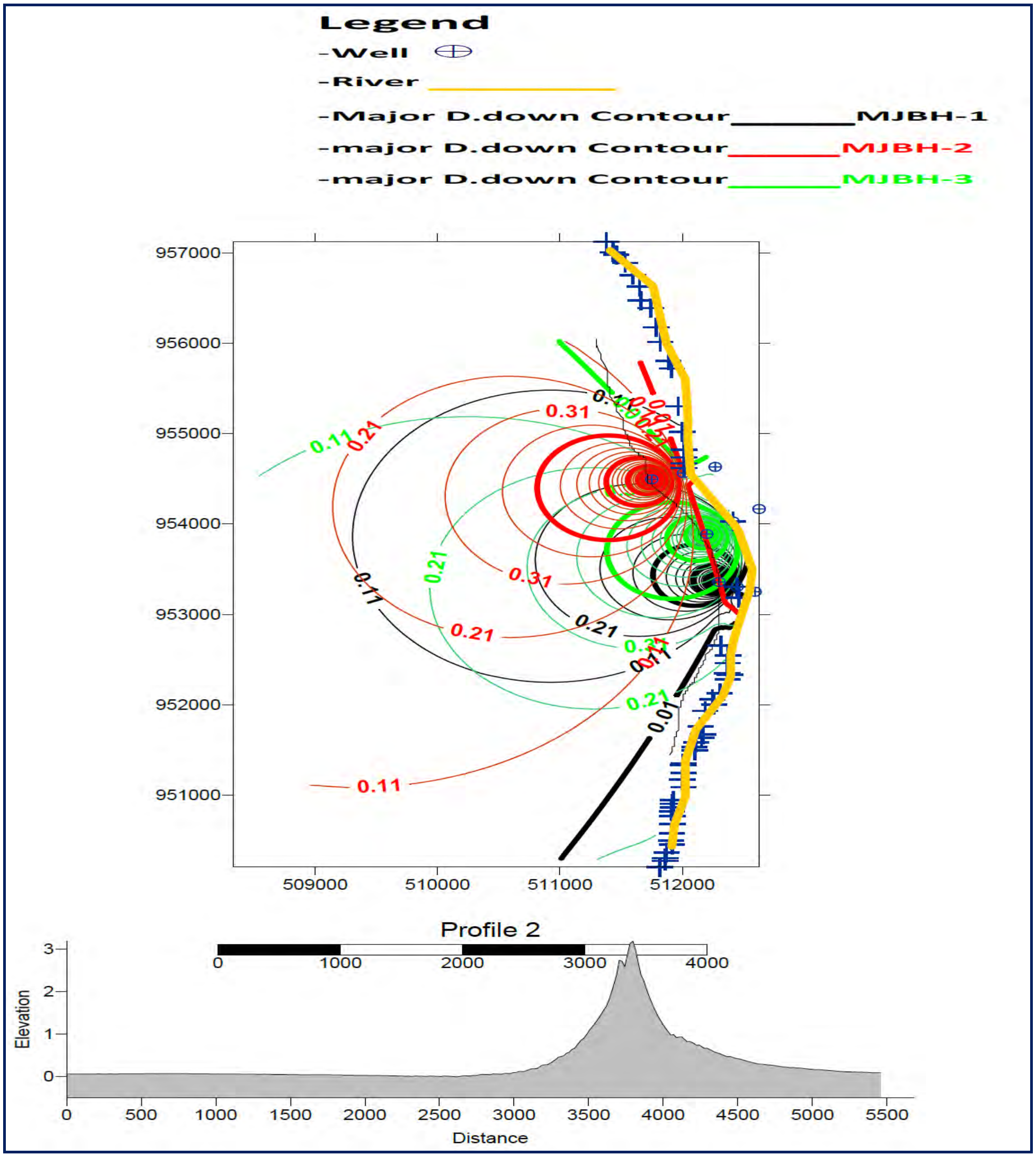

Figure 49. Schematic plan view illustrating possible well interference configuration of contour lines distributions in which the drawdowns computed by superposition for individual three pumping boreholes and the plots conducted for the particular boreholes and overlaid to note marginal overlapping states of the cones of depressions as the above plot plan view shows in case when the pumps at every boreholes are all assumed to operate by half rates of designed discharge rate capacities of the wells and the aquifer letting adopts maximum transmissivity T_{max}.

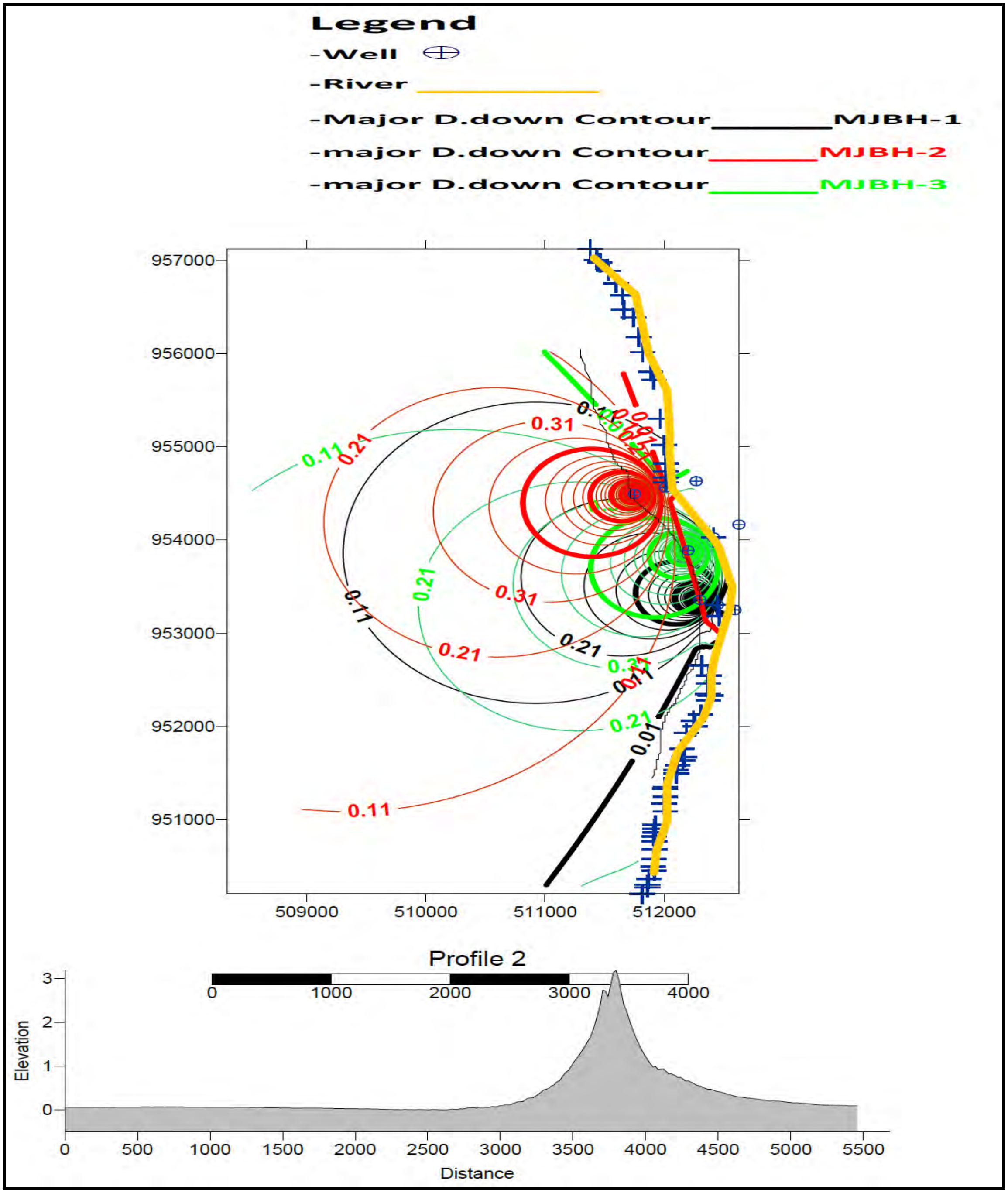

Figure 50. Schematic plan view illustrating possible well interference configuration of contour lines distributions in which the drawdowns computed by superposition for individual three pumping boreholes and the plots conducted for the particular boreholes and overlaid to note marginal overlapping states of the cones of depressions as the above plot plan view shows in case when the pumps at every boreholes are all assumed to operate by half rates of designed discharge rate capacities of the wells and the aquifer letting adopts minimum transmissivity T_{min}.

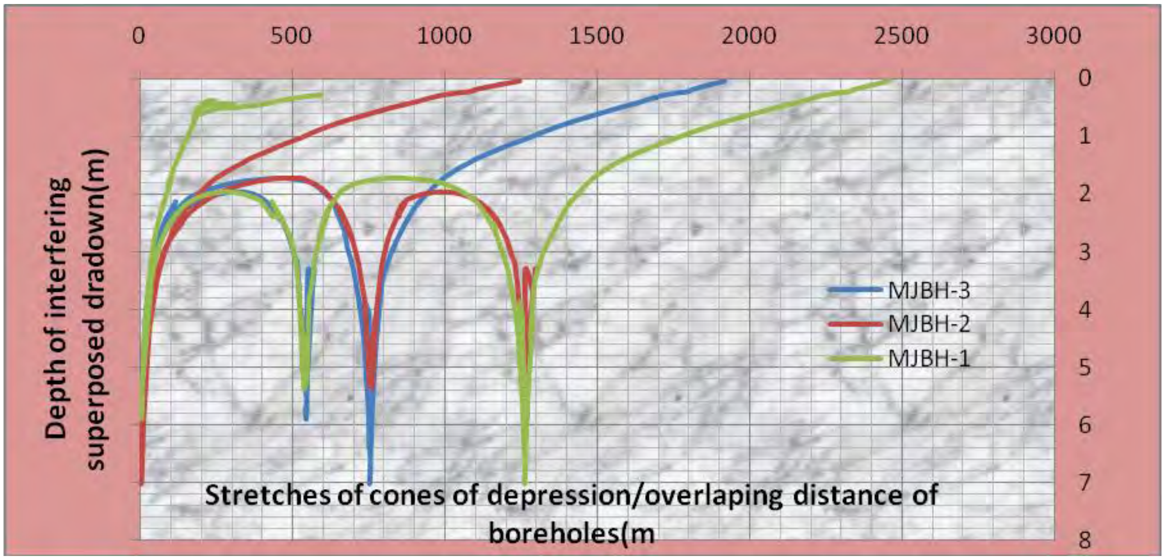

Figure 51. Schematic cross section illustrating possible well interference configuration explain potential drawdown interference between the operating boreholes when the pumps in the wells assumed to operate by half rates of the designed capacities and the aquifer attains minimum transmissivity T_{min} for case the individual drawdowns superposed for every three pumping boreholes and overlaid as the plan view of Figure 50 shows.

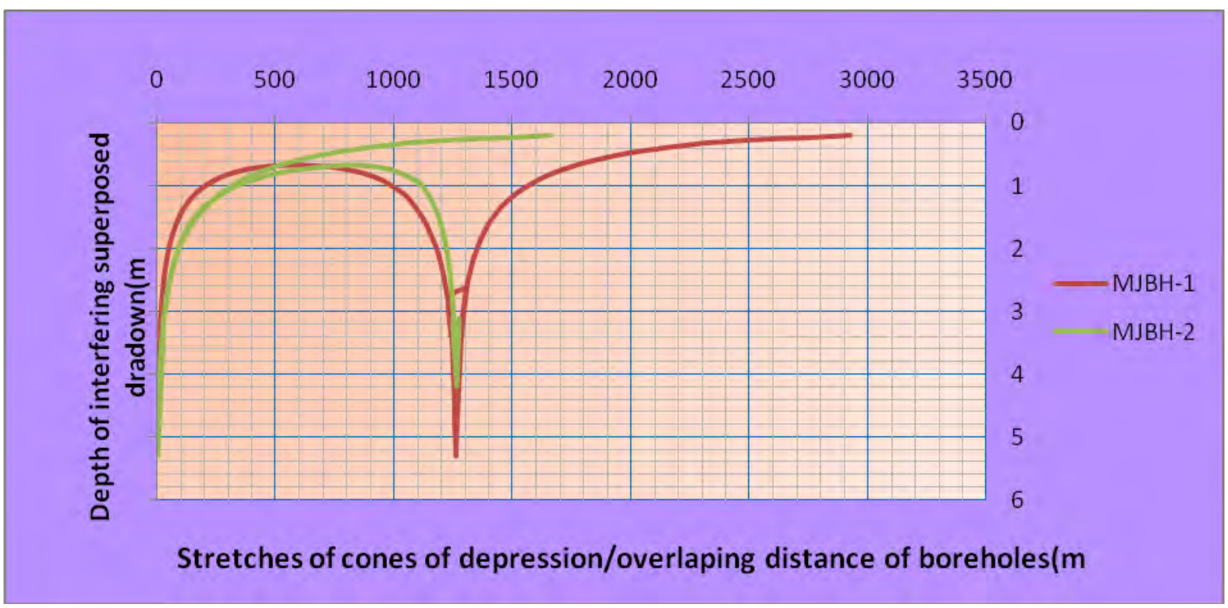

Figure 52. Schematic cross section illustrating possible well interference configuration explain potential drawdown interference between the operating boreholes when the rates of designed capacities in the wells assumed and the aquifer attains minimum transmissivity T_{min} for the case of only two wells as plan view in which particular superposed drawdown for each boreholes overlaid.

5. Conclusions and Recommendations

5.1. Conclusions

The contribution of this research is as follows

It details how fixed the radius of influences and approximated the corresponding time travels with respect to distant from the potential threatening sites and this in return may contribute better awareness while selecting and designing proper layout system for a group of wells or multiple well in a given well field, in scheduling progressive water resources management, planning of pump operations and building of suitable protections to environmental impacts thus to secure sustainable extracting of potable water from the field.

It describes how the expansions, configurations and intersecting of contour lines of simulated composite drawdowns affected by adopting different mean values of aquifer parameters along with systematically controlling of the pumping rates to evaluate varying case scenarios to reach at an outmost results in delineating the influence boundary zones for the operating wells.

Through the study, here are the summarized main conclusions of this research which have been conducted depending up on the analyses results:

1. Because of building up wards of the configuration of contour lines plots of composite drawdowns as the distance kept between the river and the boreholes not adequate and the river exists at higher elevation than the static water levels in the boreholes, this research forms a conclusion that the river delivers a flow into the aquifer and thus the Mojo boreholes abstract water from this river which is responsible in refilling the withdrawal water as long as ascending of pumping operating in the boreholes.

2. The quality of the data were tested by the graphical method through plotting the collected data drawdowns and the recovery data on drawdown versus time and residual drawdowns versus time graphs on both excel window and the aquifer testing software computer programme and the recorded data those exhibit deviation from the normal were removed and the drawdown records at the latest time had only been considered in the analyses. So that the approximated values of the transimissivities computed by the Excel method and Aquifer Test software technique via curve fitting techniques were comparably closer to each other, this implies that the organized data are dependable and the results of the tests are reliable.

3. The Mojo Perennial River is the main package of the pollutions due to the facts of the potential treats such as depots, tanneries and oil factories which have no proper waste treatments are closer and sending wastes to this river, it indirectly transfers poisons to the adjacent aquifer; therefore, the abstraction conducted from this well field to alleviate the water demand to the town cannot be free from suspicions contaminations.

4. As noticed from distribution graphs the arrangements of the composite drawdown's contours lines plots they crossing each other and overlapping such previews of overlapping arrangements of contour lines verified the state of well interference so that from this occurrence, a conclusion derived that there are wells interfering between operating boreholes at Mojo well field.

5.2. Recommendations

1. The Resident water supply authorities of Mojo town ought to secure the catchment areas of the recharging river to minimize the intrusions of pollutants chemicals into the river there by exercising the following actions: -
    - ❖ Influencing the factories owners in privilege to facilitate waste treatments plants to their factors
    - ❖ Creating awareness to local level ruling out the use of fertilizers, pesticides, other hazard chemicals, degradations of the catchments as a result of improper land use and management and cultivations
    - ❖ Cultivating forests to sustain the regulation of drawdown at well field.

2. The boreholes for irrigation schemes at the vicinity of Mojo boreholes are developing by the MoWE, so that enough space should be kept to avoid interferences these wells with the water supply boreholes.

3. Provision of high capacity of recharge ponds, by preserving closer distances between the Mojo Perennial River and the boreholes so that no account of the river flow shall be perceived by pumping boreholes in touch with the river reach since these ponds operating a role of the recharging river due to their closer proximity to the boreholes than the river, thus these high capacity ponds supply the aquifer with equivalent inflow that the river used to deliver.

4. It is wrong to select the location of boreholes site closer to the hydraulic boundary. Great precautions should be carefully taken when decision made to select proper settings of the wells site by thoroughly evaluating the sites and providing sufficient space from the possible threats and the realization radius of influence should included while designing layout system for the field.

5. Water quality test not conducted due to construction works of main lines currently in progress and water extraction for domestic consumption from the boreholes have

not been commenced until now/this study is finalized. As the previous study pointed out water production from the previous wells those established nearer to the Mojo Perennial River has been found exposed to water born and water related diseases such as typhoid and amebiasis and since the boreholes for the new scheme are similarly located closer to this river in which suspicious pollutants expected from the existing potential threats situated at the well field vicinity and this project intended to simply extracting water from these points, delivers to the service reservoir through the rising main lines and then to covey into the distribution lines there to supply for domestic uses with no treatment facilitate. Therefore; we would like to recommend water quality analyses should be conducted whilst the pumps in the boreholes will be functioning as this river delivers flow to the adjacent aquifer at the well field and the water from this source is contaminated water by different anthropogenic developments conditions described earlier. Although the potential pollutants are existing at the downstream of the boreholes locations, the influence of pumping in due course of time may come in contact with those sources as the cones of depressions expands and governs more areal coverage with continual pumping operations over longer period of times.

6. The thesis investigates only the depletion of water from the river to aquifer depending on the distance between the operating wells and the river. Hence, the total volume of water that can be extracted from the perennial river and the time needed for the process to end under varying conditions of the pump operations recommend as a topic for further study to consolidate confidences to the conclusions of this research derived and to enhance the potential utilization of the groundwater at the well field may the case related.

7. We would also like to mention a model based solute transport investigation at this area to establish the potential contaminant influences on the quality of the groundwater.

REFERENCES

Ayenew, T., Demellie, Prof., A.C. (2012). Pumping Test Lecture Note. Addis Ababa Institute of Technology. pp. 4-11.

Azzah Salah El-Din Hassan. (2013). Master Thesis. Semi-Analytical Tool for Optimal Management of Alluvial Aquifers Hydraulically Connected to Streams.

Bear, J. (1979). *Hydraulics of Groundwater*. McGraw-Hill, New York, p. 569.

Boonstra, J. and N. A. de Ridder. (1981). Numerical Modelling of Ground Water Basins. International Institute for Land Reclamation and Improvement. Wageningen, The Netherlands. pp. 4-40.

Boulton N.S. and Streltsova T.D. (1977). Unsteady flow to a pumped well in a fissured water-bearing formation. Journal of Hydrology, 35. pp. 257–269.

Bouwer, Herman. (2002). Artificial recharge of groundwater: hydrogeology and engineering. Hydrogeology Journal, No. 10:121–132.

Charlas R. Fitts. (2002). *Ground Water Science*. Copyright@ 2002. Elsevier Science Ltd. An Imprint of Elsevier Science 525 B Street, Suite 1900, San Diego, California 92101-4495, USA, http://www.academicpress.com. pp. 15-16, p. 94, pp. 216-226.

Chirlin, G. R. (1990). The Slug Test: The First Four Decades. Ground Water Management. Proceedings of the (1990). Cluster Conference. National Water Well Association. Columbus,Ohio. pp. 365-381.

Desta Horrecha Consult. (2012-213). Mojo Water Suplly Well Development Report.

Department of the Army. U.S. Army Corps of Engineers, (1999). *Ground water manual*, Engineering and Design Groundwater Hydrology. Manual No.1110-2-1421. Washington, DC 20314-1000. Chapter-4. p. 10 ; Chappter-5. pp-5-2.

Dragoni W. (1998). Some considerations regarding the radius of influence or a pumping well. Internet: <http://www.gndci.pg.cnr.itf>. pp. 21-25.

de Marsily G. (1986). *Quantitative Hydrogeology - Groundwater Hydrology for Engineers*. Academic Press, pp. 269 and 440.

EPA. (1995). Technical Guidance manual for Hydrogeologic Investigations and Ground Water Monitoring, U.S. Environmental Protection Agency. Chapter 4. pp. 1-24; pp. 4-6.

F. De Smedt, prof. dr. ir. A.C. (2009). Ground Water Hydrology. Department of Hydrology and Hydraulic Engineering Faculty of Applied Sciences, Internet: <Email: fdesmedt@vub.ac.be,Free University Brussel>. pp. 6-17.

Fetter, C.W. (2001). *Applied Hydrogeology*. (4th edition). New York, NY: Macmillan College Publishing Company. pp. 435-436 and p. 598.

Freeze, R. A. and J. A. Cherry. (1979). *Groundwater*, Prentice Hall, Englewood Cliffs, N.J. p. 604.

Handa BK (1994). *Ground water contamination in India*, in Proc. Regional Workshop on Env. Aspects of Groundwater Dev., (Singhal DC ed.), Ind. Assoc. Hydrol., Kurukshetra, pp. 1–33.

Harr, J. (1995). *A Civil Action*. Vintage Books, New York, p. 502.

I.Delleur, J. W. (Jacques Willy). (2000). The Handbook of Groundwater Engineering. School of Civil Engineering Purdue Universit West Lafayette, Indiana. edited by Jacques Delleur. Includes bibliographical references and index. ISBN 0-8493-2698-2 (CRC Press) ISBN 3-540-64745-7 (Springer-Verlag).Co-published by.CRC Press LLC.2000 Corporate Blvd., N.W. Boca Raton, FL 33431, U.S.A. pp. 61-62; pp.294-323 and 840-844.

Jacob, C. E. (1944). Notes on Determining Permeability by Pumping Tests Under Water Table Conditions. U.S. Geological Survey.

J. Wilson, Prof. A.A., (2006). Hydrology Program, ERTH403/HYD503, pp=30-32.

Kakar YP (1988). *Ground water quality monitoring in India*. Jalvigyan Sameeksha, NIH, Roorkee, Vol. III, pp. 52–63.

Kakar YP (1990). *Groundwater pollution due to industrial effluents*. Bhu-Jal News, Central Ground Water Board, Govt. of India 2: 1–12.

Karplus, Walter J., (1958). Analog simulation: New York, McGraw Hill, p. 434.

Kresic Neven (2009). *Groundwater Resources Sustainability, Management, and Restoration*. The McGraw-Hill Companies. pp. 366-415 and pp. 766-769.

Kresic Neven (2010). *Sustainability and management of springs*.MACTEC Engineering and Butterworth-Heinemann is an imprint of Elsevier 2010, Elsevier Inc. 30 Corporate Drive, Suite 400, Burlington, MA 01803, USA. pp.425-430; pp.441-566.

Kevin M. Hiscock., (2005). *Hydrogeology Principles and Practice*. School of Environmental Sciences University of East Anglia. First published 2005 by Blackwell Science Ltd. United Kingdom., pp. 176-183.

Kruseman GP, de Ridder NA. (1994). *Analysis and Evaluation of Pumping Test Data*, 2nd ed. International Institute for Land Reclamation and Improvement, Publication 47. P.O. Box 45, 6700 AA Wageningen, The Netherlands, 1994. pp. 49-50, pp. 90-101, 226-290 and 377.

K.Thorbjarnarson, Well Hydraulics and Capture Zone. MODULE. Internet: <http://groundwater.orst.edu/under/wells.html>.

Mebruk Mohammed, Dr. Ing., A.C., (2012). GWH, Well Hydraulics Lecture Note. Addis Ababa Institute of Technology. pp. 199-203 and pp. 205-220.

Philippe Renard. (2005). *Hydraulics of Wells and Well Testing*. University of Neuchatel, Switzerland. Encyclopedia of Hydrological Sciences (edt. by M.G. Anderson). 2005 John Wiley & Sons, Ltd. Switzerland. pp. 10-13 and pp.15-18.

Ruprecht JK, Schofield NJ (1991). Effects of partial deforestation on hydrology and salinity in high salt storage landscapes. J. Hydrol. 12(9): 19–38.

Rushton K.R. (2003). *Groundwater Hydrology: conceptual and computational models*. John Wiley & Sons Ltd. The Atrium, Southern Gate, Chichester. pp. 159-165.

Schoeller H (1959) Arid Zone Hydrology: Recent Developments. UNESCO, Paris, p. 125.

Singhal and R. P. Gupta. (2010). Applied Hydrogeology of Fractured Rocks, DOI 10.1007/978-90-481-8799-7. Springer Science+Business Media B.V. 2010. pp. 60-61 and 169-175.

Smedley PL. (1992). *Relationship between trace elements in water and health*, with special reference to developing countries. Interim Report 1992. BGS Tech. Report WD/92/39, p. 33.

Stevens, J., (1986). Applied Multivariate Statistics for the Social Sciences. Erlbaum, Hillsdale, NJ.

Sevee, J. 1991. *Methods and Procedures for Defining Aquifer Parameters*. In: D. M. Nielsen (editor), *Practical Handbook of Ground-Water Monitoring*. Lewis Publishers, Inc.

Chelsea, Michigan. pp. 397-448.

Tensay Getnet, MSc.Thesis, November (2011). *Sedimentation Modeling for Ribb Dam*, Addis Ababa Institute of Technology, pp.48 -53

Thomas Röhrich (2002). Aquifer Test v.3.5 User's Manual, Advanced Pumping Test & Slug Test Analysis Software. Co-developed by Thomas Röhrich and Waterloo Hydrogeologic, Inc. pp. 138-149.

Todd, D.K. (1980). *Groundwater Hydrology* (2nd edition). John Wiley and Sons, New York, pp. 181,183,186, 193 and 535.

Tweed SO, Leblanc M, Webb JA, Lubczynski MW (2007) Remote Sensing and GIS for mapping groundwater recharge and discharge areas in salinity prone catchment, south-eastern Australia. Hydrogeol. J. 15(1): 95–96.

United Nations Educational, Scientific and Cultural Organization UNESCO (2004). Determining hydrodynamic and contaminant transfer parameters of groundwater flow, *in Ground Water Studies* (eds V. S. Kovale**versus**ky, G. P. Kruseman, K. R. Rushton). IHP-VI, Series on Groundwater No. 3. UNESCO, Paris. pp. 113-114; pp. 223-229.

Walton, W. C. (1987). *Groundwater Pumping Tests, Design and Analysis*. Lewis Publishers, Inc.Chelsea, Michigan.

Welch AH Stollenwerk KG (eds) (2003). *Arsenic in Ground Water*. Kluwer Academic Publ., Dordrecht, p. 475.

APPENDIX - A

Data Modification, Aquifer Categorizing, Analyses Of Theis Curve- Fitting Matching To Approximate The Parameters Of Mojo Well Field Aquifer By Excel Tools Manually And Aquifer Test Program Automatic Curve Fitting Techniques

A1-Adjustment Conducted to the collected Data

Table A. 1: *Adjusted Drawdowns for related conditions of pumping test data from single borehole MJBH-1*

From (m)	To (m)	Casing	Length (m)	Blind length (m)	Screen length(m)	2l/r	Time (min)	F Calculated	Q (m^3/s)	Drawdown (m)	SWL (m)	Drawdown (m) Corrected for Partial Penetration	Drawdown (m) Corrected for Unconfined again Sc=sa*(1-sa/2b)
1 a. g. l.	12	2 Surface casing	12	12	0	0	0	0.733	0.045	0	12.9	0	0
0.6 a. g. l.	74.79	12.6 Blind	75.79	75.8	0	0	1	0.733	0.045	11.4	12.9	8.36	8.27
75	86.42	1.9 Screen	11.63	0	11.63	183	2	0.733	0.045	13.1	12.9	9.6	9.47
86	92.65	1 Blind	6.23	6.23	0	0	3	0.733	0.045	14.3	12.9	10.47	10.32
93	104.32	1.9 Screen	11.67	0	11.67	184	4	0.733	0.045	14.7	12.9	10.75	10.59
104	110.36	1 Blind	6.04	6.04	0	0	5	0.733	0.045	15.2	12.9	11.11	10.93
110	128.42	3 Screen	18.06	0	18.06	284	6	0.733	0.045	15.4	12.9	11.29	11.11
128	140.43	2 Blind	12.01	12	0	0	7	0.733	0.045	15.5	12.9	11.36	11.18
140	164.47	4 Screen	24.04	0	24.04	379	8	0.733	0.045	15.7	12.9	11.52	11.33
164	170.47	1 Blind	6	6	0	0	9	0.733	0.045	15.8	12.9	11.58	11.39
170	176.48	1 Screen	6.01	0	6.01	94.7	10	0.733	0.045	16.2	12.9	11.88	11.68
176	182.52	1 Blind	6.04	6.04	0	0	12	0.733	0.045	16.7	12.9	12.24	12.03
183	206.44	4 Screen	23.92	0	23.92	377	14	0.733	0.045	17	12.9	12.46	12.25
206	218.14	2 Blind	11.7	11.7	0	0	16	0.733	0.045	17.2	12.9	12.57	12.35
218	230.45	2 Screen	12.31	0	12.31	194	18	0.733	0.045	17.3	12.9	12.71	12.49
230	236.45	1 Blind	6	6	0	0	20	0.733	0.045	17.5	12.9	12.85	12.62
236	248.15	2 Screen	11.7	0	11.7	184	25	0.733	0.045	17.9	12.9	13.14	12.9
248	254.41	1 Blind	6.26	6.26	0	0	30	0.733	0.045	18.6	12.9	13.64	13.38
254	283.33	4.8 sern	28.92	0	28.92	455	35	0.733	0.045	18.6	12.9	13.6	13.34

283	300.57	2.9 Blind	17.24	17.2	0	0	40	0.733	0.045	18.7	12.9	13.71	13.45
301	323.65	3.8 Screen	23.08	0	23.08	363	45	0.733	0.045	19	12.9	13.89	13.62
324	335.17	1.9 Blind	11.52	11.5	0	0	50	0.733	0.045	19.2	12.9	14.04	13.76
335	352.46	2.9 Screen	17.29	0	17.29	272	60	0.733	0.045	19.3	12.9	14.16	13.88
352	357	0.8 Blind	4.54	4.54	0	0	70	0.733	0.045	19.4	12.9	14.23	13.95
Average			**15.42**	**7.56**	**7.86**	**124**	80	0.733	0.045	19.6	12.9	14.4	14.11
L/b		0.51	Thus it satisfies the principle L/b<0.5				90	0.733	0.045	19.8	12.9	14.54	14.25
2L/r		123.77	Thus it satisfies the principle 2L/r>30				100	0.733	0.045	20	12.9	14.68	14.38
$F=L/b[1+7\cos(\pi L/2b)(r/2L)^{0.5}]$					**0.7331**		120	0.733	0.045	20.3	12.9	14.87	14.57
							140	0.733	0.045	20.6	12.9	15.09	14.78
							160	0.733	0.045	20.8	12.9	15.26	14.94
							180	0.733	0.045	21.1	12.9	15.5	15.16
							210	0.733	0.045	21.4	12.9	15.71	15.37
							240	0.733	0.045	21.9	12.9	16.08	15.72
							270	0.733	0.045	22.2	12.9	16.24	15.87
							300	0.733	0.045	22.4	12.9	16.42	16.04
							330	0.733	0.045	22.6	12.9	16.58	16.2
							360	0.733	0.045	23	12.9	16.83	16.44
							420	0.733	0.045	23.3	12.9	17.05	16.65
							480	0.733	0.045	23.4	12.9	17.13	16.72
							540	0.733	0.045	23.6	12.9	17.29	16.88
							600	0.733	0.045	23.8	12.9	17.43	17.01
							660	0.733	0.045	23.9	12.9	17.54	17.11
							720	0.733	0.045	24	12.9	17.62	17.19
							780	0.733	0.045	24.2	12.9	17.73	17.29
							840	0.733	0.045	24.3	12.9	17.83	17.39
							900	0.733	0.045	24.5	12.9	17.95	17.5
							960	0.733	0.045	24.6	12.9	18.03	17.58
							1020	0.733	0.045	24.7	12.9	18.09	17.63
							1080	0.733	0.045	24.7	12.9	18.09	17.63
							1140	0.733	0.045	24.7	12.9	18.09	17.63
							1200	0.733	0.045	24.7	12.9	18.09	17.63
							1260	0.733	0.045	24.7	12.9	18.09	17.63
							1320	0.733	0.045	24.7	12.9	18.09	17.63
							1380	0.733	0.045	24.7	12.9	18.09	17.63

Table A. 2: *Adjusted Drawdowns for associated conditions of pumping test data from single borehole MJBH-2*

From (m)	To (m)	Casing	Length (m)	Blind length (m)	Screen length (m)	2l/r	Time (min)	F Calculated	Q(m^3/s)	Drawdowns (m)	SWL	Drawdowns (m) Corrected for Partial penetrations	Drawdown (m) Corrected for Unconfined again Sc=sa*(1-sa/2b)
0.6 m a.g.l.	12	2 Surface casing	12.00	12.00	0.00	0.00	0	0.7012	0.045	0.00	24.5	0.00	0.00
+1 m a.g.l.	109.1	17.8 Blind	110.09	110.09	0.00	0.00	1	0.7012	0.045	0.90	24.5	0.63	0.63
109.1	139.2	5 Screen	30.06	0.00	30.06	473.39	2	0.7012	0.045	4.30	24.5	3.02	3.00
139.2	150.8	2 Blind	11.64	11.64	0.00	0.00	3	0.7012	0.045	5.45	24.5	3.82	3.80
150.8	180	5 Screen	29.22	0.00	29.22	460.16	4	0.7012	0.045	6.33	24.5	4.44	4.41
180	192.7	2 Blind	12.65	12.65	0.00	0.00	5	0.7012	0.045	7.23	24.5	5.07	5.04
192.7	216.7	4 Screen	24.06	0.00	24.06	378.90	6	0.7012	0.045	8.44	24.5	5.92	5.88
216.7	222.8	1 Blind	6.03	6.03	0.00	0.00	7	0.7012	0.045	9.04	24.5	6.34	6.29
222.8	246.8	4 Screen	24.06	0.00	24.06	378.90	8	0.7012	0.045	10.40	24.5	7.29	7.23
246.8	253.4	1 Blind	6.54	6.54	0.00	0.00	9	0.7012	0.045	10.42	24.5	7.31	7.24
253.4	256.4	1/2 Blind	3.07	3.07	0.00	0.00	10	0.7012	0.045	10.96	24.5	7.68	7.61
256.4	268.1	2 Screen	11.63	0.00	11.63	183.15	12	0.7012	0.045	11.37	24.5	7.97	7.90
268.1	273.9	1 Blind	5.82	5.82	0.00	0.00	14	0.7012	0.045	11.53	24.5	8.08	8.01
273.9	297.3	4 Screen	23.40	0.00	23.40	368.50	16	0.7012	0.045	11.80	24.5	8.27	8.19
297.3	308.9	2 Blind	11.59	11.59	0.00	0.00	18	0.7012	0.045	12.90	24.5	9.05	8.95
308.9	326.4	3 Screen	17.54	0.00	17.54	276.22	20	0.7012	0.045	13.15	24.5	9.22	9.12
326.4	332.2	1 Blind	5.81	5.81	0.00	0.00	25	0.7012	0.045	13.37	24.5	9.37	9.27
332.2	355.5	4 Screen	23.33	0.00	23.33	367.40	30	0.7012	0.045	13.63	24.5	9.56	9.45
355.5	367.1	2 Blind	11.59	11.59	0.00	0.00	35	0.7012	0.045	13.82	24.5	9.69	9.58
367.1	384.6	3 Screen	17.42	0.00	17.42	274.33	40	0.7012	0.045	13.97	24.5	9.80	9.68
384.6	390.4	1 Blind	5.81	5.81	0.00	0.00	45	0.7012	0.045	14.13	24.5	9.91	9.79

390.4	402.1	2 Screen	11.69	0.00	11.69	184.09	50	0.7012	0.045	14.23	24.5	9.98	9.86
402.1	415	2 Blind	12.95	12.95	0.00	0.00	60	0.7012	0.045	14.28	24.5	10.01	9.89
Average			18.61	9.37	9.24	145.44	70	0.7012	0.045	14.46	24.5	10.14	10.02
L/b		0.496	Thus it satisfies the principle L/b<0.5				80	0.7012	0.045	14.60	24.5	10.24	10.11
2L/r		145.436	Thus it satisfies the principle 2L/r>30				90	0.7012	0.045	14.64	24.5	10.27	10.14
$F=L/b[1+7\cos(\pi L/2b)(r/2L)^{0.5}]$					**0.7012**		100	0.7012	0.045	14.70	24.5	10.31	10.18
							120	0.7012	0.045	14.73	24.5	10.33	10.20
							140	0.7012	0.045	14.83	24.5	10.40	10.27
							160	0.7012	0.045	14.89	24.5	10.44	10.31
							180	0.7012	0.045	15.00	24.5	10.52	10.38
							210	0.7012	0.045	15.06	24.5	10.56	10.43
							240	0.7012	0.045	15.12	24.5	10.60	10.47
							270	0.7012	0.045	15.19	24.5	10.65	10.51
							300	0.7012	0.045	15.30	24.5	10.73	10.59
							330	0.7012	0.045	15.40	24.5	10.80	10.66
							360	0.7012	0.045	15.40	24.5	10.80	10.66
							420	0.7012	0.045	15.45	24.5	10.83	10.69
							480	0.7012	0.045	15.60	24.5	10.94	10.79
							540	0.7012	0.045	15.68	24.5	10.99	10.85
							600	0.7012	0.045	15.77	24.5	11.06	10.91
							660	0.7012	0.045	15.84	24.5	11.11	10.96
							720	0.7012	0.045	15.92	24.5	11.16	11.01
							780	0.7012	0.045	15.98	24.5	11.20	11.05
							840	0.7012	0.045	16.04	24.5	11.25	11.09
							900	0.7012	0.045	16.09	24.5	11.28	11.13
							960	0.7012	0.045	16.15	24.5	11.32	11.17
							1020	0.7012	0.045	16.18	24.5	11.34	11.19
							1080	0.7012	0.045	16.20	24.5	11.36	11.20
							1140	0.7012	0.045	16.28	24.5	11.41	11.26
							1200	0.7012	0.045	16.38	24.5	11.49	11.33
							1260	0.7012	0.045	16.38	24.5	11.49	11.33
							1320	0.7012	0.045	16.38	24.5	11.49	11.33
							1380	0.7012	0.045	16.43	24.5	11.52	11.36
							1440	0.7012	0.045	16.48	24.5	11.56	11.39
							1500	0.7012	0.045	16.49	24.5	11.56	11.40
							1560	0.7012	0.045	16.53	24.5	11.59	11.43
							1620	0.7012	0.045	16.57	24.5	11.62	11.46
							1680	0.7012	0.045	16.60	24.5	11.64	11.48
							1740	0.7012	0.045	16.64	24.5	11.67	11.50
							1800	0.7012	0.045	16.69	24.5	11.70	11.54
							1860	0.7012	0.045	16.70	24.5	11.71	11.54

1920	0.7012	0.045	16.75	24.5	11.74	11.58
1980	0.7012	0.045	16.75	24.5	11.74	11.58
2040	0.7012	0.045	16.76	24.5	11.75	11.59
2100	0.7012	0.045	16.76	24.5	11.75	11.59
2160	0.7012	0.045	16.78	24.5	11.77	11.60
2220	0.7012	0.045	16.79	24.5	11.77	11.61
2280	0.7012	0.045	16.80	24.5	11.78	11.61
2340	0.7012	0.045	16.82	24.5	11.79	11.63
2400	0.7012	0.045	16.84	24.5	11.81	11.64
2460	0.7012	0.045	16.87	24.5	11.83	11.66
2520	0.7012	0.045	16.88	24.5	11.84	11.67
2580	0.7012	0.045	16.90	24.5	11.85	11.68
2640	0.7012	0.045	16.94	24.5	11.88	11.71
2700	0.7012	0.045	16.95	24.5	11.88	11.71
2760	0.7012	0.045	16.98	24.5	11.91	11.74
2820	0.7012	0.045	17.08	24.5	11.98	11.80
2880	0.7012	0.045	17.10	24.5	11.99	11.82
2940	0.7012	0.045	17.13	24.5	12.01	11.84
3000	0.7012	0.045	17.15	24.5	12.02	11.85
3060	0.7012	0.045	17.17	24.5	12.04	11.86
3120	0.7012	0.045	17.20	24.5	12.06	11.89
3180	0.7012	0.045	17.21	24.5	12.07	11.89
3240	0.7012	0.045	17.23	24.5	12.08	11.91
3300	0.7012	0.045	17.25	24.5	12.10	11.92
3360	0.7012	0.045	17.29	24.5	12.12	11.95
3420	0.7012	0.045	17.33	24.5	12.15	11.97
3480	0.7012	0.045	17.34	24.5	12.16	11.98
3540	0.7012	0.045	17.37	24.5	12.18	12.00
3600	0.7012	0.045	17.37	24.5	12.18	12.00
3660	0.7012	0.045	17.37	24.5	12.18	12.00
3720	0.7012	0.045	17.37	24.5	12.18	12.00
3780	0.7012	0.045	17.37	24.5	12.18	12.00
3840	0.7012	0.045	17.38	24.5	12.19	12.01
3900	0.7012	0.045	17.38	24.5	12.19	12.01
3960	0.7012	41.9	17.4	24.5	12.20	12.02
4020	0.7012	41.92	17.42	24.5	12.21	12.03
4080	0.7012	41.95	17.45	24.5	12.24	12.06

Table A. 3: *Adjusted Drawdowns for associated conditions of pumping test data from single borehole MJBH-3*

From (m)	To (m)	Casing	Length (m)	Blind length (m)	Screen length (m)	2l/r	Time (min)	F Calculated	Q(m³/s)	Drawdowns (m)	SWL	Drawdowns (m) Corrected for Partial penetrations	Corrected Drawdown (m) for Unconfined again Sc=sa*(1-sa/2b)
0.85 a. g. l.	12	2 Surface casing	12.85	12.85	0.00	0.00	0	0.7652	0.04383	0.00	14.55	0.00	0.00
0.85 a. g. l.	95.15	15.85 Blind	95.15	95.15	0.00	0.00	1	0.7652	0.04383	4.84	14.55	3.70	3.69
95.15	130.87	6 Screen	35.72	0	35.72	562.52	2	0.7652	0.04383	9.55	14.55	7.31	7.24
130.87	136.69	1 Blind	5.82	5.82	0.00	0.00	3	0.7652	0.04383	9.95	14.55	7.61	7.54
136.69	160.22	5 Screen	23.53	0	23.53	370.55	4	0.7652	0.04383	10.40	14.55	7.96	7.88
160.22	166.22	1 Blind	6	6	0.00	0.00	5	0.7652	0.04383	10.47	14.55	8.01	7.93
166.22	196.1	6 Screen	29.88	0	29.88	470.55	6	0.7652	0.04383	10.65	14.55	8.15	8.07
196.1	202.1	1 Blind	6	6	0.00	0.00	7	0.7652	0.04383	10.85	14.55	8.30	8.22
202.1	214.12	2 Screen	12.02	0	12.02	189.29	8	0.7652	0.04383	11.14	14.55	8.52	8.44
214.12	220.15	1 Blind	6.03	6.03	0.00	0.00	9	0.7652	0.04383	11.27	14.55	8.62	8.53
220.15	244.21	4 Screen	24.06	0	24.06	378.90	10	0.7652	0.04383	11.45	14.55	8.76	8.67
244.21	250.49	1 Blind	6.28	6.28	0.00	0.00	12	0.7652	0.04383	11.74	14.55	8.98	8.88
250.49	256.61	1 Blind	6.12	6.12	0.00	0.00	14	0.7652	0.04383	12.00	14.55	9.18	9.08
256.61	280.78	4 Screen	24.17	0	24.17	380.63	16	0.7652	0.04383	12.22	14.55	9.35	9.24
280.78	293.02	2 Blind	12.24	12.24	0.00	0.00	18	0.7652	0.04383	12.44	14.55	9.52	9.41
293.02	316.52	4 Screen	23.5	0	23.50	370.08	20	0.7652	0.04383	12.61	14.55	9.65	9.54
316.52	322.28	1 Blind	5.76	5.76	0.00	0.00	25	0.7652	0.04383	13.00	14.55	9.95	9.83
322.28	345.24	4 Screen	22.96	0	22.96	361.57	30	0.7652	0.04383	13.40	14.55	10.25	10.12
345.24	351.38	1 Blind	5.63	5.63	0.00	0.00	35	0.7652	0.04383	13.58	14.55	10.39	10.26
351.38	362.91	2 Screen	11.53	0	11.53	181.57	40	0.7652	0.04383	13.81	14.55	10.57	10.43
362.91	369.06	1 Blind	5.76	5.76	0.00	0.00	45	0.7652	0.04383	14.01	14.55	10.72	10.58
369.06	386.68	3 Screen	17.62	0	17.62	277.48	50	0.7652	0.04383	14.20	14.55	10.87	10.72

386.68	392.78	1 Blind	6.15	6.15	0.00	0.00
392.78	404.3	2 Screen	11.52	0	11.52	181.42
404.3	410	1 Blind	5.7	5.7	0.00	0.00
Average			**16.88**	**7.42**	**9.46**	**148.98**
L/b		0.56	Thus it does not satisfies the principle L/b<0.5 but we apply correction as the aquifer is unconfined and the difference is 0.06			
2L/r		148.98	Thus it satisfies the principle 2L/r>30			
F=L/b[1+7cos(πL/2b)(r/2L)$^{0.5}$]					**0.7652**	

60	0.7652	0.04383	14.56	14.55	11.14	10.99
70	0.7652	0.04383	14.85	14.55	11.36	11.21
80	0.7652	0.04383	15.10	14.55	11.55	11.39
90	0.7652	0.04383	15.43	14.55	11.81	11.64
100	0.7652	0.04383	15.63	14.55	11.96	11.78
120	0.7652	0.04383	15.93	14.55	12.19	12.01
140	0.7652	0.04383	16.30	14.55	12.47	12.28
160	0.7652	0.04383	16.71	14.55	12.79	12.59
180	0.7652	0.04383	16.75	14.55	12.82	12.62
210	0.7652	0.04383	16.80	14.55	12.85	12.65
240	0.7652	0.04383	16.82	14.55	12.87	12.67
270	0.7652	0.04383	16.95	14.55	12.97	12.76
300	0.7652	0.04383	17.15	14.55	13.12	12.91
330	0.7652	0.04383	17.56	14.55	13.44	13.22
360	0.7652	0.04383	17.92	14.55	13.71	13.48
420	0.7652	0.04383	18.30	14.55	14.00	13.76
480	0.7652	0.04383	18.58	14.55	14.22	13.97
540	0.7652	0.04383	18.80	14.55	14.38	14.13
600	0.7652	0.04383	19.00	14.55	14.54	14.28
660	0.7652	0.04383	19.23	14.55	14.71	14.45
720	0.7652	0.04383	19.45	14.55	14.88	14.61
780	0.7652	0.04383	19.55	14.55	14.96	14.69
840	0.7652	0.04383	19.71	14.55	15.08	14.80
900	0.7652	0.04383	19.85	14.55	15.19	14.91
960	0.7652	0.04383	19.95	14.55	15.26	14.98
1020	0.7652	0.04383	20.07	14.55	15.36	15.07
1080	0.7652	0.04383	20.20	14.55	15.46	15.16
1140	0.7652	0.04383	20.25	14.55	15.49	15.20
1200	0.7652	0.04383	20.40	14.55	15.61	15.31
1260	0.7652	0.04383	20.43	14.55	15.63	15.33
1320	0.7652	0.04383	20.50	14.55	15.69	15.39
1380	0.7652	0.04383	20.56	14.55	15.73	15.43
1440	0.7652	0.04383	20.65	14.55	15.80	15.50

1500	0.7652	0.04383	20.74	14.55	15.87	15.56
1560	0.7652	0.04383	20.80	14.55	15.92	15.61
1620	0.7652	0.04383	20.95	14.55	16.03	15.72
1680	0.7652	0.04383	21.08	14.55	16.13	15.81
1740	0.7652	0.04383	21.20	14.55	16.22	15.90
1800	0.7652	0.04383	21.25	14.55	16.26	15.94
1860	0.7652	0.04383	21.34	14.55	16.33	16.00
1920	0.7652	0.04383	21.40	14.55	16.37	16.05
1980	0.7652	0.04383	21.50	14.55	16.45	16.12
2040	0.7652	0.04383	21.55	14.55	16.49	16.16
2100	0.7652	0.04383	21.60	14.55	16.53	16.19
2160	0.7652	0.04383	21.65	14.55	16.57	16.23
2220	0.7652	0.04383	21.80	14.55	16.68	16.34
2280	0.7652	0.04383	21.90	14.55	16.76	16.41
2340	0.7652	0.04383	21.95	14.55	16.80	16.45
2400	0.7652	0.04383	22.05	14.55	16.87	16.52
2460	0.7652	0.04383	22.15	14.55	16.95	16.60
2520	0.7652	0.04383	22.19	14.55	16.98	16.63
2580	0.7652	0.04383	22.25	14.55	17.02	16.67
2640	0.7652	0.04383	22.30	14.55	17.06	16.71
2700	0.7652	0.04383	22.30	14.55	17.06	16.71
2760	0.7652	0.04383	22.32	14.55	17.08	16.72
2820	0.7652	0.04383	22.32	14.55	17.08	16.72
2880	0.7652	0.04383	22.32	14.55	17.08	16.72

A_2 - Analyses of the Corrected Pumping Test Data by EXCEL Tools by manual Curve – Fitting

***Theis's Curve-Fitting Method, Cooper and Jacob Drawdown versus Time Graph and Residual Drawdown versus Time Graph*.**

The Analytic Solution Method is consumed for analyzing pumping test data which completed in each three single wells at Mojo well field aquifer. The measured drawdowns data from every single pumping well test is fitted to match with standard simulated type – curve so as to identify category of aquifers in the area of our interest. Once the category of the aquifer was determined for water supply well fields, the pumping test data is adjusted against to the conditions of external influences those may take place during the pumping test had been conducted. Thus, a log-log graph of the measured drawdown as a function of time since pumping started was plotted for each well. Then curve fitting for each three wells with different standard type – curves is conducted manually. Subsequently the category of the aquifer at which pumping test conducted is recognized based on judgments of the visual observations from the curve fitting and lasting duration of pumping period that recorded during pumping test.

The Theis's curve-fitting method is established on the following simplified assumptions and limiting conditions for steady state and unsteady state conditions.

"Several studies suggested that the assumptions and conditions underlying the curve-fitting methods are: -

1. The aquifer is infinite in extent, with no constant head boundaries, no-flow boundaries, or any other heterogeneity;
2. The aquifer is homogeneous, isotropic, and of uniform thickness over the area influenced by the test;
3. Prior to pumping starts, there exits steady state head distribution and the flow surface is horizontal (or nearly so) over the area that will be influenced by the test;
4. The aquifer is pumped at a constant discharge rate and keeps pumping at a steady discharge rate Q when pumping well turns on at time t=t0 ;

5. The well penetrates the entire thickness of the aquifer, hence receives water by horizontal flow and there is only resistance to horizontal flow;
6. Far from the well, heads remain unaffected by pumping;
7. Close to the well, the hydraulic gradient approaches the same gradient that occurs with steady-state radial flow;
8. And with the limiting conditions, in addition, for unsteady-state methods: -
9. The water removed from storage is discharged instantaneously with decline of head. When the flow to the well is in an unsteady state, i.e. the drawdown differences with time are not negligible nor are the hydraulic gradient constant with time;
10. The diameter of the well is small, i.e. the storage in the well can be neglected (Charles R. Fitts, 2002; G.P. Kruseman and N.A. de Ridder, 1994)".

A log–log time drawdown plot for an ideal unconsolidated confined aquifer tapped by a fully penetrating well will match with the Theis type curve (Figure A1. A) and a semi-log time-drawdown plot will be characterized by an uniform slope as (Figure A1. A'). The graphic of log-log plot in the figures Part B and b below display the curves for an unconfined, homogeneous, isotropic aquifer of infinite lateral extent and with a delayed yield. These two curves are characterized by delayed yield in unconfined aquifers which show typical S-shape on a log–log plot with three time-segments (Figure A1. B) shows (B.B.S. Singhal and R.P. Gupta, 2010).

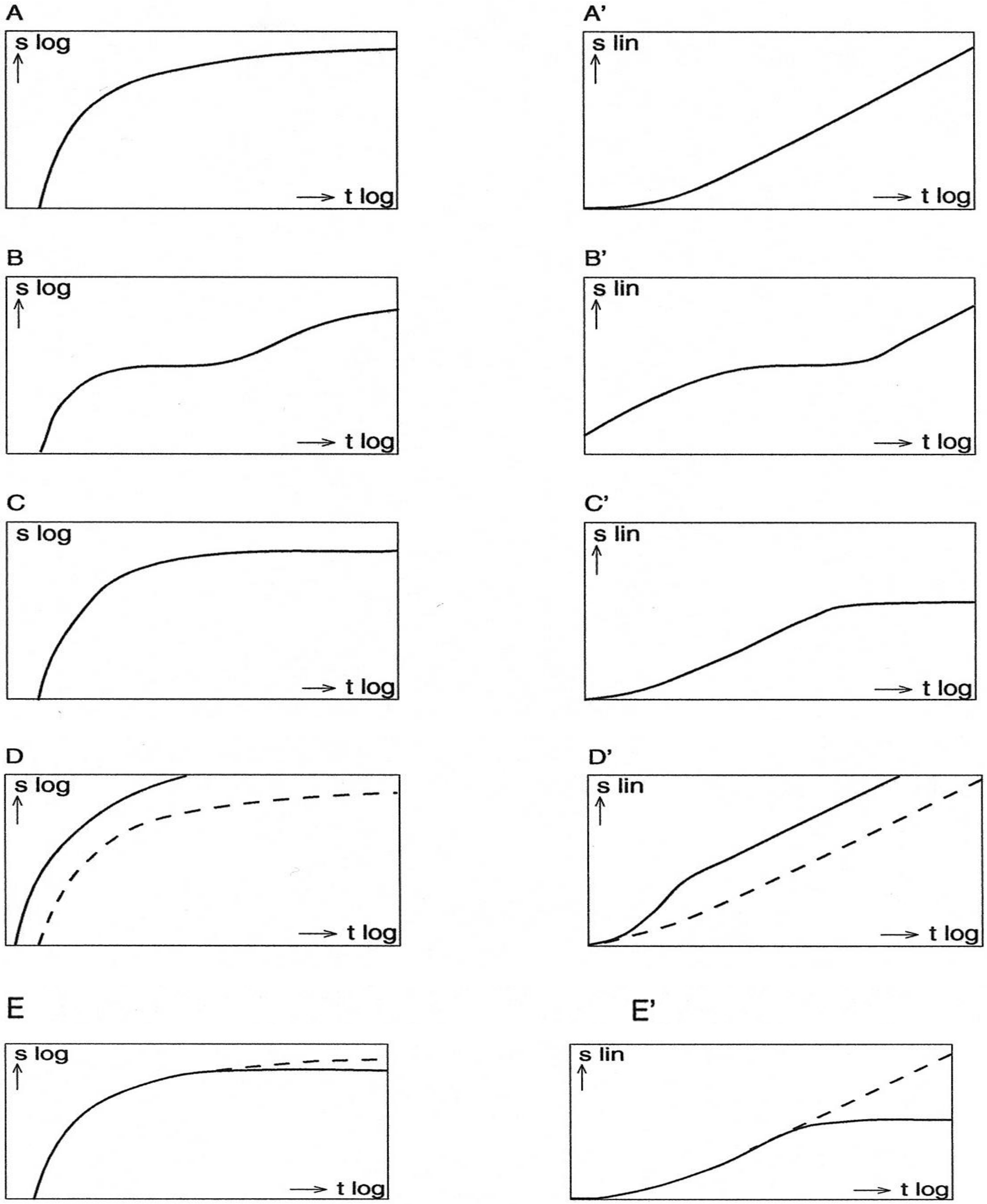

Figure A1. Comparison of log–log and semi-log curves of the theoretical drawdown versus time relationship in aquifers; A and A’: confined aquifer, B and B’: unconfined aquifer, C and C’: leaky (or semi-confined) aquifer; D and D’: effect of partial penetration, E and E’: effect of recharge boundary (Source of the diagrams, Kruseman GP, de Ridder NA, 1994).

According to the listed authors, the three time segments of the curve should be assumed as follows: -

1. "The steep early-time segment covers only a brief period after the start of pumping (often only the first few minutes). At early pumping times, an unconfined aquifer reacts in the same way as a confined aquifer: the water produced by the well is released instantaneously from storage by the expansion of the water and the compaction of the aquifer. The shape of the early-time segment is similar to the Theis type curve;
2. The flat intermediate-time segment reflects the effect of the dewatering that accompanies the falling water table. The effect of the dewatering on the drawdown is comparable to that of leakage: the increase of the drawdown slows down with time and thus deviates from the Theis curve. After a few minutes to a few hours of pumping, the time-drawdown curve may approach the horizontal;
3. The relatively steep late-time segment reflects the situations where the flow in the aquifer is essentially horizontal again and the time-drawdown curve once again tends to conform to the Theis curve". (Kruseman GP, de Ridder NA, 1994).

Based on different responses of graphic features of the pumping test data from single boreholes, pumping duration that had been narrated at the pumping tests and the basic behaviors of unconfined aquifers as the descriptions at sections 2.4.3 and 2.4.4 indicates, the category of the aquifer at well field region for this investigation (Mojo Town Water Supply well Field) groups in the classifications of ***unconfined*** aquifer.

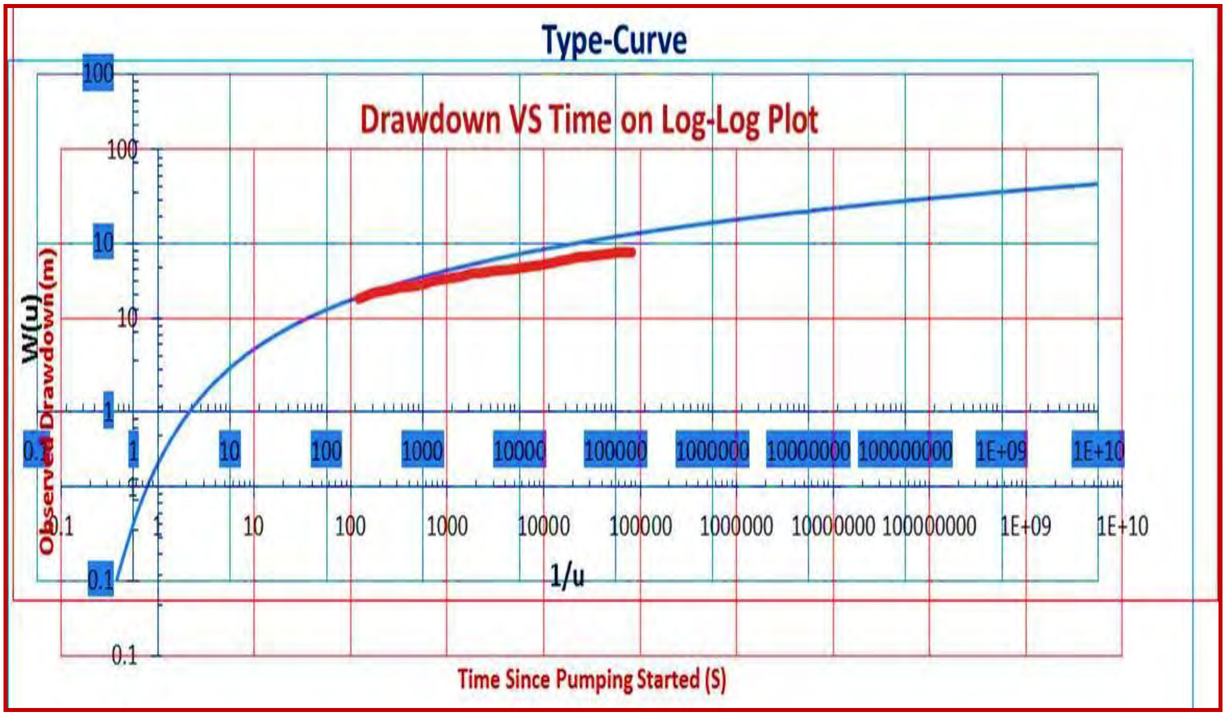

Figure A2. Plot of Observed Drawdown as a function of time in double-logarithmic paper for MJ-BH1 and the effect shows the behavior of Unconfined aquifer in response to constant pumping rate

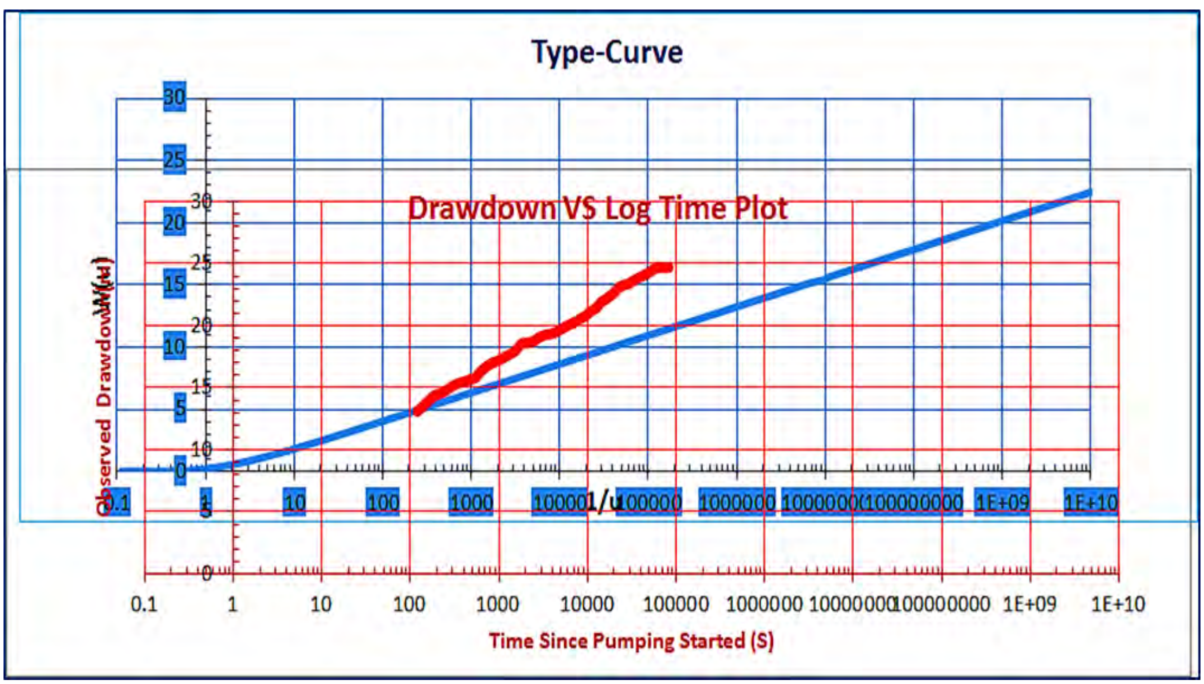

Figure A3. Observed drawdown versus time plot on Semi-Log paper for MJBH-1 shows the effect of partial penetration

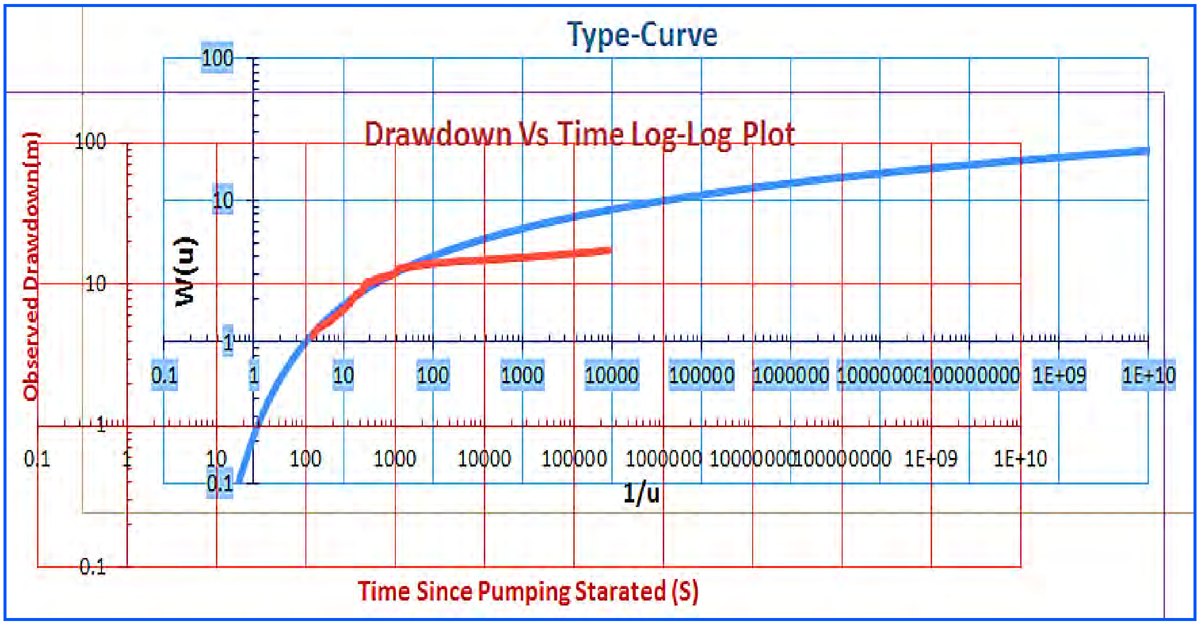

Figure A4. A Plot of Observed Drawdown as a function of time in double-logarithmic paper for MJBH-2 and the effect shows the behavior of unconfined aquifer in response to constant pumping rate

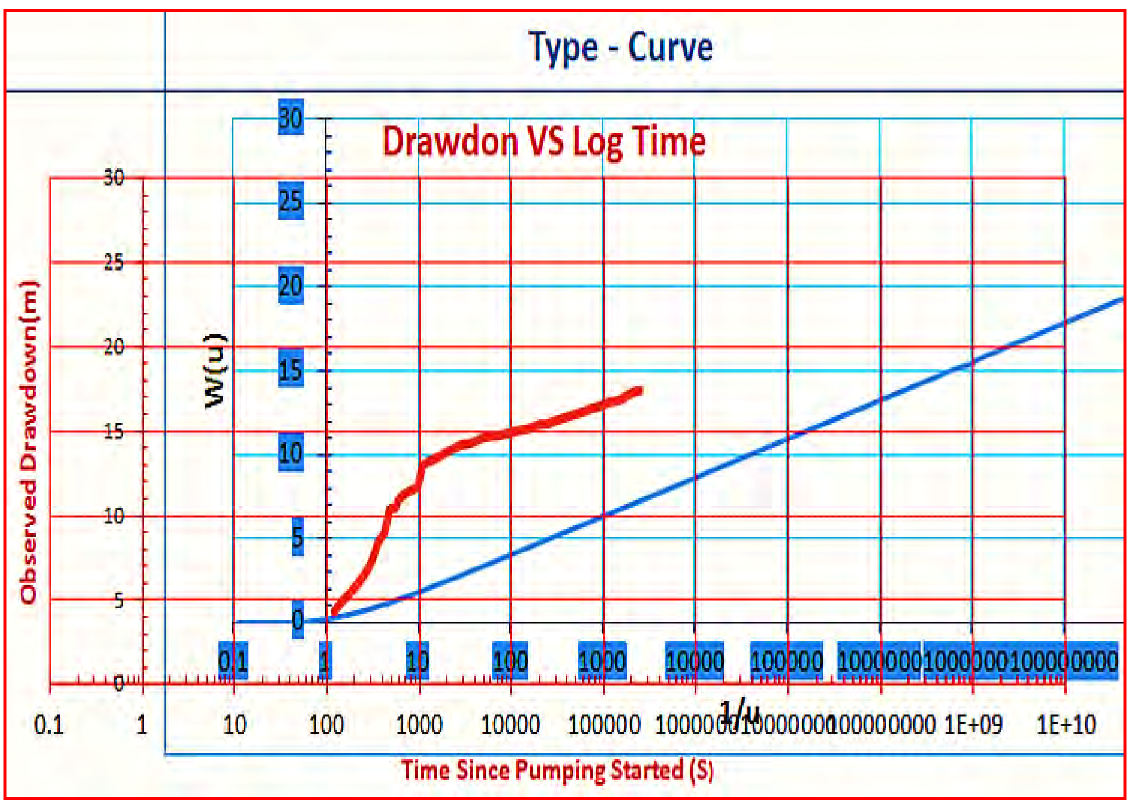

Figure A5. Observed drawdown versus time plot on Semi-Log paper for MJBH-2 shows the effect of partial penetration

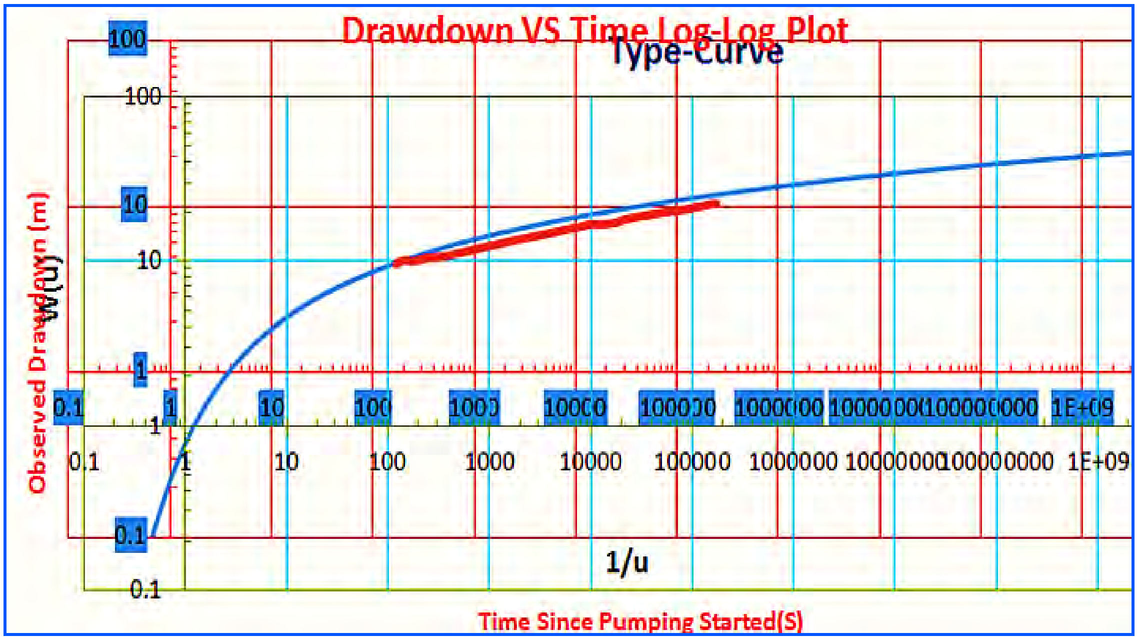

Figure A6. A Plot of Observed Drawdown as a function of time in double-logarithmic paper for MJBH-3 and the effect shows the behavior of unconfined aquifer in response to constant pumping rate

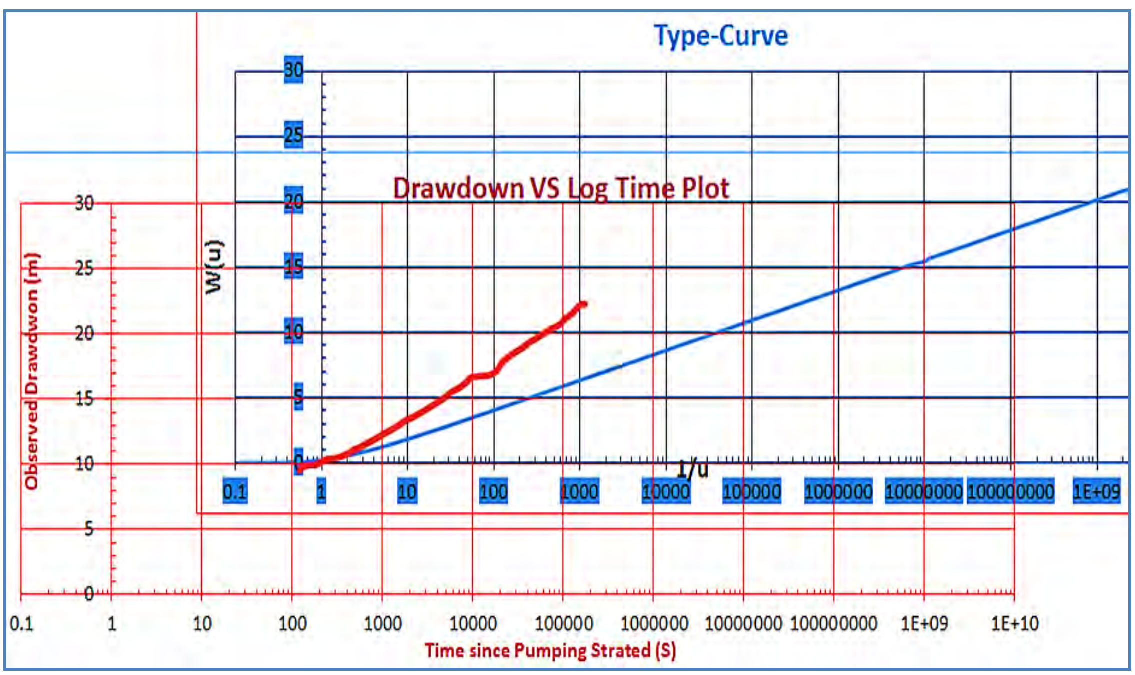

Figure A7. Observed drawdown versus time plot on Semi-Log paper for MJ-BH3 shows the effect of partial penetration

Therefore; as it can be observed from the plots of both log-log and semi-log of drawdown as a function of time since pumping started and with sensibly comparisons of the simulated standard type curves as shown in literature review parts and there also by considering the length of lasting duration of pumping periods recorded during the operation of pumping tests, the aquifer of the Mojo Water Supply Well Field is categorized into an ***unconfined*** type of the Aquifers along with ***partial penetration and recharging boundary condition****.*

a) Result of Pumping Test Analysis and Outcomes of the Aquifers Parameters

Next to the aquifer categorization, corrections for the measured drawdowns against to external influential conditions those might be encountered during the operation of pumping test is conducted before the data are going to apply for the analysis of aquifer parameters valuation. Accordingly, the measured drawdown data that observed from individual single well pumping test is adjusted for the required corrections as Table A1 illustrates.

There by using the corrected drawdown and observed data as a function of the time since pumping started is plotted on log-log scale for each well on Excel Spread Sheet. Similarly the Theis Type – Curve using well function W (u) versus 1/u with the same scale is also plotted on Excel Spread Sheet using values of W (u) on Y-axis and 1/u on X-axis from table of readily published ground water books. Table A1 shows the adjusted data of the drawdown.

Then the corrected drawdown versus time plot is fitted with the Type – Curve by moving it keeping the horizontal axis parallel and overlapping until the best matching point achieved provided that both plots ensured to have the same size and scale. As a final point in estimation of the aquifer parameters for particular wells i.e. MJBH-1, MJBH-2 and MJBH-3 is carried out manually by means of three analytical solution methods as sequentially detailed here below:-

i) Result of Pumping Test Analysis by Excel Spread Sheet (Theis Type-Curve Fitting Method for MJBH-1)

The two logarithmic plots with similar size and scale (i.e. for the corrected drawdown from MJBH-1 and Theis Type – Curve) are manually superposed and shifted keeping the axes parallel to each other until the best corresponding point is attained as shown in the Figure A8 below. So that the best fitting point is selected with values for W (u) =1 and 1/u =10 and the corresponding values for s=1.3m and t=0.16 sec.

Hence, from Theis equation by substituting it results

$$T_{TBH1} = \frac{Q}{4\pi S} W(u) = \frac{0.045}{4*\pi*1.3} * 1 = 0.00275\, {m^2}/{s}$$

$$S_{TBH1} = {4Ttu}/{r^2} = 4 * 0.00275 * 0.16 * 10/{0.127^2} = 0.0109$$

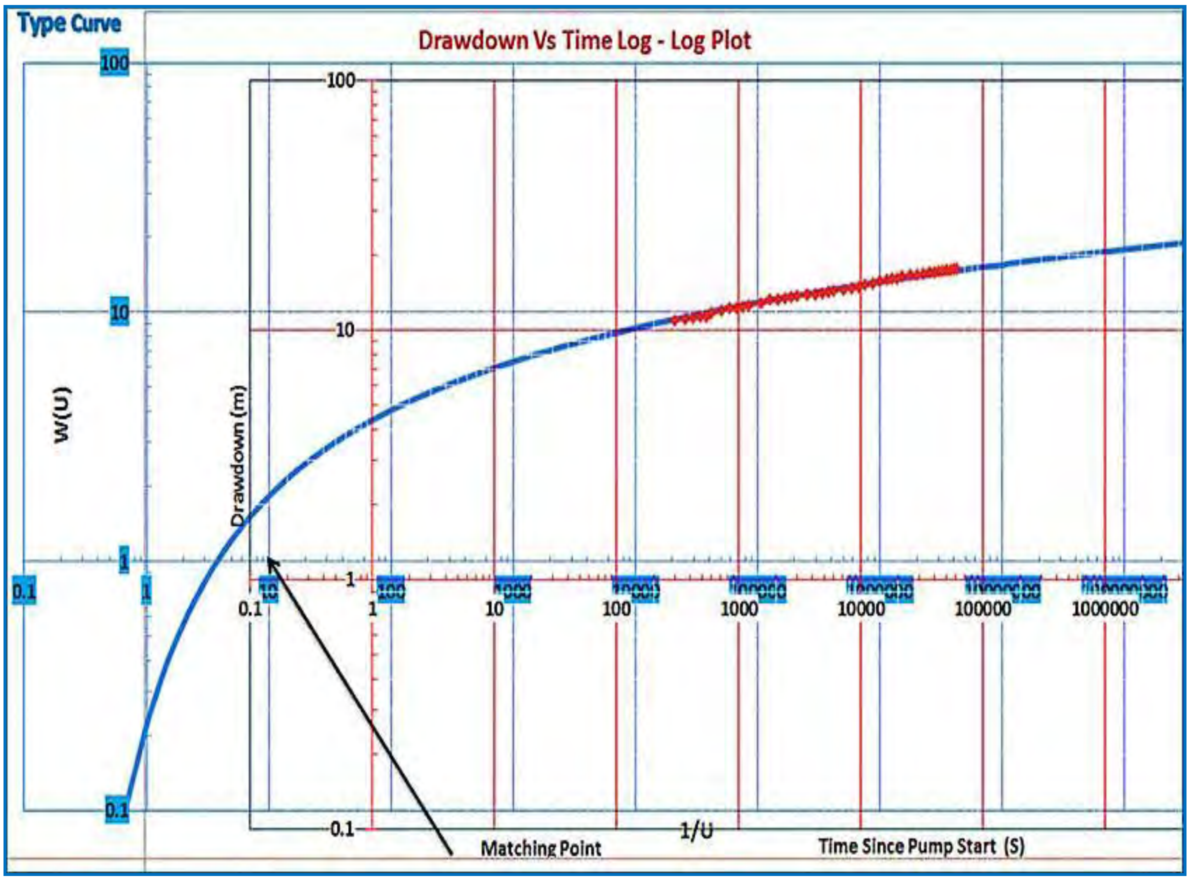

Figure A8. Adjusted field data of drawdowns versus time for pump testing observed from single well of MJBH-1 plotted on a log-log graph paper with the same scale as the theoretical Theis type curve, and superimposed on it.

ii) Result of Pumping Test Analysis by Excel Spread Sheet (Theis Type-Curve Fitting Method for MJBH-2)

The two logarithmic plots with similar size and scale (i.e. for the corrected drawdown from MJBH-2 and Theis Type – Curve) are superposed and shifted keeping the axes parallel to each other until the best corresponding point is attained as shown in the figure A9. So that the best fitting point is selected with values for W (u) =10 and 1/u =10 and the corresponding values for s=6.75m and t=0.0175 sec.

Hence, from Theis equation by substituting it gives

$$T_{TBH2} = \frac{Q}{4\pi S} W(u) = \frac{0.045}{4 * \pi * 6.75} * 10 = 0.00530\, {m^2}/{s}$$

$$S_{TBH2} = {4Ttu}/{r^2} = 4 * 0.0053 * 0.0175 * {10}/{0.127^2} = 0.00230$$

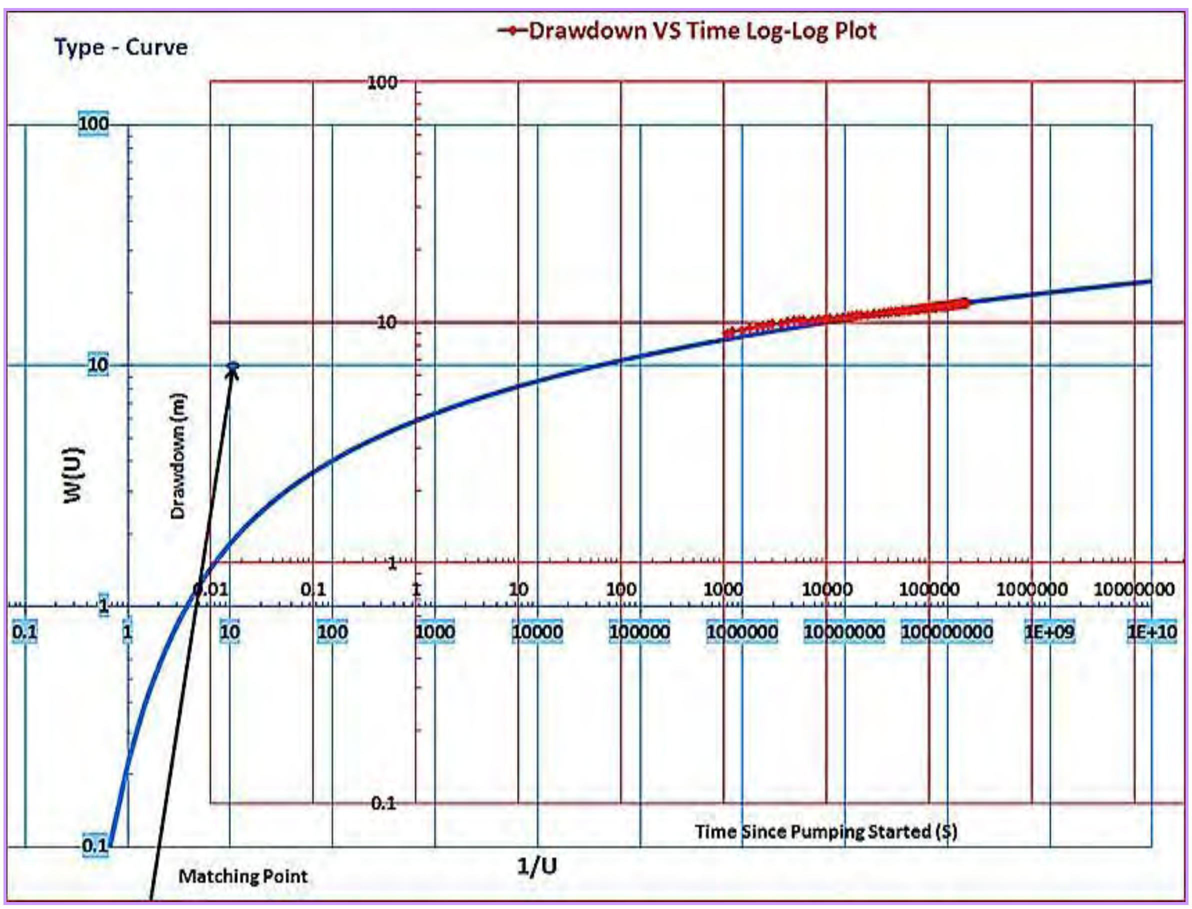

Figure A9. Adjusted field data of drawdowns versus time for pump testing observed from single well of MJBH-2 plotted on a log-log graph paper with the same scale as the theoretical Theis type curve, and superimposed on it.

iii) Result of Pumping Test Analysis by Excel Spread Sheet (Theis Type-Curve Fitting Method for MJBH-3)

The two logarithmic plots with similar size and scale (i.e. for the corrected drawdown from MJBH-3 and Theis Type – Curve) are superposed and shifted keeping the axes parallel to each other until the best corresponding point is attained as shown in the Figure A10. So that the best fitting point is selected with values for W (u) =10 and 1/u =10 and the corresponding values for s=1.3m and t=1.6 sec.

Hence, from Theis equation by substituting it gives

$$T_{TBH3} = \frac{Q}{4\pi S} W(u) = \frac{0.04383}{4 * \pi * 1.3} * 1 = 0.002683 \, ^{m^2}/_{s}$$

$$S_{TBH3} = {}^{4Ttu}/_{r^2} = 4 * 0.002683 * 1.6 * {}^{10}/_{0.127^2} = 0.10646$$

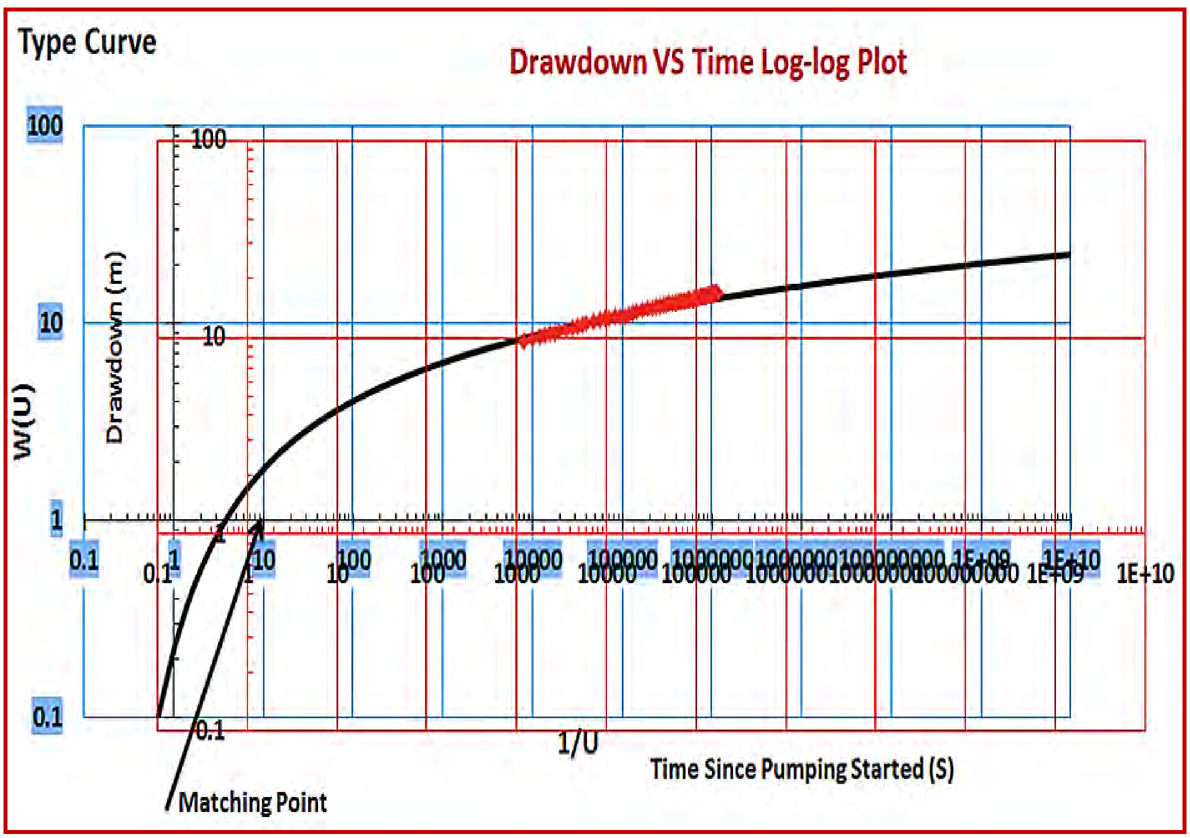

Figure A10. Adjusted field data of drawdowns versus time for pump testing observed from single well of MJBH-3 plotted on a log-log graph paper with the same scale as the theoretical Theis type curve, and superimposed on it.

iv) Result of Copper-Jacob Method for Solution of Non-Equilibrium Equation by Excel Spread Sheet for MJBH-1

The cooper – Jacob approximation is used to analyze the adjusted pumping test data of MoJo Borehole No.1 (MJBH-1) for value of u < 0.01. In an attempt to carry out the analysis for solution of non-equilibrium equation for the corrected drawdown data of the MJBH-1 applying the Copper and Jacob method, the previously described equation in the literature review section 1.4.2, is functional for the approximation of the solution.

To recall the equation:

$$s = \frac{2.3Q}{4\pi T}\log10\frac{2.25Tt_0}{r^2S} = \frac{Q}{4\pi T}\ln\frac{2.25Tt_0}{r^2S}$$

In case of this equation, as Q, r, T and S have constant values, a plot of the adjusted drawdown, s versus t on a semi - logarithmic graph paper can give a straight line as shown for MJBH-1 in Figure A11. For the values of large enough pumping time, a straight line is drawn through the adjusted drawdown data points. The slope of this straight line is calculated by analysis the value of Δs on the s - axis corresponding to one log-interval on the t - axis (one log-interval is the distance between any value and 10 times that value). This permits us to calculate T as

$$T = \frac{2.3Q}{4\pi\Delta s}$$

Then the value of S is also computed from the intercept t_0 of the fitted straight line with t-axis at a point s=0

$$S = \frac{2.25Tt_0}{r^2}$$

Accordingly from equation of the straight line fitted through the data points as the figure below depicts, the slope of the straight line is calculated as Δs = 15.097-12.138=2.959m and time (t_0) is read as t_0 = 0.0791sec. Hence, by substituting Δs value in the above equation gives T_{c1} for MJBH-1 which is designed to operate at a discharging rate of Q=45l/s

$$T_{CJ1} = \frac{2.3 * 0.045}{4 * \pi * 2.959} = 0.00278\,{}^{m^2}/_{s}$$

And also by substituting t_0 and T value in the above equation gives S_{CJ1} for MJ-BH1

$$S_{CJ1} = \frac{2.25 * 2.78 * 10^{-3} * 0.0791}{0.127^2} = 0.0313$$

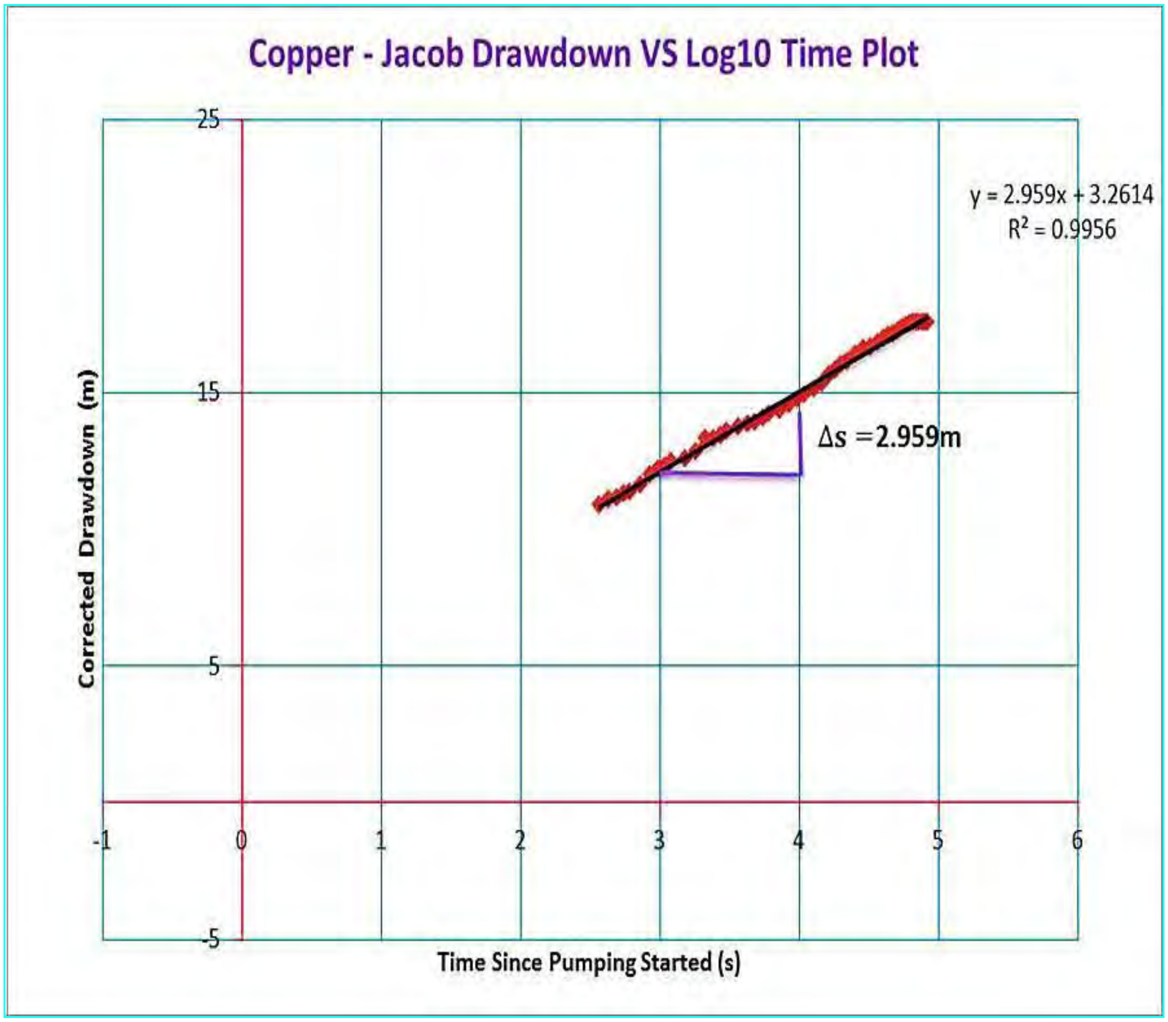

Figure A11. Copper-Jacob method for solution of non-equilibrium equation using the adjusted drawdown test data of MJBH-1. Drawdown is plotted as a function of time on semi-logarithmic paper.

v) **Result of Copper-Jacob Method for Solution of Non-Equilibrium Equation by Excel Spread Sheet for MJBH-2**

Through the same procedures as completed as for analyzing the corrected pumping test drawdown data for MJBH-1, is sequentially repeated to analyze solution for the corrected drawdown data of Mojo Borehole No.2 (MJBH-2) there by applying the Copper-Jacob approximation for the Solution Method of Non-Equilibrium Equation. Hence from equation of the straight line fitted through the adjusted data points of MJBH-2 as depicted in the figure below and the same equations speculated in the above analysis, the slope of the straight line is calculated as Δs =11.533-10.057 = 1.476m and time (t_0) is read as t_0 = 0.001536 sec. Hence, by substituting Δs value in the equation gives T_{c2} for MJBH-2 which is designed to operate at a discharging rate of Q=45l/s

$$T_{CJ2} = \frac{2.3 * 0.045}{4 * \pi * 1.476} = 0.00558 \, m^2/s$$

And also by substituting t_0 and T value in the above equation gives S_{CJ2} for MJBH-2

$$S_{CJ2} = \frac{2.25 * 5.58 * 10^{-3} * 0.001536}{0.127^2} = 0.001195$$

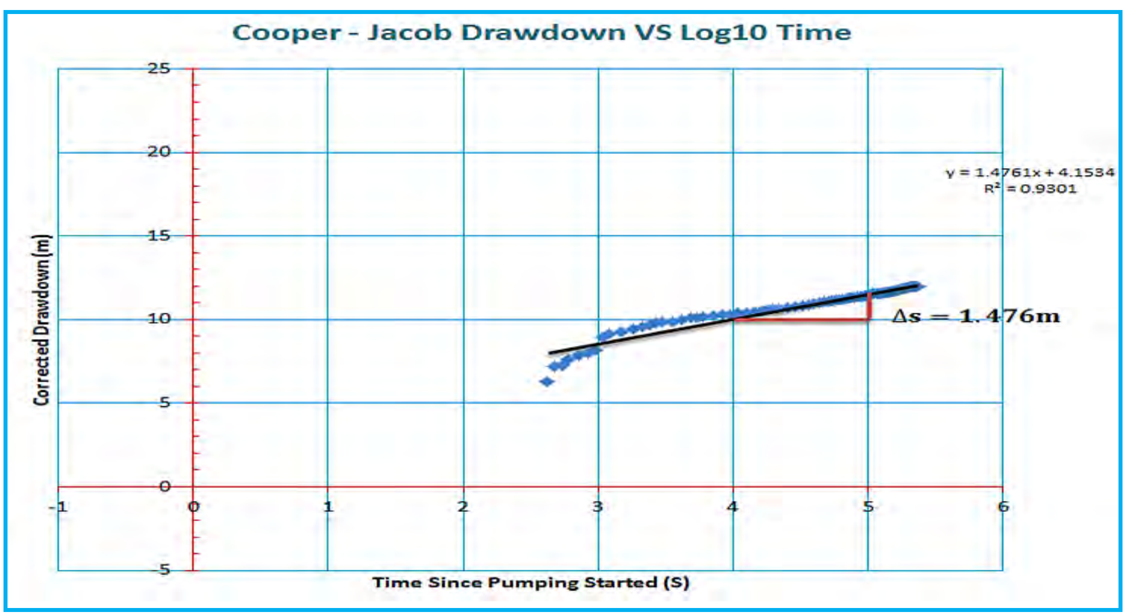

Figure A12. Copper-Jacob method for solution of non-equilibrium equation using the adjusted drawdown test data of MJBH-2. Drawdown is plotted as a function of time on semi-logarithmic paper.

vi) Copper-Jacob Method for Solution of Non-Equilibrium Equation for the Adjusted Drawdown Test Data of MJBH-3

Following the same procedures as completed as for analyzing the corrected pumping test drawdown data of MJBH-1, is successively repeated in order to analyze solution for the corrected drawdown data of Mojo Borehole No.3 (MJBH-3) there by applying the Solution Method of Non-Equilibrium Equation of the Copper-Jacob approximation. Thus from equation of the straight line fitted through the adjusted data points of MJBH-3 as depicted in the figure A13 below and using the same equation that speculated in the above analysis, the slope of the straight line is calculated as Δs = 12.543-9.41=3.133m and time (t_0) is read as t_0 = 0.992 sec. Hence, by substituting Δs value in the equation gives T_{CJ3} for MJBH-3 which is designed to operate at a discharging rate of Q=43.83l/s

$$T_{CJ3} = \frac{2.3 * 0.04383}{4 * \pi * 3.133} = 0.00256 \,{}^{m^2}/_{s}$$

And also by substituting t_0 and T value in the above equation gives SCJ3 for MJBH-3

$$S_{CJ3} = \frac{2.25 * 2.56 * 10^{-3} * 0.992}{0.127^2} = 0.3543$$

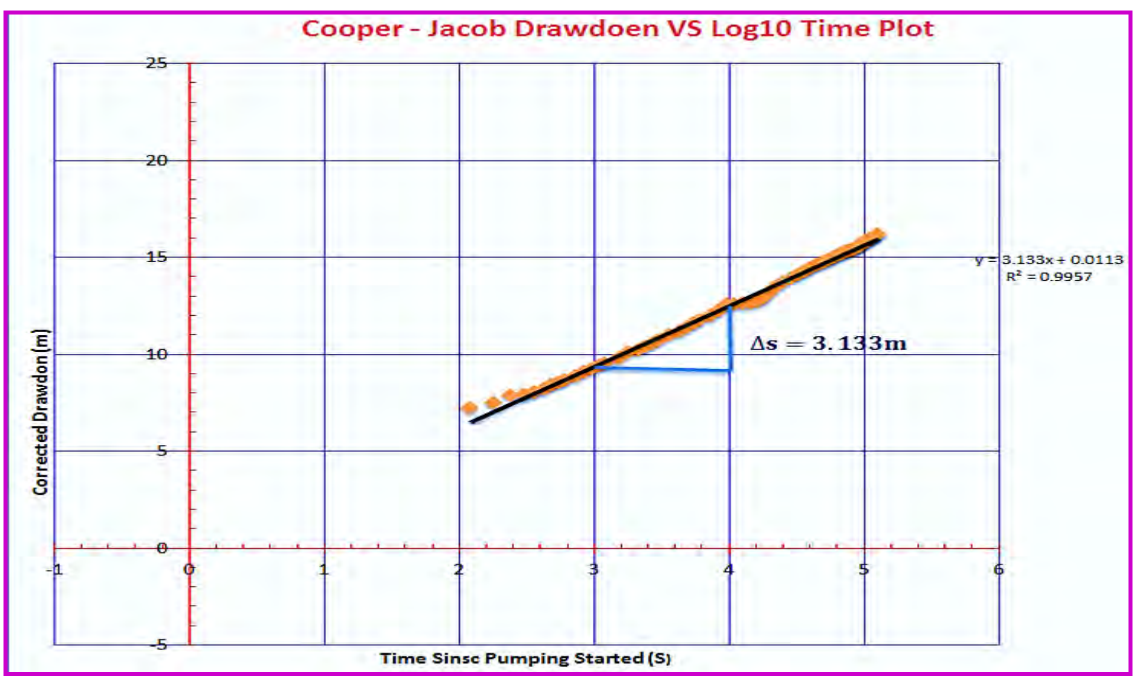

Figure A13. Copper-Jacob method for solution of non-equilibrium equation using the adjusted drawdown test data of MJBH-3.

vii) Recovery Test Method for Solution of the Non-Equilibrium Equation of Residual Drawdown for MJBH-1

At the end of a pumping test, when pumping is stopped, water levels in pumping and observation wells will begin to rise. This is referred to as the recovery of groundwater levels, while the measurements of drawdown below the original static water level (prior to pumping) during the recovery period are known as residual drawdowns (s'). Hence, a plot of residual drawdown s′, versus the logarithm of t/t′ for MJBH-1 provides a straight line as shown in figure below. The gradient of the straight line equals 2.3Q/4πT. So that Δs′, the change in residual drawdown over one log cycle of t/t′, allows finding a value of transmissivity (T) from: -

$$\mathbf{T = \frac{2.3Q}{4\pi\Delta s'}}$$

From the equation of the straight line fitted to the residual drawdown data points of MJBH-1 plotted, the slope of the straight line is calculated as Δs’=9.378-6.52= 2.858m. Then by substituting the value of Δs’ in the above equation it gives

$$\mathbf{T_{R1} = \frac{2.3 * 0.045}{4 * \pi * 2.858} = 0.00288\ m^2/_s}$$

Note: No comparable value of S can be determined by this recovery test.

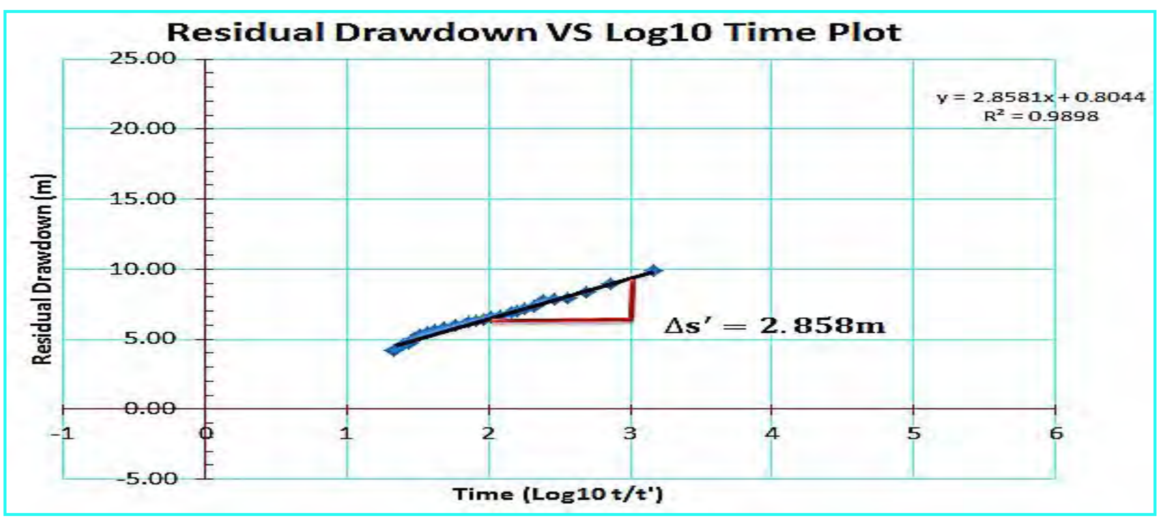

Figure A14. Recovery test method for solution of the non-equilibrium equation of MJBH-1 for residual drawdown data

viii) Recovery Test Method for Solution of the Non-Equilibrium Equation of Residual Drawdown for MJBH-2

At the end of a pumping test, when pumping is stopped, water levels in pumping and observation wells will begin to rise. This is referred to as the recovery of groundwater levels, while the measurements of drawdown below the original static water level (prior to pumping) during the recovery period are known as residual drawdowns (s'). A plot of residual drawdown s′, versus the logarithm of t/t′ for MJBH-2 is carried out and it provides a straight line as shown in figure below. Its gradient is equal to 2.3Q/4πT. So that Δs′, the change in residual drawdown over one log cycle of t/t′, allows finding a value of transmissivity (T) from: -

$$\mathbf{T = \frac{2.3Q}{4\pi\Delta s'}}$$

From the plot, the equation of the straight line is fitted to the residual drawdown data points of MJBH-2 and the slope of the straight line is calculated as Δs'=5.767- 7.631=1.864m. Then by substituting the value of Δs' in the above equation it gives

$$\mathbf{T_{R2} = \frac{2.3 * 0.045}{4 * \pi * 2.858} = 0.00442\, {}^{m^2}/_{s}}$$

Note: No comparable value of S can be determined by this recovery test.

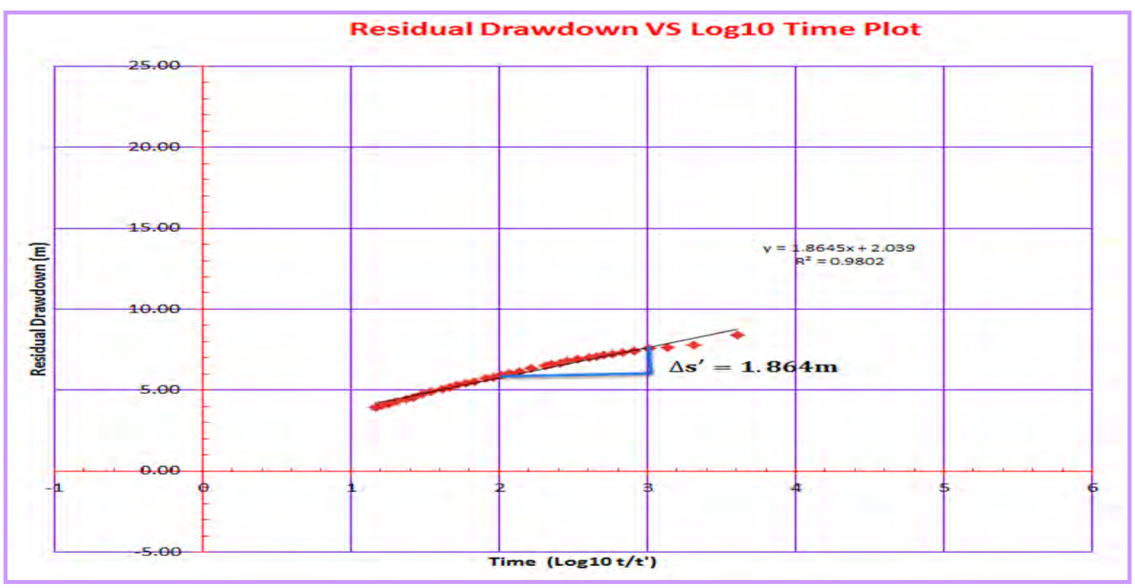

Figure A 15. Recovery test method for solution of the non-equilibrium equation of MJBH-2 for residual drawdown data

ix) **Recovery Test Method for Solution of the Non-Equilibrium Equation of Residual Drawdown for MJBH-3**

The residual drawdowns (s') of recovery test for Mojo borehole 3 (MJBH-3) is corrected for important influences the aquifer conditions. By using the recovery data a plot of residual drawdown s', versus the logarithm of t/t' for MJBH-3 is conducted on the Excel spread sheet and it provides a straight line as shown in figure below. The gradient of this line is equal to 2.3Q/4πT. So that Δs', the change in residual drawdown over one log cycle of t/t', allows finding a value of transmissivity (T) from: -

$$\mathbf{T} = \frac{\mathbf{2.3Q}}{\mathbf{4\pi\Delta s'}}$$

Therefore; from the produced plot, the equation of the straight line is fitted to the residual drawdown data points of MJBH-3 and the slope of the straight line is calculated as Δs'= 8.741-6.035=2.706m. Then by substituting the value of Δs' in the above equation it gives

$$\mathbf{T_{R3}} = \frac{\mathbf{2.3 * 0.04383}}{\mathbf{4 * \pi * 2.858}} = \mathbf{0.00296\,m^2/s}$$

Note: No comparable value of S can be determined by this recovery test.

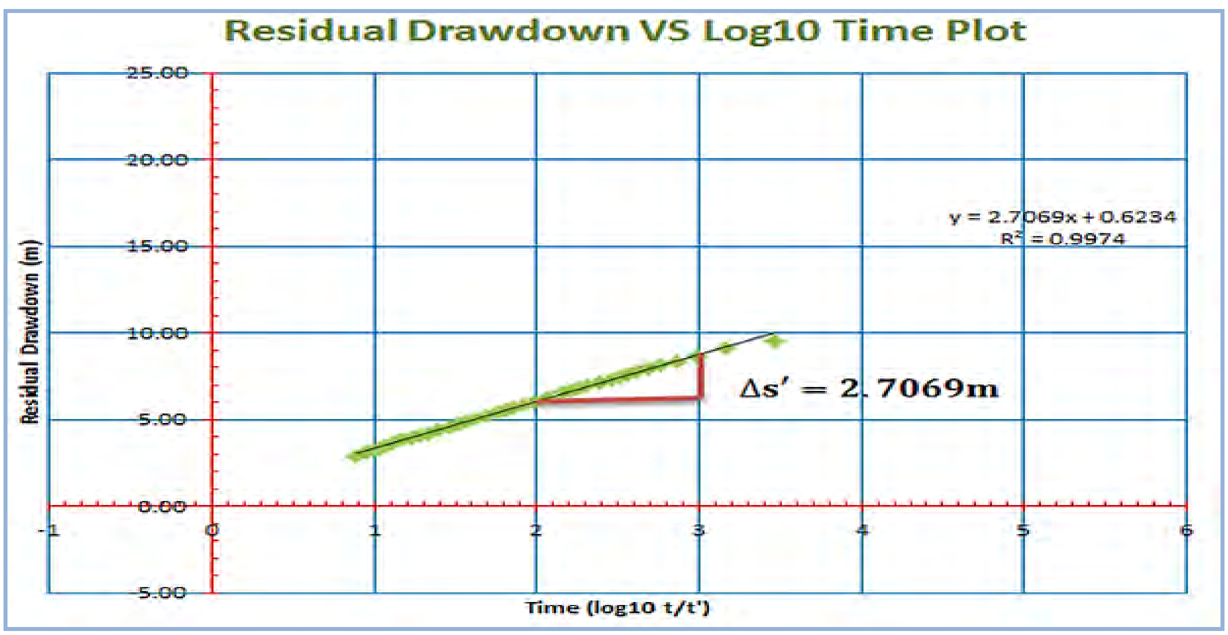

Figure A16. Recovery test method for solution of the non-equilibrium equation of MJ-BH3 for residual drawdown data

A_3 - Result of Pumping Test Analysis by Aquifer Test 3.5 Software for MJBH-1

The Aquifer Test 3.5 is the most popular software package available for graphical analysis; provide a selection of the most commonly used solution methods for data analysis and reporting of pumping test data results. Thus by making use of an Aquifer Testing Software Package the single well pumping test data from three boreholes of Mojo water supply well field is adjusted for comprehensive external substantial environments those maybe occurred and their analyses are modeled graphically for the mere tenacity of compassion between the manual curve fitting method as completed by using Excel Spread Sheet above and by means of automatic curve fitting technique deciding on, Solution Method Advisor to assist in choosing an appropriate data analysis method which is optional in this software package. In the case of manual curve fitting methods the analyses are produced for only for the pumping test data that adjusted for both partial and unconfined aquifer conditions where as in the case of Aquifer Test software, automatic curve fitting techniques the analyses conducted for three scenarios such as observed pumping test data, pumping test data adjusted only for partial penetration and data adjusted for both partial and unconfined aquifer conditions. Then similar pumping testing data which were consumed for manual curve fitting are used in this case there by organizing the data into Microsoft Excel version 5.0/1995 files and Data logger ASCII files with a variety of delimiters and column layouts for Theis 1935 and Copper and Jacob 1946 solution methods. The organized test data are then entered into the Aquifer Test Projects already created through the keyboard by directly importing from the Microsoft Excel (version 5/1995) workbook file, or from any data logger file (in ASCII format) those already saved in database of the aquifer testing projects. For the residual drawdowns, the test data are inserted to the Aquifer Test Projects being created from a spreadsheet or database, simply by cutting and pasting through the clipboard. In conclusion, by means of automatic curve fitting technique helping on the solution method advisor and also manual fitting methods are also applied based on the site situation how know, the observed field test and adjusted pumping test data are graphically analyzed. Here under the outcome of the analyses such as Drawdown versus Time and Theis analysis, for the three pumping wells of

Mojo boreholes are presented successively beginning by MJBH-1. The result illustrated hereunder for the pumping test data that is adjusted for both partial penetration and unconfined aquifer circumstances which was similarly consumed by manual curve fitting method previously concluded for MJBH-1 just for the easiness of comparisons.

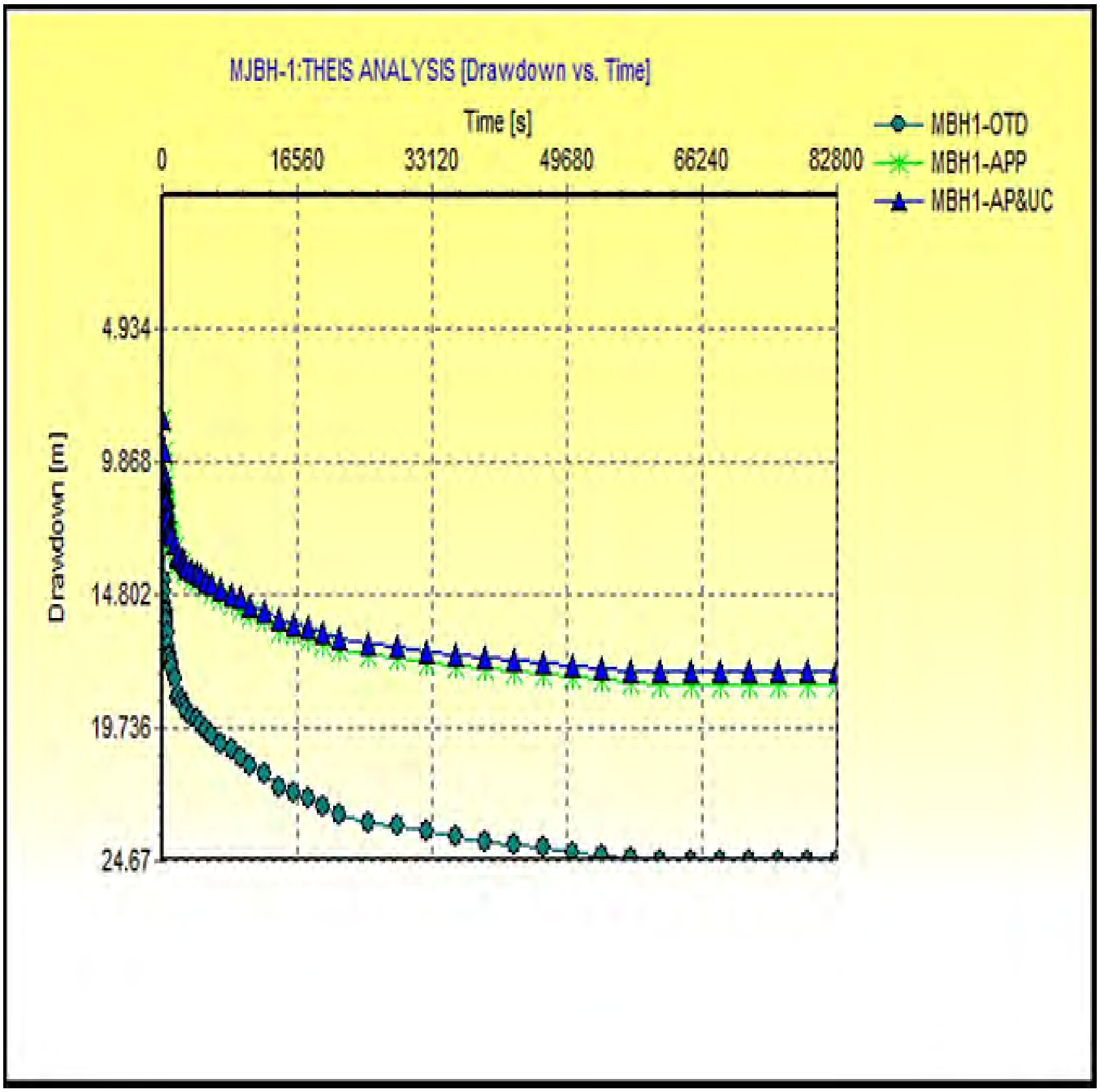

Figure A17. Theis analysis by aquifer test for observed and adusted drawdown versus time for pump testing data conducted in MJBH-1 using computer program

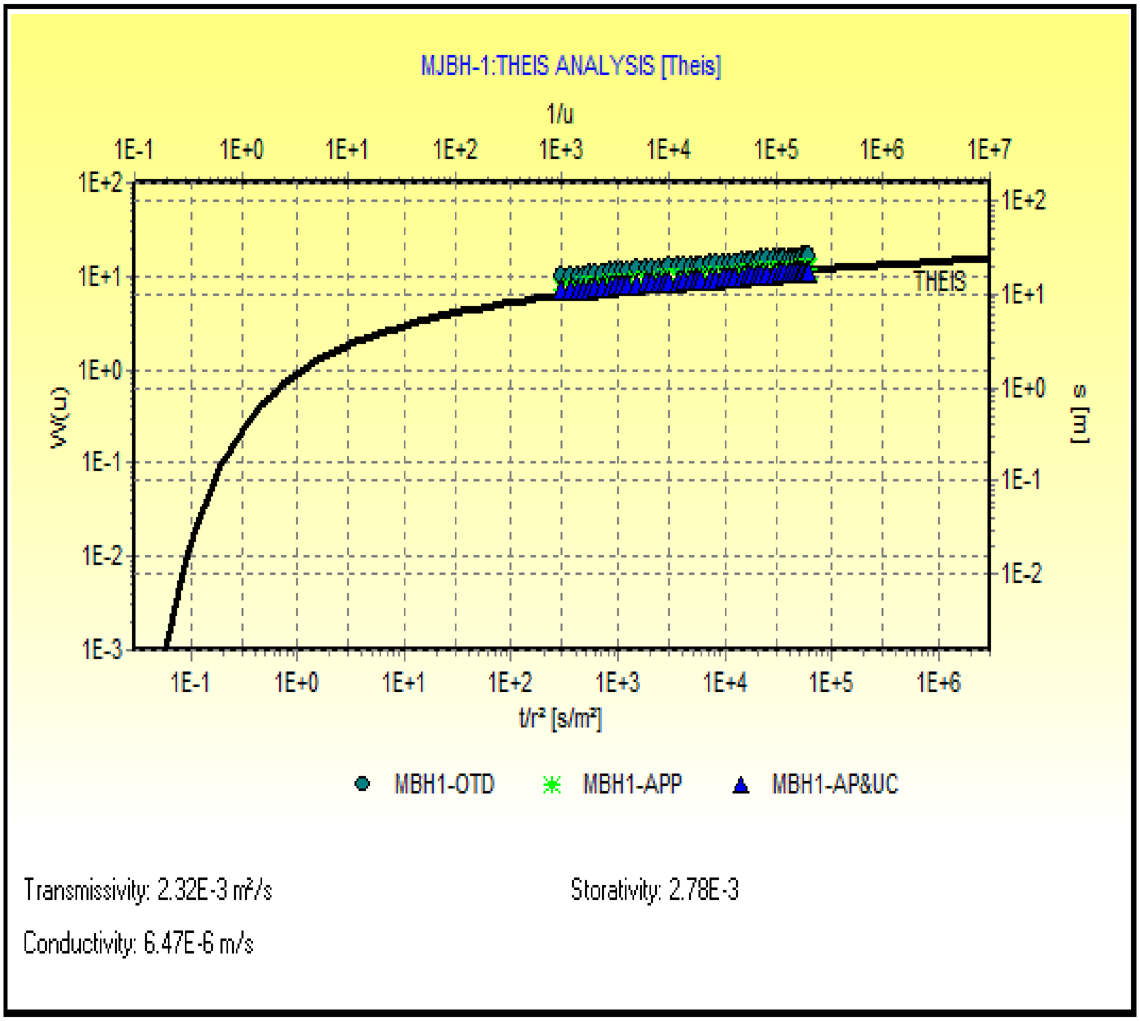

Figure A18. Curve fitting by aquifer test for observed and adjusted pumping test data conducted at MJBH-1 using an automated procedure within a computer program

b) Result of Pumping Test Analysis by Aquifer Test 3.5 Software for MJBH-2

Since all the procedures are similarly completed as carried out for the analysis of MJBH-1, the outcome of the analyses such as Drawdown versus Time and Theis analysis for MJBH-2 are presented as shown in Figures A19 and 19 below. The result illustrated for the pumping test data that is adjusted for both partial penetration and unconfined aquifer circumstances that was similarly consumed for the analysis of MJBH-2 previously concluded by manual curve fitting method to simplify the comparisons.

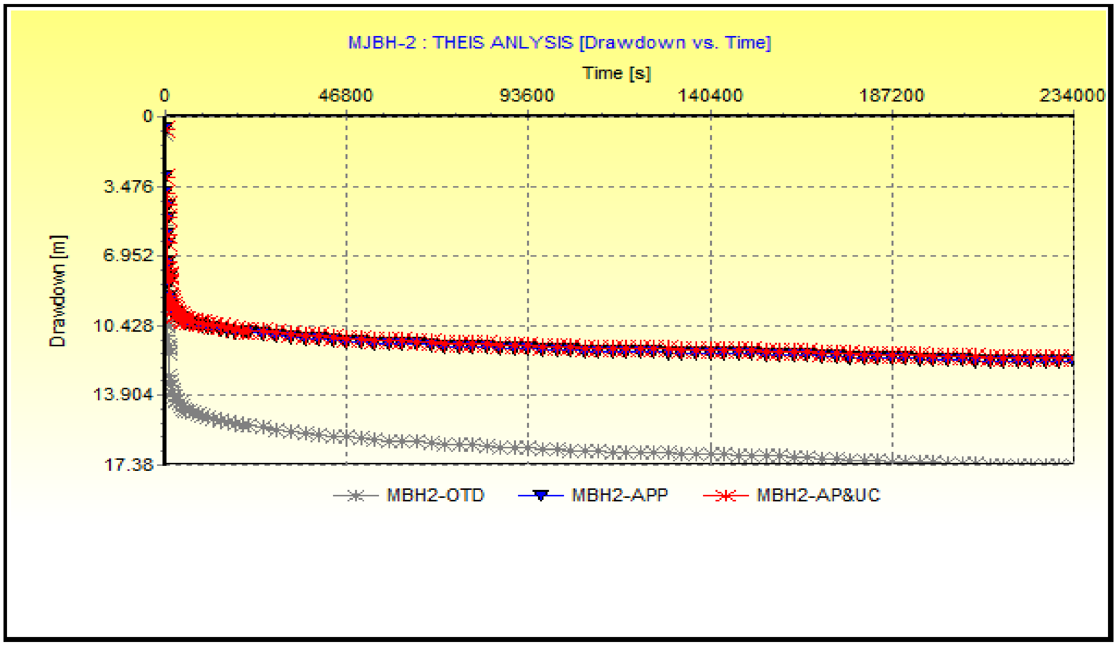

Figure A19. Theis analysis by aquifer test for observed and adjusted drawdown versus time for pump testing data conducted in MJBH-2 using computer program

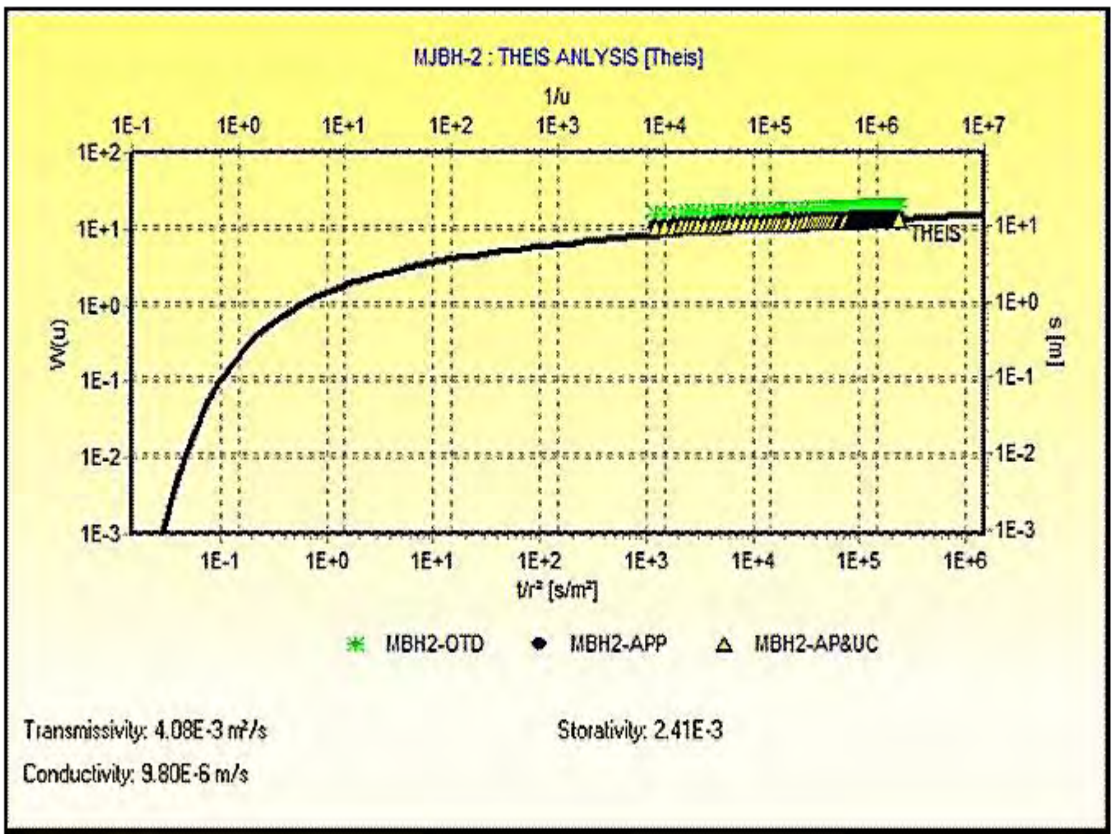

Figure A20. Curve fitting by aquifer test for observed and adjusted pumping test data conducted at MJBH-2 using an automated procedure within a computer program

c) Result of Pumping Test Analysis by Aquifer Test 3.5 Software for MJBH-3

As all the procedures are similar with the analysis of MJBH-1, the outcome of the analyses such as Drawdown versus Time and Theis analysis for MJBH-3 are presented as shown in figures below. The result illustrated for the pumping test data that is adjusted for both partial penetration and unconfined aquifer conditions is also consumed for the analysis of MJBH-3 which previously concluded by manual curve fitting method in order to simplify the comparisons.

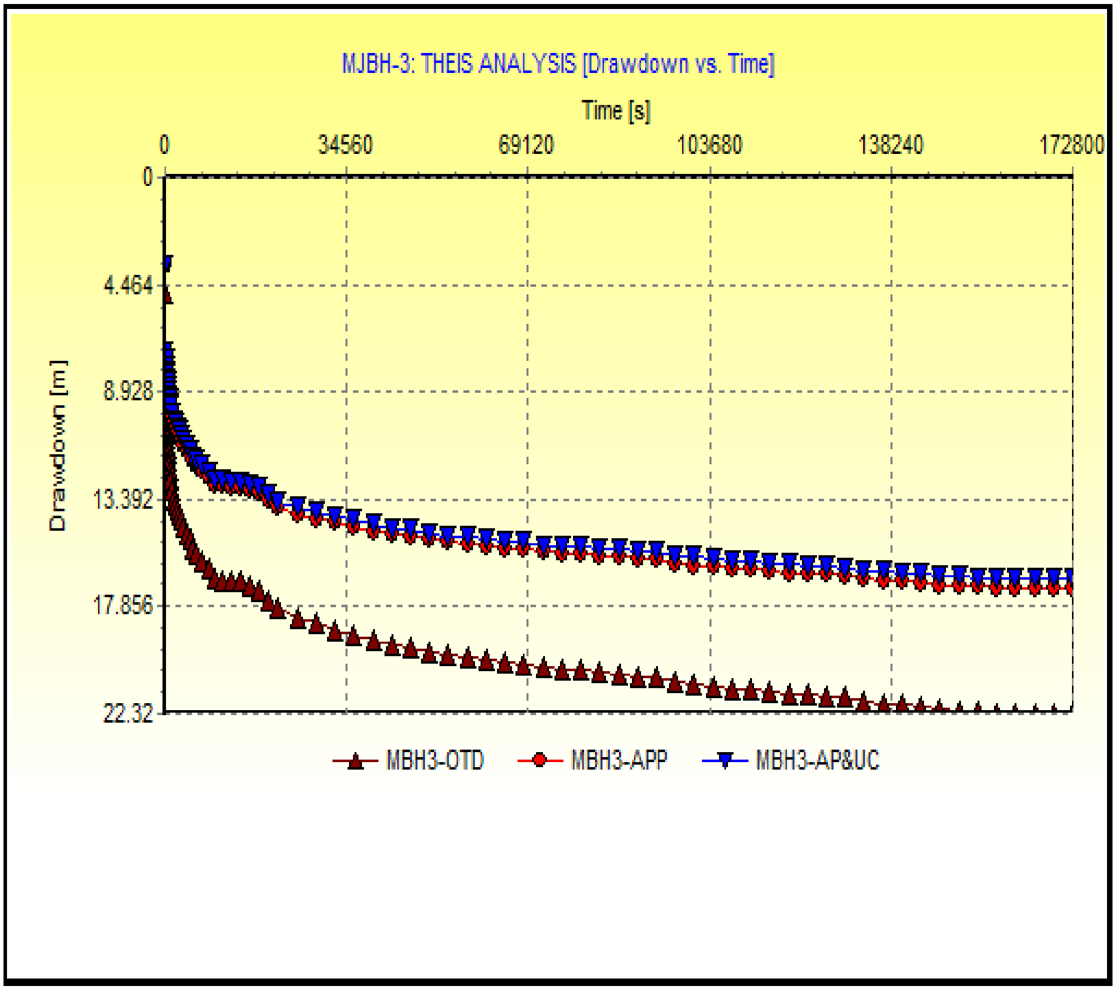

Figure A 21. Theis analysis by aquifer test for observed and adusted drawdown versus time for pump testing data conducted in MJBH-2 using computer program

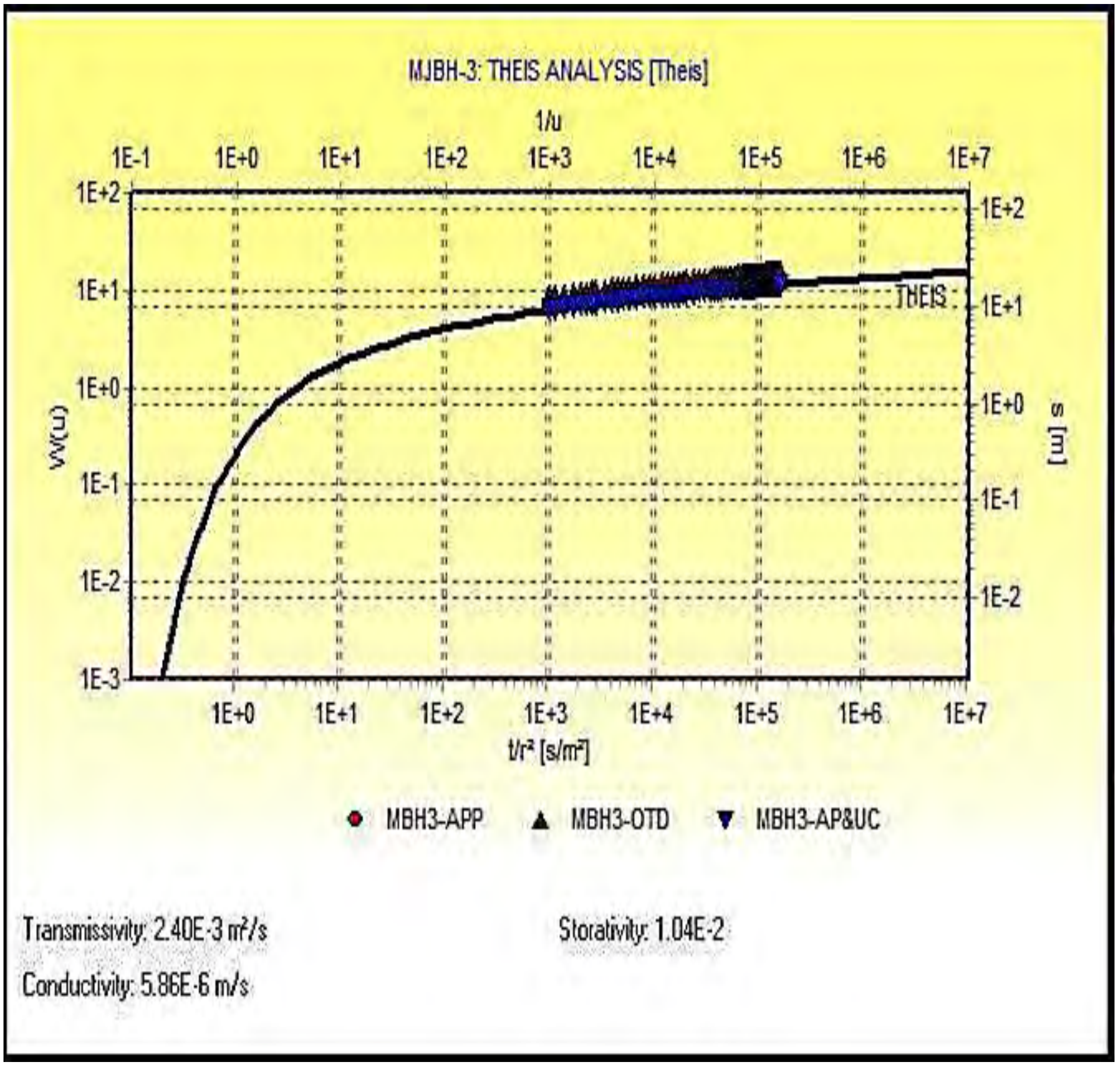

Figure A 22. Curve fitting by aquifer test for observed and adjusted pumping test data conducted at MJBH-2 using an automated procedure within a computer program

i) Result of Copper-Jacob Time – Drawdown Analysis by Aquifer Test 3.5 Software Method for MJBH-1

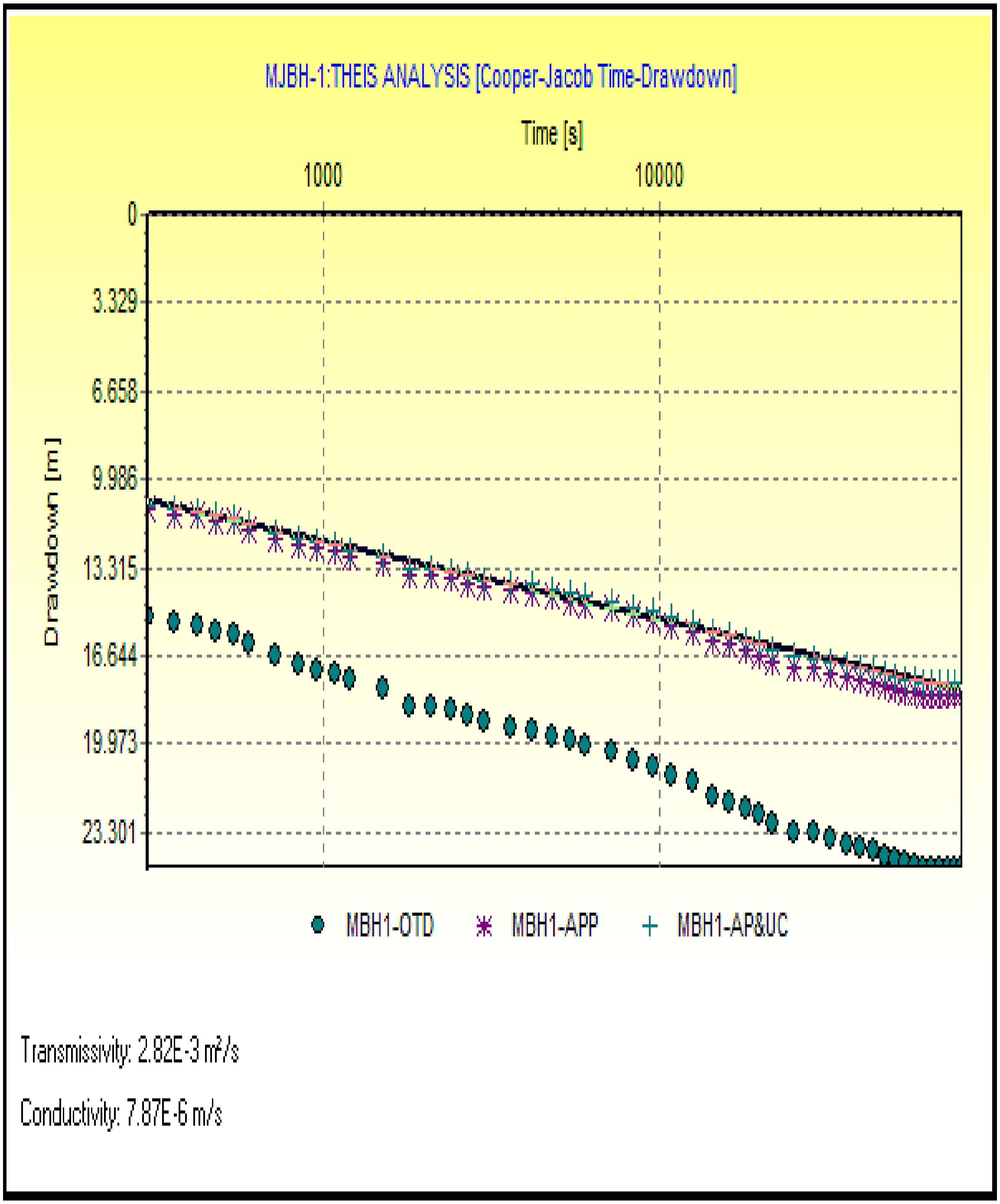

Figure A23. Cooper-Jacob time-drawdown analysis plot for solution of non-equilibrium equation using the adjusted drawdown test data of MJBH-1 by an automated procedure within a computer program. Drawdown is plotted as a function of time on semi-logarithmic paper.

ii) Result of Copper-Jacob Time – Drawdown Analysis by Aquifer Test 3.5 Software Method for MJBH-2

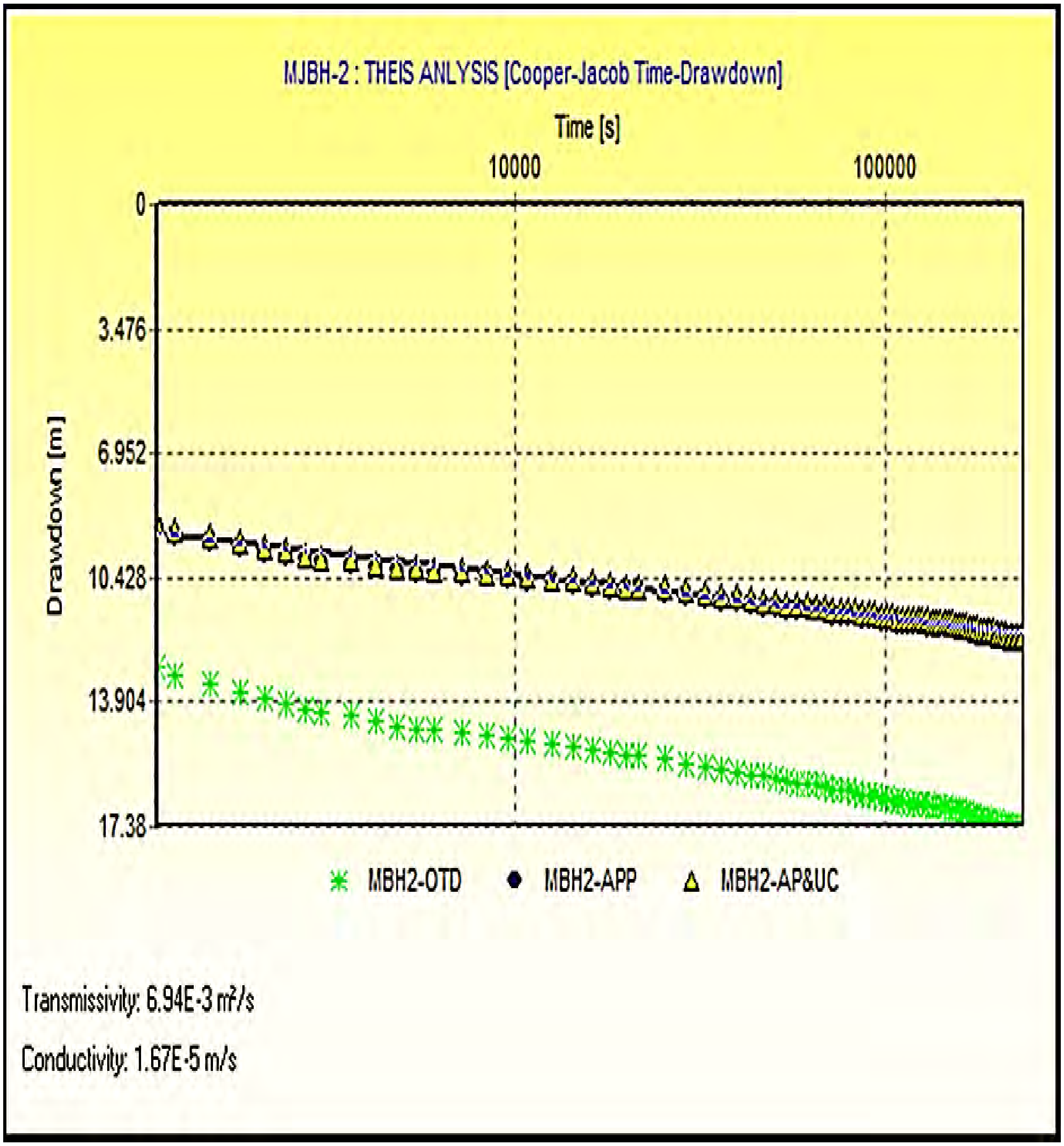

Figure A 24. Cooper-Jacob Time-Drawdown analysis plot for solution of non-equilibrium equation using the adjusted drawdown test data of MJBH-2 by an automated procedure within a computer program. Drawdown is plotted as a function of time on semi-logarithmic paper

iii) Result of Copper-Jacob Time – Drawdown Analysis by Aquifer Test 3.5 Software Method for MJBH-3

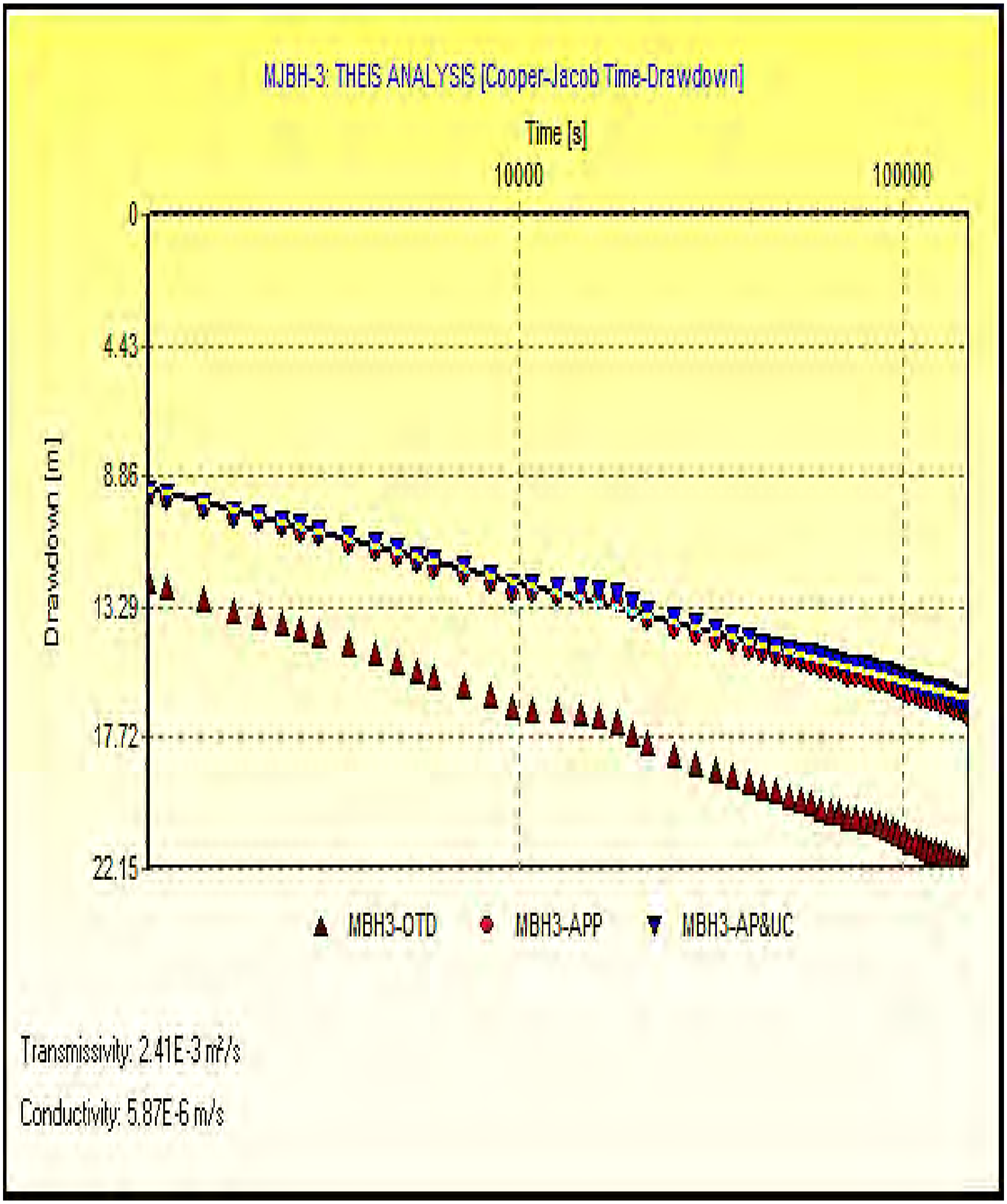

Figure A25. Cooper-Jacob Time-Drawdown analysis plot for solution of non-equilibrium equation using the adjusted drawdown test data of MJBH-3 by an automated procedure within a computer program. Drawdown is plotted as a function of time on semi-logarithmic paper

i) Result of Recovery Test by Aquifer Test 3.5 Software Analysis Method for MJBH-1

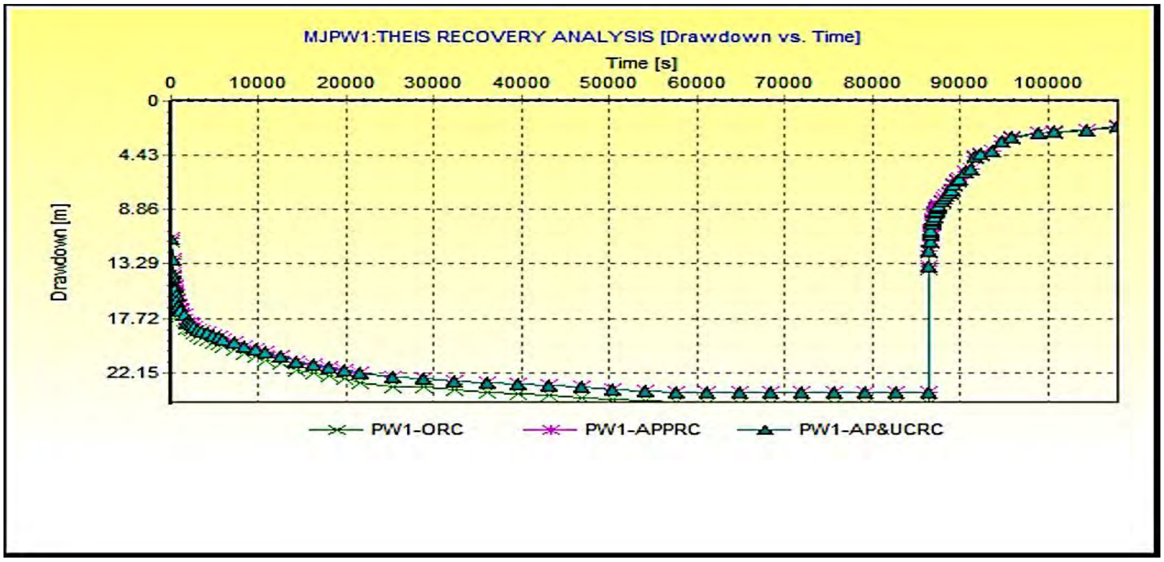

Figure A26. Theis Recovery analysis drawdown versus time graph by Aquifer Test for MJBH-1

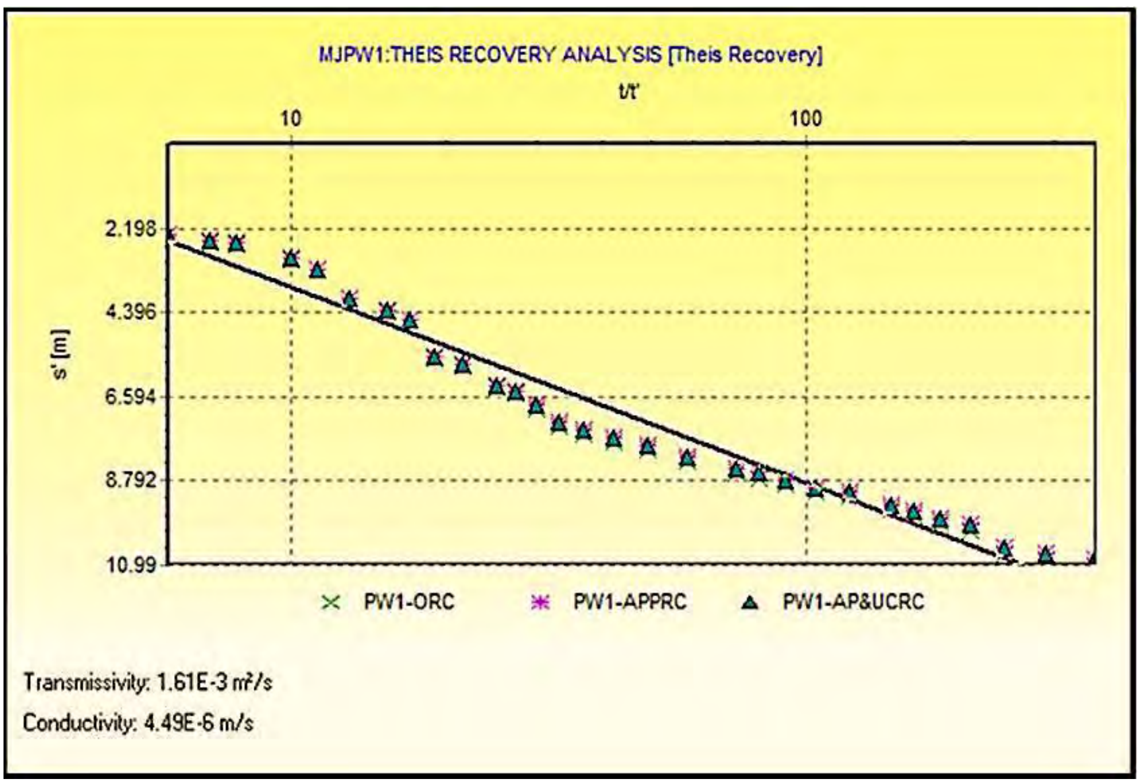

Figure A27. Theis Recovery analysis plot for solution of non-equilibrium equation using the adjusted drawdown test data of MJBH-1 by an automated procedure within a computer program. Drawdown is plotted as a function of time on semi-logarithmic paper

ii) **Result of Recovery Test by Aquifer Test 3.5 Software Analysis Method for MJBH-**2

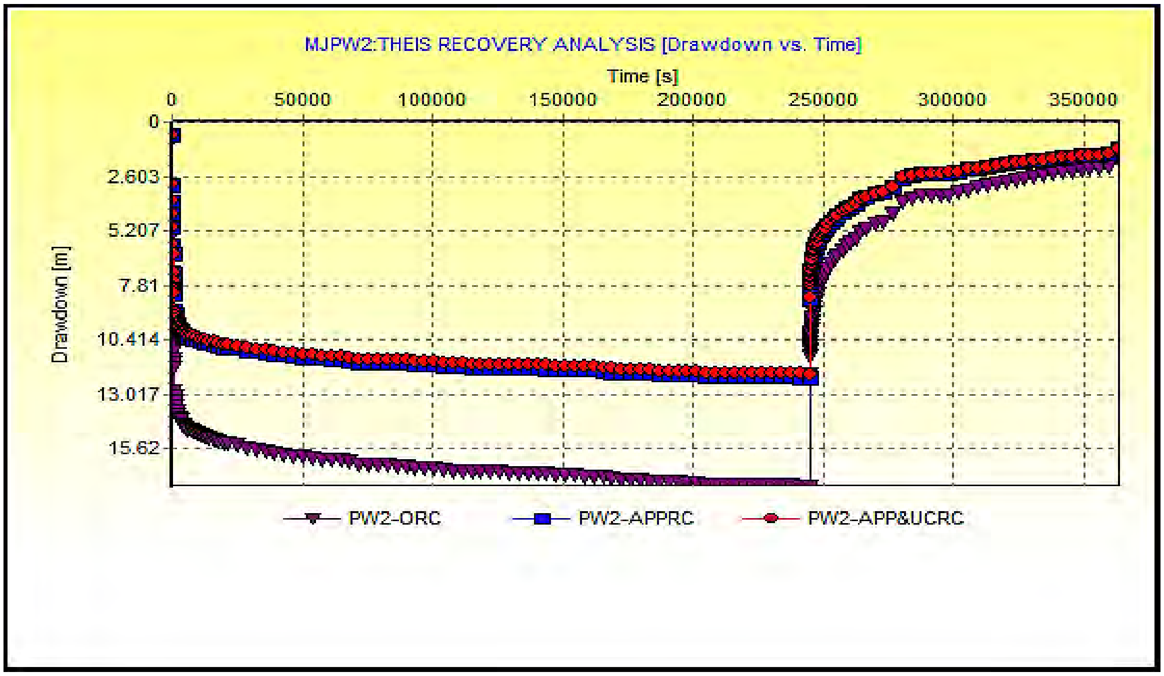

Figure A28. Theis Recovery analysis drawdown versus time graph by Aquifer Test for MJBH-2

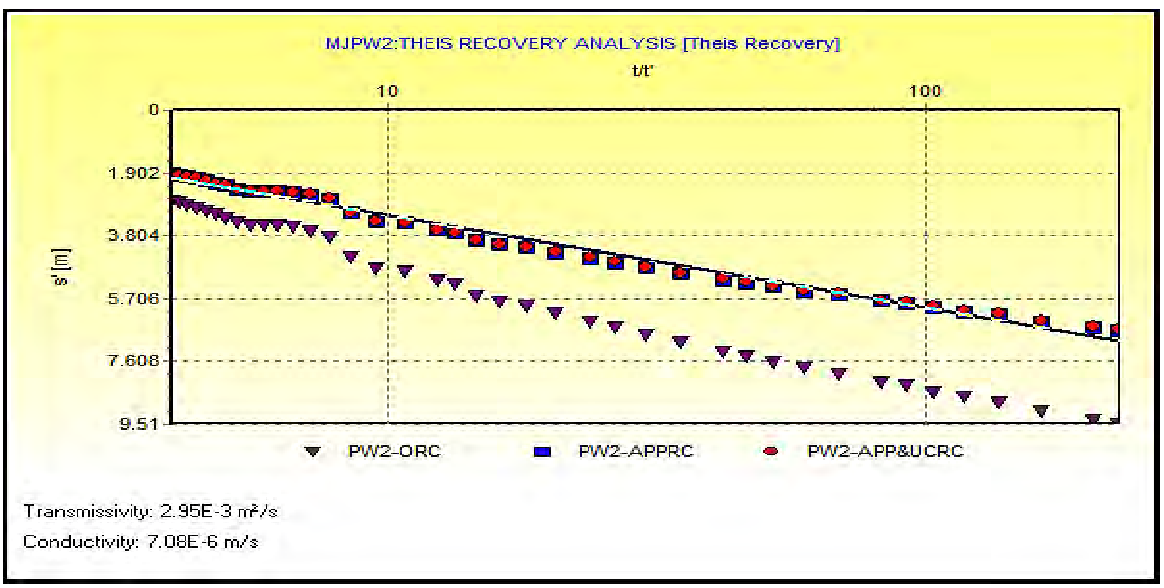

Figure A29. Theis Recovery analysis plot for solution of non-equilibrium equation using the adjusted drawdown test data of MJBH-2 by an automated procedure within a computer program. Drawdown is plotted as a function of time on semi-logarithmic paper

iii) Result of Recovery Test by Aquifer Test 3.5 Software Analysis Method for MJBH- 3

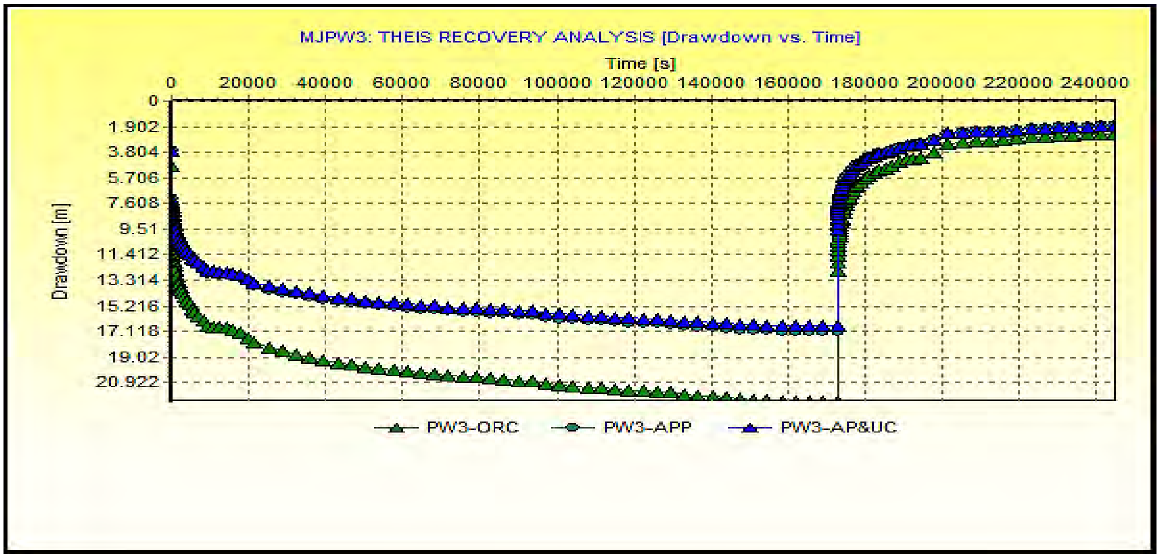

Figure A30. Theis Recovery analysis drawdown versus time graph by Aquifer Test for MJBH-3

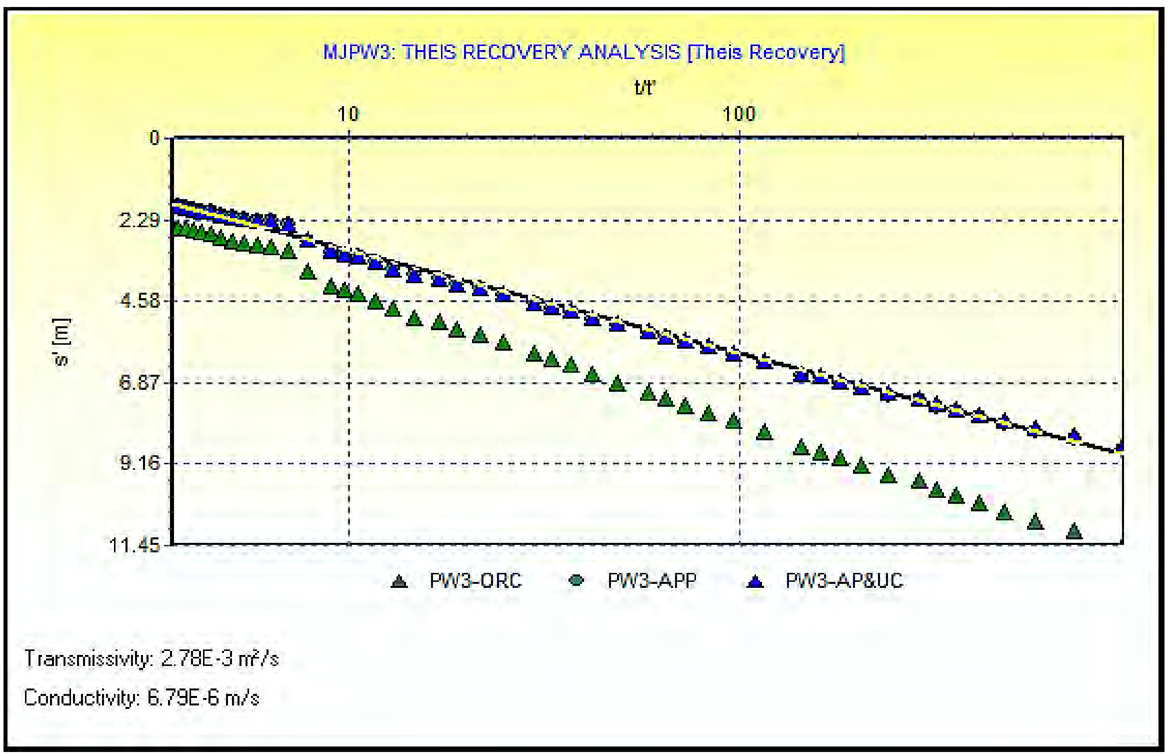

Figure A 31. Theis Recovery analysis plot for solution of non-equilibrium equation using the adjusted drawdown test data of MJBH-3 by an automated procedure within a computer program. Drawdown is plotted as a function of time on semi-logarithmic paper

Table A.4: *Summary of the results for the analyses of approximated aquifer parameters completed by excel spread sheet / manual curve-fitting/ method MJBH-1, MJBH-2 and MJBH-3 respectively*

Borehole name		MJBH-1									
Methods / Aquifer Paramaters		Theis 1935 Method			Copper-jacob Straight Line Method			Recovery Test Method		Type of Aquifer	Type of Analysis
		T_{T1}	S_{T1}	K_{T1}	T_{CJ1}	S_{CJ1}	K_{CJ1}	T_{R1}	K_{R1}		
Transmissivity (m^2/s)	T_T	2.75E-03								Unconfined	Plot drawdown versus time on log-log paper and substitute values into analytical equations
Storativity	S_T		1.09E-02								
Horizontal hydraulic conductivity (m/s)	K_T			7.69E-06							
Transmissivity (m^2/s)	T_{CJ}				2.78E-03					Unconfined	Drawdown versus time plotted on semi-log paper and substitution of values into analytical equations.
Storativity	S_{CJ}					3.07E-02					
Horizontal hydraulic conductivity (m/s)	K_{CJ}						7.78E-06				
Transmissivity (m^2/s)	T_R							2.88E-03		Unconfined	Residual Drawdown versus time plotted on semi-log paper and substitution of values into analytical equations.
Horizontal hydraulic conductivity (m/s)	K_R								8.05E-06		

Borehole name		MJBH-2									
Methods / Aquifer Paramaters		Theis 1935 Method			Copper-jacob Straight Line Method			Recovery Test Method		Type of Aquifer	Type of Analysis
		T_{T2}	S_{T2}	K_{T2}	T_{CJ2}	S_{CJ2}	K_{CJ2}	T_{R2}	K_{R2}		
Transmissivity (m^2/s)	T_T	5.31E-03								Unconfined	Plot drawdown versus time on log-log paper and substitute values into analytical equations
Storativity	S_T		2.30E-03								
Horizontal hydraulic conductivity (m/s)	K_T			1.28E-05							
Transmissivity (m^2/s)	T_{CJ}				5.58E-03					Unconfined	Drawdown versus time plotted on semi-log paper and substitution of values into analytical equations.
Storativity	S_{CJ}					1.20E-03					
Horizontal hydraulic conductivity (m/s)	K_{CJ}						1.34E-05				
Transmissivity (m^2/s)	T_R							4.42E-03		Unconfined	Residual Drawdown versus time plotted on semi-log paper and substitution of values into analytical equations.
Horizontal hydraulic conductivity (m/s)	K_R								1.06E-05		

Borehole name		MJBH-3								Type of Aquifer	Type of Analysis
Methods / Aquifer Paramaters		Theis 1935 Method			Copper-jacob Straight Line Method			Recovery Test Method			
		T_{T3}	S_{T3}	K_{T3}	T_{CJ3}	S_{CJ3}	K_{CJ3}	T_{R3}	K_{R3}		
Transmissivity (m^2/s)	T_T	2.68E-03									Plot drawdown versus time on log-log paper and substitute values into analytical equations
Storativity	S_T		1.06E-01							Unconfined	
Horizontal hydraulic conductivity (m/s)	K_T			6.54E-06							
Transmissivity (m^2/s)	T_{CJ}				2.56E-03						Drawdown versus time plotted on semi-log paper and substitution of values into analytical equations.
Storativity	S_{CJ}					3.54E-01				Unconfined	
Horizontal hydraulic conductivity (m/s)	K_{CJ}						6.25E-06				
Transmissivity (m^2/s)	T_R							2.96E-03		Unconfined	Residual Drawdown versus time plotted on semi-log paper and substitution of values into analytical equations.
Horizontal hydraulic conductivity (m/s)	K_R								7.23E-06		

Table A.5: *Summary of the results for the analysis of estimated completed by aquifer test 3.5 software method for comparison for mjbh-1, mjbh-2 and mjbh-3 respectively*

Borehole name		MJBH-1								Type of Aquifer	Type of Analysis
Methods / Aquifer Paramaters		Theis 1935 Method			Copper-jacob Straight Line Method			Recovery Test Method			
		T_{T1}	S_{T1}	K_{T1}	T_{CJ1}	S_{CJ1}	K_{CJ1}	T_{R1}	K_{R1}		
Transmissivity (m^2/s)	T_T	2.32E-03									Plot drawdown versus time on log-log paper and substitute values into analytical equations
Storativity	S_T		2.78E-03							Unconfined	
Horizontal hydraulic conductivity (m/s)	K_T			6.48E-06							
Transmissivity (m^2/s)	T_{CJ}				2.82E-03						Drawdown versus time plotted on semi-log paper and substitution of values into analytical equations.
Storativity	S_{CJ}									Unconfined	
Horizontal hydraulic conductivity (m/s)	K_{CJ}						7.88E-06				
Transmissivity (m^2/s)	T_R							1.61E-03		Unconfined	Residual Drawdown versus time plotted on semi-log paper and substitution of values into analytical equations.
Horizontal hydraulic conductivity (m/s)	K_R								4.50E-06		

Borehole name		MJBH-2								Type of Aquifer	Type of Analysis
Methods		Theis 1935 Method			Copper-jacob Straight Line Method			Recovery Test Method			
Aquifer Paramaters		T_{T2}	S_{T2}	K_{T2}	T_{CJ2}	S_{CJ2}	K_{CJ2}	T_{R2}	K_{R2}		
Transmissivity (m^2/s)	T_T	4.08E-03								Unconfined	Plot drawdown versus time on log-log paper and substitute values into analytical equations
Storativity	S_T		2.41E-03								
Horizontal hydraulic conductivity (m/s)	K_T			9.81E-06							
Transmissivity (m^2/s)	T_{CJ}				6.94E-03					Unconfined	Drawdown versus time plotted on semi-log paper and substitution of values into analytical equations.
Storativity	S_{CJ}										
Horizontal hydraulic conductivity (m/s)	K_{CJ}						1.67E-05				
Transmissivity (m^2/s)	T_R							2.95E-03		Unconfined	Residual Drawdown versus time plotted on semi-log paper and substitution of values into analytical equations.
Horizontal hydraulic conductivity (m/s)	K_R								7.09E-06		

Borehole name		MJBH-3								Type of Aquifer	Type of Analysis
Methods		Theis 1935 Method			Copper-jacob Straight Line Method			Recovery Test Method			
Aquifer Paramaters		T_{T3}	S_{T3}	K_{T3}	T_{CJ3}	S_{CJ3}	K_{CJ3}	T_{R3}	K_{R3}		
Transmissivity (m^2/s)	T_T	2.40E-03								Unconfined	Plot drawdown versus time on log-log paper and substitute values into analytical equations
Storativity	S_T		1.04E-02								
Horizontal hydraulic conductivity (m/s)	K_T			5.85E-06							
Transmissivity (m^2/s)	T_{CJ}				2.56E-03					Unconfined	Drawdown versus time plotted on semi-log paper and substitution of values into analytical equations.
Storativity	S_{CJ}										
Horizontal hydraulic conductivity (m/s)	K_{CJ}						6.25E-06				
Transmissivity (m^2/s)	T_R							2.78E-03		Unconfined	Residual Drawdown versus time plotted on semi-log paper and substitution of values into analytical equations.
Horizontal hydraulic conductivity (m/s)	K_R								6.78E-06		

A_4 - Comparisons of the Resulted Values of Aquifers Parameters from Manual and Automatic Curve Fitting Methods

From the comparisons completed among particular wells there by using the values of various transmissivities and storativities calculated and tabulated in Tables A5 and A6 via both the manual and the automatic curve fitting methods, we can recognize that values of the transmissivities approximated for the three wells are not the same and this prevails that the transmissivity in unconfined aquifers is not constant. Thus the basic assumption that Theis (1935) model anticipated that all wells in confined aquifer is an isotropic in which the transmissivity (T) is independent of direction is not more valid. Attributable to this context, “Papadopolus, 1965 stated that Theis Model is similar to an anisotropic model except that the transmissivity for the second model characterized with directional transmissivity and displays a profile of an ellipse (Papadopolus, 1965)”. This means that the maximum transmissivity (T_{max}) in the direction of high permeability or porous media, the minimum transmissivity (T_{min}) in low permeability and the average transmissivity (T_{avg}) in the mean permeability direction through media of the aquifers. Therefore, the geometric mean values of the model parameters transmissivity (T) and storage coefficient (S) is considered in evaluating the superposition modeling. Accordingly, the geometric mean values from the analysis accomplished by manual curve-fitting and that of Aquifer Test 3.5 Software methods are tabulated and presented beneath for comparing and contrasting purpose in the line of the aquifers parameters assessment. From comparisons it is noticed that the achieved geometric mean values of the aquifer parameters analyzed by means of both methods are approximately equivalent. However; the values that obtained from the analysis accomplished by Excel Spread Sheet / manual curve-fitting / technique is implemented for the evaluating real pumping and imaginary wells through the principles of superposition.

Table A.6: *Summary of Geometric Mean Results for the Analysis Completed by Excel Spread Sheet / Manual Curve-Fitting Method/*

Name of Boreholes	Aquifer Paramaters						
	Transmissivity (m^2/s)			Storativity			Horizontal hydraulic conductivity (m/s)
	T_{max}	T_{avg}	T_{min}	S_{max}	S_{avg}	S_{min}	K_{Avg}
MJBH-1 MJBH-2 MJBH-3	3.63E-03	3.40E-03	3.15E-03	2.93E-02	2.03E-02	1.12E-02	9.02E-06

Table A. 7: *Summary of Geometric Mean Results for the Analysis Completed by Aquifer Test 3.5 Software Method for Comparison*

Name of Boreholes	Aquifer Paramaters						
	Transmissivity (m^2/s)			Storativity			Horizontal hydraulic conductivity (m/s)
	T_{max}	T_{avg}	T_{min}	S_{max}	S_{avg}	S_{min}	K_{Avg}
MJBH-1 MJBH-2 MJBH-3	3.79E-03	3.00E-03	2.30E-03	4.11E-03	4.11E-03	4.11E-03	7.62E-06

APPENDIX - B

Affixed Supplementary of Tables and Figures those not included in Sections of Configurations of Cones of Depressions Contour lines for Composite Drawdown with Regard to Recharging Boundary Conditions, Establishing Radius of Influence and Wells Interferences

B1-Configurations of Cones of Depressions Contour lines for Composite Drawdown with Regard to presence of the recharge boundary condition

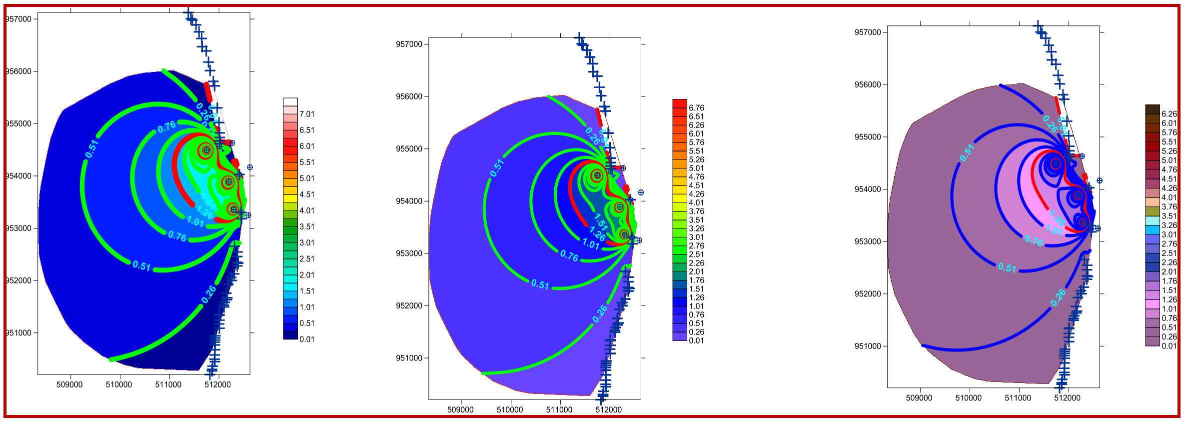

Figure B1. Plot of simulated composite drawdown contour lines distributions produced in unconfined aquifer as a result of a recharge boundary and three wells operating simultaneously located at (x_w, y_w) as indicated in Table 4 and numerous digitalized arbitrary coordinates, by having the rates of pumping of that of the designed rates capacity of the wells i.e. 0.0225 m^3/s, 0.0225 m^3/s and 0.0219 m^3/s for MJBH-1, MJBH-2 and MJBH-3 respectively, the drawdown contour lines prepared at any time (t) supposing the aquifer at well field takes the approximated transmissivities (T_{min}), (T_{avg}), (T_{max}) in sequence from left to right as shown

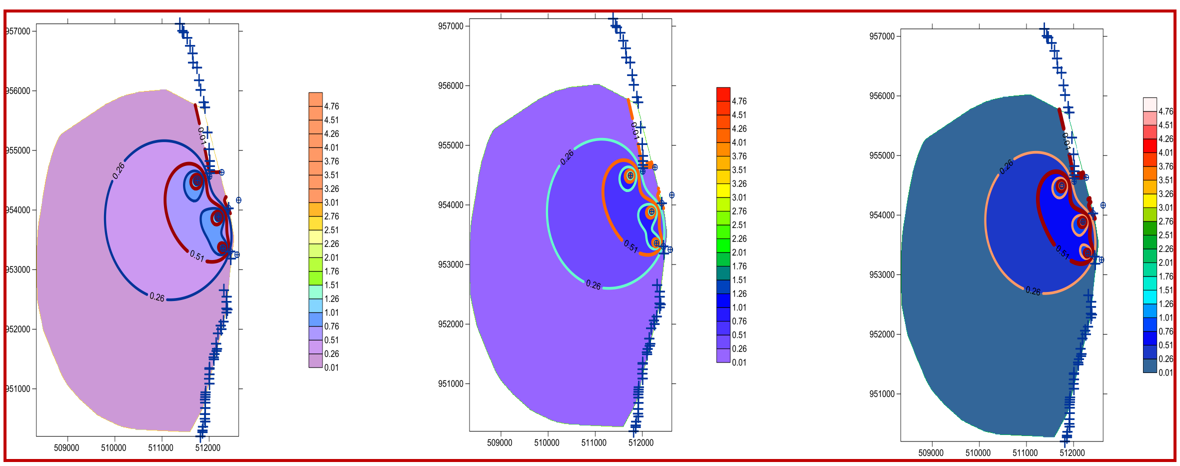

Figure B2. Plot of simulated composite drawdown contour lines distributions produced in unconfined aquifer as a result of a recharge boundary and three wells operating simultaneously located at (x_w, y_w) as indicated in Table 4 and numerous digitalized arbitrary coordinates, by reducing the rates of pumping of the wells 0.01 m^3/s for MJBH-1, MJBH-2 and MJBH-3, the drawdown contour lines prepared at any time (t) supposing the aquifer at well field takes the approximated transmissivities (T_{min}), (T_{avg}), (T_{max}) in sequence from left to right as shown

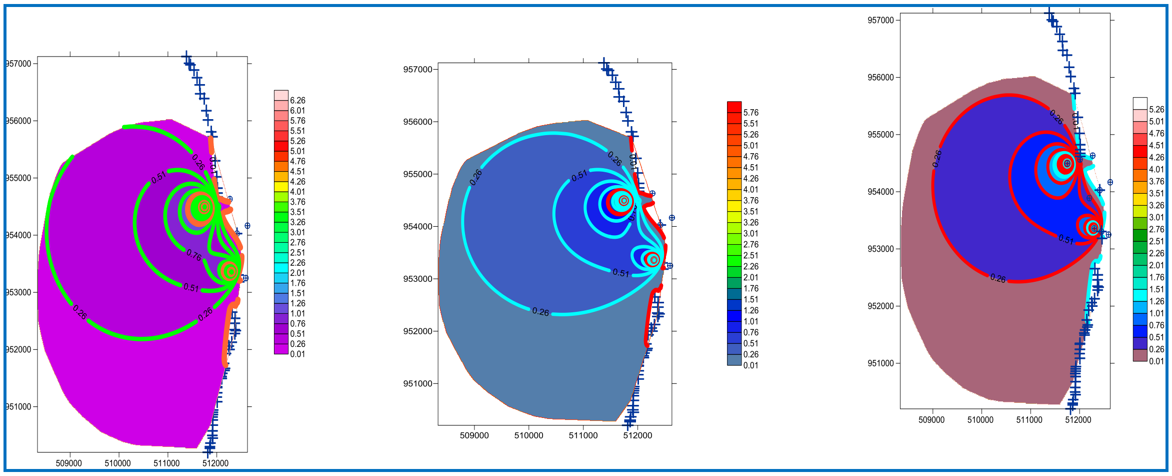

Figure B3. Plot of simulated composite drawdown contour lines distributions produced in unconfined aquifer as a result of a recharge boundary and two wells operating simultaneously located at (x_w, y_w) as indicated in Table 4 and numerous digitalized arbitrary coordinates, by having the rates of pumping of that of the designed rates capacity of the wells i.e. 0.0225 m^3/s, 0.0225 m^3/s and 0.0219 m^3/s for MJBH-1, MJBH-2 and MJBH-3 respectively, the drawdown contour lines prepared at any time (t) supposing the aquifer at well field takes the approximated transmissivities (T_{min}), (T_{avg}), (T_{max}) in sequence from left to right as shown

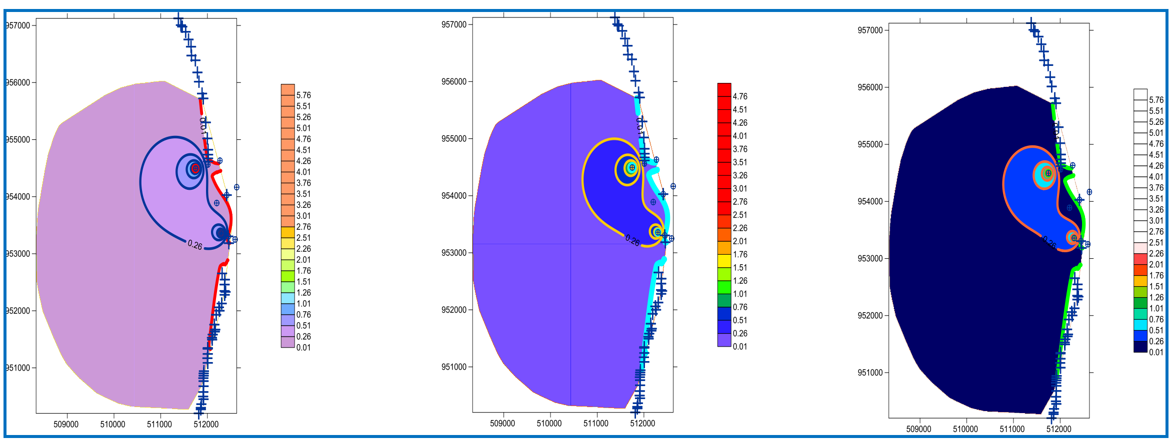

Figure B4. Plot of simulated composite drawdown contour lines distributions produced in unconfined aquifer as a result of a recharge boundary and two wells operating simultaneously located at (x_w, y_w) as indicated in Table 4 and numerous digitalized arbitrary coordinates, by reducing the rates of pumping of the wells 0.01 m^3/s for MJBH-1, MJBH-2 and MJBH-3, the drawdown contour lines prepared at any time (t) supposing the aquifer at well field takes the approximated transmissivities (T_{min}), (T_{avg}), (T_{max}) in sequence from left to right as shown

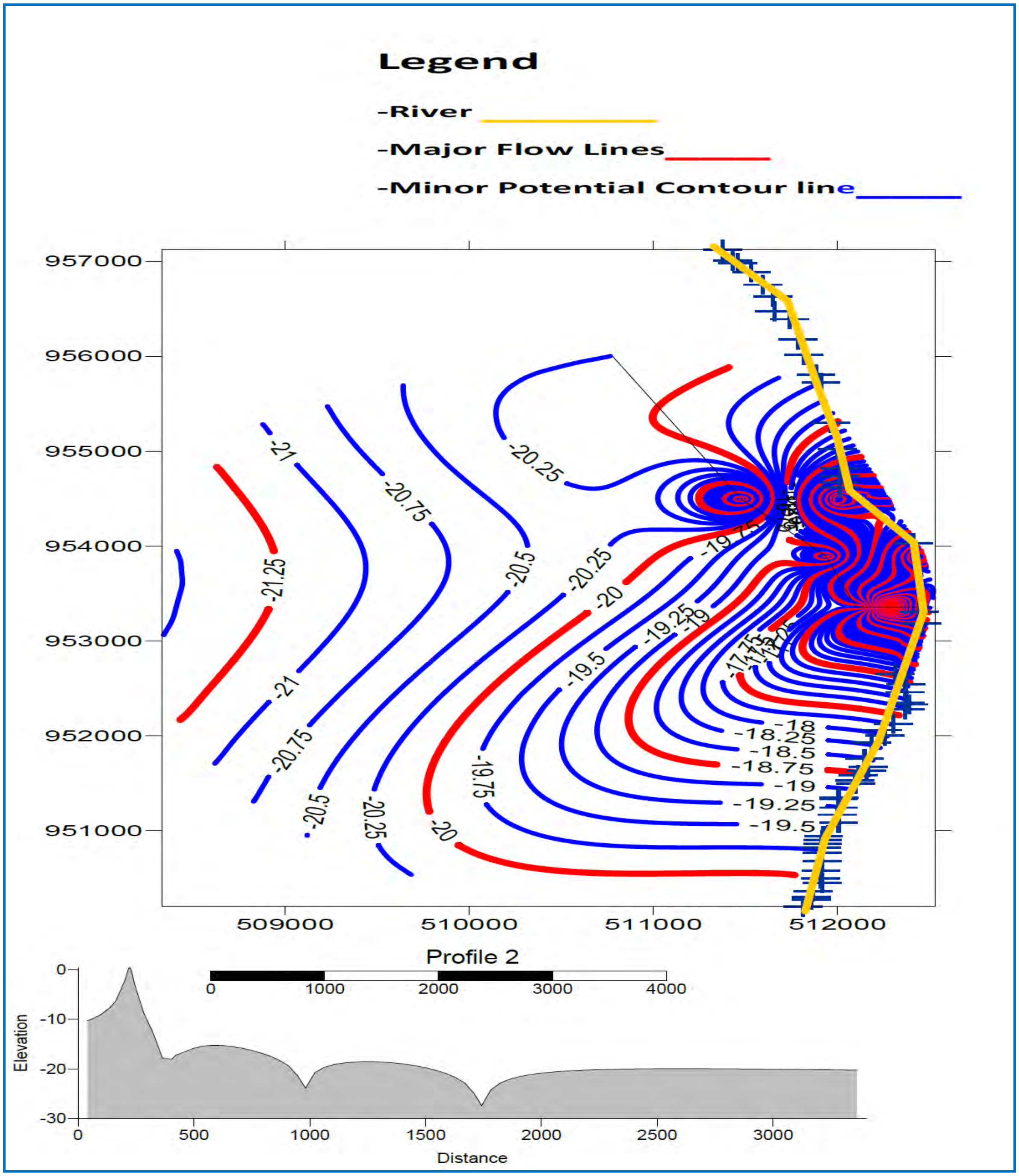

Figure B5. Plot of simulated composite drawdown potential flow distributions produced in unconfined aquifer as a result of a recharge boundary and three wells operating simultaneously located at (x_w, y_w) as indicated in Table 4 and numerous digitalized arbitrary coordinates, by deducing the rates of pumping of the wells by designed capacity of MJBH-1, MJBH-2 and MJBH-3, the drawdown flow lines prepared at any time (t) supposing the aquifer at well field takes the approximated transmissivity (T_{max})

B_3-Establishing Radius of Influence

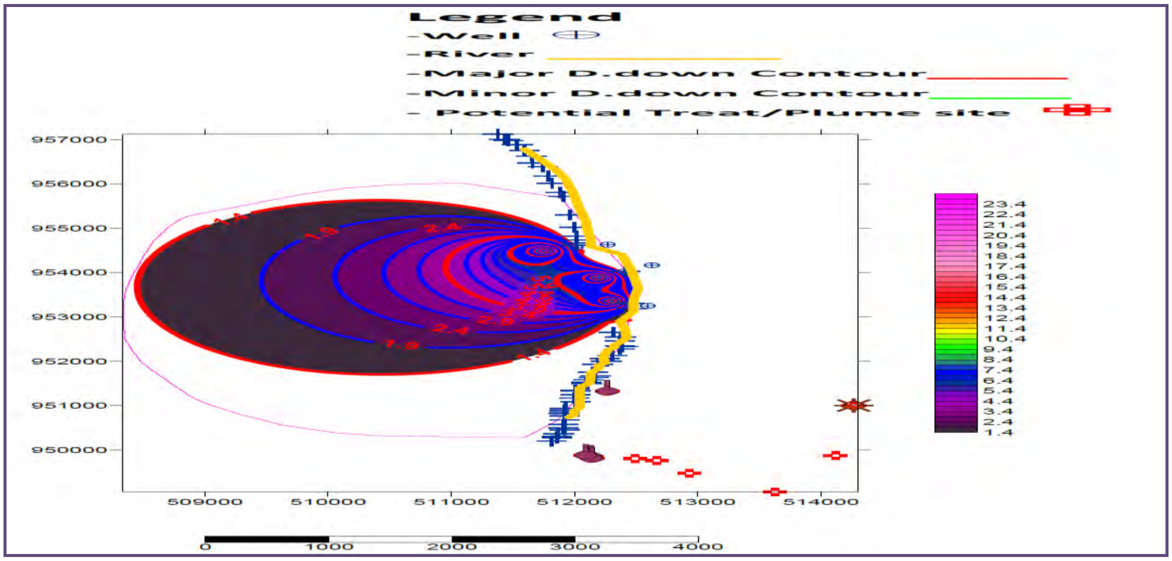

Figure B6. Schematic view of the tapered radius of influence in attempt to have defined shape of cones of depressions in the well field setting the superposed drawdowns to sink by 1.4m from the constant head in this case the boreholes are assumed to application with increased rates such as doubling that of designed capacity of pumps in the boreholes and the aquifer adopts average estimated transmissivity value

Table B. 1: *Fixed radius of influences and its corresponding time for designed discharge of the wells*

Descriptions		**Name of Boreholes**			**Remark**
		MJBH-1	**MJBH-2**	**MJBH-3**	
Parameters Adopt to the Aquifer at Mojo Well Field	***Approximated Transmissivity (m^2/s)***	0.003396	0.003396	0.003396	T_{avg}
	Storativty	0.02032	0.02032	0.02032	S_{avg}
Constant Pumping Rate(m^3/s)		0.09	0.09	0.08776	Pumps operating by double designed capacity
Fixed Radius of Influence (m)	**Extents(m)**	153.82	251.59	212.73	Contour line/Cone of depression from well origin to the recharge river region where the composite drawdown depressed to depth of 1.4m below the constant head
	Travel Time (Days)	1.42	3.8	2.76	
Fixed Radius of Influence (m)	**Extents(m)**	3852.74	3505.96	3728.35	Contour line/Cone of depression from well origin to the right edge where the composite drawdown depressed to a depth 1.4m below the constant head
	Travel Time (Days)	890.27	737.47	848.7	

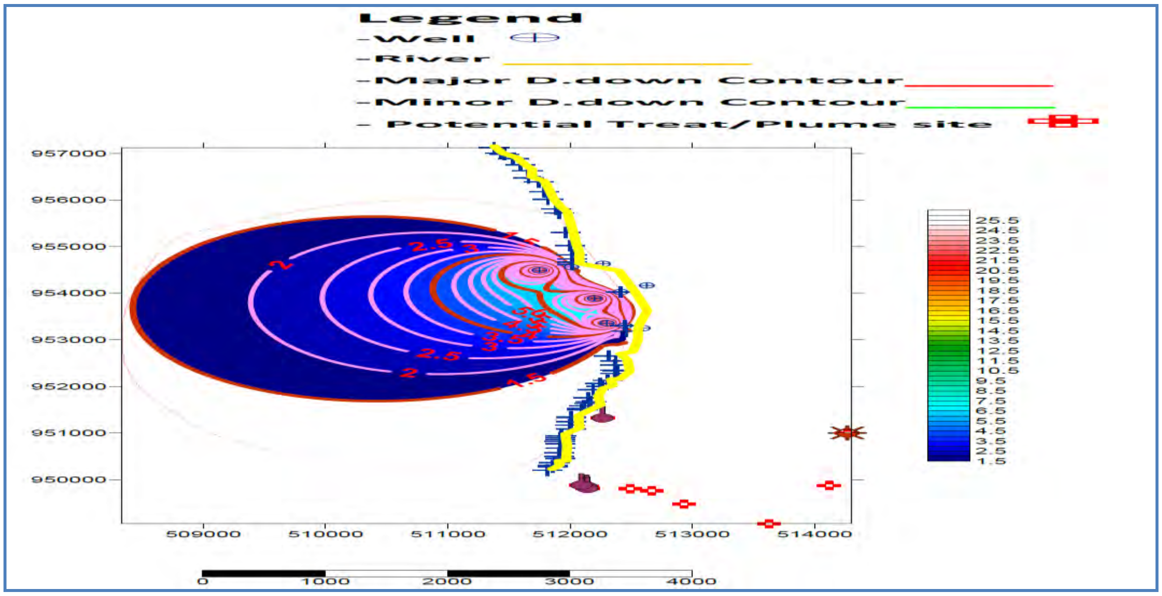

Figure B7. Schematic view of the tapered radius of influence in attempt to have defined shape of cones of depressions in the well field setting the superposed drawdowns to sink by 1.5m from the constant head in this case the boreholes are assumed to application with increased rates such as doubling that of designed capacity of pumps in the boreholes and the aquifer adopts average estimated transmissivity value

Table B. 2*: Fixed radius of influences and its corresponding time for designed discharge of the wells*

Descriptions		**Name of Boreholes**			**Remark**
		MJBH-1	**MJBH-2**	**MJBH-3**	
Parameters Adopt to the Aquifer at Mojo Well Field	***Approximated Transmissivity (m^2/s)***	0.003147	0.003147	0.003147	Minimum Transmissivity, T_{min}
	Storativity	0.02926	0.02926	0.02926	Maximum Storativity, S_{max}
Constant Pumping Rate(m^3/s)		0.045	0.045	0.04383	Pumps operating by rates of designed capacity
Fixed Radius of Influence (m)	**Extents(m)**	153.82	251.59	212.73	Contour line/Cone of depression from well origin to the recharge river region where the composite drawdown depressed to depth of 1.5m below the constant head
	Travel Time (Days)	2.200	5.900	4.290	
Fixed Radius of Influence (m)	**Extents(m)**	3852.741	3505.962	3728.353	Contour line/Cone of depression from well origin to the right edge where the composite drawdown depressed to a depth 1.5m below the constant head
	Travel Time (Days)	1383.54	1162.01	1342.67	

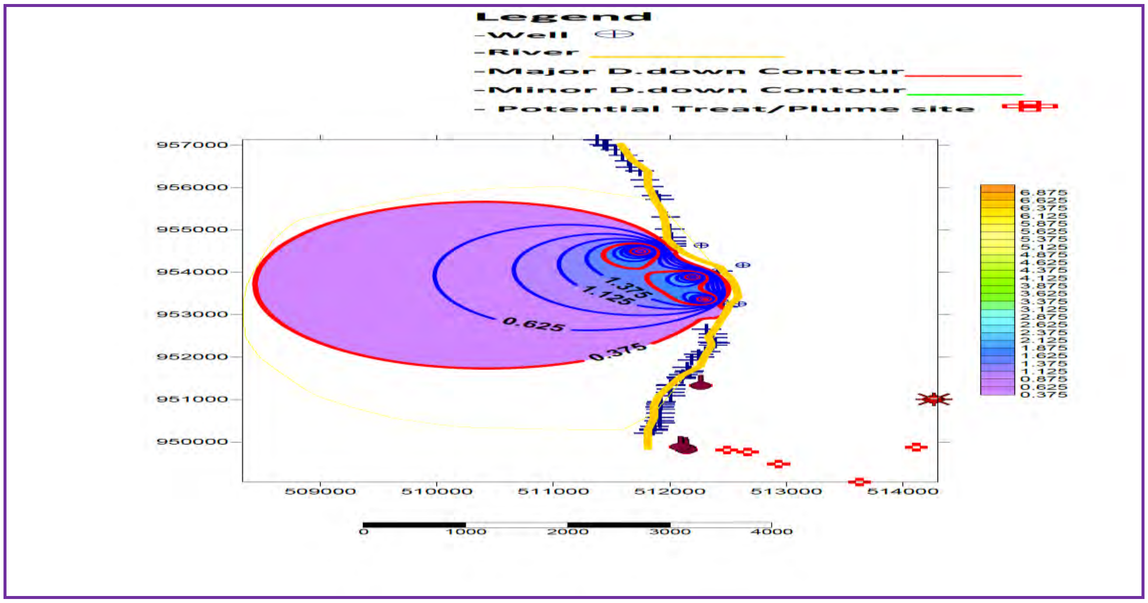

Figure B8. Schematic view of fixed radius of influence in attempt to have defined shape of cones of depressions in the well field setting the superposed drawdowns sinking by 0.375m from the constant head in this case when the boreholes are operating decreasing by the half rates from that of the designed capacity of pumps in the boreholes and the assumed aquifer adopts maximum estimated transmissivity value

***Table B. 3**: Fixed radius of influences and its corresponding time for designed discharge of the wells*

Descriptions		Name of Boreholes			Remark
		MJBH-1	MJBH-2	MJBH-3	
Parameters Adopt to the Aquifer at Mojo Well Field	***Approximated Transmissivity (m^2/s)***	0.003396	0.003396	0.003396	Average Transmissivity, T_{avg}
	Storativity	0.02032	0.02032	0.02032	Average Storativity, S_{avg}
Constant Pumping Rate(m^3/s)		0.0225	0.0225	0.021915	Pumps operating by half rates of designed capacity
Fixed Radius of Influence (m)	**Extents(m)**	288.33	301.8	208.97	Contour line/Cone of depression from well origin to the recharge river region where the composite drawdown depressed to depth of 0.375m below the constant head
	Travel Time (Days)	5.220	5.710	2.790	
Fixed Radius of Influence (m)	**Extents(m)**	3729.03	3513.28	3726.37	Contour line/Cone of depression from well origin to the right edge where the composite drawdown depressed to a depth 0.375m below the constant head
	Travel Time (Days)	812.23	720.96	887.64	

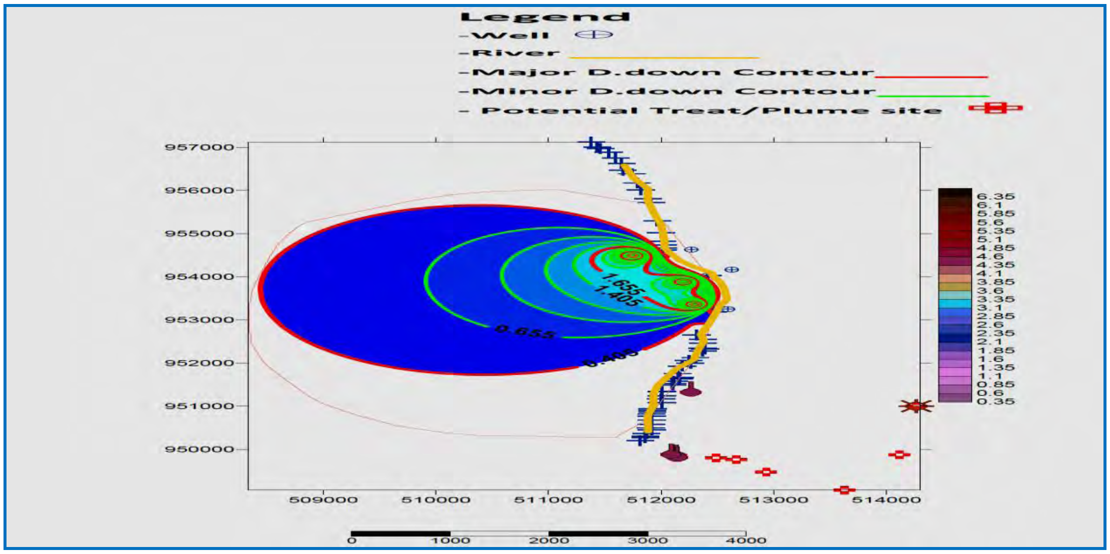

Figure B9. Schematic view of fixed radius of influence in attempt to have defined shape of cones of depressions in the well field setting the superposed drawdowns sinking by 0.405m from the constant head in this case when the boreholes are operating decreasing by the half rates from that of the designed capacity of pumps in the boreholes and the assumed aquifer adopts maximum estimated transmissivity value

Table B. 4: *Fixed radius of influences and its corresponding time for designed discharge of the wells*

Descriptions		Name of Boreholes			Remark
		MJBH-1	**MJBH-2**	**MJBH-3**	
Parameters Adopt to the Aquifer at Mojo Well Field	***Approximated Transmissivity (m^2/s)***	0.003147	0.003147	0.003147	Minimum Transmissivity, T_{min}
	Storativity	0.02926	0.02926	0.02926	Maximum Storativity, S_{max}
Constant Pumping Rate(m^3/s)		0.0225	0.0225	0.021915	Pumps operating by half rates of designed capacity
Fixed Radius of Influence (m)	**Extents(m)**	288.33	252.94	208.97	Contour line/Cone of depression from well origin to the recharge river region where the composite drawdown depressed to depth of 0.405m below the constant head
	Travel Time (Days)	3.090	6.250	1.660	
Fixed Radius of Influence (m)	**Extents(m)**	3852.741	3505.962	3728.353	Contour line/Cone of depression from well origin to the right edge where the composite drawdown depressed to a depth 0.405m below the constant head
	Travel Time (Days)	488.19	922.01	458	

B_4-Wells Interferences

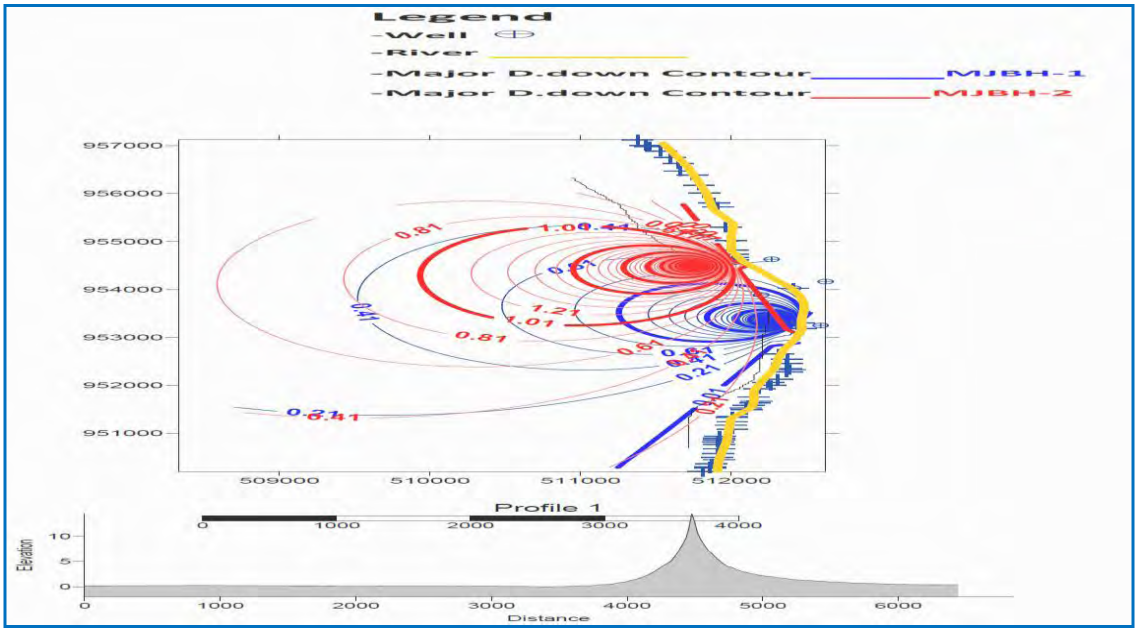

Figure B10. Plan view of two wells operating pumping rates doubling the designed discharge of the wells with case aquifer adopts maximum transmissivity

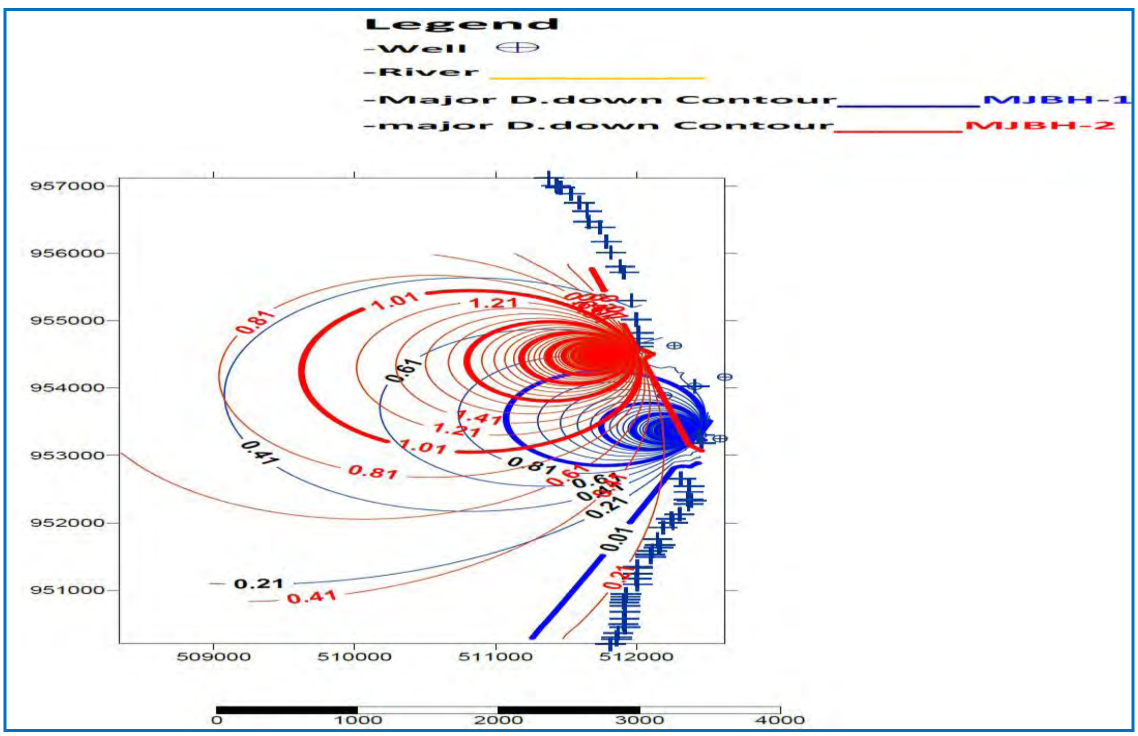

Figure B11. Plan view of two wells operating pumping rates doubling the designed discharge of the wells with case aquifer adopts minimum transmissivity

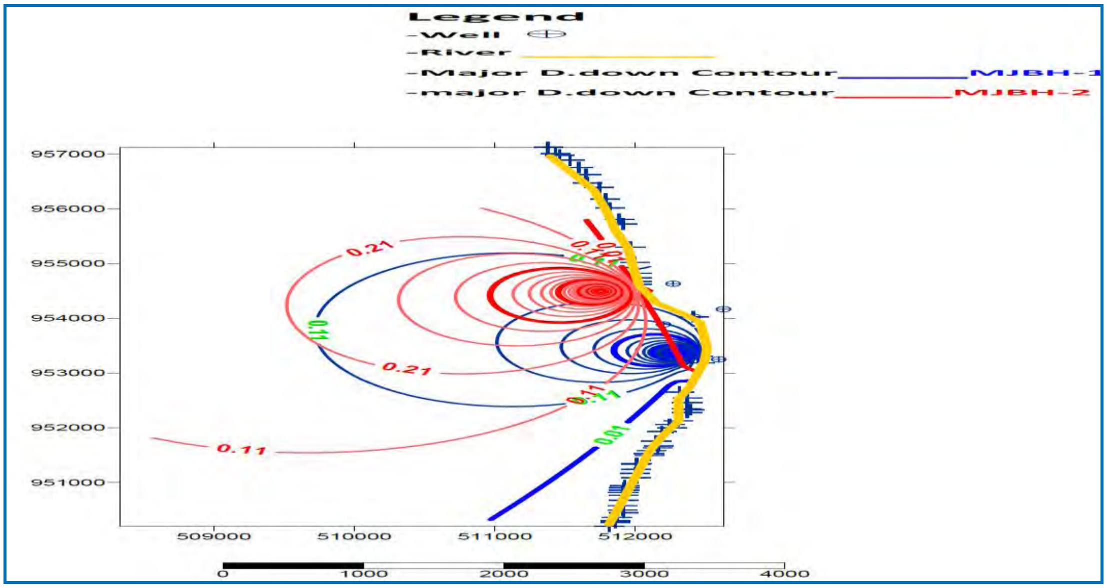

Figure B12. Plan view of two wells operating pumping rates having the designed discharge of the wells with case aquifer adopts maximum transmissivity

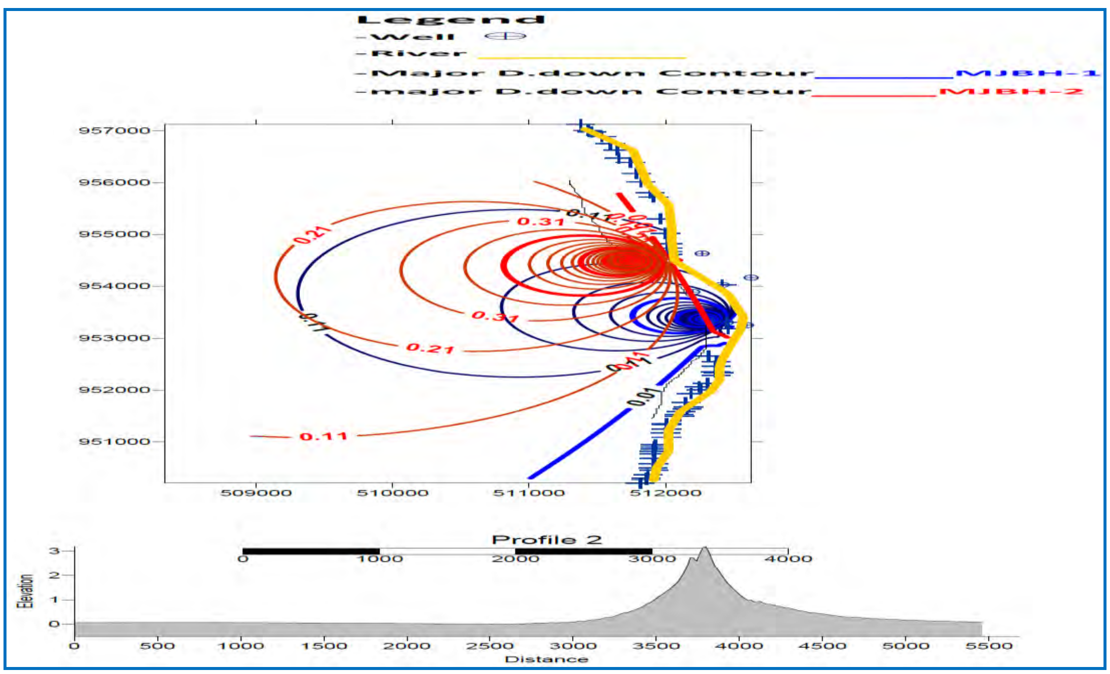

Figure B13. Plan view of two wells operating pumping rates having the designed discharge of the wells with case aquifer adopts maximum transmissivity